A STUDY ON PERFORMANCE ENHANCEMENT OF CUTTING TOOLS THROUGH PERFORATED SURFACE FOR THE MACHINING OF TITANIUM ALLOY USING PCD INSERTS

Thesis

Submitted in partial fulfillment of the requirements for the degree of

DOCTOR OF PHILOSOPHY

by

CHARITHA M RAO

DEPARTMENT OF MECHANICAL ENGINEERING
NATIONAL INSTITUTE OF TECHNOLOGY KARNATAKA
SURATHKAL, MANGALORE-575025
OCTOBER, 2019

Dedicated to….

My beloved Parents, Family

members…

&

All my Teachers and Colleagues who taught

and encouraged me with positive thoughts…

DECLARATION

By the Ph.D. Research Scholar

I hereby declare that the Research Thesis entitled **“A STUDY ON PERFORMANCE ENHANCEMENT OF CUTTING TOOLS THROUGH PERFORATED SURFACE FOR THE MACHINING OF TITANIUM ALLOY USING PCD INSERTS”** which is being submitted to the **National Institute of Technology Karnataka, Surathkal** in partial fulfillment of the requirements for the award of the degree of **Doctor of Philosophy** in **Mechanical Engineering** is a bonafide report of the research work carried out by me. The material contained in this Research Thesis has not been submitted to any other Universities or Institutes for the award of any degree.

Register Number: **145094ME14F03**

Name of the Research Scholar: **Charitha M Rao**

Signature of the Research Scholar:

Department of Mechanical Engineering

Place: NITK-Surathkal
Date:

CERTIFICATE

This is to certify that the Research Thesis entitled **"A STUDY ON PERFORMANCE ENHANCEMENT OF CUTTING TOOLS THROUGH PERFORATED SURFACE FOR THE MACHINING OF TITANIUM ALLOY USING PCD INSERTS"** submitted by **Ms. Charitha M. Rao** (Register Number: ME14F03) as the record of the research work carried out by her, is accepted as the Research Thesis submission in partial fulfillment of the requirements for the award of the degree of **Doctor of Philosophy**.

Research Guides

Prof. Shrikantha S. Rao	**Dr. Mervin A. Herbert**
Professor	Associate Professor
Department of Mechanical Engineering	Department of Mechanical Engineering
Date:	Date:

Chairman-DRPC
Date:

DEPARTMENT OF MECHANICAL ENGINEERING
NATIONAL INSTITUTE OF TECHNOLOGY KARNATAKA, SURATHKAL
MANGALORE - 575025

ACKNOWLEDGEMENT

I am indebted to my supervisors **Prof. Shrikantha S Rao**, Professor and **Dr. Mervin A Herbert**, Associate Professor, Department of Mechanical Engineering, National Institute of Technology Karnataka, Surathkal, for their excellent guidance and support throughout the research work. Their constant encouragement, help and review of the entire work during the course of the investigation are invaluable.

I wish to thank Research Progress Assessment Committee members **Dr. M. R. Ramesh**, Associate Professor, Department of Mechanical Engineering and Dr**. Pruthviraj U**, Assistant Professor, Department of Applied Mechanics and Hydraulics Engineering for their unbiased appreciation and criticism all through this research.

I am immensely grateful to **Prof. Shrikantha S Rao**, Professor and Head, Department of Mechanical Engineering for extending the Departmental facilities, which ensured the satisfactory progress of my research work.

I would like to thank all the teaching and non-teaching staff members of the Department of Mechanical Engineering, of NITK Surathkal for their continuous help and support throughout the research work.

I wish to express my sincere gratitude to **Prof. K. V Gangadharan**, for his valuable suggestions to do this research in the measurement of Vibration signals. I thank **Ms. Rashmi Banjan** of Department of Metallurgical and Materials, for her support in connection with the use of Scanning electron microscope.

I would like to thank CMTI Bengaluru for research support during all years of my research. Especially, I would like to thank **Mr. Prakash Vinod**, Head, Department of NMTC for his encouragement. I also like to thank **Dr. Ashish Warade** and **Mrs. Sushma** for their support in connection with the use of a confocal microscope.

I owe my deepest gratitude to supporting staff of the Department of Mechanical Engineering, **Mr. Jaya Devadiga**, **Mr. C A Verghese**, **Mr. Pradeep**, **Mr. Sudhakar** and **Mr. Mahaveer** for their help during conducting experiments.

I thank the Director and the administration of NITK Surathkal for permitting me to pursue my research work at the Institute.

I would like to thank **Mr. Lakshmikanth Kenni**, Assistant Professor, Department of Automobile and Aeronautical Engineering, MIT, Manipal, for helping in ANSYS Simulation and I also thank **Mr. Pradeep Kumar**, SFTC Bengaluru, for his immense support in use of DEFORM-3D software for the Dynamic Simulation process.

I would like to thank my co-researchers and friends **Dr. Sachin B**, **Mrs. Roopa R**, **Mrs. Jeane D'Souza**, **Dr. Sivaiah P**, **Mr. Subramanya R Pabhu P**, **Mr. Srivatsa T V**, **Mr. Ishwargouda Patil, Mr. Austin D'Souza**, **Mr. Vinay Verghese**, **Mr. Bala Narasimha**, **Mrs. Rashmi L Malghan**, **Mr. Karthik Rao M C**, **Mr. Anarghya** and **Dr. Muralidhar Avvari**, for their kind help, encouragement for successful completion of this research work. I would also heartfelt thanks to **Mr. Rahul** and **Mr. Rohith Rajpal** for their immense support and help in fetching vibration data.

I would like to thank **Dr. Srinivas Pai**, **Mr. Grynal D'Mello** and **Mr. Adarsh Rai**, Department of Mechanical Engineering, NMAMIT, Nitte, for their kind help and suggestions in carrying out experiments, vibration Measurement and helping in Prediction technique using Adaptive Neuro-Fuzzy Inference System. I am also thankful to **Mr. Sanoop Kottuvayal Thazha Kuni**, for helping me in coding the prediction of ANFIS.

I am indebted to all my friends of the Department of Mechanical Engineering and other Departments of NITK Surathkal for their constant help and encouragement during the entire this research work

I would also like to share the happiest moment with my parents **Mr. M R Manjunatha Rao** and **Mrs. H Suma**. Their blessings, guidance and endeavour kept my moral high throughout the research. I feel happy to express my sincere appreciation to my husband **Dr. Sachin B** for his understanding, care, support and encouragement throughout my research. I also extend my hearty thanks to **Mr. Sathyamurthy** for his continues support throughout my research and helping me in achieving success.

The list goes on and there are many others I should mention. There are people who have helped me all the way and provided me support when I didn’t even realize I needed it, or needed it now, or needed it constantly. Listing all of them would fill a book itself, so I merely will have to limit myself to a few words: I THANK YOU ALL……!

(Charitha M Rao)

ABSTRACT

In the manufacturing industry, high-speed machining technology has been widely used in metal cutting due to its remarkable advantages in improving the productivity. However, the cutting tools have minimum tool life when used for machining difficult-to-cut materials such as titanium alloys and nickel-based alloys. Titanium alloy (Ti-6Al-4V alloy) is one of the widely used materials in the application of aerospace industries, military applications, automobile industries and biomedical implants. Rapid tool wear is the main issue in machining these difficult-to-cut materials due to the high heat generation in the machining zone and high chemical reactivity at higher cutting conditions. The heat produced at shear zone during machining of Ti-6Al-4V alloy is highly centralized and temperature increases rapidly. Tribological properties at the tool-chip contact area can be improved by using a number of methods like Minimum Quantity Lubrication (MQL) and surface coatings. The surface texturing technology is a promising approach in this regard. Many researchers have discussed with different surface texturing patterns such as parallel, perpendicular and elliptical micro/nano textures on cutting inserts. These surface textures helped in improving the tribological properties. The present work is focused on surface textures with micro-hole patterns on cutting inserts, under the MQL environment. In this process, the lubricant surrounded in the micro-holes at the tool-chip interface could be squeezed to the cutting interface to reduce friction under proper viscosity and sliding speed.

A novel configuration of holes and tunnels in the inserts has been tried out successfully. The present work is divided into three phases while machining of Ti-6Al-4V alloy using the micro-hole patterned cutting insert under MQL environment. In the first phase, the modelling and simulation of micro-hole patterned cutting inserts were developed using Finite Element Analysis software. In this phase, different micro-hole patterns were developed on PolyCrystalline Diamond (PCD) cutting insert using CAD modelling and later static and dynamic analysis were carried out. From the results, it was observed that cutting inserts with micro-holes embedded on rake face and flank face had lower stress concentration. Hence, proved that cutting inserts with micro-holes with

different hole configurations had no adverse impact on mechanical properties of cutting tool materials.

In the second phase, optimization strategy is applied to identify the right configuration of surface texture and experiments were conducted based on the one factor at a time approach to study the behaviour of individual process parameters like cutting velocity, feed rate and depth of cut on the performance indexes such as cutting temperature, machining vibrations, tool flank wear, Material Removal Rate (MRR), chip-morphology and surface integrity (surface roughness, surface topography and microhardness) under MQL environment machining using normal and modified cutting inserts. It is evident from the experimental results that machining with modified inserts significantly improved the machining performance and quality of the product. One more finding, out of the present work, is the mitigation of serrated chips, when compared to chip formation in machining of Ti-6Al-4V alloys with normal inserts. The chip formation with less shear bands were obtained during machining process due to the improvement in the thermal stability property caused by a reduction in cutting temperature through micro-hole patterns. A best feasible micro-hole configuration for the machining of Ti-6Al-4V alloy under MQL environment was arrived at, as a unique solution.

In the third phase, the modified PCD insert with the chosen pattern of micro-holes was compared with Polycrystalline Cubic Boron Nitride (PCBN) inserts, for machining of the Ti-6Al-4V alloy. From the experimental results, it was found that modified PCD insert had better efficiency in reducing the cutting temperatures and also reduces the tool wear by increasing the wear resistance properties due to the micro-pool lubrications when compared to modified PCBN inserts.

Another important outcome of this research is the development of prediction model using Adaptive Neuro-Fuzzy Inference System (ANFIS) to assist in validation. This method is a combination of two soft-computing methods of ANN and Fuzzy logic. Fuzzy logic helps in the transformation of the human knowledge and the ANN helps in the learning process and reduces the rate of errors in the determination of rules in fuzzy logic. In this research, gauss membership function model was developed for the prediction of

output parameters. The comparison made between the predicted values derived from ANFIS and experimental values proved that the gauss membership function adaptation achieved accuracy of 96 % with 4-5% prediction error.

Thus, a unique surface texturing consisting of micro-holes and tunnels in the PCD inserts, for machining Ti-6Al-4V alloy has been successfully developed, tested and validated.

Keywords: *Ti-6Al-4V alloy, PCD inserts, surface texturing, Minimum Quantity Lubrication (MQL), Micro-holes, machining vibrations, PCBN inserts, chip morphology, tool wear, surface integrity, ANFIS.*

CONTENTS

Declaration

Certificate

Acknowledgements

Abstract

Contents *i*

List of Figures *ix*

List of Tables *xv*

List of Symbols and Abbreviations *xix*

CHAPTER-1 INTRODUCTION **1**

1.1 METAL CUTTING BACKGROUND 1

1.2 TITANIUM (Ti-6Al-4V) ALLOY 5

1.3 POLYCRYSTALLINE DIAMOND (PCD) AS CUTTING TOOL INSERT 7

1.4 TEMPERATURE ISSUES IN THE METAL CUTTING PROCESS 8

1.5 FACTORS INFLUENCING CUTTING TEMPERATURES DURING THE CUTTING PROCESS 9

  1.5.1 Work-material and tool-material 9

  1.5.2 Cutting tool geometry 9

  1.5.3 Selection of cutting process parameters 9

  1.5.4 Use of coolants 10

1.6 COOLING STRATEGIES 10

1.7 MINIMUM QUANTITY LUBRICATION (MQL) TECHNIQUE 12

1.8 SURFACE TEXTURING METHOD OF CUTTING TOOL INSERTS 12

1.9 FINITE ELEMENT MODELLING 15

1.10 NEED FOR THE PRESENT STUDY 16

1.11 THESIS ORGANIZATION 17

CHAPTER-2 LITERATURE REVIEW **21**

2.1 INTRODUCTION 21

2.2 MACHINABILITY OF TITANIUM ALLOY (Ti-6Al-4V) 21
2.3 MQL MACHINING PROCESS 27
2.4 SURFACE TEXTURING OF CUTTING TOOL INSERTS 28
2.5 FINITE ELEMENT ANALYSIS OF THE TURNING PROCESS 36
2.6 MODELLING AND OPTIMIZATION TECHNIQUES FOR MACHINING WITH NORMAL AND MODIFIED PCD INSERT UNDER DIFFERENT COOLING ENVIRONMENTS 40
    2.6.1 Design of Experiment using Taguchi method 40
    2.6.2 A prediction model using Adaptive Neuro-Fuzzy Inference System 44
2.7 SUMMARY OF THE LITERATURE REVIEW 46
2.8 MOTIVATION FROM THE LITERATURE REVIEW 47
2.9 OBJECTIVES OF THE CURRENT RESEARCH 49
2.10 THE SCOPE OF THE PRESENT RESEARCH 49
CHAPTER-3 EXPERIMENTAL METHODOLOGY 51
3.1 SELECTION OF WORK MATERIAL 51
3.2 DIFFERENT COOLING ENVIRONMENTS AND EXPERIMENTAL SETUP 53
    3.2.1 MQL Cooling 53
    3.2.2 Construction of MQL machining setup 54
    3.2.3 Dry machining 55
3.3 MACHINING CONDITIONS 56
3.4 EXPERIMENTAL DESIGN AND METHODOLOGY 57
    3.4.1 Experimental Methodology 57
    3.4.2 Experimental Designs 58
        3.4.2.1 Taguchi Orthogonal array (OA) design 58
        3.4.2.2 One factor at a time approach (OFATA) 61
        3.4.2.3 Adaptive Neuro-Fuzzy Inference System (ANFIS) 61
3.5 MEASUREMENT OF PERFORMANCE CHARACTERISTICS 62
    3.5.1 Cutting Temperature 62

3.5.2 Machining vibrations 63
3.5.3 Cutting Tool Wear 63
3.5.4 Surface Roughness of Machined Surface 64
3.5.5 Surface Topography of Machined Surface 64
3.5.6 Material Removal Rate (MRR) 65
3.5.7 Scanning Electron Microscope 66
3.5.8 Microhardness 67
3.5.9 Electric Discharge Super Drilling Machine 68
3.6 SUMMARY 69
CHAPTER-4 FINITE ELEMENT ANALYSIS OF TI-6AL-4V ALLOY USING PCD INSERT 71
4.1 INTRODUCTION 71
4.2 MICRO-HOLES ON POLYCRYSTALLINE DIAMOND INSERT 72
4.3 INFLUENCE OF MICRO-HOLES ON THE MECHANICAL PROPERTIES OF THE CUTTING INSERT 72
4.4 FINITE ELEMENT ANALYSIS USING DEFORM-3D 76
4.4.1 Design of Micro-hole patterns on Polycrystalline Diamond Insert 77
4.4.2 Finite Element Modelling and Simulation 79
4.5 FEM SIMULATION RESULTS AND DISCUSSIONS 82
4.5.1 FEM based Prediction of Cutting Force 83
4.5.2 FEM based Prediction of effective Stress 84
4.5.3 FEM based Prediction of effective Strain 85
4.5.4 FEM based Prediction of Temperature 85
4.6 SIMULATION OF THE MACHINING PROCESS 87
4.7.1 Effect of Micro-holes on cutting temperature 88
4.7 ANALYSIS OF SURFACE ROUGHNESS AND CUTTING TEMPERATURE IN MACHINING OF TI-6AL-4V ALLOY USING NORMAL PCD INSERT UNDER DRY AND MQL ENVIRONMENT 91
4.7.1 Analysis of Variance for Surface Roughness and Cutting 92

Temperature during machining of Ti-6Al-4V alloy using PCD insert under Dry and MQL Environment
4.8 SUMMARY 97
CHAPTER-5 MACHINING OPTIMIZATION STRATEGY 99
5.1 INTRODUCTION 99
5.2 EXPERIMENTAL PLAN 99
5.3 EFFECT OF MICRO-HOLES IN MQL ENVIRONMENT AND PROCESS PARAMETERS ON CUTTING TEMPERATURE 100
  5.3.1 Effect of the modified insert and cutting velocity under MQL environment on cutting temperature 100
  5.3.2 Effect of modified insert and feed rate under MQL environment on cutting temperature 102
  5.3.3 Effect of modified insert and depth of cut under MQL environment on cutting temperature 103
5.4 EFFECT OF MICRO-HOLES IN MQL ENVIRONMENT AND PROCESS PARAMETERS ON MACHINING VIBRATIONS 104
  5.4.1 Effect of the modified insert and cutting velocity under MQL environment on machining vibrations 106
  5.4.2 Effect of the modified insert and feed rate under MQL environment on machining vibrations 108
  5.4.3 Effect of the modified insert and depth of cut under MQL environment on machining vibrations 109
5.5 EFFECT OF MICRO-HOLES IN MQL ENVIRONMENT AND PROCESS PARAMETERS ON TOOL FLANK WEAR 111
  5.5.1 Effect of the modified insert and cutting velocity under MQL environment on Tool flank wear 111
  5.5.2 Effect of the modified insert and feed rate under MQL environment on Tool flank wear 113
  5.5.3 Effect of the modified insert and depth of cut under MQL 113

environment on Tool flank wear
5.6 EFFECT OF MICRO-HOLES IN MQL ENVIRONMENT AND PROCESS PARAMETERS ON SURFACE ROUGHNESS 117
5.6.1 Effect of the modified insert and cutting velocity under MQL environment on surface roughness 117
5.6.2 Effect of the modified insert and feed rate under MQL environment on surface roughness 118
5.6.3 Effect of the modified insert and depth of cut under MQL environment on surface roughness 119
5.7 CHIP MORPHOLOGY 121
5.8 MICROHARDNESS 125
5.9 EFFECT OF MICRO-HOLES IN MQL ENVIRONMENT AND PROCESS PARAMETERS ON SURFACE TOPOGRAPHY 127
5.9.1 Effect of the modified insert and cutting velocity under MQL environment on surface topography 127
5.9.2 Effect of the modified insert and feed rate under MQL environment on surface topography 130
5.9.3 Effect of the modified insert and depth of cut under MQL environment on surface topography 132
5.10 EFFECT OF MICRO-HOLES IN MQL ENVIRONMENT AND PROCESS PARAMETERS ON MATERIAL REMOVAL RATE 134
5.11 SUMMARY 136
CHAPTER-6 COMPARISON OF MODIFIED PCD AND PCBN INSERTS IN MACHINING OF TI-6AL-4V ALLOY 139
6.1 INTRODUCTION 139
6.2 EXPERIMENTAL PLAN 139
6.3 MODIFIED CUTTING INSERTS WITH MICRO-HOLE AS SURFACE TEXTURE 140
6.4 EFFECT OF MICRO-HOLES IN PCD AND PCBN INSERTS 141

MACHINING UNDER MQL ENVIRONMENT ON CUTTING TEMPERATURE
6.5 EFFECT OF MICRO-HOLES IN PCD AND PCBN INSERTS MACHINING UNDER MQL ENVIRONMENT ON CUTTING VIBRATION IN CUTTING SPEED DIRECTION 142
6.6 EFFECT OF MICRO-HOLES IN PCD AND PCBN INSERTS MACHINING UNDER MQL ENVIRONMENT ON CUTTING TOOL FLANK WEAR 144
6.7 EFFECT OF MICRO-HOLES IN PCD AND PCBN INSERTS MACHINING UNDER MQL ENVIRONMENT ON CHIP MORPHOLOGY 146
6.8 EFFECT OF MICRO-HOLES IN PCD AND PCBN INSERTS MACHINING UNDER MQL ENVIRONMENT ON CHIP REDUCTION COEFFICIENT 148
6.9 EFFECT OF MICRO-HOLES IN PCD AND PCBN INSERTS MACHINING UNDER MQL ENVIRONMENT ON THE SURFACE ROUGHNESS 150
6.10 EFFECT OF MICRO-HOLES IN PCD AND PCBN INSERTS MACHINING UNDER MQL ENVIRONMENT ON CUTTING MICROHARDNESS 152
6.11 SUMMARY 153
CHAPTER-7 PREDICTION OF PERFORMANCE INDEXES USING ADAPTIVE NEURO-FUZZY INFERENCE SYSTEM (ANFIS) 155
7.1 INTRODUCTION 155
    7.1.1 ANFIS Architecture 157
    7.1.2 Learning Algorithm of ANFIS 160
7.2 EXPERIMENTAL PLAN 161
7.3 ANFIS MODELLING FOR CUTTING TEMPERATURE PREDICTION 162

7.4 ANFIS MODELLING FOR CUTTING VIBRATION PREDICTION 165
7.5 ANFIS MODELLING FOR TOOL FLANK WEAR PREDICTION 169
7.6 ANFIS MODELLING FOR SURFACE ROUGHNESS PREDICTION 172
7.7 SUMMARY 175
CHAPTER-8 CONCLUSIONS AND SCOPE FOR FUTURE WORK 177
8.1 CONCLUSIONS 177
8.2 SCOPE FOR FUTURE WORK 179
REFERENCES 181
APPENDIX-I 205
APPENDIX-II 206
LIST OF RESEARCH PAPERS PUBLISHED
BIO-DATA

LIST OF FIGURES

Figure No.	Description	Page No.
Figure 1.1	Heat generation zones in the metal cutting process	8
Figure 1.2	Different techniques of sustainable manufacturing for cleaner production	13
Figure 1.3	Characteristics of sustainable manufacturing	14
Figure 2.1	Schematic diagrams showing the direction of the texture (a) perpendicular and (b) parallel to the chip flow direction. (c) Cross-patterned texture	32
Figure 2.2	Photo of the rake-face textured tools filled with and without MoS_2 solid lubricants	33
Figure 2.3	Distribution of surface textures on cutting tool rake face (a) Distribution of straight holes (b) Distribution of linear grooves	35
Figure 2.4	Fabrication of surface texturing (a) using Rockwell hardness tester (b) by scratching using diamond dresser	36
Figure 2.5	Simulation of the micro-bump textured insert using ADVANTEDGE	38
Figure 2.6	Block diagram of the process	41
Figure 2.7	Block diagram for representation of ANFIS structure	45
Figure 3.1	Microstructure and elemental analysis of Ti-6Al-4V alloy workpiece	52
Figure 3.2	Minimum Quantity Lubrication Systems	54
Figure 3.3	Schematic representation of the MQL system	55
Figure 3.4	Machining zones at (a) dry machining (b) MQL machining	55
Figure 3.5	(a) Tool Holder PDJNL1616H11 (b) Commercially available PCD Insert	56
Figure 3.6	Flow chart of the research	57
Figure 3.7	Infrared thermometer gun	62
Figure 3.8	The vibration measurement set up for fetching cutting vibration signals	63
Figure 3.9	Mitutuyo Surface Roughness Tester	64
Figure 3.10	3D optical confocal microscope	65
Figure 3.11	Weighting Scale	66

Figure 3.12	Scanning Electron Microscope	67
Figure 3.13	Vickers Microhardness Tester	68
Figure 3.14	Electric discharge super drilling machine	69
Figure 4.1	Micro-hole texture pattern (a) Design 1 and (b) Design 2	72
Figure 4.2	CAD models of normal and modified PCD insert (a) normal insert (b) Design 1 micro-hole textured insert (c) Design 2 micro-hole textured insert	74
Figure 4.3	Represents the boundary conditions for static simulations. (a) & (b) represents the applied force and applied pressure for normal insert, (c) & (d) represents the applied force and applied pressure for Design 1 insert, (e) & (f) represents the applied force and applied pressure for Design 2 insert	74
Figure 4.4	Results of FEA analysis. Stress distribution: (a) normal insert (MPa) (c) micro-hole textured design 1 (MPa) (e) micro-hole textured design 2 (MPa). Total deformation: (b) normal insert (mm) (d) micro-hole textured design 1 (mm) (f) micro-hole textured design 2 (mm).	75
Figure 4.5	Structure of DEFORM-3D	76
Figure 4.6	CAD model of the different types of Micro-hole designs on the rake face of the PCD inserts	79
Figure 4.7	Meshing of the PCD cutting insert and the Ti-6Al-4V alloy workpiece in DEFORM-3D simulation	80
Figure 4.8	Simulation of FE model (a) Normal Insert (b) Design 1 modified insert (c) Design 2 modified insert	82
Figure 4.9	Comparison of cutting force with normal and designed inserts	83
Figure 4.10	Predicted Stress distribution graph of Normal Insert and Designed Inserts	84
Figure 4.11	Predicted Strain distribution graph of Normal Insert and Designed Inserts	85
Figure 4.12	Predicted Temperature distribution graph of Normal Insert and Modified Inserts	86

Figure 4.13 Different types of Micro-hole textured inserts produced by the super drilling 88

Figure 4.14 Comparison of both experimental and simulated conditions in a variation of feed rate on cutting temperature 88

Figure 4.15 Cutting temperature distribution under simulation at (a) 0.3 mm/rev (Normal insert) (b) 0.5 mm/rev (Normal insert) (c) 0.3 mm/rev (Design 1) (d) 0.5 mm/rev (Design 1) (e) 0.3 mm/rev (Design 2) (f) 0.5 mm/rev (Design 2) 90

Figure 4.16 Main effect plots of (a) Surface Roughness and (b) Cutting Temperature based on S/N ratio for turning under DRY condition 94

Figure 4.17 Main effect plots of (a) Surface Roughness and (b) Cutting Temperature based on S/N ratio for turning under MQL condition 96

Figure 5.1 Effect of (a) cutting velocity (b) Feed rate and (c) Depth of cut on cutting temperature with normal and modified insert under MQL environment by keeping all other variables as constant at their respective mean levels 101

Figure 5.2 Raw data of vibration amplitude at a high cutting velocity of 200 m/min (a) normal insert (b) Design 1 insert (c) Design 2 insert 105

Figure 5.3 Variation of vibration amplitude of cutting velocity (a) Cutting speed direction (b) Feed direction (c) Depth of cut direction 106

Figure 5.4 Variation of vibration amplitude of Feed rate (a) Cutting speed direction (b) Feed direction (c) Depth of cut direction 108

Figure 5.5 Variation of vibration amplitude of Depth of cut (a) Cutting speed direction (b) Feed direction (c) Depth of cut direction 110

Figure 5.6 Effect of (a) cutting velocity (b) Feed rate and (c) Depth of cut on Tool flank wear with normal and modified insert under MQL environment 112

Figure 5.7 Effect of (a) cutting velocity (b) Feed rate and (c) Depth of cut on Surface roughness with normal and modified insert under MQL environment by keeping all other variables as constant at their respective mean levels. 117

Figure 5.8 Sample preparation methodology for measurement of microhardness 126
Figure 5.9 Microhardness profiles of the normal insert, Design 1 and Design 2 cutting insert machined surface 126
Figure 5.10 Confocal images of surface topography at cutting velocity = 100 m/min, feed rate = 0.5 mm/rev and depth of cut = 1 mm under MQL cooling environments (a) normal cutting insert machined surface (b) Design 1 cutting insert machined surface (c) Design 2 cutting insert machined surface 128
Figure 5.11 Confocal images of surface topography at cutting velocity = 200 m/min, feed rate = 0.5 mm/rev and depth of cut = 1 mm under MQL cooling environments (a) normal cutting insert machined surface (b) Design 1 cutting insert machined surface (c) Design 2 cutting insert machined surface 129
Figure 5.12 Confocal images of surface topography at cutting velocity 150 m/min, feed rate 0.1 mm/rev and depth of cut 1 mm under (a) normal insert machining, (b) Design 1 cutting insert machining and (c) Design 2 cutting insert 130
Figure 5.13 Confocal images of surface topography at cutting velocity 150 m/min, feed rate 0.5 mm/rev and depth of cut 1 mm under (a) normal insert machining, (b) Design 1 cutting insert machining and (c) Design 2 cutting insert 131
Figure 5.14 Confocal images of surface topography at cutting velocity 150 m/min, feed rate 0.5 mm/rev and depth of cut 0.5 mm under (a) normal insert machining, (b) Design 1 cutting insert machining and (c) Design 2 cutting insert 132
Figure 5.15 Confocal images of surface topography at cutting velocity 150 m/min, feed rate 0.5 mm/rev and depth of cut 1.5 mm under (a) normal insert machining, (b) Design 1 cutting insert machining and (c) Design 2 cutting 133

insert µm
Figure 5.16 Effect of (a) cutting velocity (b) Feed rate and (c) Depth of cut on Material Removal Rate (MRR) with normal and modified insert under MQL environment 134
Figure 5.17 MRR measurements by keeping surface roughness as reference 135
Figure 6.1 The Micro-hole texture (a) PCD Insert (b) PCBN Insert 141
Figure 6.2 Effect of varying feed rate on cutting temperature 142
Figure 6.3 Machining vibrations with modified PCD and PCBN insert with a varying feed rate 144
Figure 6.4 Effect of varying feed rate on tool flank wear 144
Figure 6.5 SEM image of a cross-section of a chip showing some chip features under MQL environment 148
Figure 6.6 The chip-reduction coefficient of modified PCD and PCBN inserts 148
Figure 6.7 Average surface roughness of machined surface with the modified PCD and PCBN insert 150
Figure 6.8 Microhardness value beneath the surface roughness machining with modified PCD and PCBN insert 152
Figure 7.1 Architecture of Adaptive Network 157
Figure 7.2 (a) A two input first-order Sugeno Fuzzy model with two rules (b) equivalent ANFIS architecture 158
Figure 7.3 Plots showing the comparison of experimental values and predicted values of cutting temperature by ANFIS 164
Figure 7.4 Scatter Plot showing the variation of cutting temperature for experimental and predicted values using ANFIS 164
Figure 7.5 3D surface plot for cutting velocity vs feed rate of cutting temperature 165
Figure 7.6 3D surface plot for feed rate vs depth of cut of cutting temperature 165
Figure 7.7 Plots showing the comparison of experimental values and predicted values of machining vibrations amplitude by ANFIS 167

Figure 7.8	Scatter Plot showing the variation of machining vibrations amplitude for experimental and predicted values using ANFIS	168
Figure 7.9	3D surface plot for cutting velocity vs feed rate of machining vibrations amplitude	168
Figure 7.10	3D surface plot for feed rate vs depth of cut of machining vibrations amplitude	169
Figure 7.11	Plots showing the comparison of experimental values and predicted values of tool flank wear by ANFIS	170
Figure 7.12	Scatter Plot showing the variation of tool flank wear for experimental and predicted values using ANFIS	171
Figure 7.13	3D surface plot for cutting velocity vs feed rate of tool flank wear	171
Figure 7.14	3D surface plot for feed rate vs depth of cut of tool flank wear	172
Figure 7.15	Plots showing the comparison of experimental values and predicted values of surface roughness by ANFIS	173
Figure 7.16	Scatter Plot showing the variation of surface roughness for experimental and predicted values using ANFIS	174
Figure 7.17	3D surface plot for cutting velocity vs feed rate of surface roughness	174
Figure 7.18	3D surface plot for feed rate vs depth of cut of surface roughness	175

LIST OF TABLES

Table No.	Description	Page No.
Table 1.1	Chemical Composition of Ti-6Al-4V alloy	6
Table 1.2	Mechanical properties of Ti-6Al-4V alloy	6
Table 3.1	Chemical composition of Ti-6Al-4V alloy (wt. %) used in the present research	52
Table 3.2	Mechanical Properties of Ti-6Al-4V alloy	52
Table 3.3	Machining Conditions	56
Table 3.4	Standard orthogonal array	60
Table 3.5	Taguchi’s L_9 orthogonal array	60
Table 3.6	OFATA experimental plan	61
Table 4.1	Mechanical properties of PCD Insert	73
Table 4.2	Different designs with varied depth and diameter of the holes	78
Table 4.3	JC material model constants for Titanium alloy (Ti-6Al-4V)	81
Table 4.4	Material Properties of PCD	81
Table 4.5	Cutting Parameter for simulation comparison with normal insert and modified inserts	82
Table 4.6	Control factors and levels for turning	91
Table 4.7	Control factor settings as per L_9 Orthogonal Array	92
Table 4.8	Control factor settings as per L_9 OA with measured values and corresponding signal to noise ratio for turning with the normal insert in dry condition	93
Table 4.9	ANOVA for Cutting Temperature based on S/N ratio for turning under dry condition	94
Table 4.10	ANOVA for Average Surface Roughness based on S/N	95

	ratio for turning under dry condition	
Table 4.11	Control factor settings as per L_9 OA with measured values and corresponding signal to noise ratio for turning with the normal insert in MQL condition	96
Table 4.12	ANOVA for Cutting Temperature based on S/N ratio for turning under MQL condition	96
Table 4.13	ANOVA for Average Surface Roughness based on S/N ratio for turning under MQL condition	97
Table 5.1	Controllable factors and their levels for OFATA	100
Table 5.2	SEM Images of tool flank wear at different machining conditions	115
Table 5.3	SEM Images of tool flank wear at different machining conditions	116
Table 5.4	SEM Images of machined surfaces at different machining conditions	120
Table 5.5	Chips images at different machining conditions	123
Table 5.6	SEM images of the chip-morphology at different machining conditions	124
Table 6.1	Material properties of PCD and PCBN inserts	140
Table 6.2	SEM images of tool flank wear	145
Table 6.3	SEM images of the chips obtained at machining with modified PCD and PCBN inserts	147
Table 6.4	SEM images of surface roughness	150
Table 7.1	Controllable Factors and their levels for experimentation	162
Table 7.2	Comparison of cutting temperature predicted by trained ANFIS model with the experimentally obtained cutting temperature for machining Ti-6Al-4V alloy	163
Table 7.3	Comparison of machining vibrations amplitude predicted	167

by trained ANFIS model with the experimentally obtained machining vibrations amplitude for machining Ti-6Al-4V alloy

Table 7.4 Comparison of tool flank wear predicted by trained ANFIS model with the experimentally obtained tool flank wear for machining Ti-6Al-4V alloy 170

Table 7.5 Comparison of surface roughness predicted by trained ANFIS model with the experimentally obtained surface roughness for machining Ti-6Al-4V alloy 173

LIST OF ABBREVIATIONS AND SYMBOLS

PCD	Polycrystalline Diamond
PCBN	Polycrystalline Cubic Boron Nitrite
MQL	Minimum Quantity Lubrication
OSHA	Occupational Safety and Human Administration
NDM	Near Dry Machining
OFATA	One Factor at a Time Approach
SEM	Scanning Electron Microscope
FEM	Finite Element Modelling
BUE	Built up Edge
MRR	Material Removal Rate
R_a	Average Surface Roughness
EDS	Energy Dispersive X-ray Spectroscopy
DOE	Design of Experiment
ANOVA	Analysis of Variance
RSM	Response Surface Methodology
GRA	Grey Relation Analysis
EDM	Electric Discharge Machining
DOF	Degrees of Freedom
GA	Genetic Algorithm
PSO	Particle Swarm Optimization
ANFIS	Adaptive Neuro-Fuzzy Inference System
FIS	Fuzzy Inference System
ANN	Artificial Neural Network

CHAPTER-1

INTRODUCTION

1.1 METAL CUTTING BACKGROUND

Machining operations constitute a large segment in the manufacturing sector. The selection of cutting tools and cutting conditions is an essential element in process planning for machining. Traditional machining operations like turning, milling, drilling, grinding etc., play an vital role in production systems (Rehorn et al. 2005). The quality of the surface finish and the dimensions of the machined part is having a direct influence on the health of the cutting edge. The failure of the cutting edge is the major cause of the unplanned interruption in a machining environment, which results in larger downtime (Jantunen 2002). The poor thermal conductivity of advanced materials results in high-temperature concentration at the chip-tool interface. This condition results in tool wear, as the bonding strength is weakened in the tool substrate due to abrasion and thermally related mechanisms. Most of the machining processes fail due to the improper surface integrity of the machined components which results in rough surface and cracks on the surface, especially in difficult-to-cut materials like Titanium alloys, ferrous alloys, nickel alloys and magnesium alloys etc. Nowadays, many industries are using difficult-to-cut materials for the long-term usage of the components. Therefore, it is necessary to improve the productivity of the products with reduced environmental impact and cost of the product.

The stability of the machine tool plays a predominant role during cutting process. Poor stability may develop chatter in the work-piece leading to its poor quality. Chatter vibrations are present in almost all cutting operations and are the major obstacles in achieving desired productivity. Regenerative chatter is the most detrimental effect on any process as it creates excessive vibration between the tool and the work-piece, resulting in poor surface finish, high-pitch noise and accelerated tool wear, which in turn, reduces machine tool life and reliability and safety of the machining operation. There are various techniques proposed by several researchers to predict and detect chatter where the objective is to avoid chatter occurrence in the cutting process to obtain better surface finish of the product, higher productivity and improved tool life. Generally, most of the researchers adopted two techniques for solving the problems: one in analyzing how to dampen the vibration of the parts and in turn its stability, the other in tool design so as to reduce the chatter and tool wear, to improve surface finish and tool life. The selection of the workpiece and the tool materials is very important in the machining process. Nowadays, applications of the composite materials are improving in fields of aerospace and military applications. However, this could not reduce the use of monolithic alloys for instance, like Titanium alloy in these areas. The major superior properties such as stability to resist corrosion, high thermal stability and high load-bearing capacity of these materials elevate it to be one of the superalloys. The component developed for aerospace applications requires huge material to be removed from the large blocks of material. The shaping of the material of components for aerospace applications is very difficult due to its complex physical morphology and superior surface finish requirements. The workpiece materials differ widely in their properties from initial to the plastic deformation process, to withstand stress, strain and the temperature during the machining process (Bayoumi and Xie 1995). Ti-6Al-4V alloy is a difficult-to-cut material owing to its low thermal conductivity and high chemical affinity properties, causing tool wear, and, it has main application in areas of aerospace engine parts, military applications and bio-medical applications. Therefore, it is necessary to improve its machining without compromising the quality, with reduced environmental impact and cost of production. Many non-conventional machining processes (Hasçalik and Çaydaş 2007; Li et al. 2015) were used to machine difficult to cut materials but these have a limitation in their productivity owing to lower material removal rate. For many years, machining industries are using conventional fluid cooling at the machining zone to overcome the rise in cutting temperature (El Baradie 1996a). But, it was found that flood cooling technique is unable to reduce the cutting temperature at the tool-chip interface at higher cutting speeds (Shaw 1984) and conventional cutting fluids are chemical contaminants that cause health issues, environmental problems and additional disposal cost (El Baradie 1996b). The efficiency of the heat removal process depends on the factors such as the heat transfer coefficient at the chip-tool interface (Nandy et al. 2009). There are many methods in cooling systems. For the machining operation at higher cutting speeds, cutting fluids with rust inhibitor and water-soluble oils can be used. Some chlorinated and sulphurized oils can also be used for heavier cuts at low cutting speeds. Chlorinated coolants may cause cracks during machining which may increase the shear area forming serrated chips (Campbell 2011). The conventional cooling/ flood cooling methods have their limitations at the higher cutting condition, due to improper penetration of coolant to the interface area, as coolant vaporizes at high cutting temperatures generated at cutting zone (Ezugwu 2004; Ezugwu et al. 2003).

To improve the cutting conditions using coolant, many different technologies have been developed in recent years for controlling the cutting temperature generated at the chip-tool interface, which increases the efficiency of machining and also increases tool life. To improve the efficiency of the machining process, some of the techniques like high-pressure cooling, cryogenic cooling, using of solid lubricants, minimum quantity lubrication and internal tool cooling using compressed air are some of the technologies being used (Sharma et al. 2009). Some researchers have been working on elimination or the reduction of cutting fluids with the awareness of environmental and health hazardous issues. The technique of Minimum Quantity Lubrication (MQL) is one of the methods used in less consumption of cutting fluid in the machining process. In MQL process, very small quantity of liquid lubricant is made to spray at the chip-tool interface with the help of a pneumatic pump and the compressed air pressure (Coz et al. 2012; Rahim and Sasahara 2011).

Heat generation is the biggest problem during the machining of titanium alloy due to its thermal conductivity. To improve the machinability of material, the cutting temperature developed at the cutting zone should be brought down. In addition to the application of cutting fluids, many researchers have studied on chatter vibrations like built-in active vibration damping, composite dampers, TiN top coating cutting tool, parameter tuning, change in tool geometries and cryogenic treatment. In metal cutting, at the interface of tool-chip and tool-workpiece, severe friction exists by way of the rubbing action between chip-tool and tool-workpiece regions with high normal load and cutting speed. A proper lubrication between the tool-workpiece interfaces will help in decreasing the tool wear which leads to an improvement in the surface finish of the workpiece. The lubrication may also help in cooling the tool, in turn, increasing its tool life. Research work has been carried out on the usage of cutting fluids as lubricants like holding the fluids at the tool-chip interface, cryogenic cooling, thermosyphon cooling and heat pipe cooling. Nowadays, surface texturing of the cutting tool is being studied for the control of tribological properties. Different types of texturing pattern are being tried out on the rake face of the cutting tool such as elliptical shape, micro/nano textures, parallel and perpendicular textures and micro-dimples, respectively. This texturing helped in controlling the tribological characteristics of the tool on a solid surface and resulted in the decrease of cutting force due to reduction in friction on the rake face which strongly depends on the direction of the texture.

Many conventional machining processes were used to machine Ti-6Al-4V alloy, but this material has a limitation in productivity due to low MRR and the high cutting temperatures generated during the machining. From the machining, it was clear that the efficiency of titanium alloy depends on the frictional conditions at the tool-chip interface. The use of a lubricant or coolant improves the frictional and thermal conditions. To improve the effectiveness of cooling method several technologies have been developed in recent years for the improvement in reduction of cutting temperature at the machining zone. Many types of research have been developed in the elimination or the reduction in consumption of cutting fluids with the increase of awareness in environmental and health issues. MQL is one of the best methods used for the minimum consumption of cutting fluids with a large reduction in cutting temperature. In this process, the very small quantity of fluid is sprayed or impinged to the tool-chip interface with the help of compressed air flow. Besides the external cooling of the cutting tool, some internal lubrication is also necessary for the improvement of tool life. Related to stability of machine tool during the cutting process, several researches have studied on chatter vibrations like built-in active vibration damping, composite dampers, TiN top coating cutting tool, parameter tuning, change in tool geometries and cryogenic treatment. In metal cutting, at the interface of tool-chip and tool-workpiece, severe friction exists due to the rubbing action between chip-tool and tool-workpiece with high normal load and cutting speed. A proper lubrication between the tool-workpiece interfaces will help in reducing tool wear and thus improving the surface finish of the workpiece. The lubrication may also help in cooling the tool, in turn, increasing its tool life.

1.2 TITANIUM (Ti-6Al-4V) ALLOY

The titanium alloy, especially Ti-6Al-4Valloy is the most attractive and commonly used alloy in aerospace applications. The machining of the Ti-6Al-4V alloy is not as easy when compared to other conventional materials. It is a two-phase α+β titanium alloy, in which aluminium is the alpha stabilizer and vanadium is the beta stabilizer. This high-strength alloy can be used at cryogenic temperatures up to about -427°C. Ti-6Al-4V alloy is mainly used in the annealed condition. Titanium and its alloys are extensively used in aviation and aerospace industries due to their excellent amalgamation of high strength-to-weight ratio maintained at elevated temperatures, fracture resistant characteristics, and excellent corrosion resistant properties (Guo et al. 2009; M'Saoubi et al. 2008; Wu et al. 2005). They are also progressively being used (or being considered for use) in other industrial and commercial applications, such as petroleum refining, chemical processing, surgical implantation, pulp and paper, pollution control, nuclear waste storage, food processing, electrochemical (including cathodic protection and extractive metallurgy) and marine applications. One of the attractive properties in the bio-medical application is its biological compatibility. Ti-6Al-4V alloy is recognized as difficult-cut- material, due to higher heat generation at the tool-chip interface. The main properties of the Ti-6Al-4V alloy are as follows: (i) It is well known that the higher cutting temperatures are produced during machining of a Ti-6Al-4V alloy which results in tool wear. (ii) Titanium has a strong alloying tendency or chemical reactivity with the cutting tool material at operating temperatures. This causes galling, welding, and smearing, along with rapid wear or cutting tool failure. (iii) The chatter in machining of the Ti-6Al-4V alloy is due to the low modulus of elasticity (iv) During the machining of titanium alloys, they exhibit the thermal plasticity leading to the unique characteristics of chip formation (Ezugwu 2005; Ezugwu and Wang 1997; Veiga and Davim 2013). Tables 1.1 and 1.2 show the chemical composition and mechanical properties of the Ti-6Al-4V alloy, respectively.

Table 1.1 Chemical Composition of Ti-6Al-4V alloy

Element	**Aluminium**	**Vanadium**	**Iron**	**Nitrogen**	**Oxygen**	**Carbon**	**Titanium**
Composition (% wt.)	5.5-6.76 %	3.5-4.5%	<0.25%	<0.05%	<0.2%	<0.08%	Balance

Table 1.2 Mechanical properties of Ti-6Al-4V alloy (Nouari and Makich 2013)

Mechanical Properties	**Ti-6Al-4V alloy**
Density	4.43×10^3 (g/cm^3)
Tensile elastic modulus	110 (GPa)
Tensile strength	931 (MPa)
Hardness	340 (HV)
Yield strength	862 (MPa)
Percentage of elongation	14
Thermal conductivity at 20°C	709 (W/m K^{-1})

1.3 POLYCRYSTALLINE DIAMOND (PCD) AS CUTTING TOOL INSERT

Polycrystalline Diamond (PCD) is one of the hardest materials like monocrystalline diamond and has considerable advantages. The PCD was developed by General Electric and Mega Diamond in 1960’s by a sintering process by sintering diamond grits. This sintering process made the material still harder compared to natural diamond. The PCD is made under high pressures and temperatures and requires specialized and expensive equipment. The PCD material contains significant bonding materials such as cobalt and nickel which are thermally unstable. When the PCD is subjected to high cutting temperatures that are produced during machining of hard ceramics or the drilling of hard rocks, the metallic properties catalyze the deteriorating diamond to graphite, which reduces the strength of the material. To avoid such formation of graphite, the separate reaction chamber is arranged before the sintering is done. Thus, by following this procedure, the cobalt melts at higher temperatures and forms voids at higher temperature and pressures. This melted cobalt void helps to maintain the pressures on diamond surface preventing the graphite formation. Hence, the strength of PCD is improved due to the high strength diamond-diamond bonds, produced by crystallites, which are grown at the contact points (Wilks & Wilks 1991).

The PCD which is available in different proportions and grades are suitable for machining non-ferrous metals and non-metals, respectively. The binders that are additionally added enable the intergrowth of the diamond structures, which affect the final product. The binder metals used commonly are carbides and sometimes nitrides and borides are also being used (Webzell 2007). The main aim of this process is to improve the production process and also to improve the material properties. The PCD inserts are being commonly used in the face milling of aluminium alloys and other nonferrous materials. They are also used in the machining of Si-Al alloys because of their ability to withstand higher abrasions during machining. The application of PCD has been widely spread in machining automobile parts like cylinder heads, intake manifolds and oil pump bodies. By considering the above properties of PCD i.e., high thermal conductivity, abrasion resistant, and improved tool life, it can be successfully used in the machining of titanium alloy.

1.4 TEMPERATURE ISSUES IN THE METAL CUTTING PROCESS

In the normal cutting process, the cutting tool is always subjected to the characteristic performances of cutting temperature, cutting forces and the tribological action, due to the contact at the chip-tool interface. Due to the effect of performance characteristics, the life of the cutting tool decreases which leads to dimensional inaccuracy and increased power requirements. As there is an increase in cutting temperature at the machining zone, the thermal stress on the cutting insert is increased which leads to thermal softening and results in tool wear (Zhao et al. 2002). The cutting temperatures attained are only important, as far as they affect the thermally activated mass transport phenomenon at the tool-workpiece interface. It may also involve the self-diffusion or alloy formation and may also involve the interfacial diffusion, resulting in creep or the softening of the tool material (Kuppaswamy 1996). The heat generation zones are as shown in Figure 1.1. It includes three zones namely primary zone, secondary zone and tertiary zone, respectively.

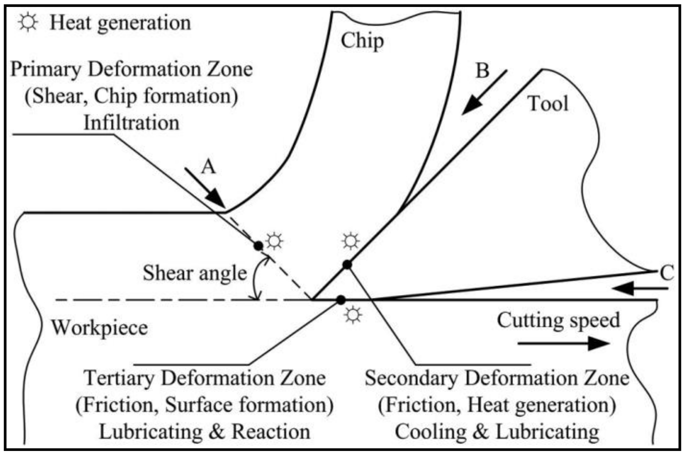
☼ Heat generation
Chip
Primary Deformation Zone
(Shear, Chip formation)
Infiltration
B
Tool
A
Shear angle
C
Workpiece
Cutting speed
Tertiary Deformation Zone
(Friction, Surface formation)
Lubricating & Reaction
Secondary Deformation Zone
(Friction, Heat generation)
Cooling & Lubricating

Figure 1.1 Heat generation zones in the metal cutting process (Yan et al. 2016)

1.5 FACTORS INFLUENCING CUTTING TEMPERATURES DURING THE CUTTING PROCESS

1.5.1 Work-material and tool-material

The machining zone temperatures are mainly affected by the thermal and mechanical properties of the work-material and tool material, respectively. The main mechanical properties such as tensile strength and hardness have the major considerations on the development of cutting temperature. In general, more heat is generated during the metal cutting process due to the chip formation process which results in higher cutting temperatures. In addition, thermal properties of work-material also affect the cutting temperature. The higher the thermal conductivity of the material, the lower is the rise in cutting temperature.

1.5.2 Cutting tool geometry

The cutting tool geometry considerably affects the cutting temperature in the machining zone. The cutting rake angle has an influence on cutting temperature as the negative rake angle requires more input energy for deformation due to the increase in contact area during machining. Similarly, the cutting temperature increases with an increase in clearance angle because as the cutting parameters are increased, the chip thickness also increases. Likewise, with the increase in nose radius, the cutting temperature also increases gradually (MacHai and Biermann 2011; Manivel and Gandhinathan 2016).

1.5.3 Selection of cutting process parameters

In the machining process, the cutting temperatures mainly depend on the process parameters such as cutting speed, feed rate and depth of cut. To some extent, cutting fluids also play a role in affecting the cutting temperature. The cutting velocity and the feed rate play an important role in the selection of cutting parameters because these are the main factors that effect the cutting temperature during machining. The process parameters are directly proportional to the cutting temperature (Kalpakjian et al. 2014; Shaw 1984).

1.5.4 Use of coolants

The main application of coolant during machining is to control the cutting temperature at the tool-workpiece interface to avoid the heat accumulation that is generated by the built-up edges in the vicinity of the cutting edge. The coolant is more likely carried away by the chips in outward flowing direction than at the machining interface. The effect of the application of cutting coolants decreases with an increase in cutting parameters in minimization of cutting temperature (Dhananchezian et al. 2011).

1.6 COOLING STRATEGIES

Turning of difficult-to-cut-materials is always concomitant with the high tool wear due to the increase in the cutting temperature. Due to the increase in cutting temperature, there is an adverse effect on cutting tool life, surface integrity and dimensional accuracy. The main aim in turning the difficult-to-cut-material is the minimization of cutting temperature with the application of cutting fluids. This application of cutting fluids helps in cooling, lubrication or the combination of both. This cutting fluid increases the tool life with a reduction in cutting temperature and improves the surface finish, eradicates the chips from machining zone (Trent and Wright 2000).

As there is a technological benefit with the use of cutting fluids, there is also a major drawback in environmental and economic problems. The cost of coolants ranges from 7% to 17% of the total machining when compared to tool cost of 2% to 4%, respectively (Klocke and Eisenblätter 1998). The obtaining and storing of cutting fluids includes the expenses and disposal of cutting fluids as they have to obey the environmental legislation such as Occupational Safety and Health Administration (OSHA) regulation (Sutherland et al. 2000) which has become stringent for the awareness on environmental and shop floor aspects. The cutting fluid will vaporize at the cutting zone during machining due to the higher cutting temperatures and forms the mist. This mist like form spreads to the atmospheric air which contaminates the surrounding area and inhalation of this lead to various diseases in labour class. This may also lead to minor skin irritation to respiratory infections and more to the carcinogenic formation. Therefore, if possible, elimination of the use of cutting fluids will be a significant economic encouragement. Due to the harmful effects and storage of cutting fluids, the manufacturing industries are being forced to implement new strategies for the reduction of cutting fluids during the machining process.

To overcome these issues with the cutting fluids, new technologies have been developed for the minimum use of cutting fluids or dry cutting. The techniques such as the use of different new tool materials, coating for tool materials, variations in the geometry of the cutting tool use of solid lubricants, surface texturing/modifications on the tool surface and the dry cutting process have been developed. The dry cutting process may eliminate the use of cutting fluid related problems such as environmental pollution and health hazardous. However, in dry machining, due to the improper cooling system, the cutting temperatures will be high and the frictional force increases with increase in the chip-tool contact area and leads to cutting tool wear (Klocke and Eisenblätter 1998). To overcome the consequences of the dry machining process, the cutting tool must be manufactured with larger rake angles to withstand the higher cutting temperatures (Sreejith and Ngoi 2000).

The cutting tool procurement with this new modifications leads to increased cost in the manufacturing process. Since dry cutting is not possible in all the processes and use of cutting fluids lead to health issues and environmental pollution, the process should be optimized so that a minimum quantity of cutting fluid is used. Several techniques have been innovated and investigated in last few decades with the application of small quantity of cutting fluid during the machining process. The most popular technique is the use of cutting fluids to alleviate the economic and environmental impacts is the Minimum

Quantity Lubrication (MQL) application. In this process very small quantity of coolant is being passed with the pressure of compressed air through the nozzle to the cutting zone interface.

1.7 MINIMUM QUANTITY LUBRICATION (MQL) TECHNIQUE

MQL process is also known as Near Dry Machining process (NDM), due to the application of cutting fluids in a small quantity with the help of compressed air which is splashed at the machining zone through the external nozzle (Machado and Wallbank 1997; Rahman et al. 2002). In MQL system, the lubrication is achieved with the help of lubricant that is passed and the cooling effect is achieved through the compressed air at the machining zone. This reduces the cutting temperature and the thermal shocks and helps in the improvisation of the surface integrity at the high tool pressures. In addition to the MQL system, it is reported that the introduction of cutting fluids through the specially designed tools with the modifications on the tool surface can bring forth better tool life. The concept of MQL in the manufacturing industry is an attractive option when compared to dry and wet machining, for the reduction in the use of cutting fluid. The main advantages of MQL are listed below:

- The concept of MQL saves time and money. For instance, as the cutting speed increases, the machining time is reduced and thereby reduction in manufacturing cost.
- Due to the use of proper lubricants, there is an improvement in the surface quality of the workpiece which promotes and enhances the product quality.
- MQL is eco-friendly due to the minimum use of cutting fluid. The environment is not much polluted and also helps in managing labour health issues.

1.8 SURFACE TEXTURING METHOD OF CUTTING TOOL INSERTS

High-speed machining technology has widely been used in metal cutting due to its remarkable advantages when compared with conventional machining such as improving productivity, decreasing thermal deformations and cutting force etc. However, when machining difficult-to-cut materials, the cutting tool life is shorter and efficiency also decreases. As a result, progressive tool wear occurs when the tool is in contact with the workpiece i.e. on the tool rake face and tool flank face. These wear processes are complex, involving both chemical and mechanical interactions between the contact surfaces which are governed by the cutting forces and the chemical composition of both tool and workpiece material, respectively (Su et al. 2014). Therefore, to improve the cutting tool life, sustainable machining techniques are getting wide acceptance due to its environmental and cost benefits. To achieve the sustainable machining system, the consumption of energy resources has to be properly monitored and optimized. The proper energy utilization can be achieved with proper monitoring and benchmarking of the energy consumption during the machining process. Nowadays, most of the manufacturing units are switching to green machining technology to reduce the use of cutting fluids and their emission of carbon to the atmosphere. Figure 1.2 shows different sustainable techniques that are tried out by the researchers recently. The characteristic of sustainable manufacturing is depicted in Figure 1.3.

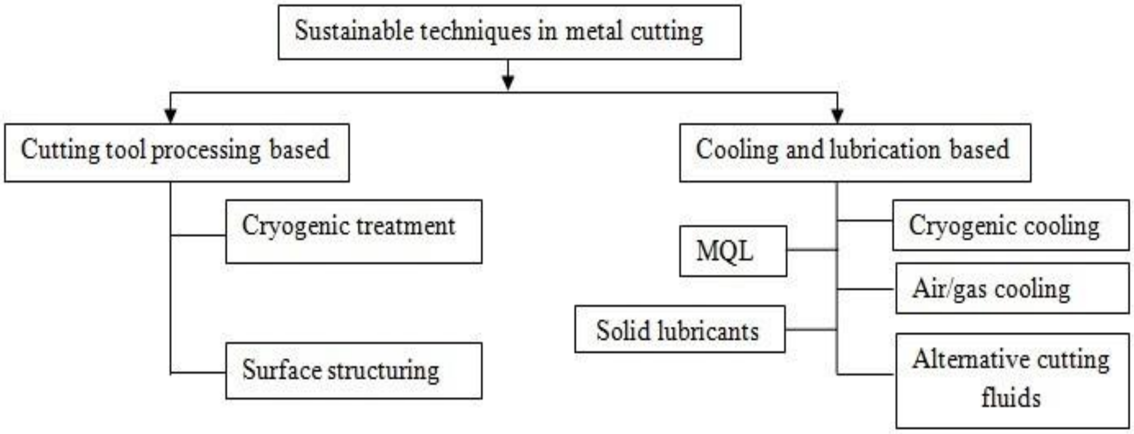
Sustainable techniques in metal cutting
Cutting tool processing based
Cooling and lubrication based
Cryogenic treatment
Surface structuring
MQL
Solid lubricants
Cryogenic cooling
Air/gas cooling
Alternative cutting fluids

Figure 1.2 Different techniques of sustainable manufacturing for cleaner production Courtesy:(Chetan et al. 2016)

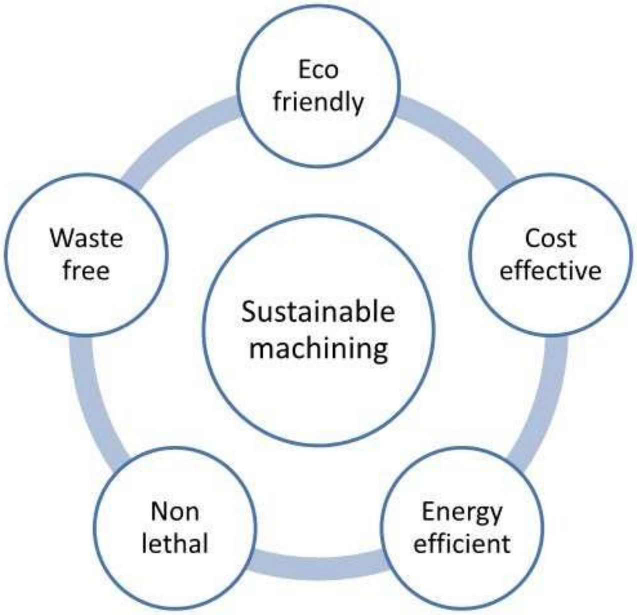

Figure 1.3 Characteristics of sustainable manufacturing Courtesy:(Chetan et al. 2016)

In recent years, surface texturing has been introduced to improve the tribological properties of lubricated surfaces. The main aim of surface texturing is to reduce the cutting tool wear, retention the lubricants and to increase the load carrying capacity. There are many machining processes for creating the micro-sized textures on the surface of the cutting tool such as lithography, electrochemical machining, electric discharge machining, photochemical machining and optical laser machining. Among these processes, the optical laser machining and electric discharge machining are found to be the advanced techniques in interacting different geometries on any of the surfaces without making any changes in the material properties. These textured surfaces also find wide applications in area of optics, microfluidic channels, acoustics and medical implants. The presence of micro-textures on the cutting tool helps in the reduction of a contact length of the chip-tool interface which in turn reduces the frictional force (Arulkirubakaran et al. 2016). This reduction in chip-tool contact length also helps in lesser tool material adhesion, thereby stabilizing the built-up edge formation resulting in an improvement in tool life.

1.9 FINITE ELEMENT MODELLING

The understanding of the fundamental mechanism of the machining process leads to proper selection of cutting tools, workpiece pattern and the selection of controllable factors without the need for lengthy and costly procedures and experimentation (Usui and Shirakashi 1982). The alternative process for the selection of machining process is the development of the mathematical model and simulating with the help of a numerical approach. One of the popular methods of numerical approach is the Finite Element Method (FEM) which is frequently used. The main aim of using FEM is to derive the prediction of the deformation process, stress-strain in the workpiece and the prediction of cutting force with the specific process parameters. Now a day's, variety of finite-element techniques are available for studying deformation during metal cutting process. It is a non-linear analysis including the re-meshing process, chip-formation mechanism, tool wear study and also the prediction of residual stress analysis (Thomas et al. 2000). In every usage of finite element process, the validation of results is validated with experimental investigations.

Many industries and research centres are looking for an alternative to understanding the metal cutting process for the improvement of quality control, setting the optimum process parameters, reduction of cost and to study the machining process. The best alternative is the finite element analysis. Many researchers have studied the application behaviours of finite element analysis to analyse the cutting temperature, stress, strain, tool wear, cutting forces and residual stresses for the improvement of the machining process. Finite element codes have been written by several researchers to solve large industrial problems in realizing the benefit of solving such problems using numerical problems. The FE codes such as Abacus, Advant Edge, third wave and DEFORM-2D and 3D are used to simulate the manufacturing process problems. DEFORM-2D and 3D are the widely used FE codes in solving the metal cutting process due to its simple and user-friendly robustness (Umbrello et al. 2007, 2008).

DEFORM-3D is a commercially available FEM tool for machining and forming processes. The metal cutting problems can be simulated using the Arbitrary Lagrangian-Eulerian (ALE) and Lagrangian techniques using DEFORM-3D. They help in finding optimum conditions than the analytical methods, with less cost and less time-consuming. The various performance parameters like stress, strain, cutting forces, cutting temperature, tool wear prediction can be graphically obtained in the software.

1.10 NEED FOR THE PRESENT STUDY

The product performance is highly impacted by the cutting tool wear, which is the natural phenomenon, observed during the machining process. The increasing demand in the manufacturing industry for higher productivity requires the use of higher cutting velocity and feed rates. Machining with higher cutting parameters inherently produces high cutting temperature, which not only reduces tool life but also reduces the product quality especially when the material is stronger and heat resistant (Dhar et al. 2006). The conventional flood cooling is not only futile but also damages the working environment by polluting with harmful gases and smokes. Machinability of the Ti-6Al-4V alloy is poor because of high strength-to-weight ratio and low thermal conductivity, which forms the serrated chips leading to tool wear with poor dimensional inaccuracy. The storage of cutting fluids and disposal of conventional coolants has many restrictions due to environmental effects in the manufacturing industries. Nowadays, devising environmental strategies is one of the biggest challenges for the manufacturing industries. To overcome these issues they are looking for many alternative cooling strategies to improve the productivity with harming the shop floor environment and human health.

Machining under MQL environment is one of the eco-friendly manufacturing processes under the green manufacturing system. In accordance with MQL machining, the surface texturing also plays a vital role in the improvement of tribological properties of the materials. There are different types of textures incorporated by different researchers to reduce the tribological properties of the materials for the improvement of productivity. Some of the texture patterns such as parallel, perpendicular micro/nano stripes, elliptical and circular shapes have been designed on the tool rake face to avoid the heat transfer. These textures were cut with the help of femtosecond laser system which does not affect any changes in material properties of the cutting tool. Most of the surface texturing techniques help in reduction of tribological properties of materials rather than cooling or lubrication. It has been proved that micro dimples and micropores filled with lubricants help in the reduction of friction and wear for sliding contact, even under high contact pressures. In an analysis of micro-pool lubrication for metal forming (Lo and Wilson 1999) showed that lubricant surrounded in the micro-holes between the tool and workpiece interface could be squeezed to the interface to reduce the friction under proper viscosity and sliding speed. Thus, it is assumed that micro-pool lubrication may also be used in metal cutting at the chip-tool interface to reduce friction and tool wear. However, very few researches have been worked with different difficult-to-cut materials like Ti-6Al-4V alloy, nickel-based alloys and superalloys using surface texturing with MQL system. Ti-6Al-4V alloy has wide applications in areas of aerospace, automobile, military and biomedical applications. So there is a necessity to carry out an extensive investigation in machining of Ti-6Al-4V alloy with micro-hole textured PCD insert. This research work focuses on lubrication of cutting inserts and explores the use of micro-hole lubrication created on the rake and flank face of the insert in different configurations. These micro-holes textured on the cutting insert are filled with lubricants and act as micro pools which help in the reduction of tool wear and friction at tool-chip contact area. It is a novel idea of improved lubrication through micro-hole surface texturing achieving good effects in tribological applications.

1.11 THESIS ORGANIZATION

To study the feasible technique for machining Ti-6Al-4V alloy with micro-hole texture PCD insert, the organization of the thesis is divided into the following chapters:

CHAPTER 1 contains brief introduction of the metal cutting process, selection of materials for machining such as Ti-6Al-4V alloy, PCD insert, cutting temperature issues, study on cooling strategies to overcome cutting temperature problems in difficult-to-cut materials, MQL machining, study of the micro-hole textured insert behavior, FEM simulation and need for the present work.

CHAPTER 2 discusses the comprehensive literature survey on the machinability of titanium alloy with their applications, and influence of process parameters. The chapter also discusses on the machining of materials with surface textured cutting tools for a reduction in tribological properties and to improve their machining performance characteristics, the literature on the effect of MQL cooling method in different machining characteristics and superalloy materials. Literature studies on finite element analysis using different software interface have also been discussed. The chapter also makes a review in the area of artificial intelligence using Adaptive Neuro-Fuzzy Inference System (ANFIS) for the prediction of performance characteristics and also includes the scope and objectives of the current research.

CHAPTER 3 elucidates the details of the selection of work material, cutting tool inserts, the specification of the tool holder, experimental methodology and the experimental designs used for turning, the development of the experimental setup for performing the experiments of research, different equipment's used to study the performance characteristics and their procedure. In the present research, the performance characteristics such as cutting temperature, cutting vibration, tool flank wear, Material Removal Rate (MRR), chip-morphology and surface integrity (surface roughness, surface topography and microhardness) are studied.

CHAPTER 4 The Taguchi design of experiment has been incorporated for the selection of number of experiments to be performed and to investigate the effect of process parameter on cutting temperature, tool flank wear and surface roughness. It also deals with the comparison between the machining of titanium alloy with commercially available PCD insert (normal insert) in dry cutting and MQL environment, respectively. Further, the FEM analysis was performed for different designs of micro-hole texture pattern on PCD insert with static analysis using ANSYS software and dynamic simulation using the DEFORM-3D software. The cutting temperature, stress, strain were predicted under simulation for comparison with experimental results.

CHAPTER 5 Studies on the effect of process parameters of turning Ti-6Al-4V alloy with modified PCD insert under MQL environment. The experiments were conducted based on one factor at a time approach (OFATA) by considering the controllable parameters such as cutting velocity, feed rate and depth of cut with normal insert, Design 1 insert and Design 2 insert, respectively, under MQL environment.

CHAPTER 6 focuses on the comparison study between the PCD and Polycrystalline Cubic Boron Nitride (PCBN) insert. The experiments were performed with OFATA approach. The machining of Ti-6Al-4V alloy with modified (Design 2) PCD and PCBN were studied to identify the better tool material selection for machining of Ti-6Al-4V alloy under MQL environment.

CHAPTER 7 presents the mathematical models developed for each response using Adaptive Neuro-Fuzzy Inference System (ANFIS) machining with modified PCD insert under MQL environment. The predicted values were compared with experimental values to know the effectiveness of the prediction system.

CHAPTER 8 contains the findings and results of current research i.e., turning of Ti-6Al-4V alloy with normal and modified inserts under MQL environment and also compared with modified PCBN insert, with final conclusions. The recommendation and directions for future work are also briefly discussed based on the obtained results and observations of the current work.

CHAPTER-2

LITERATURE REVIEW

2.1 INTRODUCTION

This chapter contains survey of literature on various aspects of issues involved in machining of Titanium alloy. Also, various optimizations and modelling techniques with their effect on machining performance characteristics while machining the difficult-to-cut material have been presented. The chapter also explains various simulation processes of metal cutting using FEM analysis, reported in literature.

2.2 MACHINABILITY OF TITANIUM ALLOY (Ti-6Al-4V)

Titanium alloys with their good strength to weight ratio, low thermal conductivity and superior corrosion resistance have recently been widely used in aerospace, biomedical and petroleum industries (Rahman et al. 2006; Wang et al. 2014b). Titanium alloy has been considered as the difficult to machine material due to its high thermal conductivity, low modulus of elasticity, high-temperature strength and high chemical reactivity (Su et al. 2006).

Properties of titanium alloys are as follows: (Ezugwu 2005; Ezugwu and Wang 1997; Veiga and Davim 2013)

- Titanium and its alloys are poor thermal conductors. As a result, the heat generated when machining titanium cannot be dissipated quickly; rather, most of the heat is concentrated on the cutting edge and tool face which leads to tool wear.
- The chemical reactivity of titanium alloy is stronger with the cutting tool material at the operating conditions. Due to this reactivity, it causes galling, smearing and

chipping of the workpiece surface. It may also cause low fatigue strength of machined surface and increase tool wear.

- Due to the low modulus of elasticity of titanium alloys, chatter may occur during machining.
- During the machining of titanium alloys, they exhibit thermal plasticity leading to the unique characteristics of chip formation. Also, the high dynamic strength during cutting process induces abrasive sawtooth edges resulting in tool notching.
- The strange work hardening characteristics of titanium alloys induce the built-up-edge in the cutting tool and increase the shearing angle, which results in the increase of bearing load.

Pramanik (2014) investigated various problems in machining of titanium alloys such as the variation in chip thickness due to the instability of the shear strength during the cutting conditions. The cutting temperature increases with the decrease in the density, due to higher thermal stress. Residual stresses are generated with the temperature gradient during cooling of huge castings of stock materials. To overcome these problems, many methods were proposed to improve the productivity of machining titanium alloys such as the application of vibration analysis kit, thermally enhanced machining, applications of coolants and hybrid machining techniques. Liang et al. (2015) investigated the possible studies on the benefit of Ni_3Al binder on WC-based cemented carbides insert in the dry turning of the Ti-6Al-4V alloy. In this study, the cutting performances and wear mechanisms were studied based on analyzing the morphologies and compositions of worn surface of coated WC insert. By this coating technique of WC-$10Ni_3Al$, the crater and flank wear were reduced and attributed to its synergistic mechanism of chemical inertness and high hardness induced due to the mechanical properties of the binder material. Çalışkan and Küçükköse (2015) studied the machining of Ti-6Al-4V alloy using a CN/TiAlN coating that was deposited on cemented carbide insert as an attempt in increasing the productivity of the alloy. The effect of the coated insert was observed on the output performances such as cutting force, chip formation and surface integrity. The results observed were that, there was improvement in tool wear resistance and tool life was improved by 15% when compared to uncoated tools. The machining of the Ti17 alloy was performed with and without high-pressure water jet assistance using uncoated WC/Co cutting tools. The effect of water pressure and cutting speed were investigated on the tool wear and cutting forces. There was a 30% improvement in the productivity of the product (Ayed et al. 2015). Dorlin et al. (2015) developed a cutting force predictive model to optimize the process parameters in the cylindrical and face turning of the Ti6Al4V alloy. The results emphasized the significance of the contact mechanism in ploughing mechanisms and also on the intensity of cutting forces. Deiab et al. (2014) motivated on implementation of cooling strategies in manufacturing cells for sustainable manufacturing practices. The use of vegetable oils in machining of Ti-6Al-4V alloy using uncoated tungsten carbide insert was proposed as a sustainable alternative than synthetic emulsions. The cooling strategies such as cryogenic cooling, dry machining, MQL and Minimum Quantity Cooled Lubrication (MQCL) were proposed. The machining of Ti-6Al-4V alloy with rapeseed vegetable oil in MQL and MQCL turns out to be a sustainable alternative. Huang et al. (2014) studied the performance of dry milling aeronautical thin-walled components of titanium alloy using two different types of tools. The two different tools were variable and uniform pitch tools in milling aeronautical thin wall component of the Ti-6Al-4V alloy. The cutting vibration performance was reduced in milling with variable pitch tool compared to uniform pitch tool. Chiappini et al. (2014) studied the mechanics of chip formation in turning of Ti-6Al-4V alloy with varying spindle speed. This variable spindle speed technique was incorporated due to which it suppresses the regenerative chatter without any malignant changes in the effect of the productivity.

The key problem associated in machining of the Ti-6Al-4V alloy is the cutting tool wear and the mechanism involved in tool failure was studied by Arrazola et al. (2009); Balažic and Kopač (2010); Bhatt et al. (2010); Jaffery and Mativenga (2009). It is very hard to machine Ti-6Al-4V alloy with the variety of available tools because of its material hardness characteristics. Therefore, harder tool materials which are available in the market are not suitable for machining Ti-6Al-4V alloy attributable to its chemical affinity that easily reacts with the base material and causes tool wear. Another reason is that it easily welds to the tool which forms the built-up edge of the chips which results in tool wear. Therefore, many investigations have been made to reduce the tool wear with the proper assistance with selection of tool material and proper machining conditions (SU et al. 2012). The common cutting tools used in the machining of the Ti-6Al-4V alloy are the high-speed steel and tungsten carbide inserts. The low thermal conductivity property of Ti-6Al-4V alloy, allows these tools to be used on in the lower cutting velocities. In machining at higher cutting velocities, it may lead to the development of higher cutting temperatures at the cutting zone resulting in tool wear. Therefore, the proper selection of cutting tools in machining of the Ti-6Al-4V alloy at higher speeds is a tedious task. Many of the researchers have worked with coated cutting tools for the betterment of the productivity. Oosthuizen et al. (2010) studied the performance of various conventional tool materials and proved that they have poor machinability features during machining of Ti-6Al-4V alloy when compared to PCD insert. Nabhani (2001) examined that the PCD cutting tool insert has the lowest wear and produce better surface finish during the machinability of titanium alloys when compared with the conventionally available tungsten carbide grades for machining of Titanium. During machining of titanium alloys, to attain the higher cutting speeds the cutting tool should suppress the heat generated at the cutting process as much as possible while dissipating it quickly. The higher thermal conductivity of the PCD tool could therefore possibly allow for high-speed machining of titanium alloys. Cherukuri and Molian (2003) found a significant enhancement in tool life during the machining of titanium alloy (Ti-6Al-4V) with PCD cutting tool when compared with the carbide tools. The important features and importance of polycrystalline diamond are the higher cutting removal rates, uniform surface finish, more uniform particle size distribution, harder/tougher particles and 300% greater than monocrystalline diamond. Hence, PCD cutting tool is the best alternative in machining of Ti-6Al-4V alloy than the conventional carbide tools. In order to achieve the machining of Ti-alloy at higher cutting speeds, the heat generated at the cutting zone should be suppressed and should dissipate quickly. In this way, the PCD cutting tool has better thermal conductivity property and can machine at higher cutting speed to achieve better dimensional accuracy (Narutaki et al. 1983). Ota et al. (2009) discovered the cutting efficiency using PCD cutting tool which is having high thermal conductivity in machining Ti-alloy. Mori et al. (1999) also initiated that PCD cutting tools have better longer tool life when compared to the carbide inserts in high-speed machining of Ti-6Al-4V alloys. Amin et al. (2007) studied the effectiveness of PCD inserts and also compared with the uncoated WC-cobalt insert in end milling of the Ti-6Al-4V alloy. The comparison was made in relevant to cutting speed, tool life with material removal, tool wear rates and the chip morphology. Hence, PCD cutting tool is ideally chosen for the investigations in machining of Ti-6Al-4V alloy in the present research.

The quality of the product mainly depends on the dimensional accuracy of the work material. The surface finish of the product is the technical estimation to evaluate the productivity of machine tools and machined components. A proper surface roughness helps in accomplishing the product creep resistance, fatigue resistance, precision fits and aesthetics requirements of components. Thus, the characterization and measuring of surface roughness is an important concept for the interpretation of the machining performance. Revankar et al. (2014) investigated the machining of Ti-6Al-4V alloy using PCD insert under different lubricating modes. The cutting performances such as surface roughness and surface hardness were measured. The results proved the substantial benefit of machining was obtained under the MQL environment. The cutting parameters had a great effect on cutting performances. The optimization technique using Taguchi method was for minimization of surface roughness in machining of Ti-6Al-4V alloy using different cutting inserts such as nano coated carbide insert (Nithyanandam et al. 2014), cermet inserts for finishing operation (Selvakumar et al. 2012) and tungsten carbide insert (Ramesh et al. 2012). The investigation was performed using response surface methodology and found that feed is the major effecting parameter on the surface roughness. Response surface methodology is mainly used as a prediction model for surface roughness in terms of the speed, feed and depth of cut in the literature (Nandy et al. 2009; Zębala et al. 2015). It was found that cutting parameters such as cutting speed and feed rate are the significant machining parameters affecting surface roughness while the effect of depth of cut is negligible. It has also been noted that higher cutting speed and lower feed rate produce better surface finish due to high temperatures. Dass and Chauhan (2011) utilized the factorial design for obtaining better cutting conditions in minimization of surface roughness. The surface roughness prediction in terms of process parameters such as cutting velocity, feed rate and depth of cut, using response surface model has been widely used in many literatures and found that feed rate and cutting speed are the main factors which are affecting the surface roughness (Chauhan and Dass 2012; Dabnun et al. 2005; Sahin and Motorcu 2004).

One of the significant phenomena during machining is machining vibrations, which significantly affect the machining process and quality of the finished product (Fang et al. 2012). Machining vibrations is a major problem during machining of Titanium alloy (Ti-6Al-4V) because of its characteristics like low elastic modulus which allow deflection of the slender workpiece under tool pressure, causing its deflection and moving away from the cutting tool. This leads to deflection, vibration and chatter thereby causing tolerance problems (Pramanik 2014; Veiga and Davim 2013). The vibration phenomena in metal cutting demonstrate the abnormalities occurring during cutting and the troubles of the machine tool itself (Song et al. 2005). The use of the sensor in tool condition monitoring has made the machining process more efficient by watching the cutting tool and process without penetrating or interrupting the operation (Bhuiyan et al. 2014). The application of Acoustic Emission (AE) in tool condition monitoring has been praised due to its high-frequency content and uninterrupted by surrounding noise. The AE is a type of transient elastic wave generated by the rapid release of energy from a localized source within the material (Ren et al. 2014). On the other hand, vibration signature has received a wide popularity in tool condition monitoring for its fast data collection and interpretation ability (Ebersbach and Peng 2008). Use of accelerometers/vibration sensors offers some extra advantages over other sensing techniques. This includes ease of implementation and the fact that no modifications to the machine tool or the workpiece fixtures are required (Chen et al. 2011).

2.3 MQL MACHINING PROCESS

The MQL system is the possible solution for the optimum lubrication system. This system is an alternative for both the dry and wet machining. The quantity of lubricant applied in MQL system is reduced to the minimum. The maximum flow rate of MQL is 60ml/hr. The prime lubrication system substantially reduces the frictional heat generated at the machining zone and also considerably reduces the machining cost (Madhukar et al. 2016). The reduction in cutting zone temperature in MQL system is due to the convection of compressed air and partial evaporation of cutting fluid (Ezugwu 2005). Various researchers have applied the use of MQL during the machining of difficult-to-cut materials to reduce the heat conducted at cutting zone in various manufacturing processes. Sarıkaya et al. (2016) performed the experimental investigation on surface roughness and tool wear in machining of superalloy Haynes 25 under the dry, wet and MQL environments. The MQL mist was applied at the cutting rake face of the insert and found that the cutting temperature was reduced significantly at the cutting zone. The MQL cooling condition showed better results in turning characteristics when compared to dry and wet machining. Kuzu et al. (2015) experimentally studied the compacted graphite iron material under the dry and MQL environment. Machining of material under the MQL system showed substantial reduction of the cutting force, tool wear and surface roughness by 5%, 10% and 25%, respectively. The reason for the improvement under MQL environment is due to the reduction of frictional force at the contact asperities. Kouam et al. (2015) investigated the effect of MQL and dry machining in turning of aluminium 7075-T6. Sharma and Sidhu (2014) succeeded in reducing the cutting temperature and low surface roughness under MQL environment when compared with the dry turning of AISI D2 steel. Due to better lubrication through MQL environment, Chinchanikar and Choudhury (2014) achieved superior tool life when compared to dry machining of hard turning using High Power Impulse Magnetron Sputtering coated carbide tools. Shokrani et al. (2012) classified Ti-6Al-4V alloy as one of the difficult to cut materials and also stressed the health and environmental issues for the use of cutting fluids with the government regulations which resulted in higher machining cost. The main problems associated with machining Ti-6Al-4V alloy is that of low thermal conductivity resulting in poor surface quality and reduction in tool life. To overcome these problems associated with cutting fluids, the environmentally conscious methods such as MQL cooling, dry cutting and cryogenic cooling were implemented. Ramana et al. (2011) studied the machining performance of Ti-6Al-4V alloy using uncoated carbide inserts with different cooling strategies and also studied the optimization process for the reduction of surface roughness. Dhar et al. (2006) investigated the performance characteristics such as cutting temperature, product quality and chip formation during machining of AISI-1040 steel with uncoated tungsten carbide insert under MQL environment and obtained beneficial results when compared to the dry machining process. From the literature, it is evident that the MQL is the suitable cooling technique in machining difficult-to-cut materials and also in agreement with government regulations without harming much, the environment and health issues.

2.4 SURFACE TEXTURING OF CUTTING TOOL INSERTS

The stability of the machine tool plays a predominant role during the cutting process. Poor stability may develop chatter in the work-piece leading to its poor quality. Chatter vibrations are present in almost all cutting operations and they are major obstacles in achieving the desired productivity. Regenerative chatter is the more detrimental to any process as it creates excessive vibration between the tool and the work-piece, resulting in a poor surface finish, high-pitch noise and accelerated tool wear which in turn reduces machine tool life, reliability and safety of the machining operation. There are various techniques proposed by several researchers to predict and detect chatter where the objective is to avoid chatter occurrence in the cutting process in order to obtain better surface finish of the product, higher productivity and tool life. Generally, most of the researchers adopted two techniques for its solution, one in analyzing how to dampen the vibration of the parts and in turn its stability, the other in tool design to reduce the chatter and tool wear, to improve surface finish and tool life. Daghini et al. (2009) identified that the use of the composite dampers for the cutting tool to damp the cutting tool vibrations has given good surface finish on the workpiece by minimizing the chatters. Harms et al. (2004) have worked on a tool adaptor with built-in active vibration damping device to dynamically stabilize the turning process for reducing the chatters. Fahad et al. (2012) investigated in their research that, the TiN topcoat appears to reduce the total contact area on the rake face, while the Al_2O_3 coating especially reduces intensity (weight per cent) of rake face material transfer and hence restricts the extent of sticking. Mahdavinejad and Saeedy (2011) quoted that, the process parameters, namely feed rate and cutting speed have substantial effects on the quality of turning operation. In improvement of surface roughness, feed rate parameter has to be minimized in contrast with increasing cutting speed. Since, at higher cutting speeds and lower feed rates, the built up edge formation decreases, results in minimum cutting forces and machine vibrations, respectively. Thakur et al. (2009) mentioned that the variation of shear angle due to cutting parameters is an effective indicator to get indirect information of the machinability indices such as cutting force, chip thickness, tool-chip contact length, temperature, etc. In the study, it was found that as the shear angle increases, thin chips are generated, and the velocity of the chips is high, resulting in the reduction of cutting forces and friction. Patil et al. (2013) explained that the cryogenic treatment increases wear resistance and has been attributed to the transformation of soft retained austenite into the harder martensitic phase, and the formation of fine carbide particles in the metal structure. These changes are the principal reasons for the dramatic improvement in wear resistance.

Coming to tool design, many researchers worked on different parameters of the tool, but not much work related to the improvement of lubrication between the interface of tool-workpiece and tool-chip is seen in the past literature. In metal cutting, at the interface of tool-chip and tool-workpiece, severe friction exists due to the rubbing action between chip- tool and tool-workpiece with high normal load and speed. Frictional heating of the cutting tool will be produced by the relative motion between contact surfaces of tool/work-piece/chip, which leads to high temperature at the interface of chip-tool and tool-workpiece. As an effect, wear increases at a faster rate due to high temperature, load and sliding speed at the interfaces, which lead to chatter on the workpiece surface. A proper lubrication between the tool-workpiece interfaces will help in reducing wear and thus improving the surface finish of the workpiece. The lubrication may also help in cooling the tool, in turn, increasing its tool life.

In the present scenario of the machine tool, the jet of water with soap solution is ejected to the interface and it may act as a coolant for the system. But generally speaking, this may act only as a coolant but does not help in lubrication. These fluids (cutting fluids) must be held between the interfaces to avoid more wear at the tooltip. Some researchers have been investigated on lubrication through the cutting tool. To depict few, Shaw (2005) explained the main objectives of using cutting fluids in machining operations and the reduction of temperature and friction in the cutting region by modes of lubrication and cooling. The cutting fluid must be introduced to the tool-chip and tool-workpiece interfaces for the action of effective lubrication, which is not possible in normal cutting speed; else the objective of cutting fluid will be restricted to cooling. Cryogenic cooling has also shown a significant reduction in friction and wear, cutting force, and cutting tool temperature, in comparison with conventional coolant (Hong et al. 2002).

Besides the external cooling of the cutting tool, some internal cooling and lubrication approaches have been attempted. Among those methods, thermosyphon cooling by Jen et al. (2007) and heat pipe cooling by Chiou et al. (2005) were reported. In a drilling application, reduction of drill tip temperature by 60% was achieved using a thermosyphon drill. In the earlier study by virtually all the above-mentioned techniques focus on cooling rather than lubrication, i.e., how to remove heat after it is generated rather than how to reduce the heat generation due to frictional sliding between interfaces.

Etsion (2004) and Wang et al. (2014a) conducted theoretical and practical investigations on the effects of laser surface texturing on the tribological performances of mechanical components including mechanical seals, piston rings and bearings. They used a laser system to create micro dimples on a regular surface pattern on a contact surface. As a result of the textured surface, significant improvement was found in the load capacity, friction coefficient and wear resistance. This micro dimple acts as a micro-hydrodynamic bearing in full/mixed lubrication or a micro-reservoir in starved lubrication.

Sugihara and Enomoto (2009) conducted a series of face milling experiments for aluminium alloys and noted that some serious problems exist in case of aluminium alloys because of their low lubricity against the cutting tool surface in deep-hole drilling, tapping and milling. To overcome this problem, tools with micro/nano-textured surface utilizing femtosecond laser technology was proposed. As a result, a cutting tool with banded micro/nano textures was developed, which improved the anti-adhesive effect and lubricity of the cutting tool. Further, they developed the DLC-coated cutting tools with the micro/nano-textured surfaces to overcome the aluminium alloy problems since chips readily and severely adhere to the cutting tool surface. The experiments were performed in dry and wet conditions to improve anti-adhesive properties. The anti-adhesive effect was not sufficiently achieved in wet cutting also. To overcome this, they developed a cutting tool with the microstrips parallel to cutting edge. This textured surface with the DLC-coating significantly improved the anti-adhesive property (Sugihara and Enomoto 2012, 2013).

Xing et al. (2014b, 2014a; 2014c) studied the surface texturing of Al_2O_3/TiC ceramic cutting tools for machining of AISI 1045 hardened steel. The pretreatment of Al_2O_3/TiC ceramic cutting tools was modified with the help of a femtosecond laser system. The morphology of the cutting tool exposed to different pulse energies was measured using the scanning electron microscope and atomic force microscope. The effect of the pulsed energy on the wear resistance was investigated with preheated tools. The results show that the cutting forces have no change in preheated tools and conventional tools. Meanwhile reduction in the cutting temperatures and increased adhesions of chips on the rake face was observed with the laser preheated tools. Further, a novel cutting tool of Al_2O_3/TiC with different coatings was developed with laser technologies for the improvement of cutting performance and wear reduction. Firstly, the Al_2O_3/TiC cutting tool was coated with WS_2/Zr and secondly, with nano-textures deposited with WS_2/Zr composite soft coatings and thirdly, filled with Molybdenum

Sulphide (MSo_2) solid lubricant. The cutting tests were conducted both on the conventional tool and the developed tool. The outcome of the results shows that the WS_2/Zr coated Al_2O_3/TiC cutting tool without nano-textures has improvement in lubricity at the tool-chip interface. The other parameters such as cutting force, cutting temperature, friction coefficient and tool wear were reduced with the nano-textured tools compared with the conventional tools.

Kawasegi et al. (2009) developed a cutting tool with different microscale or nanoscale textures on their surfaces as shown in Figure 2.1. This texturing helped in controlling the tribological characteristics of the tool on a solid surface. Turning experiments were performed on aluminium alloy under MQL environment. This texture resulted in the decrease of cutting force due to the frictional reduction on the rake face which strongly depends on the direction of the texture. Lei et al. (2009) experimentally studied the micro pool lubricated cutting tools by machining the mild steel. The micro-holes were drilled with the help of the femtosecond laser system and the stability of the tool was analyzed by using FEM analysis. This resulted in the reduction of cutting force by 10-30% with micro pool lubrication and 30% reduction in chip-tool contact length. Coiling chips were produced with no adverse effect on the tool insert performance.

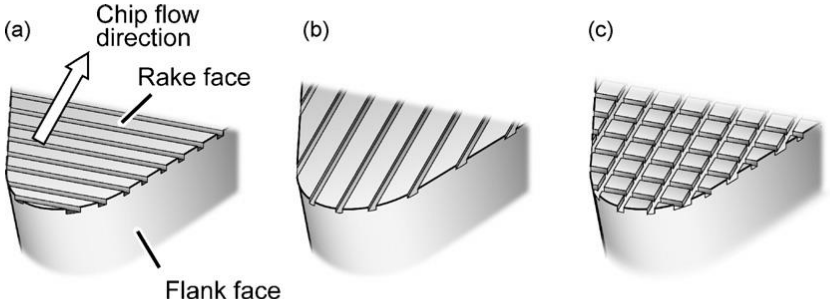

Figure 2.1 Schematic diagrams showing the direction of the texture (a) perpendicular and (b) parallel to the chip flow direction. (c) Cross-patterned texture (Kawasegi et al. 2009).

Ma and Zhu (2011) influenced the surface texture in the form of elliptical-shape dimples with different depths, diameters, area ratios, and different operation parameters on friction coefficient were investigated under the hydrodynamic lubrication condition. As a result, the optimum area ratio is independent of the operating parameters and the texture parameters. Secondly, as the optimum diameter decreases, the depth increases with the larger velocity and smaller load. Jianxin et al. (2012) performed experiments on surface textures with different geometrical characteristics on the rake face of the Tungsten carbide or Cobalt (WC/Co) carbide tools. These textured rake faces were filled with molybdenum disulfide (MoS_2) solid lubricants as shown in Figure 2.2. Dry tests were carried out with the textured tool and the conventional tool. Results prove that the elliptical grooves on the rake face filled with solid lubricant have significantly reduced in the cutting force, tool-chip interface and the friction coefficient compared with the conventional tool.

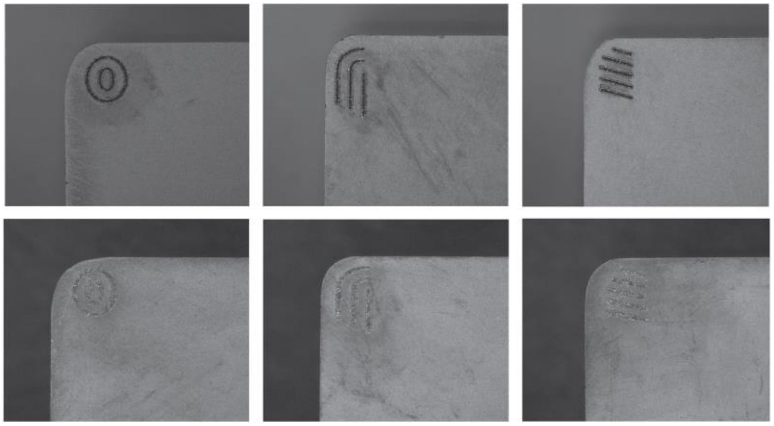

Figure 2.2 Photo of the rake-face textured tools filled with and without MoS_2 solid lubricants (Jianxin et al. 2012)

Enomoto et al. (2012) conducted experiments on steel materials since it is harder than the aluminium alloys, for the improvement of wear resistance. To overcome wear resistance problem, the previously developed textured cutting tools and the newly developed TiAlN-coated tools with the stripe-grooved surface were used on a face milling operation. Experiments were conducted with different types of textures with variation in the depth of the grooves and in parallel or orthogonal direction. Experimental results of face milling operation on the steel material improved the wear resistance with micro/nano grooves on tool surface resulted in TiAlN-coated tools of parallel edges significantly improving wear resistance and the lubricity of the cutting tool. Da Silva et al. (2013) studied the abrasive wear resistance of micro textured tools and compared those with conventional cutting tools. To compare this, square cemented carbide inserts containing the three-layered coatings (TiCN-Al_2O_3-TiN) were textured with the linear, parallel and perpendicular patterns in the chip direction. Machining test results were met with the micro-abrasion wear test to highlight the laser texturing on the cemented carbide textured tools. The textured tools with perpendicular grooves led to a significant increase in the tool life than the parallel grooves. Kümmel et al. (2015) studied that by laser surface texturing, the rake face was textured with different textures like dimples and channels for the changing of adhesion tendency of Built up Edge (BUE) on cutting tool inserts. The dimple textures on the cutting tool can best stabilize the BUE compared with non-textured cemented carbide tool with respect to the corner radius wear. The results clearly indicate that adhesion of the workpiece can be modified with the textured surface than with the non-textured cutting tools. Su et al. (2014) fabricated the microgrooves and micro-holes with different geometrical characteristics on a Polycrystalline Diamond (PCD) tools using fiber laser surface texturing. The investigations of microtextures were carried based on the effect of process parameters. As a result of this, the influence of topography and quality of microtextures can be improved with lower scanning speed and average output power with the proper process parameters.

Sharma and Pandey (2016) have reviewed on the recent advances in textured tools. They have discussed various patterns, either on rake face or flank face, which have resulted in the decrease of the cutting forces, temperatures and improved wear resistance properties. The main aim of this review was to provide meticulous information on a recently developed topic such as sustainable manufacturing by using the textured tools in turning operation. Li et al. (2016) demonstrate the application of micro-electro-discharge machining with high-frequency vibration in machining linear micro-grooves and micro-holes in a straight line on WC/8% Co (MA) and WC/15% TiC/ 6%Co (MB) cemented carbide cutting tool rake face or scrap reeling slot as shown in Figure 2.3. Results showed the accumulation of debris were reduced and the wear resistance was improved.

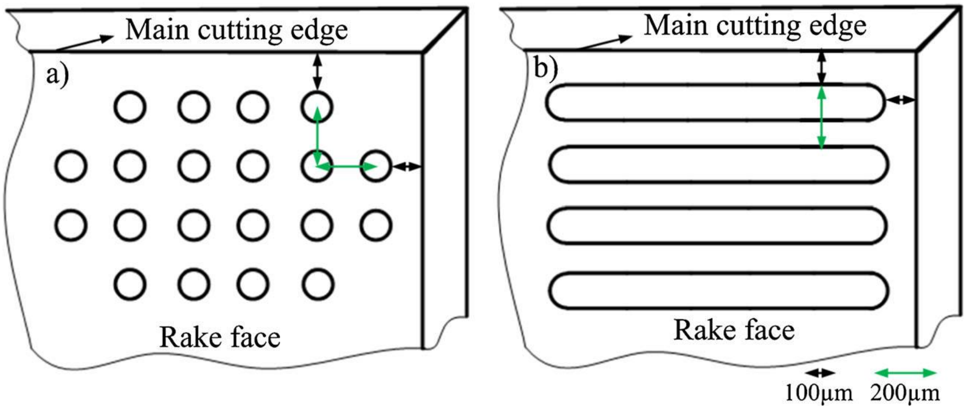

Figure 2.3 Distribution of surface textures on cutting tool rake face (a) Distribution of straight holes (b) Distribution of linear grooves (Li et al. 2016)

Jesudass and Kalaichelvan (2018) performed the experiments on steel and aluminium to study the performance of micro-textured high-speed machining inserts. The surface textures were performed with the help of Rockwell hardness tester, Vickers hardness tester and scratching with the diamond press on a single point cutting tool as shown in Figure 2.4. The experiments were performed with the commercially available tool and with a micro-textured tool for comparison with varying speed feed and depth of cut. The results showed the reduction in cutting temperature, the force with textured tools compared to non-textured tools. Niketh and Samuel (2018) investigated the effectiveness of micro-textured tools in drilling application for sustainable machining of the Ti-6Al-4V alloy. The micro-textures have been created on both the flute and margin side of drill bits for the first time. The experimental results of drilling with micro-textures evidenced that it is the feasible technique for the minimization of energy losses since there is a reduction in frictional force during the cutting regime of the Ti-6Al-4V alloy. Hao et al. (2018) developed a new technology for the improvement in the anti-adhesive property of cutting tool by micro-textures on the cutting tool surface with composite lyophilic/lyophobic wettability technique on the PCD insert in machining of the Ti-6Al-4V alloy. The micro-textures were produced with the help of a fiber laser system. As a result, the PCD insert with lyophilic/lyophobic wettability's composite material reduced the frictional force and tool wear compared to un-textured and micro-grooved tools. This new technology with different micro-textures on cutting tool provides a new way in the enhancement of cutting performances and mitigates the tool wear.

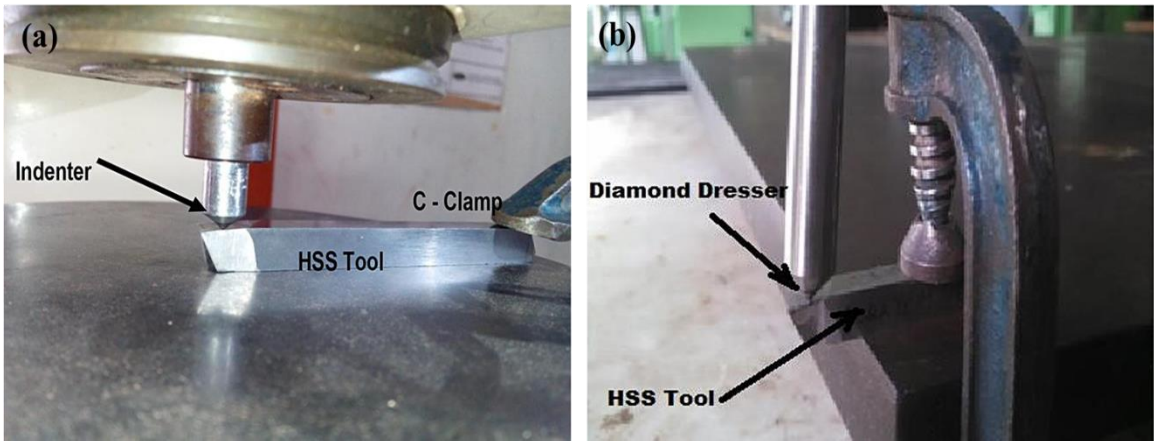

Figure 2.4 Fabrication of surface texturing (a) using Rockwell hardness tester (b) by scratching using diamond dresser (Jesudass and Kalaichelvan 2018)

2.5 FINITE ELEMENT ANALYSIS OF THE TURNING PROCESS

The turning process is the nonlinear problem, in which the local deformation, material nonlinearities and unknown boundary conditions are involved in the contact area. The experimental method to study this process is time-consuming and expensive because of the wide range of parameters involved such as materials, cutting conditions, tool geometry etc. The alternative to overcome this is the development of mathematical models. Among the many numerical techniques, Finite Element Method (FEM) is the best suitable method used for solving these numerical problems. The machining study is quite tedious since it involves many metallurgical and physical properties on materials, elasticity, heat transfer, plasticity and lubrication. Many academicians and researchers have used the finite element as an alternate method in studying machining processes such as cutting forces, cutting temperatures, residual stress and strain, deformation and chip formation for the improvement in the productivity. Vijay Sekar and Pradeep Kumar (2011) studied the machining performance of machining of Ti-6Al-4V alloy using finite element method. In this study, they had used four different Johnson-Cook (JC) material model equations for the investigation of the deformation process using the DEFORM-3D software. The prediction results proved the excellent correlation in terms of stress, strain, cutting temperature and some deviations in measuring cutting force and chip-formation. The results were compared with experimental values. Zhang et al. (2015) implemented the different JC material models for the better selection of parameters in machining of the Ti-6Al-4V alloy. They used two different JC material models with three different cutting models. The cutting models with different formulations were based on Lagrangian, Couple Lagrangian-Eulerian (CEL) and Arbitrary Eulerian-Lagrangian (ALE). The performance characteristics measured were chip compression ratio, chip geometry, plastic deformation and cutting temperature distributions. Ma et al. (2015) studied the assessment of micro-grooved WC-Co insert in machining of AISI1045 steel using the ADVANTEDGE finite element simulation. The effects were observed in terms of chip-formation, thrust force and chip-tool contact length. The micro-grooves were examined with different groove width, depth and the edge distance. The results were compared with the non-grooved tools. Ma et al. (2015) investigated the micro-bump WC-Co insert in machining of AISI-1045 steel using ADVANTEDGE software. They studied the effect of the micro-bump textured insert with the non-textured insert. The micro-bump insert simulation is as shown in Figure 2.5. It was found that micro-bumps on rake face had a reduction in cutting force and consequently in lowering of energy consumption. The results were compared with experimental values.

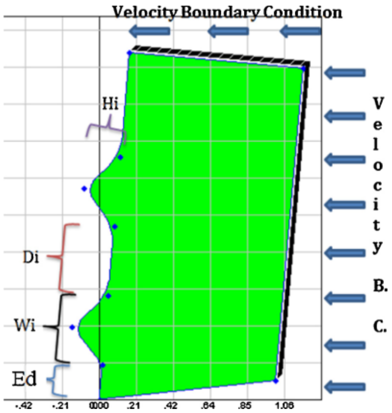

Figure 2.5 Simulation of the micro-bump textured insert using ADVANTEDGE (Ma et al. 2014)

Wu et al. (2016) developed three different pulsating heat pipes for self-lubrication of cutting tools with four, six and eight turns. The simulation was based on a 3D thermal model using the ABAQUS 6.12 software interface. The main purpose of this research was to eradicate the ill effects caused by cutting fluids and shifting towards sustainable manufacturing. Ali et al. (2012) carried machining modelling of Ti-6Al-4V alloy in milling operation to predict the reaction force, pressure and stress concentration in the high-speed milling process. The finite element modelling helps in reduction of manufacturing cost and also helps in the improvement of tool life using suitable cutting parameters. Srivastava et al. (2011) studied the high-speed machining of Ti-6Al-4V alloy using the super-finished cutting edge generated using micro-machining process. The chip-tool contact length was obtained analytically and also measured using the cutting force. The cutting forces and chip-morphology were predicted with the FEM using the ABAQUS software. This helped in the improvement of the super-finished tool in the betterment of tool-life.

Bragov et al. (2009) combined the experimental and theoretical approach to study the high strain rate behaviour and the failure of the Ti-6Al-4V alloy. The modified Gurson’s plasticity model was suggested since it considers the dependence on the type of loading. The material model values such as compressive and tensile test parameters were obtained using the split-Hopkinson test. Hua and Shivpuri (2004) studied the prediction of chip-morphology and segmentation of Ti-6Al-4V alloy using implicit, Lagrangian, non-isothermal rigid-viscoplastic FEM in orthogonal machining. DEFORM-2D software was used to study the chip-formation behaviour and their segmentation process. Ceretti et al. (1996) used the DEFORM-3D software to study the cutting operations in orthogonal and oblique cutting operation. Ezilarasan et al. (2014) explored the cutting simulation process in machining of Nimonic C-263 superalloy using carbide inserts. The DEFORM-3D was used as a software interface in the simulation process. Zębala and Słodki (2013) implemented the finite element model to study the chip breakers in machining of difficult-to-cut material Inconel 718. The algorithm was built to study the chip breakers mechanism and also observed the temperature distribution during the machining process. Arrazola et al. (2014) studied the machining of Inconel 718 with 3D finite element method based simulation and also compared the residual stress values with the experimentation. Attanasio et al. (2010) developed tool wear model and tool geometry in machining of AISI 1045 steel using ISO P40 carbide with FEM simulation using the DEFORM-3D software. The FEM model was utilized to study the influence of tool wear and the stresses at the tool rake face. Lorentzon et al. (2009) and Lorentzon and Järvstråt (2008) studied the chip formation mechanism and developed a tool wear model in the simulation process on machining of Inconel 718. They had proved that advanced friction model is most important than the Coulomb's friction model in the prediction of tool wear. They also observed that the chips obtained during machining below 50 m/min produced were long and continuous whereas the chips obtained at machining above 100 m/min were segmented with built-up-edge.

2.6 MODELLING AND OPTIMIZATION TECHNIQUES FOR MACHINING WITH NORMAL AND MODIFIED PCD INSERT UNDER DIFFERENT COOLING ENVIRONMENTS

2.6.1 Design of Experiment using Taguchi method

Design of Experiment (DOE) is the best analytical, economic and statistical tool for conducting the experiments in any machining processes. Instead of trial and error method, many parameters with their variables can be studied at the same time with these efficient design charts (Montgomery 2017). DOE is the best method for the experimental plan so that any number of factors or parameters can be analyzed and the optimized results can be obtained. The analysis is made with help of a software application known as MINITAB with new versions. To understand the effect of each and every parameter the Analysis of Variance (ANOVA) need to be performed. From this ANOVA test, the effect of the contribution of each parameter on the performance index can be obtained. After defining the effects and contributions of the parameters, next is to optimize, that is to know the levels of process parameters in the best possible response. The performance characteristics capability is dependent on process parameters and effect of noise factors through a nonlinear function. The main objective of the system is to study the nonlinearity of the robust design that would result in a small variation in the value of the quality characteristics around the desired value (Phadke 1995). The block diagram is as shown in Figure 2.6, respectively.

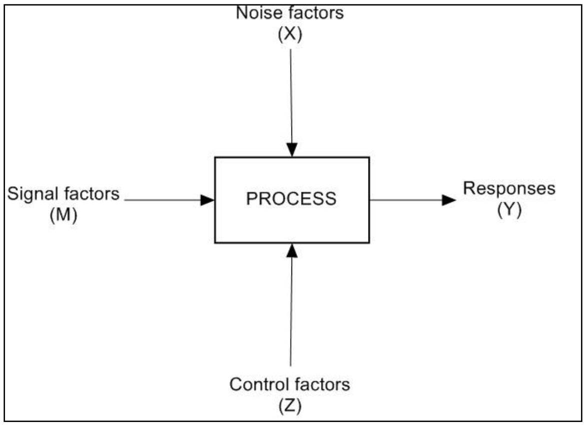

Figure 2.6 Block diagram of the process (Montgomery 2017)

The P-diagram or process diagram consists of the control factors, signal factors, noise factors and the response variable. The output response variable is represented by the letter ‘Y’ which represents the quality characteristics. The other factors which influence the number of parameters are divided into three classes:

Noise Factors (X): Certain parameters that are functioning involuntarily are known as Noise factors. Those parameters which are difficult to control or which are expensive in controlling their levels are also called as noise factors. The change in the noise factor level can be observed at different environments, different units and also with variation in time. The noise factors with statistical characteristics such as mean and variance can be specified but the actual values in preferred situation cannot be known. The major quality loss is due to the deviation in ‘y’ response specified by the signal factor ‘S’ is caused due to the noise factors.

Signal Factors (M): It is the parameter that is set by the operators to express the actual projected value of the product. For example, setting of the speed in Table fan for specifying the amount of breeze is a signal factor and also the specification of angle in steering wheel during turning of an automobile is also the function of signal factor. Other examples are in a digital communication as data is transmitted between 0 and 1 bits of signal factor and the photocopying of the original document using a printing. The design engineer selects the signal factors based on his knowledge depending upon the product that is being manufactured.

Control Factors (Z): These parameters are freely specified by the designer, since it is his responsibility to determine the best values of the specified parameters. Each control factors can be set with multiple values known as levels and these levels of certain control parameters can be changed which do not affect in the manufacturing cost. However, when the levels of all other parameters are changed, the manufacturing cost also changes. The Control factors that affect manufacturing cost are called tolerance factors, whereas the other control factors will simply be called control factors.

The Taguchi method was developed by a Japanese statistician Dr Genichi Taguchi. He developed this technique to improve the quality of the process characteristics of the production processes. This pioneering technique with fractional factorial designs helps in the optimization of the process with the minimum number of experiments. Hence, the Taguchi method has been used worldwide in engineering field successfully (Ross 1996). The experimentations that have been processed based on conventional designs are a tedious process and time to consume with a large number of data. To overcome this drawback, the Taguchi method is designed with orthogonal arrays which help in the selection of arrays based on the process parameters with a minimum number of experiments (Taguchi 1986). The product quality is termed in terms of quality loss function in Taguchi’s method. The loss function is the square of deviation of the performance characteristics. Taguchi has utilized the Signal-to-Noise ratio (S/N) as the choice of quality characteristics. This S/N ratio value is been used instead of standard deviation due to the decrease in the mean values because the standard deviation decreases with a decrease in mean values and vice-versa. Therefore, many researchers have been using the Taguchi method for optimizing the single objective functions in any machining processes of manufacturing industries.

Senthilkumar et al. (2014) used the Taguchi method for the minimization of the cutting performance such as tool wear and surface roughness, respectively in machining of hardened steel alloy. The 53.86% and 15.95% of the reduction in tool wear and surface roughness were observed in machining hardened steel and also by performing ANOVA it was observed that tool insert shape is also one of the most effecting parameters during machining. Debnath et al. (2016) optimized the performance factors such as tool wear and surface roughness under MQL environment using the Taguchi Technique in turning the mild steel. By the ANOVA test it was observed that feed rate is the most influencing parameter followed by cutting speed on surface roughness and tool wear. Ravi Kumar and Kulkarni (2017) analyzed the hard turning of titanium alloy using the Taguchi method. The L_9 orthogonal array was selected as an experimental plan. The experimentation was performed on a CNC machine and the objective is to optimize the cutting parameter and to minimize the surface roughness and tool wear. Prashanth and Krishnaraj (2017) studied the optimization of titanium alloy under the transient cutting speed. The machining parameters such as cutting speed on tool life, the flow rate of the coolant and surface roughness were discussed. Signal to noise ratio and the orthogonal array are employed for the optimization of titanium alloy using the Taguchi method. Pradeep Kumar and Thirumurugan (2012) described the comprehensive study in end milling of titanium alloy. The investigations were performed in obtaining the optimized process parameters in minimizing the tool to reduce machining cost and to improve the surface finish of the product quality. The optimization of end milling process was performed using the Taguchi method. Ren et al. (2015) studied the multi-objective optimization method for the end milling of Ti-5Al-5Mo-5V-1Cr-1Fe alloy using the Taguchi method and grey relation analysis. The Taguchi method was optimized using the signal-to-noise ratio. Further, the single optimized parameters were converted to multi-objective optimization. The results proved the importance of cutting parameters that influencing the performance characteristics. Revuru et al. (2018) studied the sustainable lubricants in machining of the Ti-6Al-4V alloy. Soybean oil-based lubricant was used as a lubricant under MQL environment. Five different conditions such as dry, cutting fluid with and without micro-graphite and soybean oil with and without graphite were investigated. The cutting performances such as surface roughness, tool wear and cutting force were measured during machining and optimized using the Taguchi method. The ANOVA test was carried out to check the effects of the contribution of each parameter during the machining process under different lubricating conditions.

2.6.2 A PREDICTION MODEL USING ADAPTIVE NEURO-FUZZY INFERENCE SYSTEM

Adaptive Neuro-fuzzy Inference Systems (ANFIS) is becoming popular in the modern machining world due to its capability to model and to epitomize fuzziness in the day-to-day activities. The design of a control system model is characterized by rigorous performance and sturdiness requirements and depends on the model-based methods. Many systems are not responsive to the conventional models due to the nonlinearity in behaviour and lack of knowledge of the process to study (Rowe et al. 1996). Nonlinear identification is, therefore, becoming the important tool for improvement in the control system which is a time-saving and cost-effective tool. Among different methods, fuzzy logic has become the most gradually establishing technique. Adaptive control is a technique for designing a controller with adjustable parameters and embedded with the adjusting of parameters. To control the system online, the adaptive strategies have been applied. The ANFIS system was first proposed by Jang in 1993. During the proposed time it was named as Adaptive Network Fuzzy Inference system and later changed to Adaptive Neuro-Fuzzy Inference system. This system is built on the basis of IF-THEN rules and proper selection of membership functions. This system consists of a neural network as well as fuzzy logic basics. The block diagram of ANFIS is as shown in Figure 2.7.

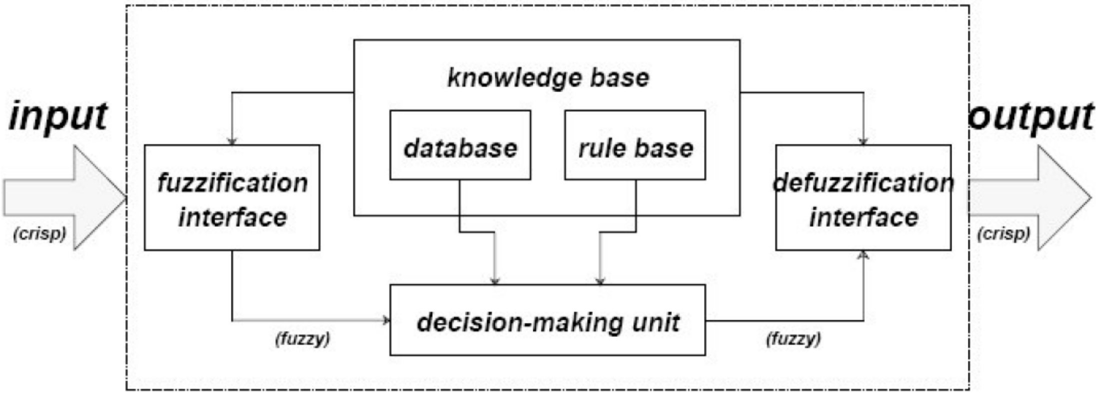

Figure 2.7 Block diagram for representation of ANFIS structure

Kovac et al. (2013) examined the machining parameter that is influencing the surface finish in face milling operation. They implemented new regression models and fuzzy logic techniques for prediction of surface roughness. From the results, it was observed that the accuracy of the prediction was improved in the fuzzy logic system when compared with the conventional regression system. Sarkheyli et al. (2015) processed a new hybrid technique attached to the ANFIS and modified genetic algorithm, to model a relationship between the process parameters and cutting performance, related to wire electrical discharge machining process parameters. The performance characteristics such as surface roughness and material removal rate were predicted. The results were compared with ANN and ANFIS-GA. From the statistical analysis, it was proved that ANFIS-MGA had better accuracy in enhancing the optimal solution. Palanisamy and Senthil (2017) investigated in the machining of 15-4 PH SS under a cryogenic environment with uncoated WC insert. For the prediction of output parameters such as cutting force and surface roughness, an artificial intelligence model using ANFIS has been developed to compare the experimental results with predicted values. Çaydaş et al. (2009) reconnoitred the application of ANFIS model to predict the surface roughness of machined surface roughness. Maher et al. (2015) evolved the use of ANFIS model to predict the surface finish in CNC machining process and concluded that developed ANFIS model helped in predicting better accuracy. Harsha et al. (2018) with the intention to reduce the machining cost by reducing the tool wear and surface roughness in machining of Ti-6Al-4V alloy used various techniques such as artificial neural network and ANFIS in this investigation. They concluded that ANFIS had a superiority effect when compared with the neural network in prediction accuracy.

2.7 SUMMARY OF THE LITERATURE REVIEW

- The traditional cooling technique has a disadvantage during machining process since it could not reduce the cutting temperature at the machining zone in the high-speed machining process. It also harms the working environment by polluting with harmful gases that are released, affecting the labour health and also disposal of the used cutting fluids is one of the biggest issues which increase machining cost.
- The possibility of dry machining processes was proposed which was inactive in avoiding the BUE formation on the cutting tool which leads in the severe tool wear and reduces the efficiency of the product.
- The MQL technique of cooling strategy has better influence in the machining process when compared to dry machining. The MQL system reduced the cutting temperature in the machining zone and helped in the improvement of the surface roughness and reduced the tool wear, which helped in the improvement of tool life and reduced the machining cost.
- Different cutting tools are available in the market for the machining of the Ti-6Al-4V alloy. But all the material available does not hold good for the machining due to their material properties and high strength to weight ratio. The different coating technologies are also applied to improve the wear resistance properties.
- In addition to different cooling strategies, many other internal cooling techniques have come into existence for the reduction of cutting temperature in the machining zone. The techniques such as thermosyphon cooling, modifications in the cutting tools, surface texturing on cutting tool rake and flank face etc.,

- The cutting tool with different surface textures leads to reduction in tribological properties and also reduces the cutting temperature which in turn reduces the tool wear and improves the surface roughness of the machined material.
- The different surface textures such as elliptical shape, parallel and perpendicular micro/nano-stripes and also micro dimples and micro bumps were produced on the tool rake face with different micro-machining techniques such as femtosecond laser machining and electrical discharge machining etc.
- To evaluate the surface textures patterns on cutting tools, several analytical, numerical and computational analysis have been performed. The best-suited method is the numerical approach with the finite element simulations. The finite element simulations are solved based on the materials physical and thermal properties.
- There are many techniques available for the optimization and prediction of the process parameters. Many techniques, either conventional or artificial techniques have been implemented to verify the optimized parameters in the machining process.

2.8 MOTIVATION FROM THE LITERATURE REVIEW

Nowadays, the trend is towards developing sustainable manufacturing processes, due to the severe government regulations over the usage of cutting fluid. The surface texturing of cutting tool insert is one of the leading internal cooling techniques because of its environmental clean machining and also the non-toxic nature of not harming the working environment. From the literature, it was found that surface texturing of cutting tool insert with cooling strategies had many advantages like proper cooling system with less consumption of cutting fluid, reduced wastage in coolant and reduction of cutting temperature due to localization of heat generated at cutting zone. In the available literature, many researches have focused on machining of difficult-to-cut alloys with different texture patterns. Hence, the present research has focused on surface texturing machining under MQL environment, with different arrangements of hole patterns. From the previous reviews, it was found that MQL cooling strategy has helped in improvement in the dimensional accuracy with improvement in wear resistance properties of the cutting tool. So this cooling effect with surface textured cutting tool under the MQL environment predominantly increases the turning performances greatly. In the current research, a micro-hole textured insert with different micro-hole orientations and sizes is implemented to study the effect of process parameters on machining performances.

However, very few researchers have worked with the difficult-to-cut materials such as superalloys, steels and smart materials by using the surface textured cutting inserts under the MQL environment. Ti-6Al-4V alloy is one of widely used difficult to cut material superalloy in areas of aerospace, military, automobile and bio-medical implants due to its low density and high strength to weight ratio and also has excellent non-corrosive property. Since the Ti-6Al-4V alloy has many key applications, there is a necessity in studying its machining properties with different techniques for the improvement in product quality with minimum machining cost. From the literature, it is observed that very few research works have been made to observe the effects of process parameters on cutting performance in machining of Ti-6Al-4V alloy, especially using micro-hole textured PCD insert under MQL environment. It is evident from reviews that machining using PCD inserts is the best alternative due to its higher tool life, and higher thermal conductivity property, and also economical. Hence, the current work focuses on the machining of Ti-6Al-4V alloy with different micro-hole textured PCD inserts. There is hardly any research finding related to dynamic analysis of machining a superalloys like Ti-6Al-4V with the help of modified insert using an analytical software (in this case DEFORM-3D) . The current work also focuses on performance characteristics such as cutting temperature, machining vibrations, tool flank wear and surface integrity which includes surface roughness measurement, surface topography and micro-hardness and comparison with the different designs and also different tool materials with micro-hole and non-textured inserts.

It is also important for the correlation of the process parameters on performance characteristics, by implementing different models to improve the product quality and also to minimize the manufacturing cost. In the literature, no attempt has been made in modelling and optimizing the turning process of Ti-6Al-4V alloy using the micro-hole textured insert under the MQL environment.

2.9 OBJECTIVES OF THE CURRENT RESEARCH

The objectives of the current research are as follows:

- Modification of the rake and flank faces of the PCD cutting insert for the machining of Ti-6Al-4V alloy.
- Carrying out dynamic analysis of the machining of Ti-6Al-4V alloy with modified inserts, using 3-Dimensional analysis.
- Comparative study of the effect of MQL on different machining parameters, during machining with normal insert and modified inserts for machining Ti-6Al-4V alloy.
- To determine the optimum cutting conditions for single response optimization for achieving better turning performance characteristics.
- Comparative studies on the performance factors for modified PCD and PCBN inserts during machining.
- Developing a Neuro-Fuzzy simulation strategy for effective decision making.

2.10 THE SCOPE OF THE PRESENT RESEARCH

- The experimental setup was developed with the external MQL setup connected to CNC turning lathe and cutting vibration measuring device such as accelerometers were mounted on the tool holder.
- Different designs of the micro-hole textured surface were created with variations in orientation and dimensions of micro-holes. Further for the validation of patterns, static simulations were performed using ANSYS 16.0 and the dynamic simulations were performed with the help of DEFORM-3D 10.0 software.

- From the static and dynamic simulations, best micro-hole designs were selected and the experimentation was carried out with measuring the cutting performances such as cutting temperature, machining vibrations, tool flank wear, chip-morphology and surface integrity. These experiments with PCD micro-hole textured inserts were compared with normal commercially available PCD insert.
- The Taguchi L9 orthogonal array was opted for the experimental trials to study the comparison between the dry environment and MQL environment machining. ANOVA test was conducted to study the levels of process parameters selected machining of Ti-6Al-4V alloy using PCD insert.
- One parameter at a time approach experimental design has been considered to investigate turning performance of the modified and normal PCD inserts under MQL environment.
- Further, to prove the importance of modified PCD insert, the comparison study with modified PCBN insert is performed using the one factor at a time approach.
- Prediction system using ANFIS model has been developed to validate the experimental results. The Taguchi L_{27} orthogonal array is considered for development of correlation models between input parameters and output responses.

CHAPTER-3

EXPERIMENTAL METHODOLOGY

This chapter presents details about the experimental procedure and the experimental setup for turning Ti-6Al-4V alloy. Information about different equipments used for measuring the performance characteristics, selection of process parameters selection are also presented here. The performances parameters namely, cutting temperature, machining vibrations, tool flank wear, chip morphology and surface integrity (surface roughness, surface topography and microhardness) have been considered in the present research as the main characteristics of turning experiments.

3.1 SELECTION OF WORK MATERIAL

There are many titanium alloys available in the market. In the present work, Ti-6Al-4V alloy of aerospace grade 5 with the combination of (α+β) phases is selected as the work material. The emerging applications of the Ti-6Al-4V alloy are in the field of aerospace industry, automobile industry, military applications and bio-medical implants due to the outstanding properties like high corrosion resistance, high hardenability with a low modulus of elasticity and density (Ezugwu and Wang 1997; Rahman et al. 2003). The chemical composition and microstructure of Ti-6Al-4V alloy are described in Figure 3.1. The machined samples were first polished to mirror finish using the emery paper of different grades and polished with diamond paste. The specimen was swabbed to 20 seconds in a Kroll’s reagent (distilled water 92ml+Nitric acid 6ml+Hydrofluric acid 2ml) to reveal the microstructure of Ti-6Al-4V alloy. Further, the specimen was observed under a Scanning Electron Microscope (SEM) for evaluation of microstructure and the Energy Dispersive X-ray Spectroscopy (EDAX) was used to evaluate the chemical composition of the Ti-6Al-4V alloy. The chemical composition and the mechanical properties of Ti-6Al-4V alloy specimen that is used in present research are shown in Table 3.1 and 3.2, respectively. These machinability characteristics of the Ti-6Al-4V alloy make it very attractive in the field of automotive and aerospace applications. The main disadvantage of this material is it lacks in the surface quality due to the built-up-edge formation in chips leading to tool wear.

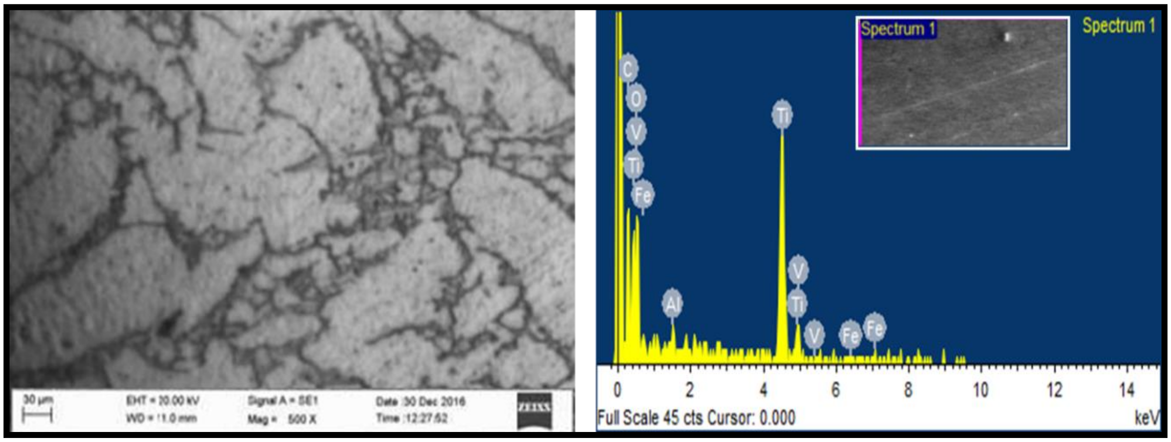

Figure 3.1 Microstructure and elemental analysis of Ti-6Al-4V alloy workpiece

Table 3.1 Chemical composition of Ti-6Al-4V alloy (wt. %) used in the present research

Element	Aluminium	Vanadium	Carbon	Iron	Oxygen	Nitrogen	Hydrogen	Titanium
Weight (%)	6.2	4.1	0.05	0.19	0.13	0.01	0.02	Bal

Table 3.2 Mechanical Properties of Ti-6Al-4V alloy

Element Property	**Metric Units**
Density	4.51 g/cm^3
Modulus of elasticity	113.8 GPa
Ultimate Tensile Strength	955 MPa
Hardness, Vickers	340 HV
Poisson’s ratio	0.34

3.2 DIFFERENT COOLING ENVIRONMENTS AND EXPERIMENTAL SETUP

3.2.1 MQL Cooling

Different lubrication systems are employed to regulate the cutting temperature at machining zone to obtain better surface finish. In the present research, the MQL system has been utilized which is one of the low-cost external coolant systems. The cooling system consists of mist lubricant made to flow through the nozzle to the tool-chip interface as shown in Figure 3.2. Dropco made DAOML-2/PS/FS/1 MQL machining setup has been used in the present research. The oil in the tank is pressurized with the compressed air to obtain the splash mist at cutting zone interface through the nozzle. The diameter of the nozzle orifice is about 1mm and the delivery pressure is maintained upto 4 kgf/cm^2. Coconut oil (density 925 kg/m^3 and viscosity 28.58mm^2/sec) has been used as cutting fluid in this work because of its thermal and oxidative stability which is higher than that of other vegetable-based cutting fluids used in machining industries. Vardhaman et al. (2018) evaluated the effect of lubricants on friction coefficient, chip-morphology, tool wear and surface quality using the dry machining and MQL machining with the use of coconut oil as a lubricant. The wettability property of coconut oil had good absorption in the machining zone resulting with minimum friction and reduction in tool wear.

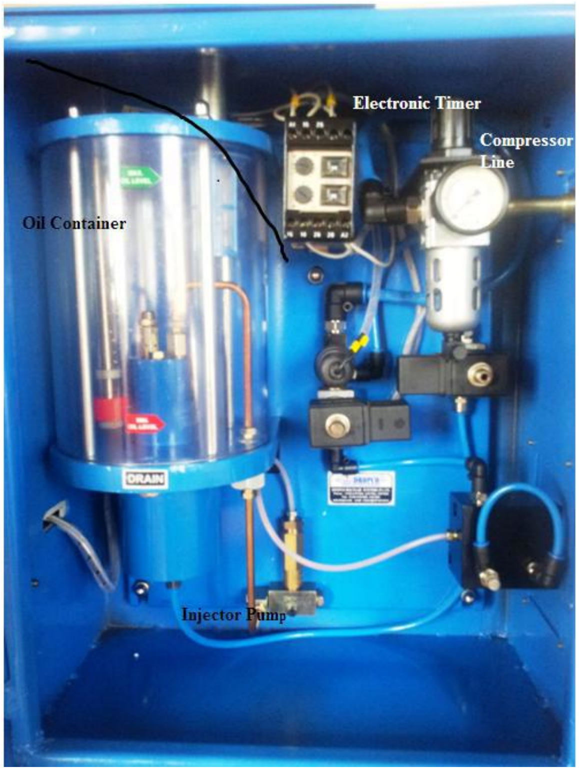

Figure 3.2 Minimum Quantity Lubrication Systems

3.2.2 Construction of MQL machining setup

The MQL system consists of the following components such as a compressor, oil reservoir, an outlet nozzle, timer and a pneumatic pump. The schematic representation of the MQL system is as shown in Figure 3.3. The oil reservoir is of 2liters capacity which is connected to the pneumatic pump to inject the oil. A filter regulator is fitted in the airline to regulate the flow of air and oil mixture and oil filter to filter the oil with 149 micron. A pressure switch is used to maintain the air pressure and a solenoid is used for the working of the pneumatic pump and to control both the oil and airline in the system. To regulate the frequency pump, an electronic timer B1DCA-X was used, which is having an adaptable time range from 0.6 seconds to 60 minutes with 8 ranges. The discharge rate from the pump is 0.40cc/stroke. Anticipated discharge can be obtained by adjusting the duration of stroke and interval between 2 strokes. There is a provision in the form of a transferrable fixture at the spindle centre to attach the nozzle. The nozzle will be attached to the portable fixture located at the spindle centre. This flexibility in design makes it easy to place the injection nozzle at any preferred position throughout the machining process.

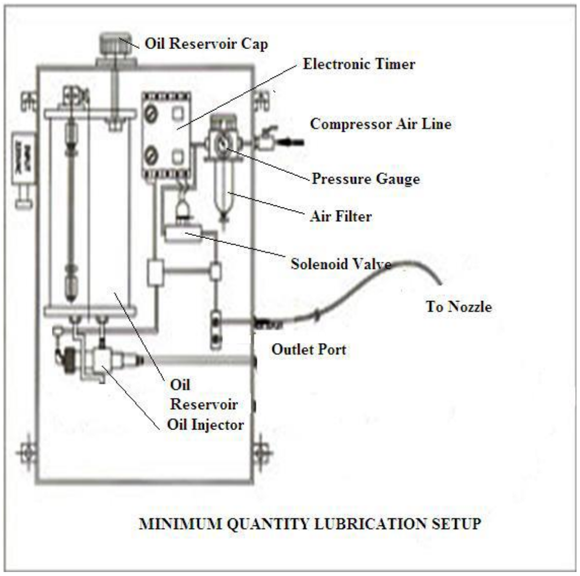
Oil Reservoir Cap
Electronic Timer
Compressor Air Line
Pressure Gauge
Air Filter
Solenoid Valve
To Nozzle
Outlet Port
Oil
Reservoir
Oil Injector
MINIMUM QUANTITY LUBRICATION SETUP

Figure 3.3 Schematic diagram of the MQL system

3.2.3 Dry Machining

In the dry machining process, there is no application of coolant or lubricant at the machining zone. The dry and MQL machining zone images are depicted in Figure 3.4.

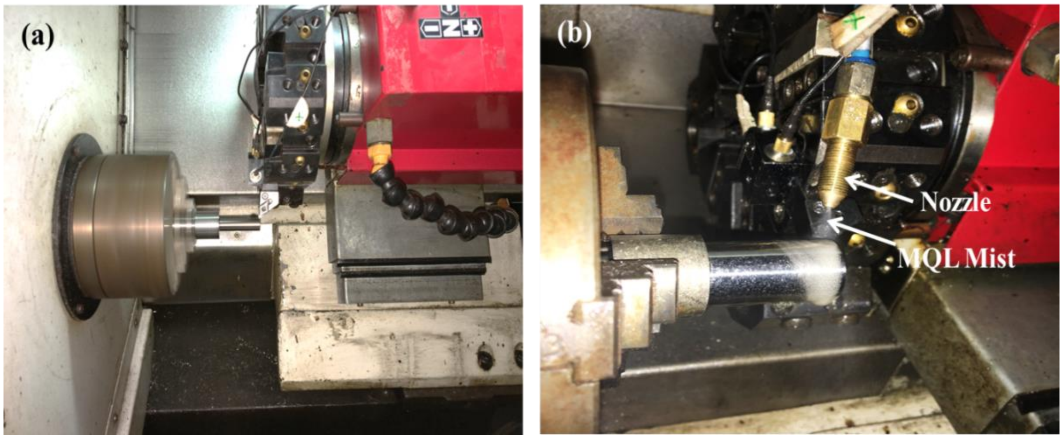
(a)
(b)
Nozzle
MQL Mist

Figure 3.4 Machining zones at (a) dry machining (b) MQL machining

3.3 MACHINING CONDITIONS

The turning experiments were performed on a Ti-6Al-4V alloy of billet 25 mm diameters using a 'MAXTURN' CNC lathe made by MTAB India Pvt. Ltd. Chennai. The CNC lathe has an extreme spindle rotation of 6000 rpm and 15 kW drive motor. Table 3.3 gives the information about the experimental conditions that are considered in the present research. Figure 3.5 shows the PDJNL1616H11 tool holder and the DNMG110408 PCD cutting insert used in machining Ti-6Al-4V alloy in the present research.

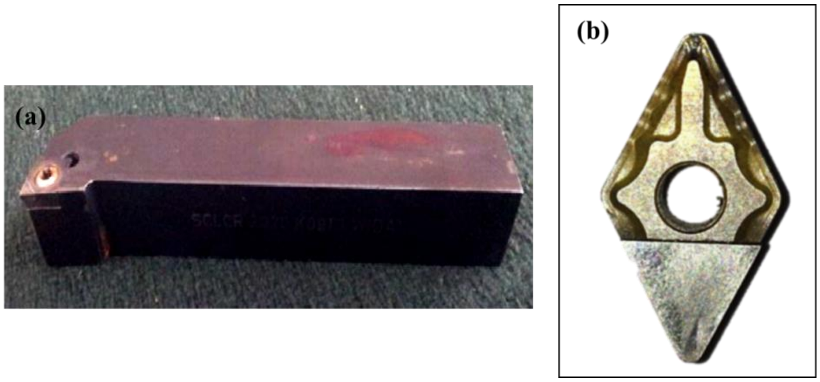

Figure 3.5 (a) Tool Holder PDJNL1616H11 (b) Commercially available PCD Insert

Table 3.3 Machining Conditions

Workpiece material and dimensions	Ti-6Al-4V alloy billet of ø 25 mm x 100 mm length
Cutting Insert	ISO Specification of DNMG110408 PCD Insert, JD-Diamond Tools made
Tool holder	ISO Specification of PDJNL1616H11, Kennametal made
Cutting insert geometry	Angle of clearance : 0°; Rake angle: 6° which is positive; major Edge cutting angle: 93°; Inclination angle of cutting edge: -5° and Nose radius: 0.8 mm.
Mode of lubrication supply	MQL environment machining with compressed air of 4- kgf/cm^2, flow rate of 60 ml/hr.
Lubricant used	Coconut oil (vegetable based oil)

3.4 EXPERIMENTAL DESIGN AND METHODOLOGY

3.4.1 Experimental Methodology

The experimental methodology of the present research is as shown in Figure 3.6. The experimental design was performed based on the L_9 orthogonal array for the selection of the cooling environment. Later the experiments were performed based on one factor at a time approach (OFATA) to study the effects of each process parameter on the performance characteristics of the turning Ti-6Al-4V alloy. For the prediction purpose L_{27} orthogonal array design based on Taguchi method was selected and prediction using Adaptive Neuro-Fuzzy Inference system was analyzed.

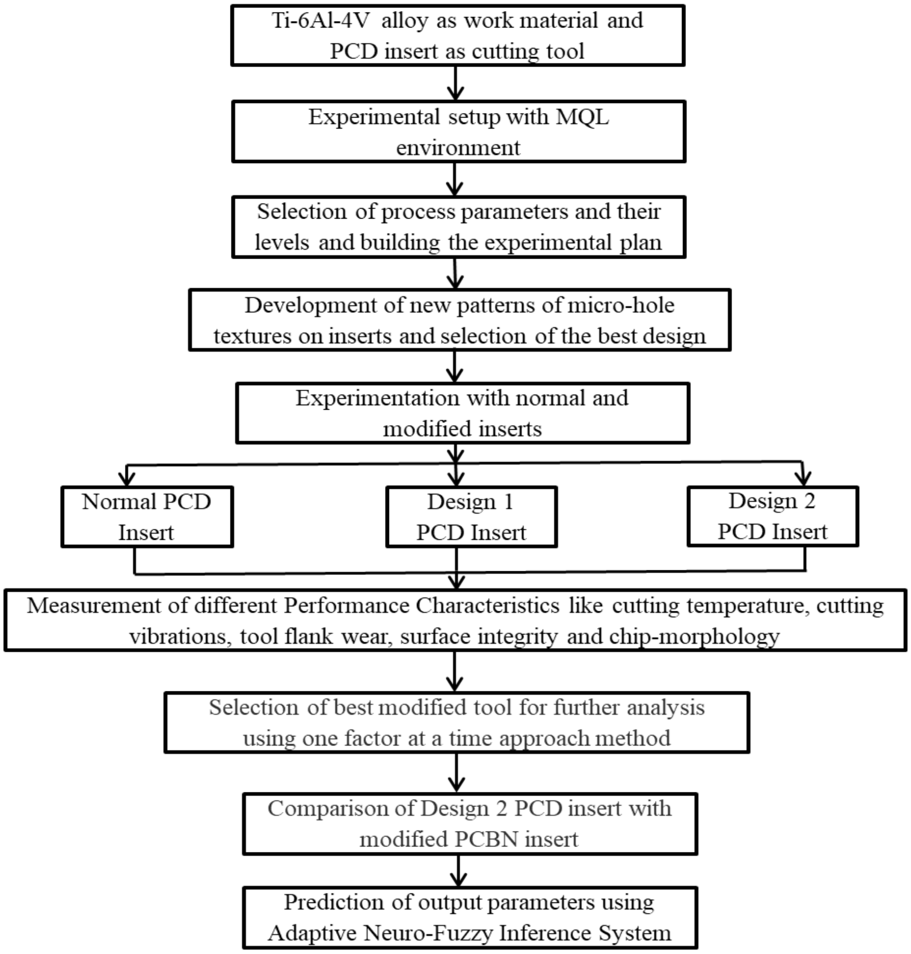
Ti-6Al-4V alloy as work material and PCD insert as cutting tool
Experimental setup with MQL environment
Selection of process parameters and their levels and building the experimental plan
Development of new patterns of micro-hole textures on inserts and selection of the best design
Experimentation with normal and modified inserts
Normal PCD Insert
Design 1 PCD Insert
Design 2 PCD Insert
Measurement of different Performance Characteristics like cutting temperature, cutting vibrations, tool flank wear, surface integrity and chip-morphology
Selection of best modified tool for further analysis using one factor at a time approach method
Comparison of Design 2 PCD insert with modified PCBN insert
Prediction of output parameters using Adaptive Neuro-Fuzzy Inference System

Figure 3.6 Flow chart of the research

3.4.2 Experimental Designs

3.4.2.1 Taguchi Orthogonal array (OA) design

The robust parametric design (RPD) is an engineering methodology intended as a cost-effective approach for improving the quality of products and processes. The goal of parametric design is to choose the levels of the control variables that optimize a defined quality characteristic. The objective of engineering design, a major part of research and development (R&D), is to produce drawings, specifications, and other relevant information needed to manufacture products that meet customer requirements. Knowledge of scientific phenomena and past engineering experience with similar product designs and manufacturing processes form the basis of the engineering design activity. However, a number of new decisions related to the particular product must be made regarding product architecture, parameters of the product design, the process architecture, and parameters of the manufacturing process. A large amount of engineering effort is consumed in conducting experiments to generate the information needed to guide these decisions. Efficiency in generating such information is the key to meeting market windows, keeping development and manufacturing costs low, and having high-quality products (Montgomery 1987).

Taguchi has tabulated 18 basic orthogonal arrays that are called standard orthogonal arrays. In many case studies, one of the arrays from Table 3.4 can be used directly to plan a matrix experiment. An array's name indicates the number of rows and columns it has, and also the number of levels in each of the columns. Thus, the array L_4 (2^3) has four rows and three 2-level columns. The array L_{18} $(2^1 3^7)$ has 18 rows; one 2-level column; and seven 3-level columns. Thus, there are eight columns in the array L_{18} $(2^1 3^7)$. When there are two arrays with the same number of rows, the second array will be represented by a prime, thus the two arrays with 36 rows are referred to as L_{36} and L'_{36}. The 18 standard orthogonal arrays along with the number of columns at different levels for these arrays are listed in Table 3.4.

The number of rows of an orthogonal array represents the number of experiments. For an array to be a viable choice, the number of rows must be at least equal to the degrees of freedom required for the case study. The number of columns of an array represents the maximum number of factors that can be studied using that array. Further, in order to use the standard orthogonal array directly, one must be able to match the number of levels of the factors with the number of levels of the columns in the array. Usually, it is expensive to conduct experiments. Therefore, the designer uses the smallest possible orthogonal array that meets the requirements of the case study (Taguchi 1986). The minimum number of experiments to select from the orthogonal array is given by the equation (3.1). The minimum number of experiments required (E_{min})

$$E_{min} = (L-1)*F+1 \quad (3.1)$$

Where F is the number of controllable factors and L is the levels considered for each controllable parameter. Hence, the L_9 orthogonal array has been selected to perform the experimental trials and to analyze the ANOVA and also to find the optimized parameters and their effects on performance characteristics. The L_9 orthogonal array is as shown in Table 3.5. The experimental trials and the Taguchi analysis were performed with the help of statistical software using MINITAB 17.0. By the help of this software interface, the main effect plots, mean plots and ANOVA results could be obtained.

Table 3.4 Standard orthogonal array

Orthogonal array	Number rows	Maximum number of Factors	Maximum number of columns of these levels			
			2	3	4	5
L4	4	3	3	-	-	-
L8	8	7	7	-	-	-
L9	9	4	-	4	-	-
L12	12	11	11	-	-	-
L16	16	15	15	-	-	-
L’16	16	5	-	-	5	-
L18	18	8	1	7	-	-
L25	25	6	-	-	-	6
L27	27	13	-	13	-	-
L32	32	31	31	-	-	-
L’32	32	10	1	-	9	-
L36	36	23	11	12	-	-
L’36	36	16	3	13	-	-
L50	50	12	1	-	-	11
L54	54	26	1	25	-	-
L64	64	63	63	-	-	-
L’64	64	21	-	-	9	-
L81	81	40	-	40	-	-

Table 3.5 Taguchi’s L_9 orthogonal array

Experimental Trial	Control Factors		
	Cutting velocity (m/min) (V)	Feed rate (mm/rev) (F)	Depth of cut (mm) (D)
1	1	1	1
2	1	2	2
3	1	3	3
4	2	1	2
5	2	2	3
6	2	3	1
7	3	1	3
8	3	2	1
9	3	3	2

3.4.2.2 One factor at a time approach (OFATA)

One factor at a time approach type of experimental design is considered to distinguish the effects of each control factors on the performance characteristics of turning operation. In this process, one control factor is varied at a time by keeping other factors constant at their respective levels. Several researchers have worked on the OFATA for their experimental designs (Manna 2013; Manjaiah et al. 2016; Sharma et al. 2015). Table 3.6 shows the experimental design plan using the OFATA method, where V2, F2 and D2 represent the levels of the control factors cutting velocity (m/min) (V), feed rate (mm/rev) (F) and depth of cut (mm) (D), respectively.

Table 3.6 OFATA experimental plan

Experimental Trial	**Control Factors**		
	Cutting velocity (m/min) (V)	**Feed rate (mm/rev) (F)**	**Depth of cut (mm) (D)**
1	V1	F5	D3
2	V2	F5	D3
3	V3	F5	D3
4	V4	F5	D3
5	V5	F5	D3
6	V3	F1	D3
7	V3	F2	D3
8	V3	F3	D3
9	V3	F4	D3
10	V3	F5	D3
11	V3	F5	D1
12	V3	F5	D2
13	V3	F5	D3
14	V3	F5	D4
15	V3	F5	D5

3.4.2.3 Adaptive Neuro-Fuzzy Inference System (ANFIS)

ANFIS is one of modified fuzzy inference system which is the combination of both the soft computing techniques, namely artificial neural network (ANN) and the fuzzy logic for predicting the performance characteristics in turning operation which is helpful to the manufacturing processes to maintain the surface integrity as well as the quality of the final product. It is one of the meta-heuristic techniques for the prediction of the output parameters. In the present research, Taguchi's L_{27} orthogonal array has been selected with three control parameters having three levels each. In this Taguchi orthogonal array, 85% of the experimental trial is used to perform the training of the process and the remaining 15%, which are chosen randomly from the experimental plan are used for testing or validating of the prediction model.

3.5 MEASUREMENT OF PERFORMANCE CHARACTERISTICS

3.5.1 Cutting Temperature

The cutting zone temperature was measured with the help of a calibrated infrared thermometer of model 'Center 350' having ±1% accuracy as shown in Figure 3.7. The resolution of the infrared thermometer is 0.5°C or 0.5°F and the measurement are about -20°C to 500°C with the preset emissivity at 0.98. In this type of measurement, the thermometer gun was held by hand manually and the infrared beam was focused on the machining zone. The cutting temperature may not be much accurate due to the interruptions caused during turning such as the chip formation and the mist generated during the MQL spray.

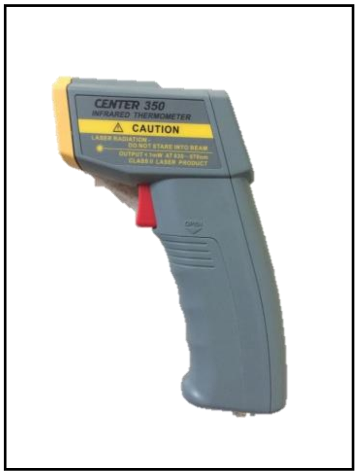

Figure 3.7 The Infrared thermometer gun

3.5.2 Machining vibrations

The machining vibrations were measured with the help of triaxial accelerometer. The triaxial accelerometer sensor was mounted on a tool holder with a Data Acquisition (DAQ) system of National Instruments NI SB-9234 to obtain the vibration signals. The triaxial accelerometer output has been connected to DAQ via Bayonet Neill-Concelman (BNC) cables and is connected to the computer. In the present study, main vibration signals were measured during machining. LabVIEW 14.0 was used as a software interface for data acquisition. Data were acquired at a sampling frequency of 25.6 kHz so that sufficient data can be acquired. The vibration setup is as shown in Figure 3.8.

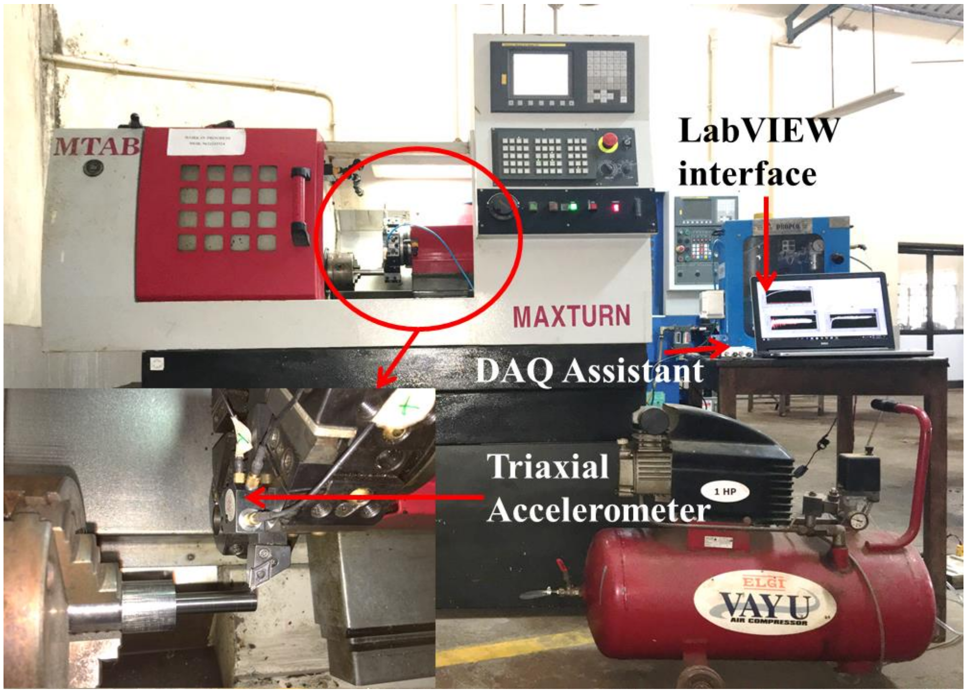

Figure 3.8 The vibration measurement set up for fetching cutting vibration signals

3.5.3 Cutting Tool Wear

Most commonly observed cutting tool wear during machining which can be measured are crator wear, flank wear and notch wear. In the present research, the cutting tool flank wear is mainly considered and measured using the Scanning Electron Microscope (SEM) which is explained here. The tool flank wear was observed for each new insert, machining with a constant machining time of 5 minutes for all different inserts i.e., normal and modified inserts.

3.5.4 Surface Roughness of Machined Surface

The surface roughness for each trial of normal and micro-hole textured tool insert machined workpiece was measured using ‘Mitutuyo SJ301’ type Surface roughness tester. The cut-off length (λ_c) used to calculate surface roughness was around 4 mm along the cutting direction. Three sample reading was taken on each machined workpiece and average of three readings was taken as final surface roughness measurement values. The Mitutuyo surface roughness tester of the contact type is as shown in Figure 3.9.

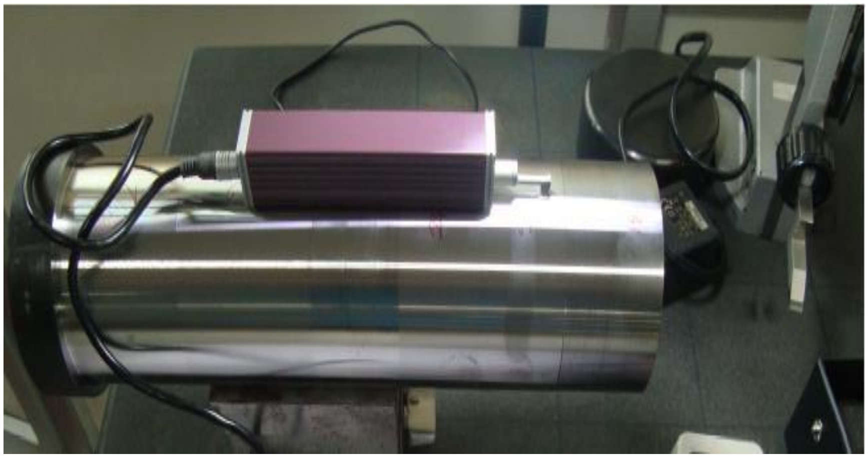

Figure 3.9 Mitutuyo Surface Roughness Tester

3.5.5 Surface Topography of Machined Surface

To measure the 3-Dimensional surface topography or to know the intensity peaks of the machined surface machined under normal and modified cutting inserts LESTOLS4100 model confocal laser 3D surface tester with the resolution of 0.8µm was used. The area of workpiece measured was about 2560 µm x 2560 µm for the investigation. The 3D confocal surface topography tester is as shown in Figure 3.10.

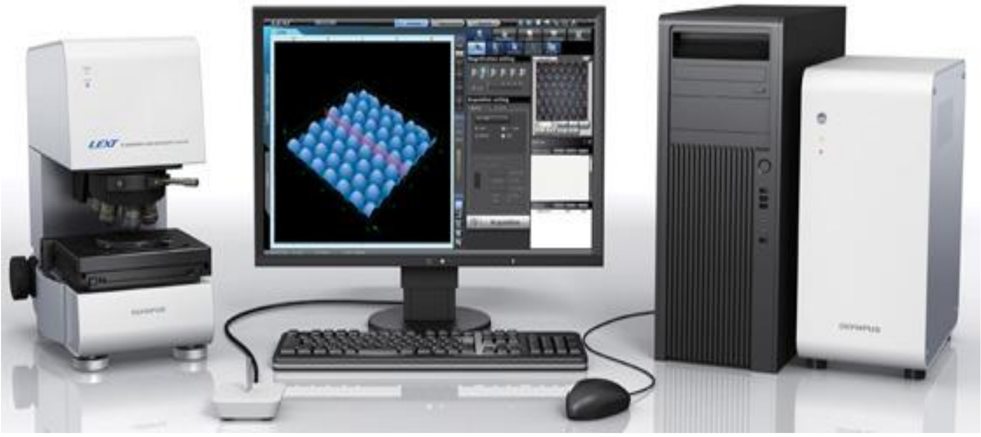

Figure 3.10 3D optical confocal microscope

3.5.6 Material Removal Rate (MRR)

Contech made CA 3102 model weighing scale was used to measure the weight of the workpiece before and after machining as shown in Figure 3.11. Each specimen was weighed using a digital weighing balance having an accuracy of 0.001 gram and maximum weighing capacity of 3.2 kg. The material removal rate (MRR) was determined using the weight loss method and computed from Equation 3.2.

$$\text{MRR} = \frac{W_i - W_f}{t} \quad \text{(gm/min)} \qquad (3.2)$$

Where,

W_i = Initial weight of the workpiece before machining (grams),

W_f = Final weight of the workpiece after machining (grams),

t = Total machining time (10 mins).

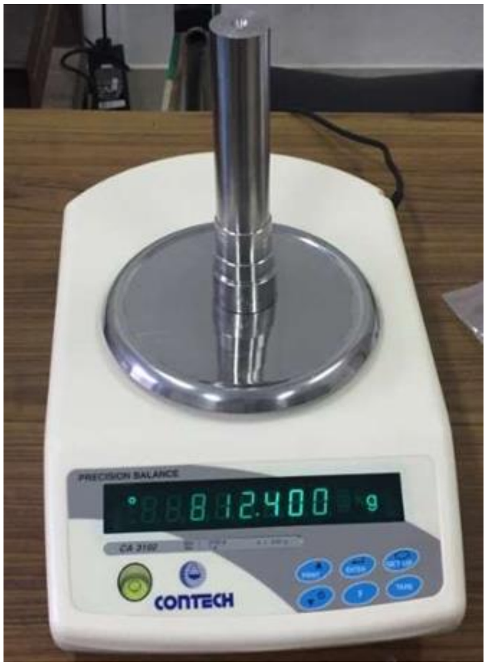

Figure 3.11 Weighting Scale

3.5.7 Scanning Electron Microscope

The SEM was used to measure the tool wear, chip-morphology and the surface defects characteristics of the machined surface. ‘JEOL-JSM-638OLA’ model SEM with 30KV resolution is as shown in Figure 3.12. It was used to measure the performance characteristics and the images were procured with different magnifications for investigation and extensive analysis. To verify the chemical compositions of the Ti-6Al-4V alloy workpiece an ‘Oxford’ made ‘X-ACT’ type Energy Dispersive X-ray spectroscopy (EDAX) was used to measure the chemical compositions.

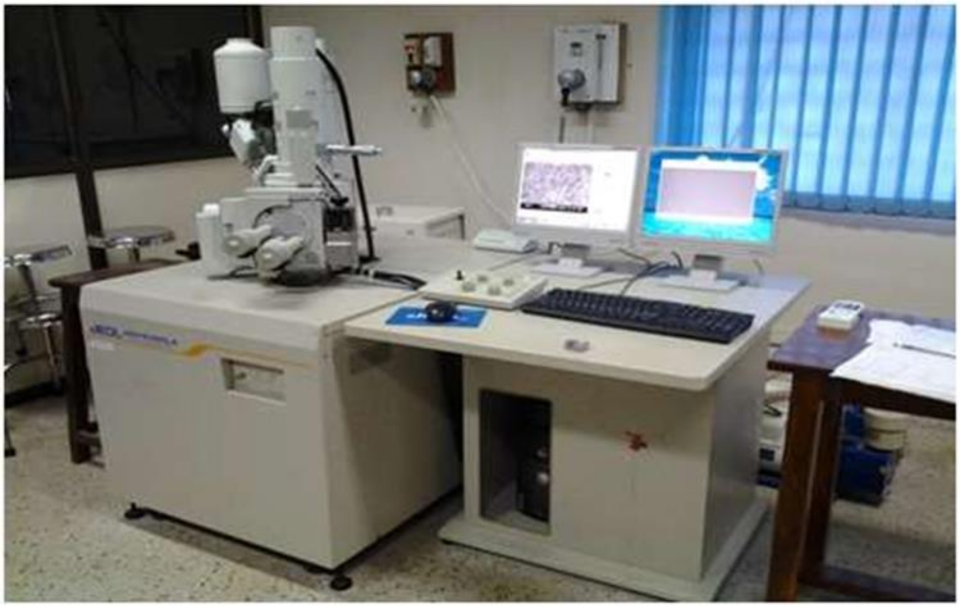

Figure 3.12 Scanning Electron Microscope

3.5.8 Microhardness

The microhardness is the subsurface hardness that is measured from the machined surface. To obtain the subsurface hardness, the machined sample is cut into required dimension using ‘Fanuc pobocut α-OiB’ model wire electric discharge machining into a semicircular shape to study the surface integrity characteristics. Further, the cut samples were cleaned with acetone and polished to the mirror finished surface using different grades of silicon papers and diamond paste and samples were mounted using cold mount. This prepared sample was used to measure the microhardness surface integrity using OMNI TECHMVH-AUTO type Vickers microhardness tester as shown in Figure 3.13. The sample was mounted on the translation stage and was magnified with different magnifications and the micro-indenter of 20µm was used for indentation of material. Each hardness test was conducted three times and the average of the three values was finally considered as the actual value.

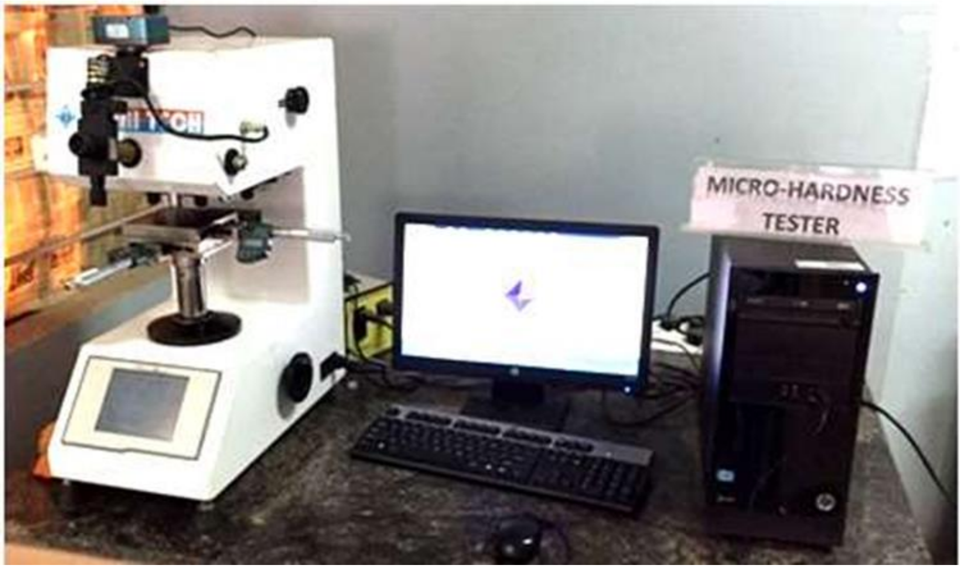

Figure 3.13 Vickers Microhardness Tester

3.5.9 Electric Discharge Super Drilling Machine

To drill the perforations on the tool rake face to obtain the desired micro-hole pattern for the surface texturing of cutting tools, ‘Electronica’ made electric discharge super drilling machine was used to drill the sufficient number of micro-holes on the rake and flank face of the cutting insert. Water was used as a dielectric medium during hole machining. Copper wire with different diameters was used for perforations. Figure 3.14 shows the electric discharge super drilling machine.

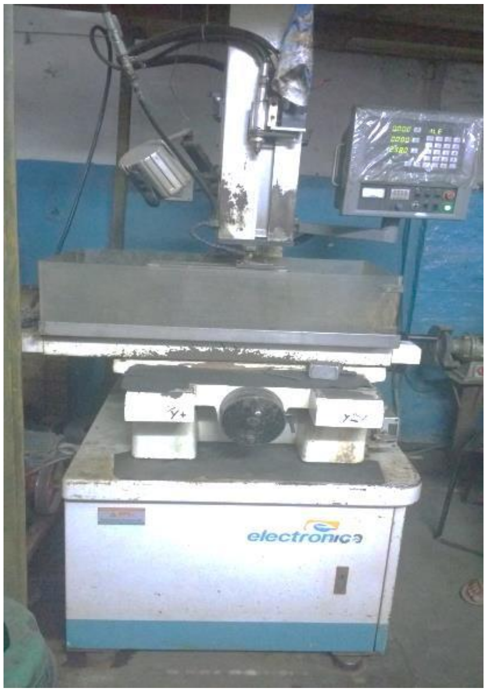

Figure 3.14 Electric discharge super drilling machine

3.6 SUMMARY

This chapter gives an overview of the Ti-6Al-4V alloy material and its chemical compositions as well as mechanical properties. It also explains the experimental set up with MQL system and the vibration system which is integrated during the machining of the Ti-6Al-4V alloy. The chapter briefly elaborates on the experimental design plans using different techniques such as Taguchi method, one factor at a time approach method and also use of ANFIS prediction tool that is involved in the experimentation. Lastly, it describes the different equipments which are used to measure the performance characteristics and the procedure of measurement.

The next chapter gives the detail explanation of simulation and experimental analysis of micro-hoe textured PCD insert for the machining of Ti-6Al-4V alloy.

CHAPTER-4

FINITE ELEMENT MODELLING, SIMULATION AND ANALYSIS OF MACHINING Ti-6Al-4V ALLOY USING PCD INSERT

4.1 INTRODUCTION

The modelling, simulation and analysis of the orthogonal metal cutting process are discussed in this chapter. Surface texturing is an emerging trend in the manufacturing industry, meant to improve the tribological properties during machining of difficult to cut materials. In this research, micro-hole pattern type surface texturing is implemented on the PCD cutting insert to overcome the tribological problems with better lubricating technology. In the first stage the micro-hole design patterns were designed on PCD insert in different configurations. To verify the design pattern such that it doesn’t distort the mechanical properties of cutting insert, the static analysis of PCD insert was performed using ANSYS 16.0 software. In the static analysis, Von-Mises or principal stress and total deformation of the cutting insert were observed by applying pressure and force based on the cutting parameters. Next, a metal cutting model was developed using the updated Lagrangian formulation with a built-in automatic re-meshing algorithm using plain stress assumptions. The developed model is capable of simulating the cutting conditions based on flow stress, frictional condition and the thermo-mechanical properties of the tool and work material. The FE model geometry, the application of boundary conditions and meshing used for this research are discussed here. Finally, to validate the simulation results, experiments have been conducted based on the simulated machining conditions and the results are compared. Further to study the basic characteristics of turning Ti-6Al-4V alloy, the experimental trials were performed using Taguchi technique under dry and MQL environment. This technique provides an idea of the effect of process parameter on performance characteristics.

4.2 MICRO-HOLES ON POLYCRYSTALLINE DIAMOND INSERT

The cutting tool material which has been used for this research work was Polycrystalline Diamond (PCD). Micro-holes are drilled on the rake and flank face along the cutting edge. The idea of making micro-holes along the cutting edge is to take care of the tool-chip contact region. Spherical holes were studied in this research. Figure 4.1 shows the micro-hole texture patterns. Deeper holes are drilled to accommodate more lubricant. Figures 4.1 (a) and (b) show two different patterns of micro-hole textures made on PCD inserts. The depth and diameter of these micro-holes are varied to select the best design pattern.

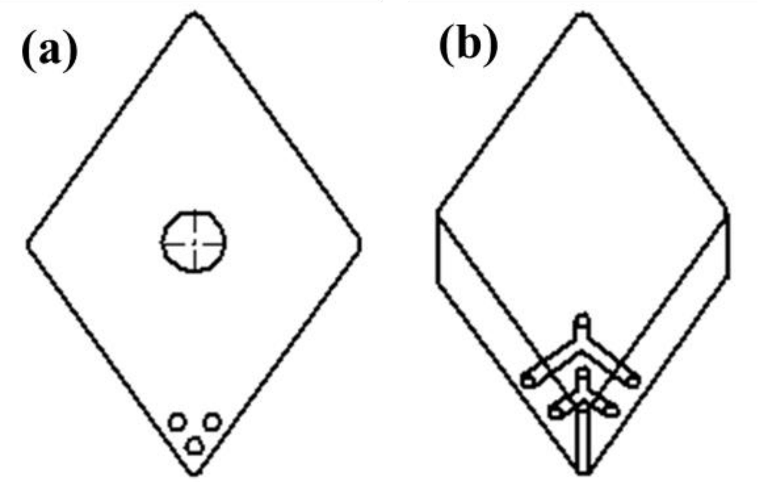

Figure 4.1 Micro-hole texture pattern (a) Design 1 and (b) Design 2

4.3 Influence of Micro-holes on the mechanical properties of the cutting insert

The effects of micro-holes on the mechanical strength of the tool along with the stress and the total deformation while machining can be evaluated by performing Finite Element Analysis (FEA). Figure 4.2 (a) depicts the CAD modelling for PCD insert without micro-hole texture. The nose radius is 0.8 mm and the clearance angle is 0°, respectively. Based on the cutting force, a normal pressure is applied on the main cutting edge at the tool-chip interface which results in an average pressure of 500 MPa. The feed force of 275 N is uniformly distributed as a nodal force along the main cutting edge as shown in Figure 4.3. The bottom surface of the cutting insert is constrained along the x-direction while the two backside faces are constrained in y and z directions, respectively. Figures 4.2 (b) and (c) demonstrate the CAD modelling of PCD insert with different micro-hole patterns. The same boundary conditions are applied for PCD inserts with micro-holes. Table 4.1 shows the mechanical properties of the PCD insert.

Table 4.1 Mechanical properties of PCD Insert

Density (ρ)	3500kg/m^3
Modulus of Elasticity (E)	800GPa
Poisson's Ratio (υ)	0.07

The simulation results are shown in Figures 4.4 (a - f). The Von-Mises stress field for the cutting insert without micro-holes (Figure 4.4(a)) indicates a highly non-uniform stress distribution at the main cutting edge. In cutting insert with micro-holes, the normal profile of stress concentration as shown in Figures 4.4 (c) and (e) are almost similar but there is variation in stress magnitude which is less than the stress magnitude of the insert without micro-holes. No significant stress concentration has been observed for embedded holes of inserts on the rake face. The Figures 4.4 (b), (d) and (f) depict the total deformation of inserts with and without micro-holes. The profiles for all the three cases are alike but they differ in terms of deformation magnitude and gradient. The micro-hole cutting inserts have a lower deformation when compared with normal insert. Overall, the deformations of all the cases are observed to be less and it differs only with few millimetres. Hence, it could be determined from static analysis that micro-holes on the flank and rake face of cutting insert don't affect any mechanical strength of the cutting insert. This observation was supported by actual experiments because tools with micro-holes should not experience any catastrophic failure.

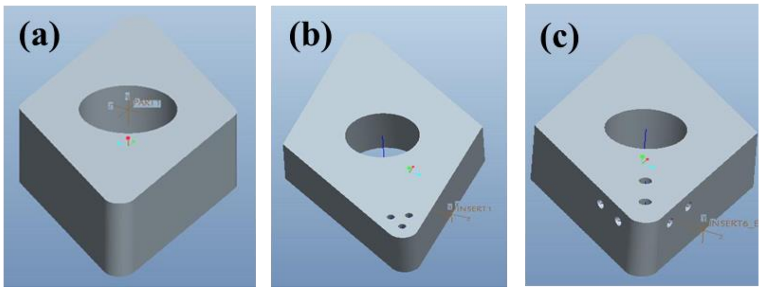

Figure 4.2 CAD models of normal and modified PCD insert (a) normal insert (b) Design 1 micro-hole textured insert (c) Design 2 micro-hole textured insert

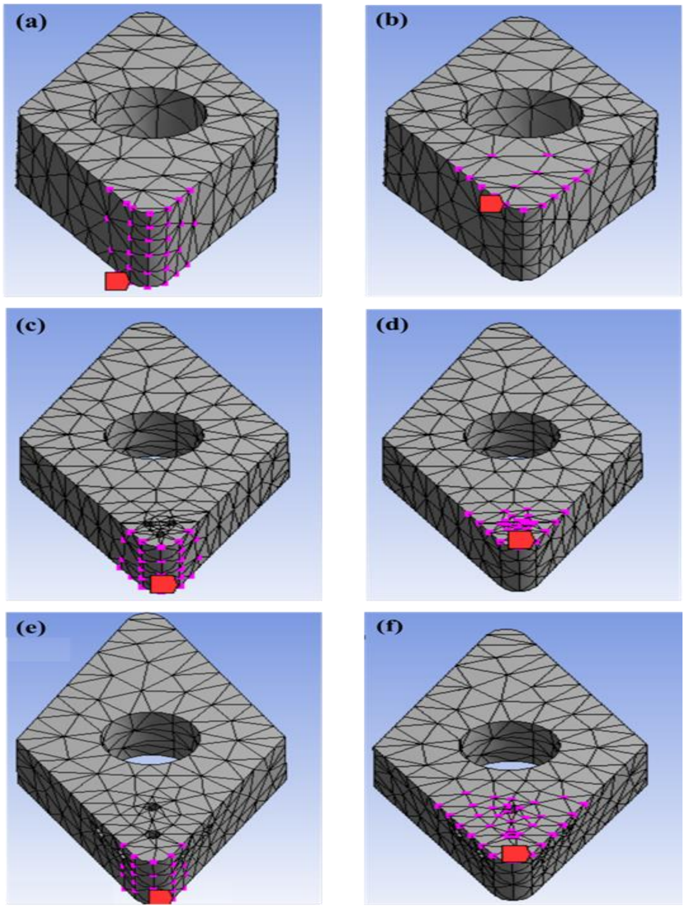

Figure 4.3 Represents the boundary conditions for static simulations. (a) & (b) represents the applied force and applied pressure for normal insert, (c) & (d) represents the applied force and applied pressure for Design 1 insert, (e) & (f) represents the applied force and applied pressure for Design 2 insert

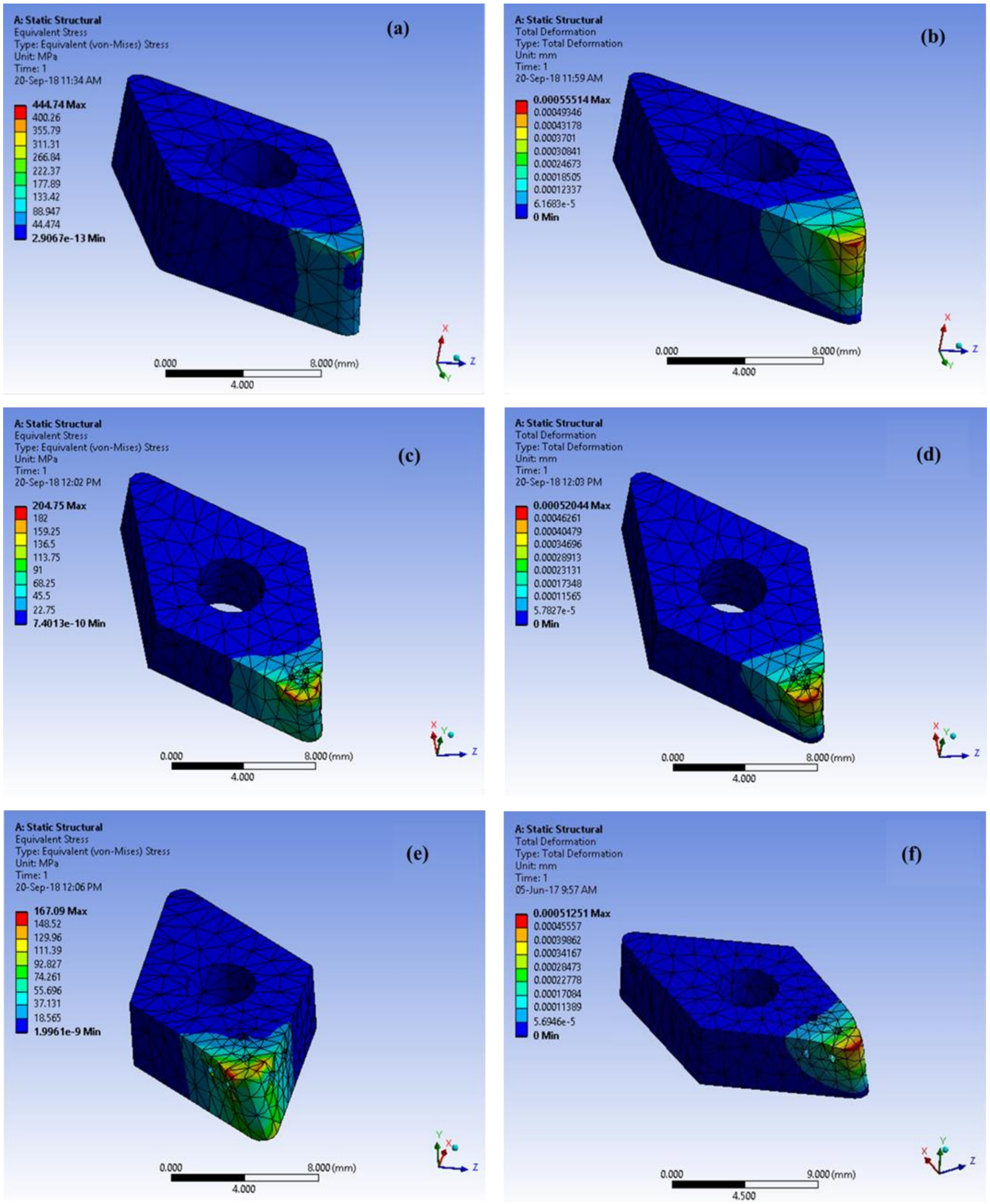

(a)
A: Static Structural
Equivalent Stress
Type: Equivalent (von-Mises) Stress
Unit: MPa
Time: 1
20-Sep-18 11:34 AM
444.74 Max
400.26
355.79
311.31
266.84
222.37
177.89
133.42
88.947
44.474
2.9067e-13 Min
0.000
8.000 (mm)
4.000
X
Y
Z
(b)
A: Static Structural
Total Deformation
Type: Total Deformation
Unit: mm
Time: 1
20-Sep-18 11:59 AM
0.00055514 Max
0.00049346
0.00043178
0.0003701
0.00030841
0.00024673
0.00018505
0.00012337
6.1683e-5
0 Min
0.000
8.000 (mm)
4.000
X
Y
Z
(c)
A: Static Structural
Equivalent Stress
Type: Equivalent (von-Mises) Stress
Unit: MPa
Time: 1
20-Sep-18 12:02 PM
204.75 Max
182
159.25
136.5
113.75
91
68.25
45.5
22.75
7.4013e-10 Min
0.000
8.000 (mm)
4.000
X
Y
Z
(d)
A: Static Structural
Total Deformation
Type: Total Deformation
Unit: mm
Time: 1
20-Sep-18 12:03 PM
0.00052044 Max
0.00046261
0.00040479
0.00034696
0.00028913
0.00023131
0.00017348
0.00011565
5.7827e-5
0 Min
0.000
8.000 (mm)
4.000
X
Y
Z
(e)
A: Static Structural
Equivalent Stress
Type: Equivalent (von-Mises) Stress
Unit: MPa
Time: 1
20-Sep-18 12:06 PM
167.09 Max
148.52
129.96
111.39
92.827
74.261
55.696
37.131
18.565
1.9961e-9 Min
0.000
8.000 (mm)
4.000
Y
X
Z
(f)
A: Static Structural
Total Deformation
Type: Total Deformation
Unit: mm
Time: 1
05-Jun-17 9:57 AM
0.00051251 Max
0.00045557
0.00039862
0.00034167
0.00028473
0.00022778
0.00017084
0.00011389
5.6946e-5
0 Min
0.000
9.000 (mm)
4.500
Y
X
Z

Figure 4.4 Results of FEA analysis. Stress distribution: (a) normal insert (MPa) (c) micro-hole textured design 1 (MPa) (e) micro-hole textured design 2 (MPa). Total deformation: (b) normal insert (mm) (d) micro-hole textured design 1 (mm) (f) micro-hole textured design 2 (mm).

4.4 FINITE ELEMENT ANALYSIS USING DEFORM-3D

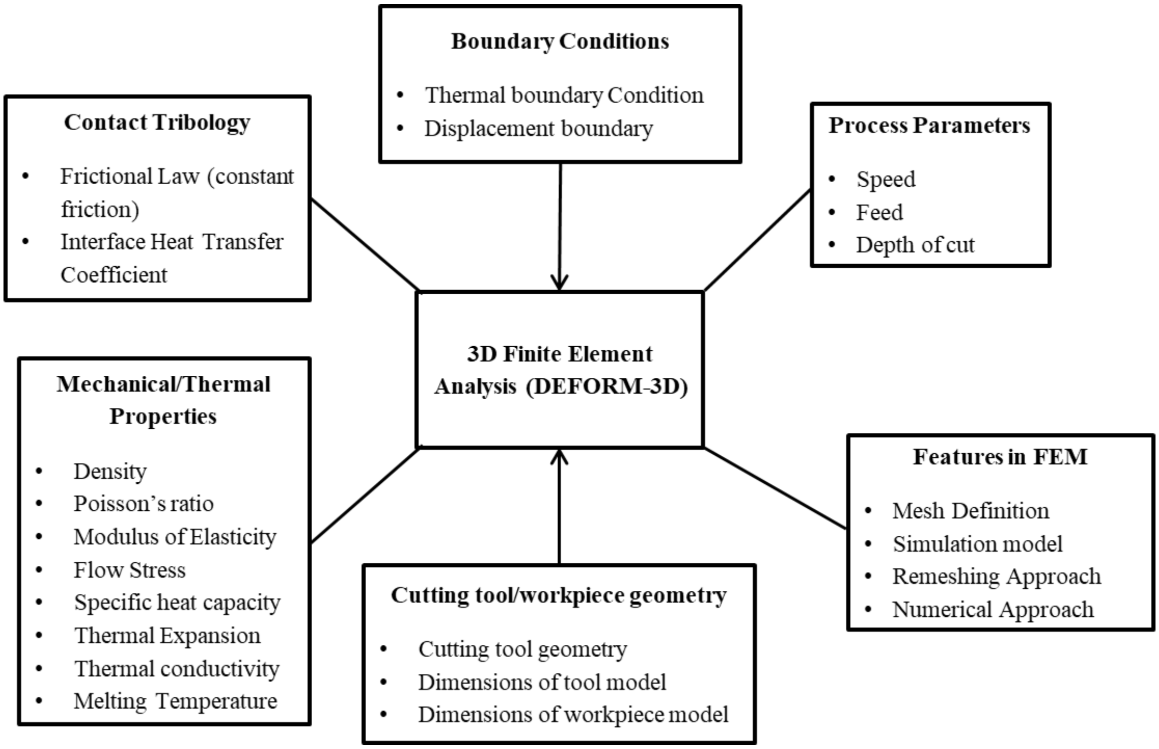
Boundary Conditions
• Thermal boundary Condition
• Displacement boundary
Contact Tribology
• Frictional Law (constant friction)
• Interface Heat Transfer Coefficient
Process Parameters
• Speed
• Feed
• Depth of cut
3D Finite Element Analysis (DEFORM-3D)
Mechanical/Thermal Properties
• Density
• Poisson's ratio
• Modulus of Elasticity
• Flow Stress
• Specific heat capacity
• Thermal Expansion
• Thermal conductivity
• Melting Temperature
Features in FEM
• Mesh Definition
• Simulation model
• Remeshing Approach
• Numerical Approach
Cutting tool/workpiece geometry
• Cutting tool geometry
• Dimensions of tool model
• Dimensions of workpiece model

Figure 4.5 Structure of DEFORM-3D

DEFORM-3D 10.0 is a commercially available FE tool that is used for the analysis for forming and as well as machining process. The analysis of metal cutting operation can be simulated in two ways i.e., the Lagrangian method and as well as Arbitrary Lagrangian-Eulerian method (ALE). The software produces both the graphical and pictorial representation for the explanation of the simulation process. The DEFORM-3D software helps in solving the finite element method problems related to metal cutting process, which is very less expensive and also a less time-consuming way to find the optimal solution. The performance factors such as stress, strain, deformations, cutting force, tool wear, chip morphology, temperature distributions and many more could be visualized graphically in the software interface. The finite element method in DEFORM-3D is solved by following the three simple steps as below to model the machining operation and the structure of DEFORM-3D is as shown in Figure 4.5.

The three segments of DEFORM-3D software are:

- Pre-Processor
- Machining module
- Post-Processor

In the metal cutting simulation problems, the components can be imported from CAD system in Stereo-Lithography (STL) format and the geometry, material properties, meshing and the movement of the tool can be specified in the pre-processor segment. In the pre-processor segment, the work material properties (Ti-6Al-4V alloy) and tool material (PCD) properties are defined and the simulation is performed in step increment based on the cutting conditions and the model is stored in the database format. The boundary conditions are applied in this segment only.

In the second segment of the machining module, the type of analysis to be performed is selected and also the various inputs such as the number of elements, number of simulation steps, process conditions and orientation of tool and workpiece can also be assigned. After assigning the initial conditions, the model is simulated to obtain the prediction results based on the step increments. Finally, in the third segment, the post-processor, the simulation results can be viewed graphically in step increments of the machining. In this process, the metal cutting of Ti-6Al-4V alloy using PCD insert can be simulated along with the formation of chips, which is solved using the updated Lagrangian formulation with Johnson-Cook (JC) material model.

4.4.1 Design of Micro-hole patterns on Polycrystalline Diamond Insert

Polycrystalline Diamond (PCD) is chosen as the material for the cutting tool in this research work. Micro-holes are made on the rake face and flank face of the cutting tool insert very close to the chip-tool contact area to reduce the heat generated through the micro-pool lubrication along the cutting edge. In designing the hole pattern, circular holes are selected because this shape is easy to be drilled using drill bits. Different types of designs are modelled and simulated to select the best designs for further experimentation. The Diameter of holes is varied from 0.4mm to 0.8mm and the depth of the hole from 1mm to 3mm, respectively, with equidistance of 1mm and 2mm. Table 4.2 shows the different designs with varied depth and diameter of the holes. The main goal is to drill deep holes so that they contain more lubricants for better cooling. Figure 4.6 shows the CAD model of different designs of the micro-hole pattern on the rake and flank face of the PCD insert.

Table 4.2 Different designs with varied depth and diameter of the holes

Design Pattern	**Dimensions**
Design 1	0.4mm Dia. and 1mm equidistance between the holes
Design 2	0.6mm Dia. and 1mm equidistance between the holes
Design 3	0.6mm Dia. and 2mm equidistance between the holes
Design 4	0.4mm Dia. and 2mm equidistance between the holes
Design 5	0.4mm Dia. 0.6mm Through Hole, 2mm equidistance between the holes
Design 6	0.6mm Dia. 0.6mm Through Hole, 2mm equidistance between the holes
Design 7	0.6mm Dia. 0.8mm Through Hole, 2mm equidistance between the holes

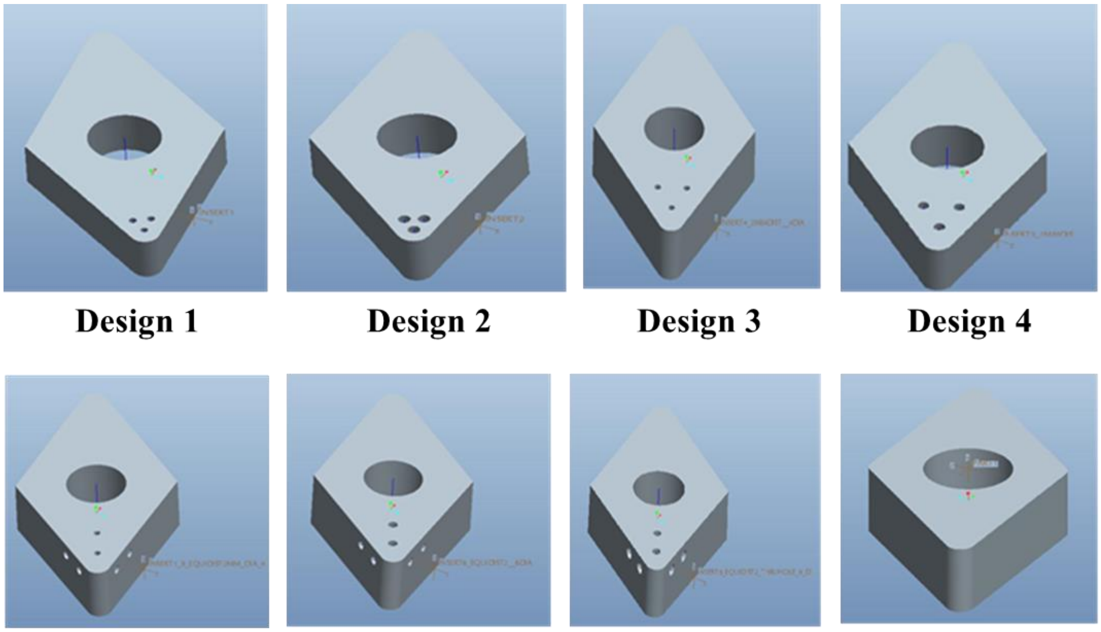

Design 1 Design 2 Design 3 Design 4

Design 5 Design 6 Design 7 Normal Insert

Figure 4.6 CAD models of the different types of Micro-hole designs on the rake face of the PCD inserts

4.4.2 Finite Element Modelling and Simulation

To evaluate the effect of micro-holes on the mechanical strength of the cutting tool when in use, the Johnson-Cook (JC) model is used extensively in deformation process due to its flexible nature of data in flow stress, which is suitable for FEM simulation code. But there is a need to gauge different material models based on the applicability in the context of deforming simulations. The JC material constitutive model considered for this analysis is based on Lesuer (2000) which is shown in Table 4.3.

Finite Element modelling is performed using DEFORM-3D™ based on an updated Lagrangian formulation which considers the mesh to be attached to the workpiece during deformation. The chip shape is formed due to the function of deformation process, where the machining conditions and material constants need not be predetermined. The workpiece material is fully constrained and the tool material movement is allowed in the Y-axis (Vijay Sekar and Pradeep Kumar 2011). The thermo-mechanical and physical properties of the workpiece and tool materials of Titanium alloy (Ti-6Al-4V) and PCD were calculated from material properties and are incorporated into the FEM model as shown in Table 4.3 and 4.4, respectively. The workpiece model is modelled as plastic and the tool insert as rigid material. Fourteen thousand tetrahedral elements were taken for the workpiece material. PRO-E Creo 5 software is used to model the micro-holes on cutting tools that are drilled along the preferred orientations on insert DNMG110408 tool geometry and micro-hole pattern as shown in Table 4.2 are considered.

3D tool model with micro-holes in different orientations and related tool material properties are imported into the DEFORM-3D™ software package during the formulation of machining simulation. The cutting tool is defined by 16,000 elements and was re-meshed with 2, 40,000 elements for the better distribution of the output parameters like cutting force, stress distribution, strain distribution and temperature distribution. The meshed model of tool and workpiece are shown in Figure 4.7.

The 3D FEM simulation of the machining process is carried out with varying cutting velocity maintaining feed rate and depth of cut as constant. Table 4.5 shows the cutting parameters for which the simulation has been performed. The simulation is performed with the micro-hole textured tool and the normal insert. The results after completion of simulation such as cutting force, stress distribution, strain distribution and temperature distribution are validated with experimental results. The simulation results are shown in Figure 4.8.

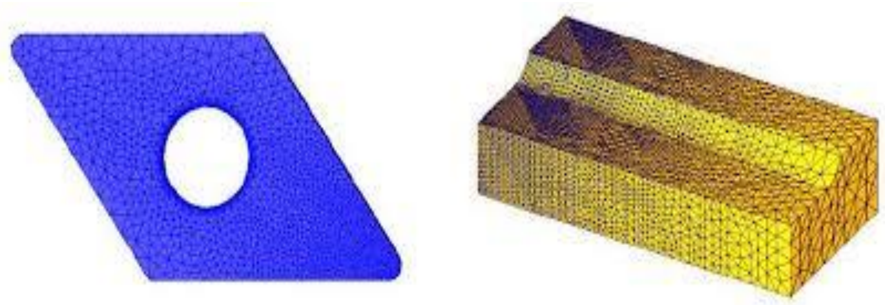

Figure 4.7 Meshing of the PCD cutting insert and the Ti-6Al-4V alloy workpiece in DEFORM-3D simulation

Table 4.3 J-C material model constants for Titanium alloy (Ti-6Al-4V)

Young’s modulus	380 GPa
Thermal conductivity	4.63 W/m K
Poisson’s ratio	0.23
Heat capacity	565 J/kg K
Thermal expansion	6.5 x 10^{-6} /K
Emissivity	0.07
Yield strength (A)	896 MPa
Hardening modulus (B)	656 MPa
Strain rate sensitivity coefficient (C)	0.128
Thermal softening coefficient (m)	0.8
Hardening coefficient (n)	0.5
Melting temperature of the work material (T_m)	1650 °C
Plastic strain rate ($\dot{\varepsilon}_0$)	$1s^{-1}$

Table 4.4 Material Properties of PCD

Young’s modulus	890 GPa
Thermal conductivity	543 W·m^{-1}·K^{-1}
Poisson’s ratio	0.07
Heat capacity	790 J·kg^{-1}·°C^{-1}
Thermal expansion	2.5 x 10-6
Emissivity	0.63

Table 4.5 Cutting Parameter for simulation comparison with normal insert and modified inserts

Sl.No.	Cutting Speed (m/min)	Feed (mm/rev)	DOC (mm)
1	100	0.5	1
2	125		
3	150		
4	175		
5	200		

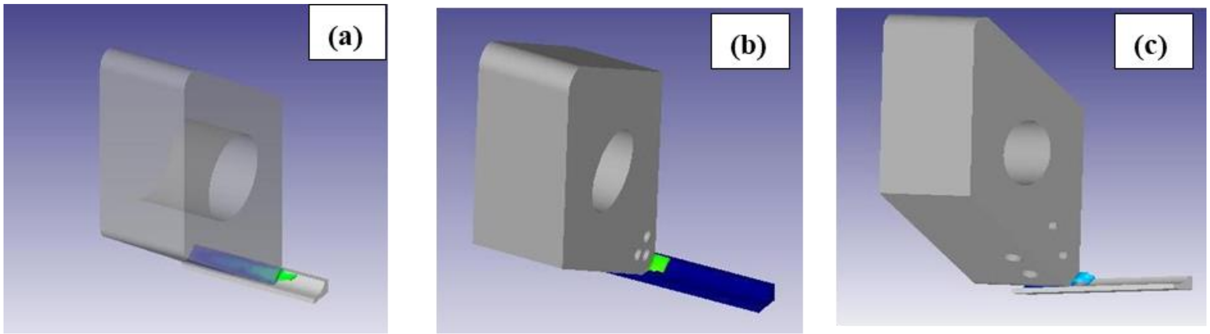

Figure 4.8 Simulation of FE model (a) Normal Insert (b) Design 1 modified insert (c) Design 2 modified insert

4.5 FEM SIMULATION RESULTS AND DISCUSSIONS

The results of Finite Element Analysis for cutting force, effective stress, strain and temperature distributions with input material model for different designs are shown here. The analysis is performed with varying Cutting velocities ranging from 100m/min to 200m/min and with constant feed rate and depth of cut (Ozcelik et al. 2011). The Finite Element output is measured around at near steady-state conditions to ensure the comparisons with normal insert.

4.5.1 FEM based Prediction of Cutting Force

Figure 4.9 describes the predictions of cutting force by FEM Simulation model comparing with the normal insert and the designed insert. The predicted cutting force increased for normal insert with the variation in cutting velocity from 100 m/min to 125 m/min and showed the decrease, followed by marginal increase from 125 m/min to 175 m/min and steadily decreased between 175m/min to 200m/min. The increase in the cutting force is due to the strain hardening effect which alters the trend slightly and then decreases between 175 m/min to 200 m/min is due to increase in cutting temperature resulting in thermal softening of the workpiece in the normal insert. Finally, there is a clear reduction in cutting force in case of micro-hole textured inserts. Compared to that normal insert, a reduction in cutting force by 14-22% is noticed when machining steel with micro-hole textured insert (Arulkirubakaran et al. 2016). The cutting forces are also impacted by the friction coefficient and also the friction law. The higher the friction values, the cutting force also increases. In this work, the JC-model is employed with μ=0.3 coulomb friction constant in friction modelling (Filice et al. 2007). Several simulations were performed with the same conditions to study the repeatability of the results since the experimentation is costlier. All the simulations showed similar results.

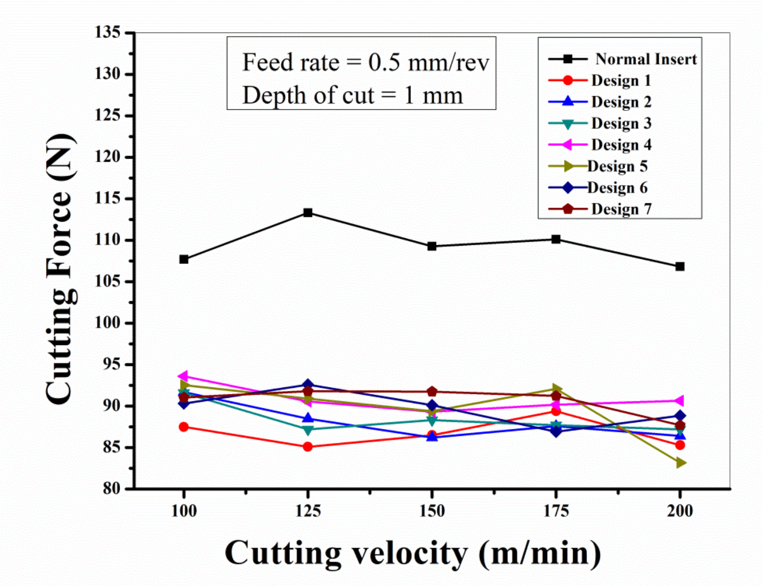

Figure 4.9 Comparison of cutting force with normal and designed inserts

4.5.2 FEM based Prediction of effective Stress

Figure 4.10 presents the effective stress variations in FE models of the normal insert and different designed patterns of inserts. The effective stress plot for all designed inserts reveals that minimum stresses are usually found in the primary deformation region where there is a contact between tool and workpiece. The stress distribution at the deformed surface is residual in nature and decreases at the uncut surface and at chip deformed surface. The seven designs prove good stability in modelling, proposing that JC law is good when evaluating global output stress.

All the seven designs predict similar ranges (1738-1860 MPa) for effective stress, proposing that material constants of the model combine to produce the similar stress pattern during machining when compared with the normal insert. The stress concentrations are less near the segments in the designed pattern at their deformation zones. The normal insert shows irregular stress distribution at primary and secondary zones when compared to designed inserts due to the rise in cutting temperature which increases the cutting force. It should be noted that there is no specific stress concentration due to the micro-holes on the rake face of the insert.

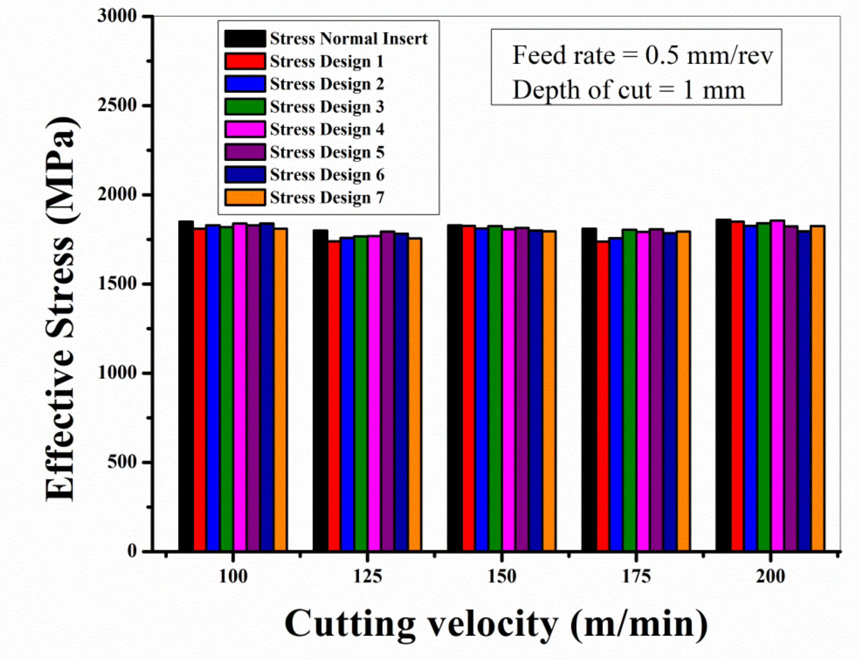

Figure 4.10 Predicted Stress distribution graph of Normal Insert and Designed Inserts

4.5.3 FEM based Prediction of effective Strain

Figure 4.11 shows the effective strain variation of predicted values with FE models of the normal insert and different designed patterns of inserts. The strain distribution in the plastic region is higher at the primary deformation region followed by secondary region and very less at the free end of the chip. The chip formation in titanium alloy suggests a complex formation mode of chips resulting in segments and serrations even at lower cutting speeds. In other material, this type of formation occurs only during high-speed cutting. The simulated chip formation for different designs shows similar strain patterns which is due to the micropool lubrication of the cutting insert. There appear to be minor variations in the primary and secondary deformation zone.

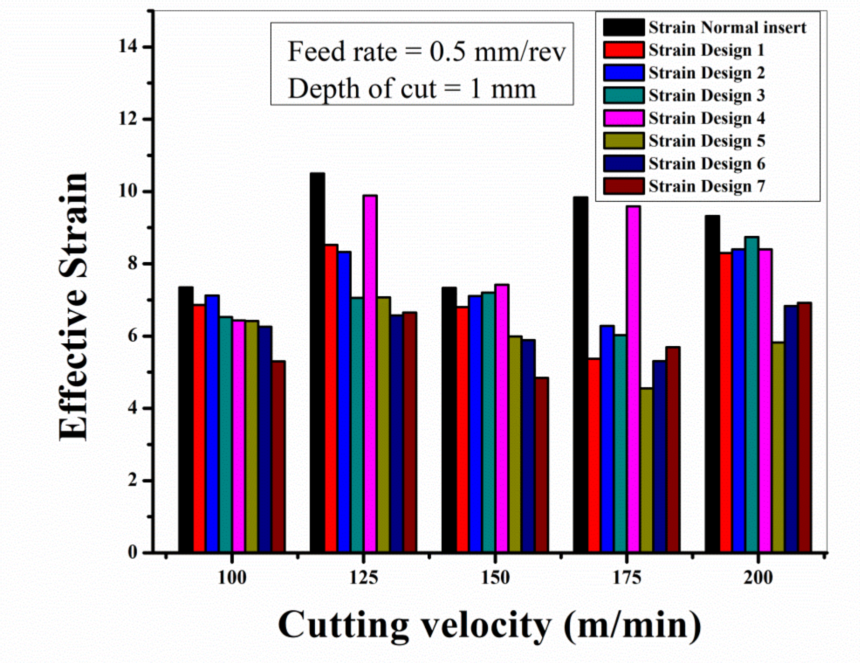

Figure 4.11 Predicted Strain distribution graph of Normal Insert and Designed Inserts

4.5.4 FEM based Prediction of Temperature

Figure 4.12 shows the temperature predictions with FE models for normal insert and different designed patterns of inserts. The heat transfer takes place in the primary region where the deformation takes place. The primary heat generated in machining process is transferred at shear zone where the plastic work material is converted to heat and at the chip-tool interface, the frictional heat is generated. The Titanium alloy has low thermal conductivity, which ensures less heat dissipation resulting in rapid tool wear of cutting tool insert which reduces the tool life. Hence, lubrication is necessary with cutting fluids or the cryogenic coolants for the removal of generated heat. In this FEM simulation model, the workpiece is treated as plastic and the cutting tool as a rigid material to understand the heat transfer during the deformation of titanium alloy in the machining process. The experimental temperature will usually be more near chip-tool interface followed by a shear plane and least at the uncut surface.

The difference in temperature is less for micro-holed textured inserts when compared with normal inserts. This can prove that micro-hole textured pattern helps in a decrease of tool wear which finally increases the tool life. The minimum value can be attributed to the variation in the value of ‘m’, the thermal softening coefficient in the model. The cutting velocity can also affect the temperature distribution. Generally, the temperature distribution may be less than normal value because of short-cutting process in the simulation.

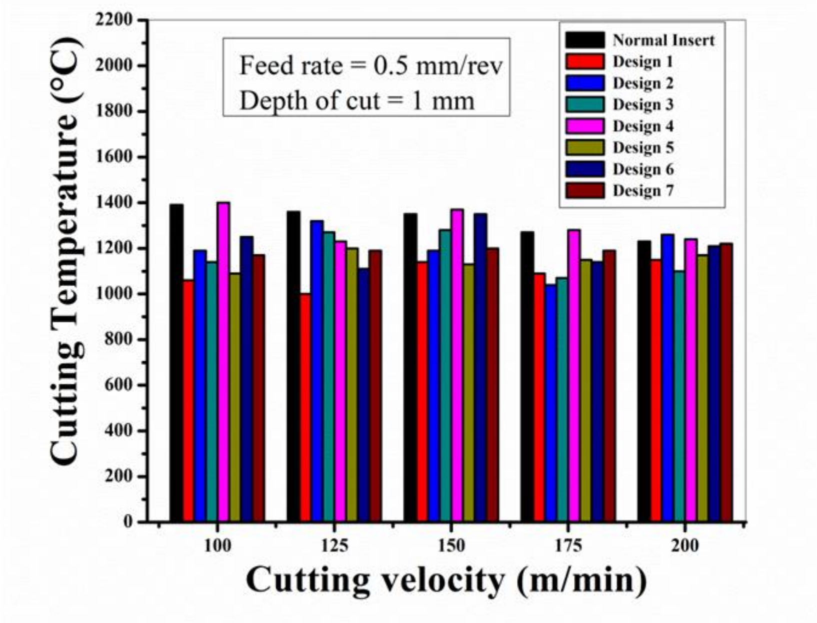

Figure 4.12 Predicted Temperature distribution graph of Normal Insert and Modified Inserts

4.6 SIMULATION OF THE MACHINING PROCESS

The simulation of the machining process was formulated with the updated Lagrangian method using DEFORM 3D 10.0 software. Ti-6Al-4V alloy was considered as the workpiece and defined as an elasto-plastic material. JC material model is as shown in Equation 4.1 was used with the empirical constants contained in Table 4.3. This equation was used internally to calculate the cutting temperature during machining (Karpat 2011).

$$\sigma = [A + B\,\varepsilon^{n}]\,[1 + C \ln (\varepsilon' / \varepsilon'_{o})]\,[1 - \{(T-T_{room}) / (T_{melt} - T_{room})\}^{m}] \tag{4.1}$$

The workpiece was considered to be fixed along the bottom in all directions. This Finite Element Analysis (FEA) package has a continuous re-meshing technique with 16,000 tetrahedral elements. In achieving the finer mesh, the workpiece was assumed as a curved shape. The micro-hole textures on the cutting insert were so oriented to facilitate easier flow of chips. The tool geometry was considered in accordance with DNMG110408 ISO standardization of PCD insert. The 3D modelled micro-hole textured cutting inserts and normal insert developed are as shown in Figure 4.3 (a-c).

The newly designed cutting inserts with micro-holes in different orientation were imported in DEFORM 3D software and used as a rigid body. Mesh of 14,000 elements defined the cutting insert and tooltip was re-meshed with 1, 40,000 elements for better distribution of output parameters such as cutting temperature and chip morphology. To identify the frictional effects between the tool and the workpiece, the constants such as Coulomb friction factor (μ), shear friction factor (m) and pressure dependent friction factor (p) are required for 3D modelling of deformation process. The material properties of Ti-6Al-4V alloy and PCD cutting insert are given in Table 4.3 and Table 4.4, respectively. The simulation process was carried out with varying feed rate (0.3, 0.4 and 0.5 mm/rev) at constant cutting velocity (150 m/min) and depth of cut (1 mm). Trial and error approach was adopted to evaluate the models. After the evaluation of the model, it was used to simulate the deformation process of the modified cutting inserts. The simulation results such as cutting temperature were validated with experimental results.

The actually modified inserts that were fabricated using super drilling machine which are shown in Figure 4.13.

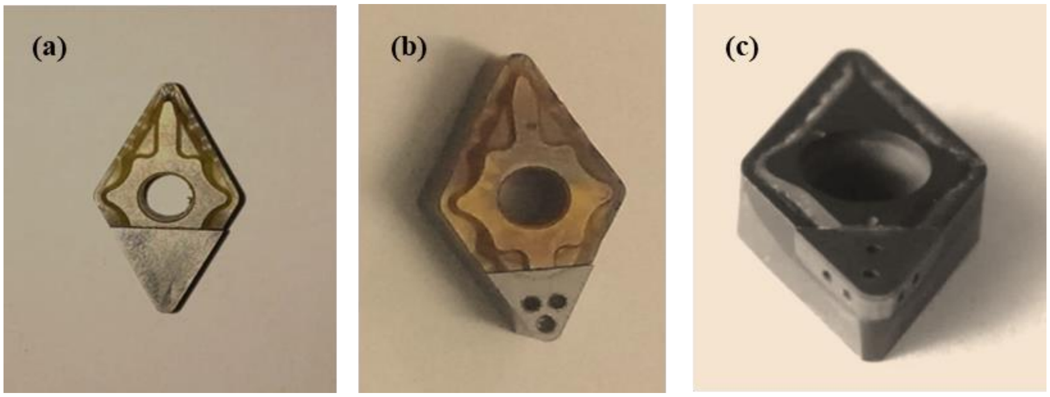

Figure 4.13 Different types of Micro-hole textured inserts produced by the super drilling

4.6.1 Effect of Micro-holes on cutting temperature

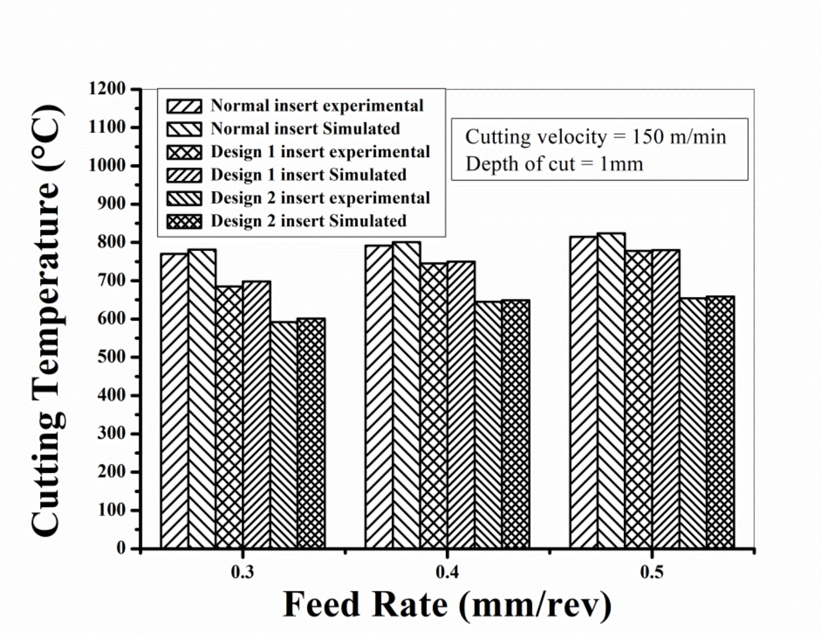

Figure 4.14 Comparison of both experimental and simulated conditions in a variation of feed rate on cutting temperature

Figure 4.14 depicts the cutting temperature at the tool-chip contact area during machining of Ti-6Al-4V using different tools like normal insert, Design 1 and Design 2, measured with the help of infrared thermometer with ±1% accuracy. It was clearly observed that the cutting temperature at contact region was found to be 592°C at 0.3 mm/rev and increased to a maximum of 654°C at 0.5 mm/rev for Design 2 insert when compared with other types of modified inserts.

The cutting temperature at the tool-chip contact region during simulation was plotted in Figure 4.14. The cutting temperature recorded for Design 2 insert at 0.3 mm/rev was 601°C and 659°C at 0.5 mm/rev. The comparison of both the simulated and experimental cutting temperature had a good agreement with varying feed rate. During experimental condition, the cutting temperature was reduced to 19-23% and in the simulated condition, it was 18-24% reduction, observed for the Design 2 insert at higher feed rate when compared to that of the normal insert and Design 1 insert. However, micro-hole textured inserts with lubricant substantially enhanced the effective lubrication by means of micro-pool lubrication mechanism with less chip-tool interface resulting in lesser frictional force. Substantial reduction in cutting temperature by 8-21% was noticed during machining simulation (Figure 4.15 (a-f)) with Design 2 cutting insert when compared to normal insert for same varying feed rate. This prediction is validated by experimental results. Reduction in cutting temperature can be attributed to the less chip-tool interface, less coefficient of friction resulting in better lubrication effect and better wear resistant properties (Jianxin et al. 2012).

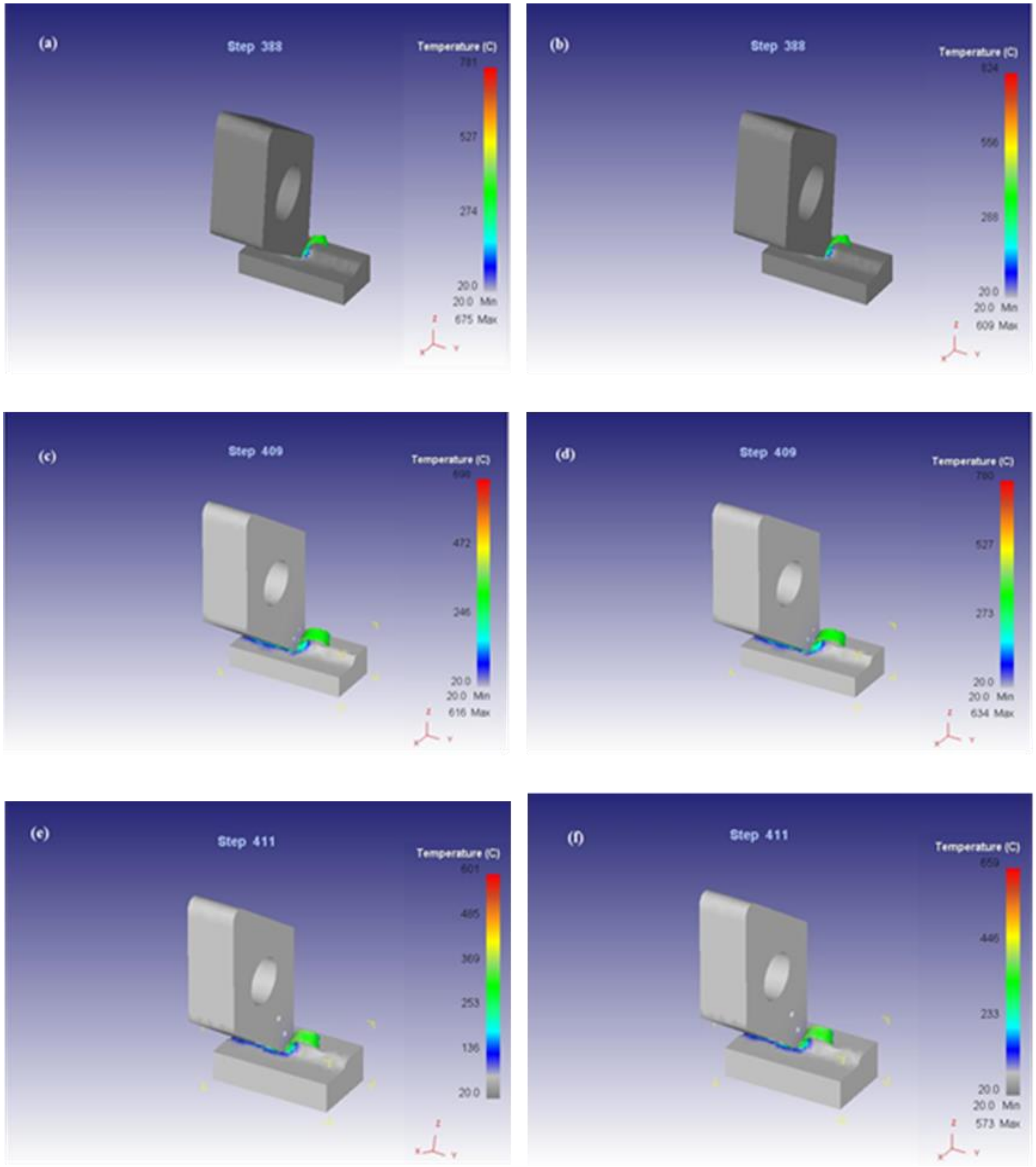
(a)
Step 388
Temperature (C)
781
527
274
20.0
20.0 Min
675 Max
z
x
y
(b)
Step 388
Temperature (C)
824
556
288
20.0
20.0 Min
609 Max
z
x
y
(c)
Step 409
Temperature (C)
698
472
246
20.0
20.0 Min
616 Max
z
x
y
(d)
Step 409
Temperature (C)
780
527
273
20.0
20.0 Min
634 Max
z
x
y
(e)
Step 411
Temperature (C)
601
485
369
253
136
20.0
z
x
y
(f)
Step 411
Temperature (C)
659
446
233
20.0
20.0 Min
573 Max
z
x
y

Figure 4.15 Cutting temperature distribution under simulation at (a) 0.3 mm/rev (Normal insert) (b) 0.5 mm/rev (Normal insert) (c) 0.3 mm/rev (Design 1) (d) 0.5 mm/rev (Design 1) (e) 0.3 mm/rev (Design 2) (f) 0.5 mm/rev (Design 2)

4.7 ANALYSIS OF SURFACE ROUGHNESS AND CUTTING TEMPERATURE IN MACHINING OF Ti-6Al-4V ALLOY USING NORMAL PCD INSERT UNDER DRY AND MQL ENVIRONMENT

This section deals with an investigation on machining Ti-6Al-4V alloy using PCD insert under dry and MQL environment. Taguchi technique was employed to derive the best optimum results under dry and MQL environment. The control factors such as cutting velocity, feed rate and depth of cut were selected to determine the best machining conditions to achieve better surface quality and reduce cutting temperature using normal PCD insert. In the current research three parameters, namely cutting velocity, feed rate and depth of cut were identified as controllable factors. The selection of feed rates and depth of cut were based on the insert manufacturer and the cutting velocity was selected based on the trial experiments. Each parameter was investigated with three levels to study the non-linearity behaviour of the process parameters. The identified controllable factors and their levels are depicted in Table 4.6. According to Taguchi quality design concept for three levels and three parameters, a standard L_9 Orthogonal Array (OA) was selected as shown in Table 4.7.

Table 4.6 Control factors and levels for turning

Control Factors	**Levels**		
	1	**2**	**3**
Cutting Speed (m/min)	100	125	150
Feed (mm/rev)	0.3	0.4	0.5
Depth of Cut (mm)	0.25	0.50	0.75

Table 4.7 Control factor settings as per L_9 Orthogonal Array

Trial No.	Cutting Speed (m/min)	Feed (mm/rev)	Depth of Cut (mm)
1	100	0.3	0.25
2	100	0.4	0.50
3	100	0.5	0.75
4	125	0.3	0.50
5	125	0.4	0.75
6	125	0.5	0.25
7	150	0.3	0.75
8	150	0.4	0.25
9	150	0.5	0.50

4.7.1 Analysis of Variance for Surface Roughness and Cutting Temperature during machining of Ti-6Al-4V alloy using PCD insert under Dry and MQL Environment

In the present work, the objective is to minimize the surface roughness and temperature. Hence, "smaller the better type" category is used for surface roughness and temperature (Phadke 1995). The S/N ratios associated with the objective functions for each trial of the OA are given by:

$$\eta_1 = -10\log_{10}(R_a^2) \tag{4.2}$$

$$\eta_2 = -10\log_{10}(\text{Temp}^2) \tag{4.3}$$

The corresponding S/N Ratios for each trail of the L_9 orthogonal array were determined using equation (4.2) and (4.3) for surface roughness and temperature are presented in Table 4.8 and 4.11, respectively, which gives the combinations of experimental machining parameters and parameter levels in the L_9 orthogonal array. A total of 9 experiments were conducted in accordance with the parameter level of each factor and observed values of surface roughness and temperature were noted. Further, the values were converted to the corresponding S/N ratio.

The level of the parameter with the highest value of S/N ratio is the best combination level. The optimal parameter setting for the dry cutting condition is found to be the lowest cutting speed of 100m/min, the lower feed rate of 0.3mm/rev and highest depth of cut 0.75 mm for minimizing surface roughness. Whereas for minimizing temperature 125m/min cutting speed, the lower feed rate of 0.5mm/rev and lowest depth of cut of 0.25mm are the optimum parameter settings for the dry cutting condition. The main effect plots Figure 4.16 (a) and (b) are generated using MINITAB statistical software for exploring the effects of control factors on surface roughness and temperature.

To examine the effects of control factors quantitatively, the Analysis of Variance (ANOVA) based on S/N ratio has been performed under dry cutting condition. The ANOVA is accomplished by separating total variability of S/N ratio, which is measured by the sum of squared deviations from the total mean of S/N ratio into contributions by each of the factors and the error. The summary of ANOVA results for surface roughness is shown in Table 4.10. It can be seen from the ANOVA that feed rate (44.96%) and depth of cut (36.9%) have major contributions, whereas cutting velocity (17.8%) has a less significant role in minimizing the surface roughness.

It is clear from ANOVA results of Table 4.9 that the feed rate (50.5%) and cutting speed (28.85%) are the major contributors, whereas depth of cut plays less significant roles in minimizing the temperature at the dry cutting condition.

Table 4.8 Control factor settings as per L_9 OA with measured values and corresponding signal to noise ratio for turning with the normal insert in dry condition

Trial No.	Cutting velocity (m/min)	Feed rate (mm/rev)	Depth of Cut (mm)	Average Surface Roughness (R_a)(µm)	Cutting Temperature (°C)	S/N ratio of R_a	S/N ratio of Temperature
1	100	0.3	0.25	0.85	100	1.41162	-40.0000
2	100	0.4	0.50	1.06	118	-0.50612	-41.4376
3	100	0.5	0.75	0.87	125	1.20961	-41.9382
4	125	0.3	0.50	1.02	100	-0.17200	-40.0000
5	125	0.4	0.75	0.97	135	0.26457	-42.6067
6	125	0.5	0.25	1.18	90	-1.43764	-39.0849

7	150	0.3	0.75	0.74	140	2.61537	-42.9226
8	150	0.4	0.25	0.99	128	0.08730	-42.1442
9	150	0.5	0.50	1.13	118	-1.06157	-41.4376

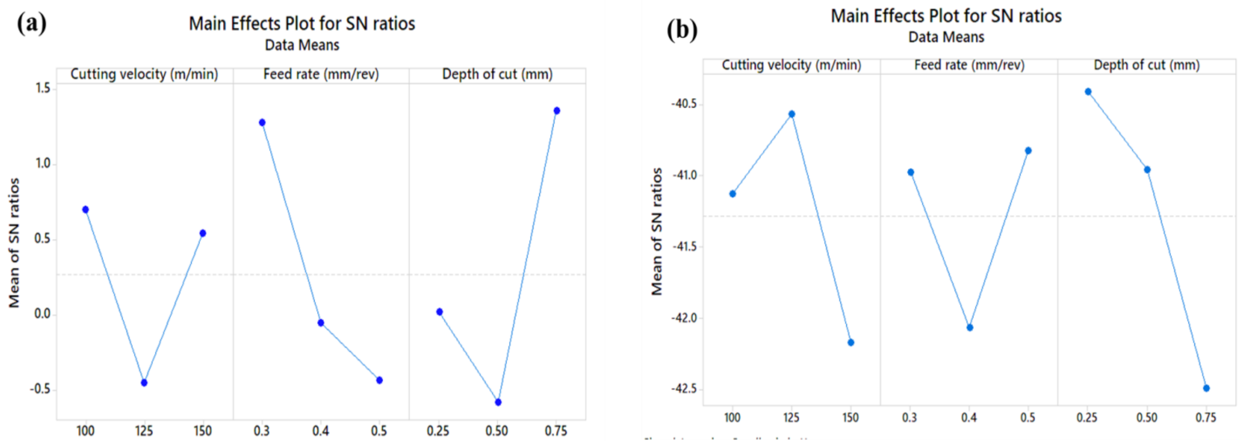

Figure 4.16 Main effect plots of (a) Surface Roughness and (b) Cutting Temperature based on S/N ratio for turning under DRY condition

Table 4.9 ANOVA for Cutting Temperature based on S/N ratio for turning under dry condition

Factor Code	Degrees of freedom	Sum of squares	Mean squares	% Contribution
Cutting velocity	2	3.9765	1.98825	28.85
Feed rate	2	6.9684	3.48419	50.55
Depth of cut	2	2.7529	1.37647	19.97
Residual error	2	0.0852	0.04260	0.618
Total	8	13.7830	6.89151	100

Table 4.10 ANOVA for Average Surface Roughness based on S/N ratio for turning under dry condition

Factor Code	Degrees of freedom	Sum of squares	Mean squares	% Contribution
Cutting velocity	2	2.3461	1.17305	17.8
Feed rate	2	5.9389	2.96947	44.96
Depth of cut	2	4.8700	2.43498	36.9
Residual error	2	0.05212	0.02606	0.39
Total	8	13.2071	6.60356	100

The level of the parameter with the highest value of S/N ratio is the best combination level. The optimal parameter setting for MQL cutting condition is found to be lowest cutting speed of 100m/min, the lower feed rate of 0.5mm/rev and depth of cut 0.5 mm for minimizing surface roughness. Whereas for minimizing temperature 125m/min cutting speed, the lower feed rate of 0.3mm/rev and lowest depth of cut of 0.25mm are the optimum parameter settings for MQL cutting condition. The main effect plots Figure 4.17(a) and (b) are generated using MINITAB statistical software.

To examine the effects of control factors quantitatively, the Analysis of Variance (ANOVA) based on S/N ratio has been performed under MQL cutting condition. The ANOVA is accomplished by separating total variability of S/N ratio, which is measured by the sum of squared deviations from the total mean of S/N ratio into contributions by each of the factors and the error. The summary of ANOVA results for surface roughness is shown in Table 4.13. It can be seen from the ANOVA that feed rate (63.89%) and depth of cut (27.03%) have major contributions, whereas cutting velocity (8.79%) has a less significant role in minimizing the surface roughness.

It is clear from ANOVA results of Table 4.12 that the feed rate (45.41%) and cutting speed (40.91%) are the major contributors, whereas the depth of cut plays less significant roles in minimizing the temperature at MQL cutting condition.

Table 4.11 Control factor settings as per L_9 OA with measured values and corresponding signal to noise ratio for turning with the normal insert in MQL condition

Trial No.	Cutting velocity (m/min)	Feed rate (mm/rev)	Depth of Cut (mm)	Surface Roughness (R_a)(μm)	Temperature (°C)	S/N ratio of R_a	S/N ratio of Temp
1	100	0.3	0.25	0.42	80	7.53501	-38.0618
2	100	0.4	0.50	0.47	119	6.55804	-41.5109
3	100	0.5	0.75	0.52	115	5.67993	-41.2140
4	125	0.3	0.50	0.65	70	3.74173	-36.9020
5	125	0.4	0.75	1.05	95	-0.42379	-39.5545
6	125	0.5	0.25	0.69	79	3.22302	-37.9525
7	150	0.3	0.75	0.68	92	3.34982	-39.2758
8	150	0.4	0.25	0.59	102	4.58296	-40.1720
9	15	0.5	0.5	0.48	110	6.37518	-40.8279

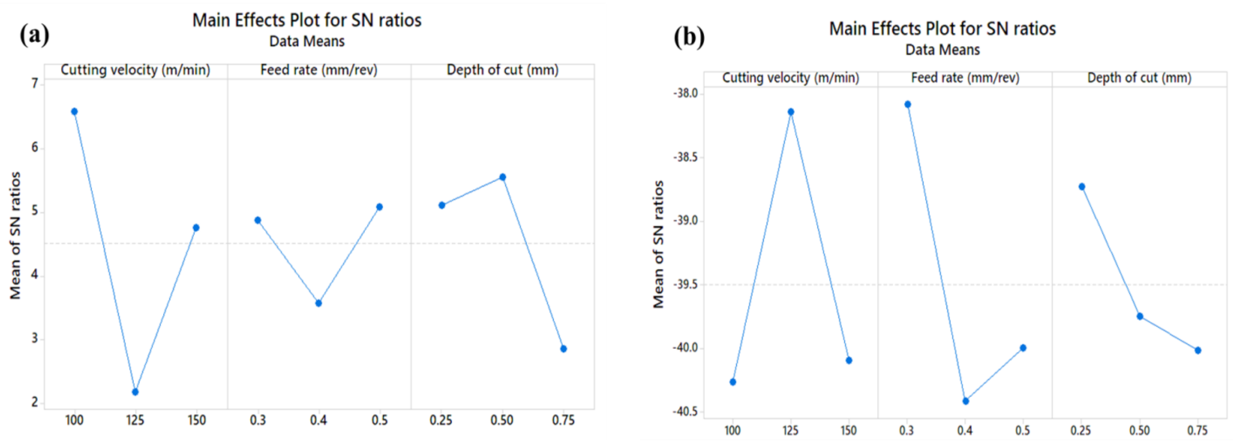

Figure 4.17 Main effect plots of (a) Surface Roughness and (b) Cutting Temperature based on S/N ratio for turning under MQL condition

Table 4.12 ANOVA for Cutting Temperature based on S/N ratio for turning under MQL condition

Factor Code	Degrees of freedom	Sum of squares	Mean squares	% Contribution
Cutting velocity	2	8.3727	4.18633	40.91
Feed rate	2	9.2927	4.64633	45.41
Depth of cut	2	2.7620	1.38099	13.49
Residual error	2	0.0350	0.01751	0.17
Total	8	20.4623	10.23116	100

Table 4.13 ANOVA for Average Surface Roughness based on S/N ratio for turning under MQL condition

Factor Code	Degrees of freedom	Sum of squares	Mean squares	% Contribution
Cutting velocity	2	4.0566	2.0283	8.79
Feed rate	2	29.4755	14.7377	63.89
Depth of cut	2	12.4721	6.2360	27.03
Residual error	2	0.1287	0.0644	0.27
Total	8	46.1328	23.0664	100

4.8 SUMMARY

The machining of difficult-to-cut material Ti-6Al-4V alloy was simulated using FEM-based DEFORM-3D software and static analysis was done using ANSYS software. The cutting force, cutting temperature at chip interface, effective stress, effective strain and total deformations were analyzed. Further, the validation of the simulation results was carried out by conducting experiments. Taguchi optimization was performed for machining Titanium alloy (Ti-6Al-4V) with PCD insert for minimizing the surface roughness and the temperature. The results indicate that MQL has substantial benefit over dry cutting and PCD is justified as a viable cutting tool for machining of titanium alloy. Based on the analysis of the experimental results, the following conclusions are drawn:

- An attempt has been made to make use of micro-holed textured PCD insert for reducing tool wear and increase of the tool life. The modelling of different micro-holed textured inserts was designed in CAD environment.
- The simulation of cutting force, cutting temperature at the interface, total deformations, effective stress and effective strain distributions were successfully achieved.
- In the static analysis, since there was no significant stress concentration due to embedded micro-holes on rake and flank face, it was observed that there is a reduction in cutting force due to the micro-pool lubrication. Therefore, it can be concluded that the micro-holes embedded on the tool rake face do not affect the

mechanical strength of the insert. This is further validated with experimental results and proved that no catastrophic failure occurred for tools with micro-holes.

- In FEM analysis of different micro-hole textured inserts, the design 2, 4, 6 and 7 showed better performance in terms of stress, strain, temperature and cutting force, when compared with other designs and normal insert. Finally, Design 4 and Design 6 were selected as best micro-hole textured patterns and were studied for further validation.
- A combination of MQL, lower cutting speed and depth of cut and higher feed rate is helpful in achieving minimum surface roughness during turning of Titanium alloy (Ti-6Al-4V).
- The feed rate (63.89%) and depth of cut (27.03%) have major effects on minimizing surface roughness. The MQL plays the vital role in minimizing surface roughness.
- The feed rate (45.41%) and cutting speed (40.91%) have key roles in minimizing the temperature in the machining process.
- The temperature level is reduced in the MQL due to its cooling and lubrication effect when compared with the dry cutting condition.
- From this chapter it was observed that the FEM analysis and Tagughi optimization process helped to find that there was no catastrophic failure in the machining of Ti-6Al-4V alloy using micro-hole textured insert and also it helped in proper selection of micro-hole texture pattern. From Taguchi analysis it was observed that machining under MQL environment provided the best performance when compared to dry environment.
- So further in next chapter it is evident that the experimental analysis was performed with best selected pattern and compared the results with the normal cutting insert using the one factor at a time approach method.

CHAPTER-5

MACHINING OPTIMIZATION STRATEGY

5.1 INTRODUCTION

This chapter elucidates the effect of the individual parameters like cutting velocity, feed rate and depth of cut under the MQL environment on performance characteristics such as cutting temperature, machining vibrations, tool flank wear, chip morphology, material removal rate (MRR) and surface integrity (surface roughness, surface topography and microhardness). SEM images have been utilized to analyze the tool flank wear, chip morphology and surface defects analysis.

5.2 EXPERIMENTAL PLAN

The experimental design is based on one parameter at a time approach. This type of experimental design is used to study the effect of each process parameter on the performance characteristics of the turning operation. In this approach, one parameter is varied at a time while the other parameters are kept constant at their respective levels. The control variables that have been chosen to perform the OFATA is shown in Table 5.1. The selection of cutting parameters is purely based on the preliminary tests that have been conducted. The turning of Ti-6Al-4V alloy using normal and modified PCD insert under MQL environment was performed on the ‘MAXTURN’ CNC lathe. The workpiece of diameter 25 mm and 100 mm long billet was used in operation. In the study, the performance factors such as cutting temperature, machining vibrations, tool flank wear, chip morphology, MRR and surface integrity were investigated under MQL environment.

Table 5.1 Controllable factors and their levels for OFATA

Controllable Factors	**Levels**				
	1	**2**	**3**	**4**	**5**
Cutting velocity (m/min)	100	125	150	175	200
Feed Rate (mm/rev)	0.1	0.2	0.3	0.4	0.5
Depth of cut (mm)	0.5	0.75	1	1.25	1.5

5.3 EFFECT OF MICRO-HOLES AND PROCESS PARAMETERS ON CUTTING TEMPERATURE IN MQL ENVIRONMENT

5.3.1 Effect of the modified insert and cutting velocity under MQL environment on cutting temperature

Figure 5.1(a) represents the cutting temperatures obtained at the machining zone at varying cutting velocity condition with different modified cutting inserts and normal insert under MQL environment. From Figure 5.1(a), it was pragmatic that as cutting velocity increases, the temperature at the machining zone increases with modified cutting inserts and normal inserts. This might be due to the development of higher friction between the tool and workpiece which causes more heat generation resulting in increased cutting temperature. Among different cutting inserts, modified Design 2 cutting insert reduced the cutting temperatures significantly as shown in Figure 5.1(a). It can be seen from Figure 5.1(a) that at a low cutting velocity of 100 m/min, the obtained machining zone temperature in normal and Design 1 and 2 cutting insert was 102.8°C, 90.6°C and 81.3°C, respectively. At this condition, the cutting temperature reduction found in Design 2 cutting insert was 21 % and 10% over the machining with normal and Design 1 insert under MQL conditions, respectively. Similarly, at a higher cutting velocity of 200 m/min, the respective cutting temperature reductions found in Design 2 was 24% and 21% compared to normal and Design 1 insert under MQL condition, respectively.

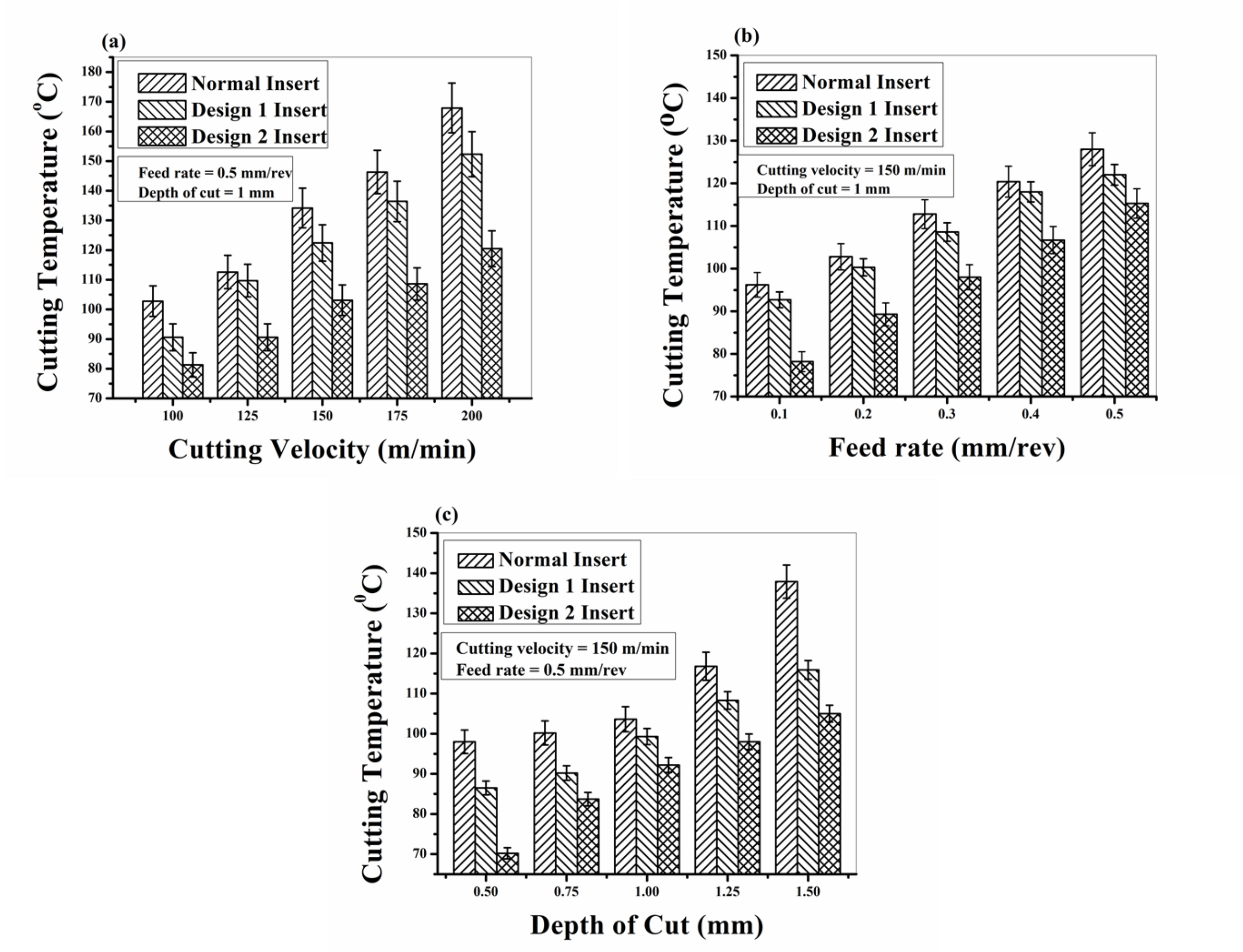

Figure 5.1 Effect of (a) cutting velocity (b) Feed rate and (c) Depth of cut on cutting temperature with normal and modified insert under MQL environment by keeping all other variables as constant at their respective mean levels

From Figure 5.1(a), it can be observed that the cutting temperature in normal insert increases sharply with the rise in cutting velocity due to a rise in friction between the contact asperities. Whereas in Design 1 modified insert machining, almost similar results were found. This might be due to the low friction which is a result of cooling lubrication effects during machining. The reason for temperature reduction in Design 2 insert is because the lubrication was directly applied to the heat generation zones through holes made in the cutting tool insert. As the lubrication is released to the normal atmospheric pressure, it absorbs the heat during the cutting process. As a result, the heat generated when machining Ti-6Al-4V alloy can dissipate quickly by supplying MQL to the heat generation zones through micro-holes made in the rake face and flank face surfaces. This indicates generation of low friction between the tool and workpiece. In overall, the respective temperature reduction range found in machining with Design 2 insert over the normal insert and Design 1insert was 20- 40% and 10-30%, respectively, with the cutting velocity varying from 100 m/min to 200 m/min. Wu et al. (2016) also obtained the same cutting temperature results during the machining of Ti-6Al-4V alloy by using the pulsating heat pipe in self lubrication of cutting tools.

5.3.2 Effect of modified insert and feed rate under MQL environment on cutting temperature

As shown in Figure 5.1(b), as the feed rate increases, the cutting temperature at the machining zone increases. The reason might be firstly, as feed rate rises, the friction between the tool and workpiece increases, which causes the rise of heat generation at contact asperities, resulting in the generation of higher temperature at machining zone. Secondly it might also due to in a specific time, the area of machining zone exposed to friction during cutting process increases with higher feed rate. This makes time available for heat dissipation at the tool-chip interface relatively lesser and hence, contributes to increased temperature. Figure 5.1(b) depicts that at a low feed rate of 0.1 mm/rev, the corresponding temperature values for machining with normal insert, Design 1 and 2 cutting insert was 96.2°C, 92.7°C and 78.2 °C, respectively. At this point, machining with normal insert and Design 1 cutting inserts also have developed the equal temperatures. At this situation, the machining with Design 2 cutting insert reduced the cutting temperatures by 18% and 16%, respectively over the normal insert and Design 1 cutting insert machining conditions. Likewise, the respective temperature drop in machining with Design 2 inserts was 10% and 5 % compared to normal insert and Design 1 cutting insert machining conditions at a high feed rate of 0.5 mm/rev. From the obtained results, it was observed that significant machining zone temperature reduction was found in Design 2 cutting insert over the other cutting inserts. Results show that when the feed rate increases, the lubrication effect decreases. When the feed rate increases, the cutting temperature also increases which results in changes in tool-chip contact. Another reason is that during experimentation accumulation of chips was observed at machining zone due to higher feed rates which causes reduction of penetration capacity of coolant into machining zone. As a whole, the temperature drop range found in Design 2 was 10-18% and 5-15%, respectively, over the machining with normal insert and Design 1 cutting insert with an increase of feed rate from 0.1 – 0.5 mm/rev, respectively.

5.3.3 Effect of modified insert and depth of cut under MQL environment on cutting temperature

As the depth of cut increases, cutting temperature increases under all cutting insert machining conditions as depicted in Figure 5.1(c). This results in increase of rubbing action between the tool and workpiece as depth of cut increases, which causes an increase in cutting temperature. At a high depth of cut of 1.5 mm, machining with Design 2 cutting insert produced 105°C at the machining zone, whereas, machining with normal insert and Design 1 insert developed 137.9°C and 115.8°C, respectively. At this condition, the cutting temperature reduction found in Design 2 cutting insert was 24% and 10%, respectively compared to normal insert and Design 1 cutting insert machining conditions. From Figure 5.1(c), it was perceived that lower cutting zone temperatures were found in machining with Design 2 cutting insert over the other cutting inserts. This difference in cutting temperature is mainly due to the lubrication effect witnessed through the micro-holes, causing reduction of friction between the tool-chip interfaces. From the results, the overall temperature reductions found in machining with Design 2 cutting insert was in the range of 15-30% and 10-35%, respectively compared to machining with normal insert and Design 1 cutting insert under MQL environment.

5.4 EFFECT OF MICRO-HOLES AND PROCESS PARAMETERS ON MACHINING VIBRATIONS IN MQL ENVIRONMENT

Vibration is significant during machining of Ti-6Al-4V alloy, because of significant relative motion between tool and workpiece, which causes self-excited vibrations, leading to the generation of cyclic forces and thereby chatter. This causes waviness of the surface, which may lead to a further variation of chip thickness and forces, leading to increased vibration. With respect to machining with normal insert and modified cutting insert Design 1 and Design 2 for turning operation, there is a peak showing a substantial increase in vibration amplitude at around 2- 4 kHz, corresponding to the natural frequency of the tool holder which is around 3.1 kHz, for a tool overhang length of 100 mm, with increase in tool wear. Similar observations were made by Fang et al. (2012) while analyzing vibration signals during high-speed machining of Inconel 718, where a comparison of wavelet-based denoising techniques was carried out. The raw data that is fetched during machining with the highest cutting velocity is depicted in Figure 5.2, respectively.

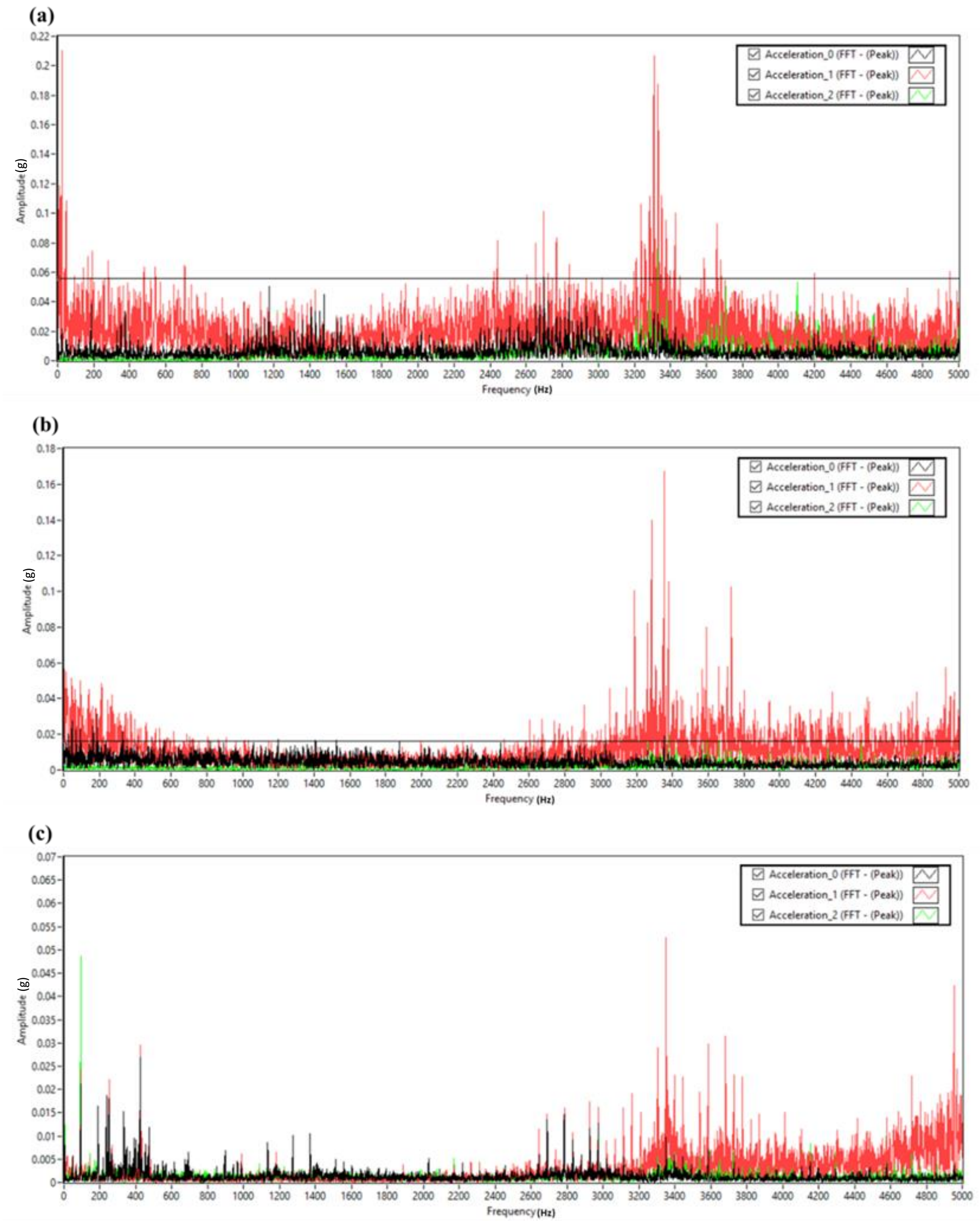

Figure 5.2 Raw Data of vibration amplitude at a high cutting velocity of 200 m/min (a) normal insert (b) Design 1 insert (c) Design 2 insert

5.4.1 Effect of the modified inser5t and cutting velocity under MQL environment on machining vibrations

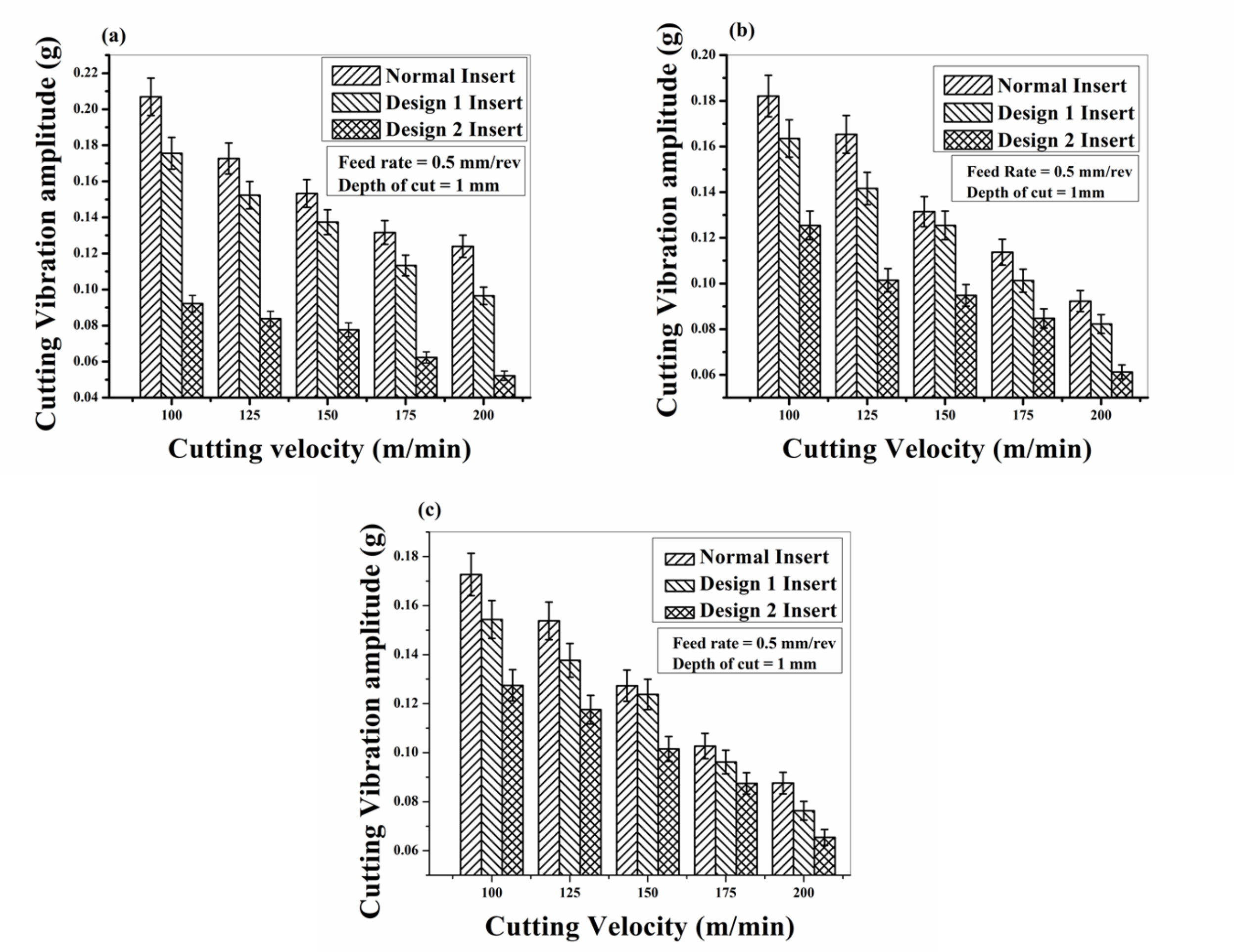

Figure 5.3 Variation of vibration amplitude of cutting velocity (a) Cutting speed direction (b) Feed direction (c) Depth of cut direction

Figure 5.3(a) shows the variation of vibration amplitude in cutting speed direction (V_y), Feed direction (V_x) (Figure 5.3(b)) and Depth of cut direction (V_z) (Figure 5.3(c)) with normal insert and modified cutting inserts Design 1 and Design 2 under different machining conditions. The comparison of results shows that the vibration amplitudes have significantly higher values in the case of machining with normal insert when compared with modified cutting insert. In this research cutting vibration fetched in cutting speed direction is considered for analysis since the other two directions have negligible machining vibrations as shown in Figure 5.3. The cutting vibration amplitude of feed direction and depth of cut direction is very minimal when compared to the cutting speed direction. The same observations were also observed by Grynal et al. (2016) during the machining of Ti-6Al-4V alloy using tungsten carbide insert. The vibration amplitude in cutting speed direction is significantly higher in the normal insert and Design 1 modified cutting insert, thereby making it sensitive to the variation of flank wear on the insert with increasing the cutting parameters. This variation in the behaviour of the vibration amplitudes with flank wear can be attributed not only to the initial condition of tool edge but also to the behaviour of the flank wear as it develops on the tool. Development of flank wear is more severe in case of normal insert and Design 1 cutting insert when compared with Design 2 cutting insert. Due to the presence of micro-hole lubrication the cutting temperature is reduced from which the tool wear will decrease leading to the decrease in cutting vibration.

From Figure 5.3(a) it is evident that as the cutting velocity increases cutting vibration decreases in both modified cutting inserts and normal insert machining. This effect is owing to an increase in cutting temperature with an increase in cutting velocity. It leads to softening of machining material and also reduces the coefficient of friction at the tool-chip interface which results in an increase in shear plane angle causing a decrease in the shearing area. This decreases the cutting vibration. It is apparent from Figure 5.3(a) that lower amplitude of cutting vibration was observed in machining with Design 2 cutting insert when compared to machining with normal insert and Design 1 cutting insert. It has been noted that the values of amplitude of cutting vibration at the cutting velocity of 100 m/min, the feed rate of 0.5 mm/rev and depth of cut of 1 mm was 0.09218 g for Design 2 cutting insert and 0.20691 g and 0.17557 g for normal insert and Design 1 cutting insert, respectively. It was found that machining with Design 2 cutting insert reduced 55.44 % and 47.49 % of the amplitude of cutting vibration over the machining with normal insert and Design 1 cutting insert, respectively. This effect is mainly due to the better lubrication characteristics of modified cutting insert causing the lower coefficient of friction at tool-chip interface resulting in less weldability of chips to the tool rake face. Modified cutting inserts micro-pool lubrication enables reduction of cutting temperature. This results in reduced adhesion between tool and workpiece interacting surfaces. It increases the tool hardness, lowers tool wear and hence, low cutting vibration. In the present work, when cutting velocity increased from 100 m/min to 200 m/min at constant feed rate of 0.5 mm/rev and depth of cut of 1 mm, the machining with Design 2 cutting insert reduced cutting vibration by 50.37 % and 36.55% over normal insert and Design 1 cutting insert as shown in Figure 5.3(a).

5.4.2 Effect of the modified insert and feed rate under MQL environment on cutting vibration

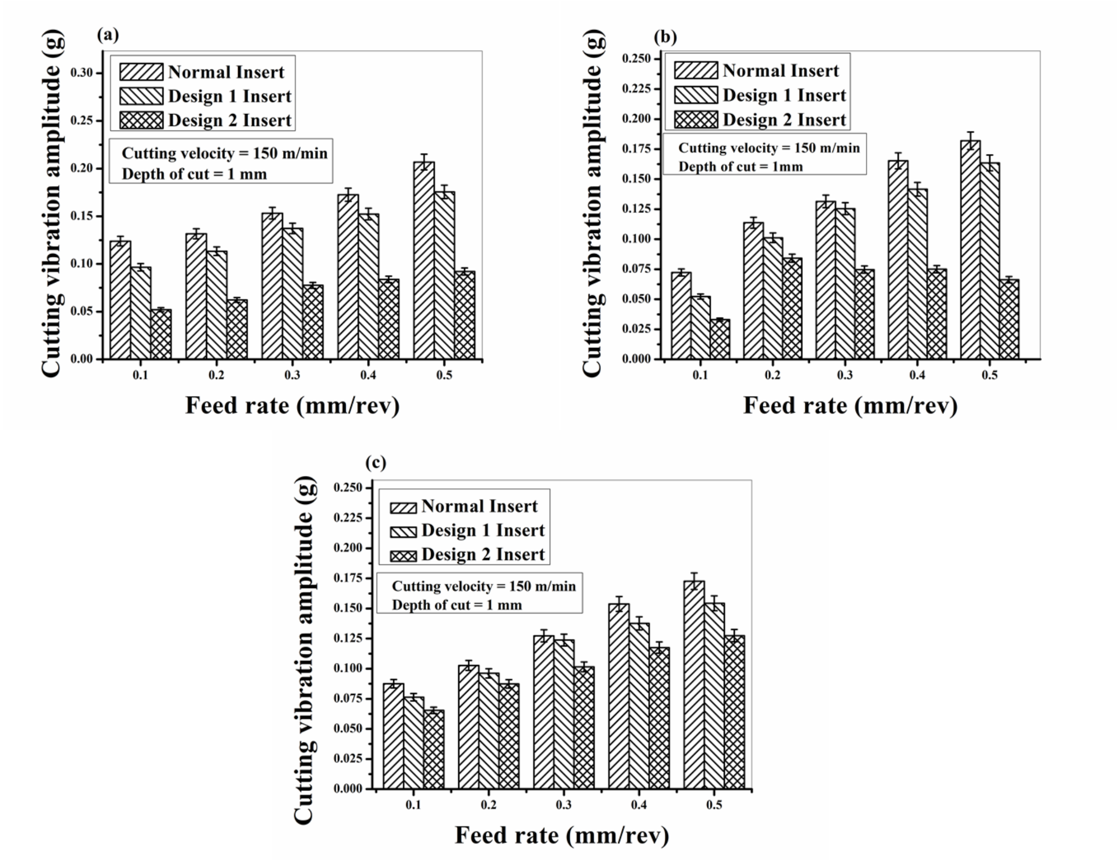

Figure 5.4 Variation of vibration amplitude of Feed rate (a) Cutting speed direction (b) Feed direction (c) Depth of cut direction

Figure 5.4 depicts the machining vibrations in all three directions i.e., cutting force (Figure 5.4(a)), feed direction (Figure 5.4 (b)) and depth of cut direction (Figure 5.4 (c)), respectively. From the Figure 5.4 (a), it is evident from cutting speed direction that as there is an increase in feed rate, the cutting vibration amplitude is also increased in both normal inserts and modified cutting inserts. This is because as feed rate increases, the material removal rate will be high and the plastic deformation of machining material increases, which increases the amplitude of machining vibrations. It is apparent from Figure 5.4 (a) that Design 2 cutting insert depicts the minimum amplitude of cutting vibration when compared to normal insert and Design 1 cutting insert respectively. It was observed that cutting vibration got reduced by amplitude of 37.5% and 31.8% in Design 2 cutting insert, when compared with normal insert and Design 1 cutting insert, respectively. This is due to the effect of modified cutting insert lubrication method, which helps in the continuous supply of coolant to the chip-tool interface, resulting in lower cutting temperatures. This minimum cutting temperature helps to reduce the chips adhesion to the cutting tip resulting in minimum vibration.

5.4.3 Effect of the modified insert and depth of cut under MQL environment on machining vibration

Figure 5.5 depicts the machining vibrations in all three directions i.e., cutting force (Figure 5.5 (a)), feed direction (Figure 5.5 (b)) and depth of cut direction (Figure 5.5 (c)), respectively. From the cutting speed direction of machining vibrations is shown in Figure 5.5 (a), it is palpable that the machining vibrations amplitude increases with increase in the depth of cut in both normal inserts and modified cutting inserts. The machining vibrations amplitude in Design 2 cutting insert shows the minimum machining vibrations level when compared to normal insert and Design 1 cutting insert, respectively. It was observed that the cutting vibration amplitude of Design 2 cutting insert was reduced by about 20%-25% over the normal and Design 1 cutting inserts as the depth of cut increased from 0.5 mm to 1.50 mm, respectively. This variation is mainly due to the reduction in cutting temperature which is due to the micro-pool lubrication through the modified inserts, which provides the cushioning effect from the MQL mist spray and also helps in reducing friction at the chip-tool interface resulting in minimum machining vibrations.

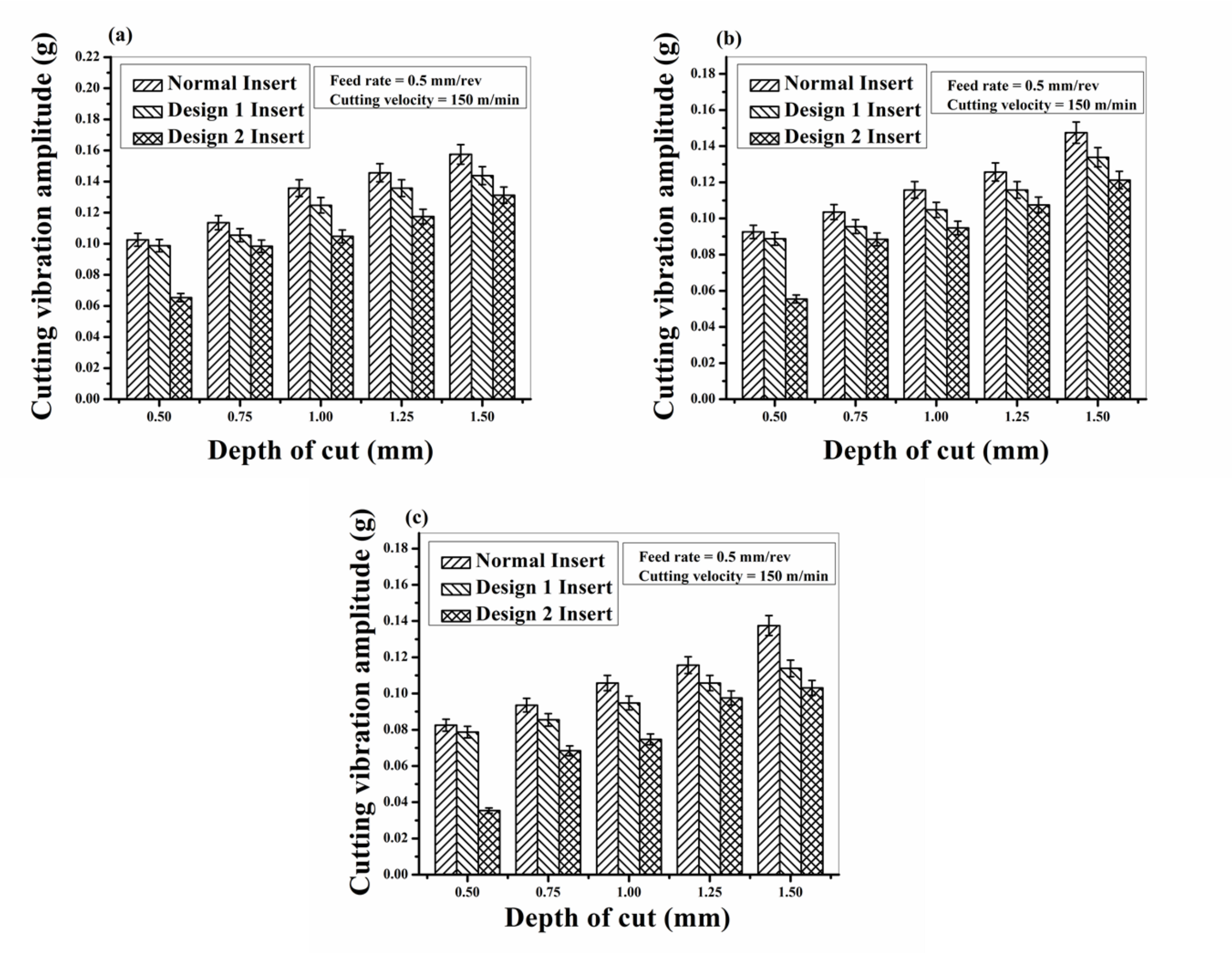

Figure 5.5 Variation of vibration amplitude of Depth of cut (a) Cutting speed direction (b) Feed direction (c) Depth of cut direction

5.5 EFFECT OF MICRO-HOLES AND PROCESS PARAMETERS ON TOOL FLANK WEAR IN MQL ENVIRONMENT

5.5.1 Effect of the modified insert and cutting velocity under MQL environment on Tool flank wear

Tool flank wear is the most important tool wear occurring in a machining operation. Flank wear is primarily attributed to the rubbing of the tool along the mechanical surfaces. The variation in flank wear with the cutting velocities after 5 mins of machining with normal insert, Design 1 and 2 cutting insert is shown in Figure 5.6 (a). Tool flank wear was measured for different cutting velocities and increasing trend was observed. This is because, at higher cutting velocity, high cutting temperature develops within a tiny time. Also, the contact area decreases between the tool and chip interface at high cutting velocity, causing cutting edge very closely exposed to high cutting temperatures leading to thermal softening of the tool material resulting in more tool wear when cutting tool contacts the workpiece at such conditions.

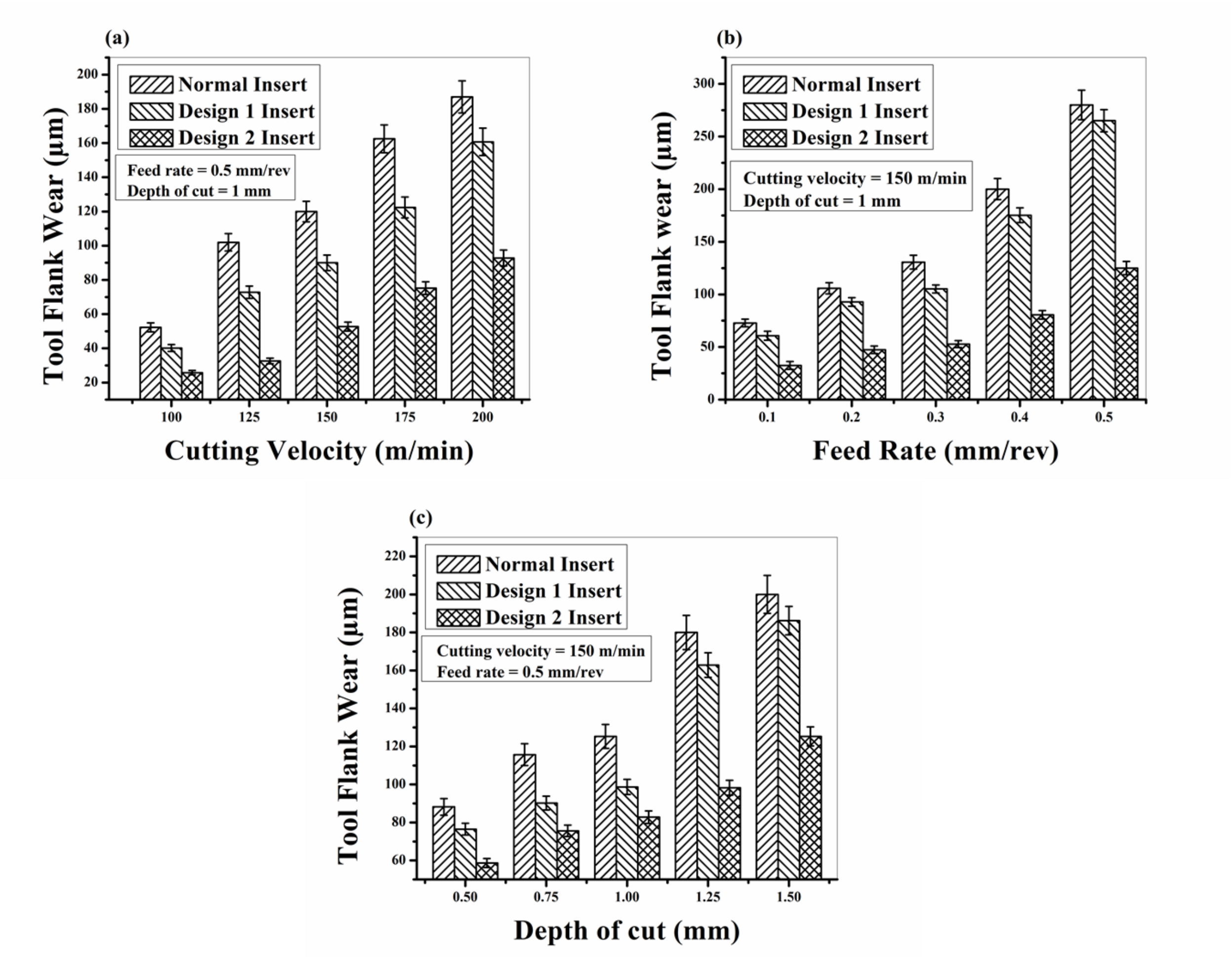

Figure 5.6 Effect of (a) cutting velocity (b) Feed rate and (c) Depth of cut on Tool flank wear with normal and modified insert under MQL environment

From Figure 5.6 (a), it was observed that at a low cutting velocity of 100 m/min, flank wear was 58.7µm in machining with Design 2 cutting insert, whereas, it was 88.2 µm and 86.5 µm for machining with normal and Design 1 cutting insert, respectively. It was found that flank wear reduction in machining with Design 2 was 51% and 36%, respectively, compared to normal insert and Design 1 cutting insert. This is due to the control of abrasion and attrition wear mechanisms through a reduction in the cutting zone temperature and less adhesion between the chip-tool by the application of MQL at cutting zones through the micro-pool lubrication. The micro-hole orientation on the tool rake face and the flank face helps in proper lubrication at the chip-tool interface. It was found that the tool flank wear reduction in Design 2 with an increased cutting velocity from 100 m/min to 200 m/min, constant feed rate of 0.5 mm/rev and constant depth of cut of 1 mm was 92.8 µm whereas, it was 187 µm and 160.7 µm for normal insert and Design 1 cutting insert, respectively.

5.5.2 Effect of modified insert and Feed rate under MQL environment on Tool flank wear

From Figure 5.6 (b), it was observed that as feed rate increases, flank wear increases under normal and modified insert machining conditions. This trend leads to the higher cutting temperatures caused by higher material removal rates at higher feed rates. It results in higher tool flank wear. Another reason might be the increase of cutting force with an increase in feed rate which reduces the strength of the tool. It is seen from Figure 5.6 (b), that at a low feed rate of 0.1 mm/rev, the respective tool flank wear measurements were 72.8 µm, 60.7 µm and 32.5 µm for normal insert, Design 1 and 2 cutting insert, respectively. At this point, the respective tool flank wear reduction was found in machining with Design 2 cutting insert with 56% and 47% over the machining with normal insert and Design 1 cutting insert. This variation is mainly due to the better control of cutting temperature with the micro-pool lubrication through MQL. Through micro-pool lubrication, there is less adhesion of chips to the cutting tool, which reduces the tool flank wear. On the whole, the results show that Design 2 cutting insert reduces the flank wear from 55% and 53% when compared with normal insert and Design 1 cutting insert with the increase in feed rate from 0.1 mm/rev to 0.5 mm/rev, respectively.

5.5.3 Effect of modified insert and depth of cut under MQL environment on Tool flank wear

Figure 5.6 (c) indicates that as the depth of cut increases, tool flank wear also increases in the normal insert and modified insert machining conditions. This effect is due to more contact between the tool and workpiece at high depth of cuts, causing generation of higher friction between the contact asperities. It leads to thermal softening of tool resulting in more tool wear. At a low depth of cut of 0.5 mm, the tool flank wear observed were 88.2 µm, 76.5 µm, and 58.7 µm with normal insert and modified inserts Design 1 and 2, respectively. The flank wear reductions found in Design 2 cutting insert at this point was 33.4% and 23.2% over the machining with normal insert and Design 1 cutting insert. Compared to other cutting inserts under MQL condition, the significant reduction of flank wear was found in machining with Design 2 cutting insert as depicted in Figure 5.6 (c). This result in control of adhesion and abrasion wear mechanisms due to the mist of lubricant through micro-holes. It provides for lower cutting temperatures. When the depth of cut increases from 0.5 mm to 1.5 mm at a constant cutting velocity of 150 m/min and feed rate of 0.5 mm/rev, machining with Design 2 cutting insert reduces flank wear from 37.35% and 32.7 % compared to normal insert and Design 1 cutting insert, respectively.

Table 5.2 illustrates the SEM images of the tool flank wear at various cutting conditions after 5 minutes of machining in the micro-holed textured insert and normal commercially available insert under MQL environment. Abrasion and adhesion wear mechanisms were observed on the flank face of the cutting insert under micro-holed inserts and normal inserts. Higher flank wear was observed in normal insert machining compared to micro-holed designed insert. The higher temperature in normal insert machining causes the strong adhesion of chips to the rake face forming built-up edges (BUE). From Table 5.2, the adhesion of the machined material to the cutting tool is evident. Table 5.3 shows the creator wear and notch wear at the rake face of the cutting inserts.

Table 5.2 SEM Images of tool flank wear at different machining conditions

Cutting conditions	Cutting Inserts		
	Normal Insert	Design 1 Insert	Design 2 Insert
Low Cutting velocity (100 m/min)	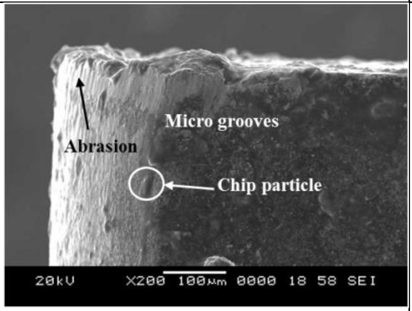 Abrasion Micro grooves Chip particle 20kV X200 100μm 0000 18 58 SEI	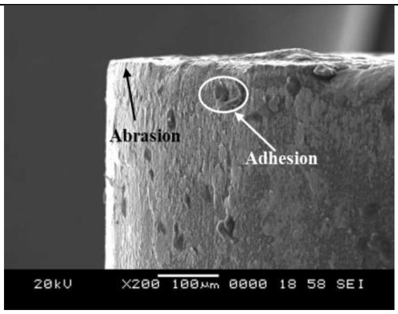 Abrasion Adhesion 20kV X200 100μm 0000 18 58 SEI	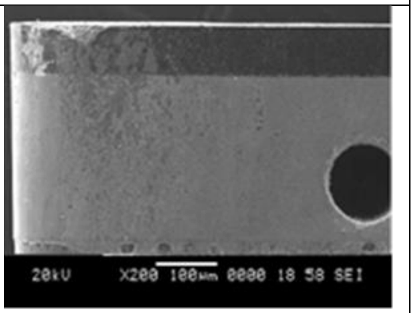 20kV X200 100μm 0000 18 58 SEI
High Cutting velocity (200 m/min)	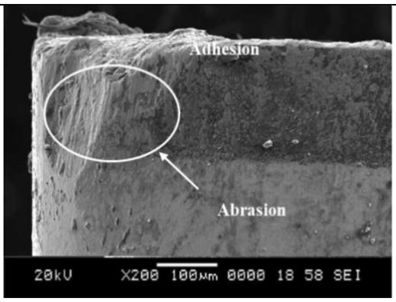 Adhesion Abrasion 20kV X200 100μm 0000 18 58 SEI	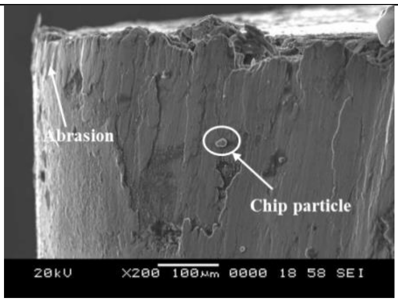 Abrasion Chip particle 20kV X200 100μm 0000 18 58 SEI	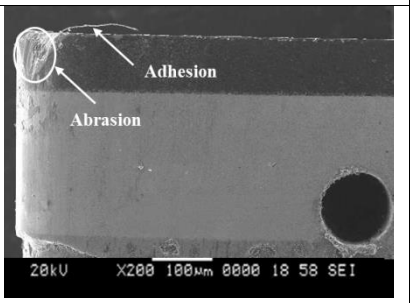 Adhesion Abrasion 20kV X200 100μm 0000 18 58 SEI
Low Feed rate (0.1 mm/rev)	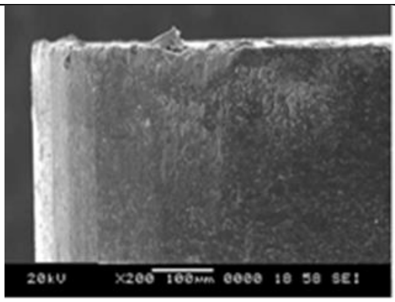 20kV X200 100μm 0000 18 58 SEI	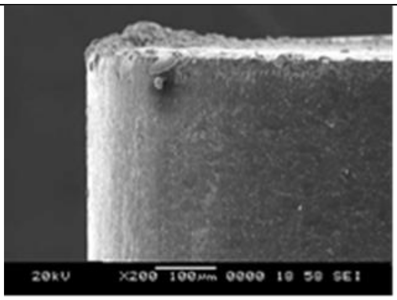 20kV X200 100μm 0000 18 58 SEI	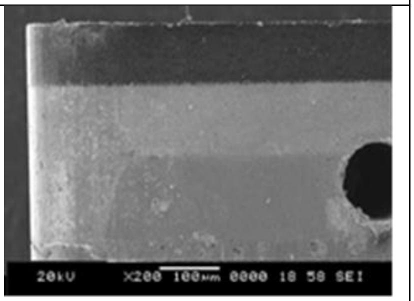 20kV X200 100μm 0000 18 58 SEI
High Feed rate (0.5 mm/rev)	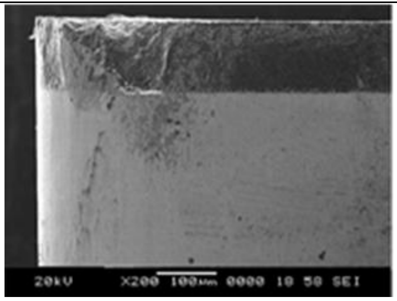 20kV X200 100μm 0000 18 58 SEI	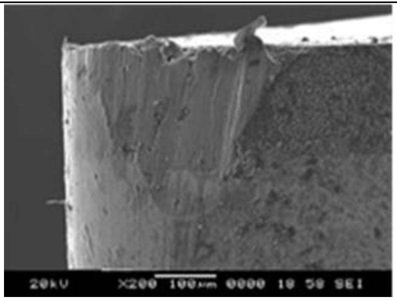 20kV X200 100μm 0000 18 58 SEI	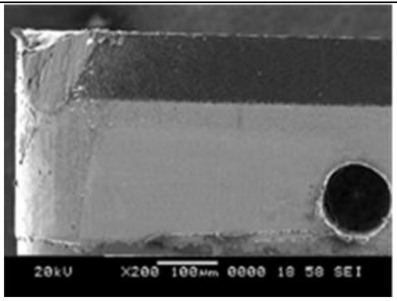 20kV X200 100μm 0000 18 58 SEI

Low depth of cut (0.5 mm)	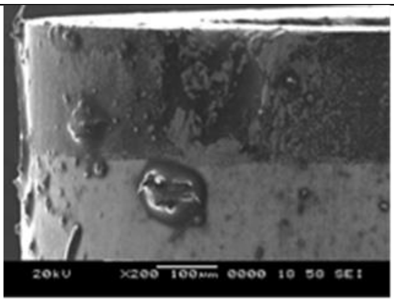 20kV X200 100µm 0000 10 50 SEI	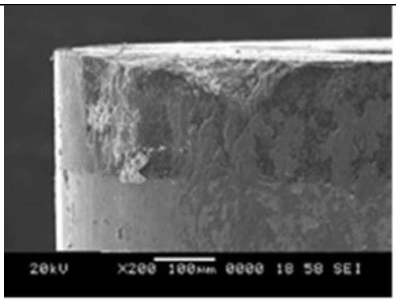 20kV X200 100µm 0000 18 50 SEI	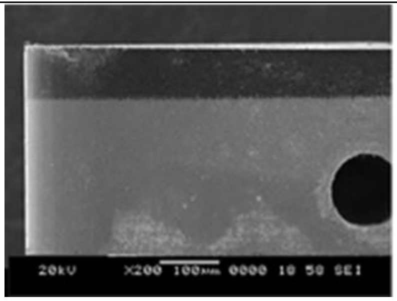 20kV X200 100µm 0000 10 50 SEI
High depth of cut (1.5 mm)	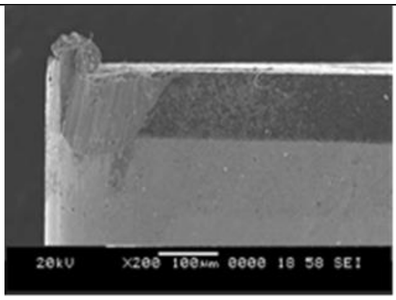 20kV X200 100µm 0000 18 50 SEI	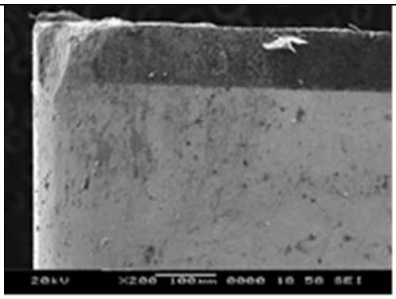 20kV X200 100µm 0000 18 50 SEI	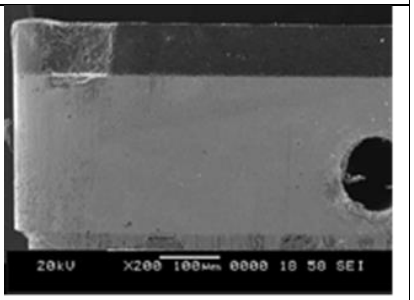 20kV X200 100µm 0000 18 50 SEI

Table 5.3 SEM Images of tool flank wear at different machining conditions

Cutting conditions	Cutting Inserts		
	Normal Insert	Design 1 Insert	Design 2 Insert
Low Cutting velocity (100 m/min)	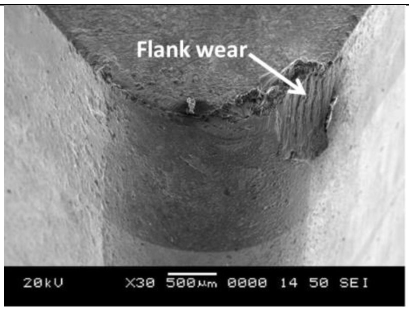 Flank wear 20kV X30 500µm 0000 14 50 SEI	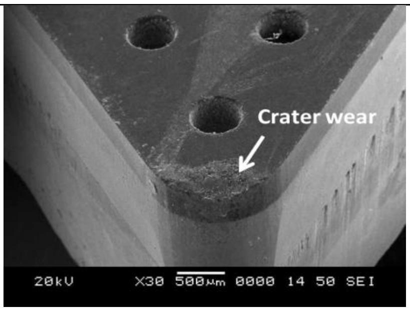 Crater wear 20kV X30 500µm 0000 14 50 SEI	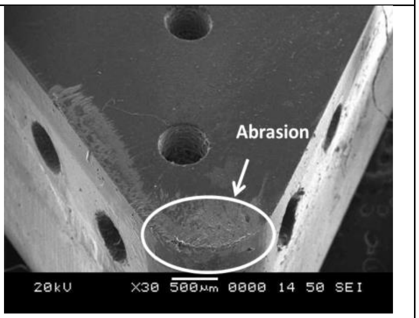 Abrasion 20kV X30 500µm 0000 14 50 SEI
High Cutting velocity (200 m/min)	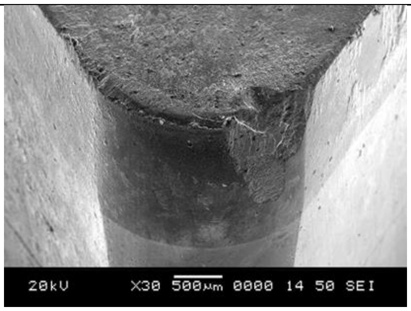 20kV X30 500µm 0000 14 50 SEI	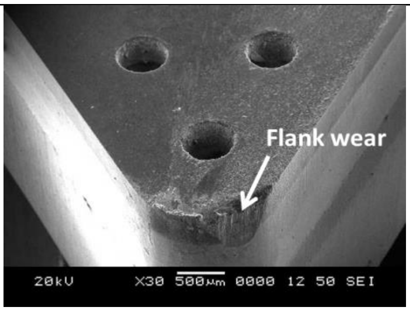 Flank wear 20kV X30 500µm 0000 12 50 SEI	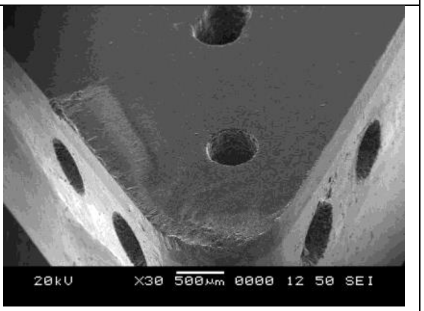 20kV X30 500µm 0000 12 50 SEI

5.6 EFFECT OF MICRO-HOLES AND PROCESS PARAMETERS ON SURFACE ROUGHNESS IN MQL ENVIRONMENT

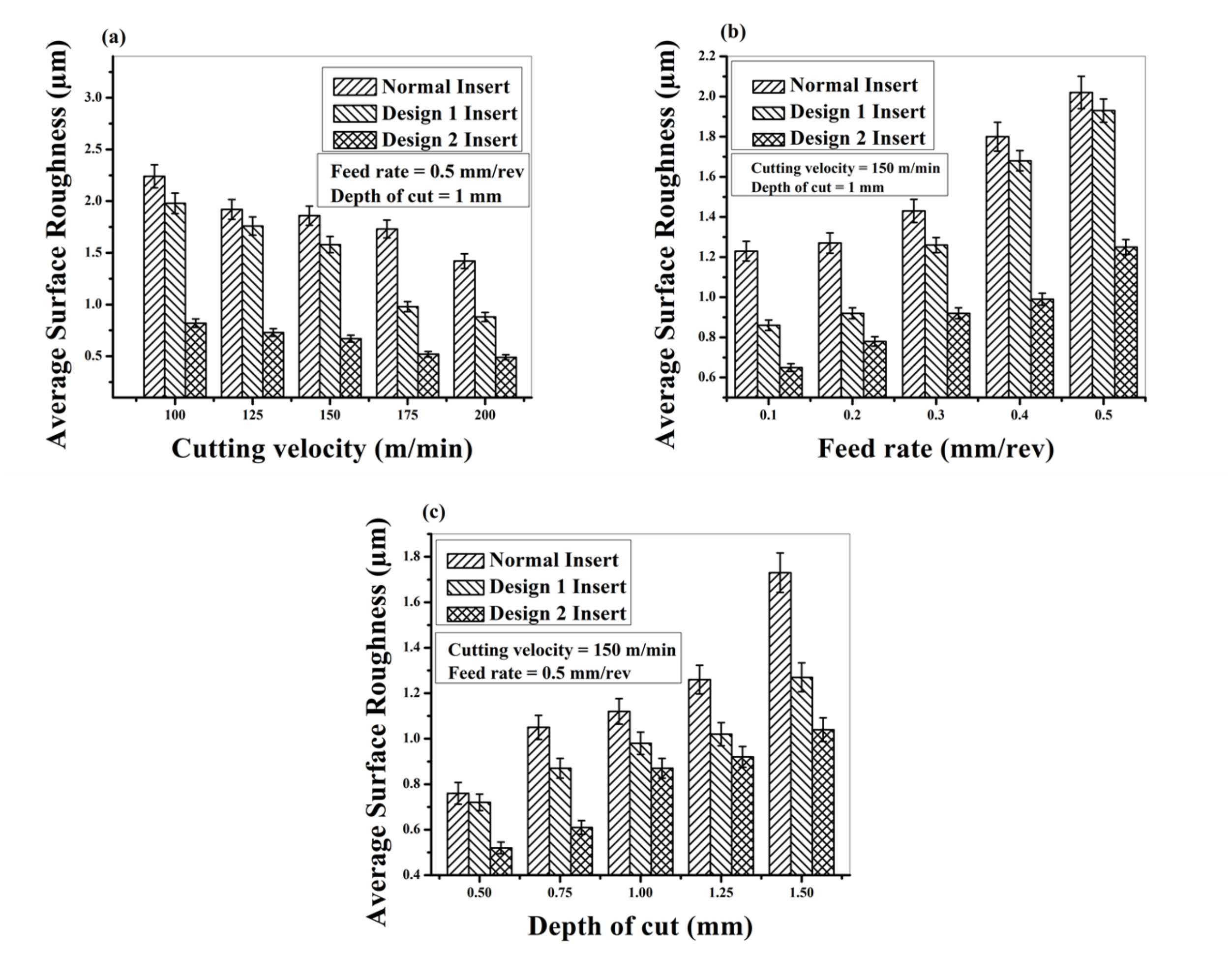

Figure 5.7 Effect of (a) cutting velocity (b) Feed rate and (c) Depth of cut on Surface roughness with normal and modified insert under MQL environment by keeping all other variables as constant at their respective mean levels.

5.6.1 Effect of the modified insert and cutting velocity under MQL environment on surface roughness

In the current study, the average surface roughness value (R_a) was considered for representing the surface finish of the machined surfaces since, it is the most commonly used in manufacturing industries across the world. The effect of the modified insert and cutting velocity on surface roughness is as shown in Figure 5.7 (a). In this graph decreasing trend was observed for all machining conditions. This effect is due to increase of cutting temperature with increase in cutting velocity. This causes thermal softening of workpiece material and removal of more and more surface discontinuities and flaws at high cutting velocities resulting in reduced surface roughness (Pawade and Joshi 2011). At the cutting velocity of 100 m/min, the obtained surface roughness in Design 2 cutting insert was 0.86 µm whereas, it was 2.24 µm and 1.98 µm for normal insert and Design 1 cutting insert, respectively as depicted in Figure 5.7 (a). At this point, the decrease of surface roughness in Design 2 cutting insert was 61% and 56% compared to normal insert and Design 1 cutting insert, respectively. At a higher cutting velocity of 200 m/min, the obtained surface roughness values for the respective machining with normal insert and Design 1 cutting insert was 1.42 µm and 0.88 µm, whereas, for Design 2 cutting insert, it was 0.49 µm as shown in Figure 5.7 (a). At this point, the reduction of surface roughness found in Design 2 cutting insert was 65% and 44% over the normal insert and Design 1 cutting insert machining conditions. The surface finish of the machined surface is greatly influenced by the tool flank wear. At all cutting velocities, Design 2 cutting insert machining substantially reduced the surface roughness value when compared to other machining environments as shown in Figure 5.7 (a). This results in substantial control of machining zone temperatures with the micro-pool lubrication at the machining zone, led to lower tool wear. Thus the generation of tool marks is lesser and less debris (which comes from adhesion wear) on the machined surfaces deposited.

5.6.2 Effect of modified insert and feed rate under MQL environment on surface roughness

Figure 5.7 (b) shows the variation of surface roughness with an increase in the feed rate. When the feed rate increases, increasing trend was observed for surface roughness in the modified cutting insert and normal insert machining. This is due to the higher temperature developments at the high feed rate causing an increase in tool wear. Hence, tool profile marks are formed on the machined surface. It is clear from the Figure 5.7 (b) that lower surface roughness values were observed in Design 2 cutting insert when compared to machining with normal insert and Design 1 cutting insert. The surface roughness value at a feed rate of 0.1 mm/rev, cutting velocity of 150 m/min and depth of cut of 1mm was 1.23 µm, 0.86 µm and 0.65 µm, respectively, in machining with normal insert, Design 1 and Design 2 cutting insert. It was noted that machining with Design 2 cutting insert reduces the surface roughness value by 47% and 24% over the normal insert and Design 1 cutting insert. This is due to the lubrication through micro-holes on the rake and flank face of the cutting insert causing lower coefficient of friction. It reduces the cutting force leading to minimum vibrations, resulting in minimum feed marks on the machined surface. Another reason maybe the observed chip breakability improvement in Design 2 cutting insert leading to less accumulation of chips near the cutting zone. Thereby absolute avoidance of frictional contact between the chips and the machined surface is observed. When the feed rate increases from 0.1 mm/rev to 0.5 mm/rev at a cutting velocity of 150 m/min and depth of cut of 1 mm, Design 2 cutting insert reduces the surface roughness from 38% and 35% compared to machining with normal insert and Design 1 cutting insert, respectively.

5.6.3 Effect of modified insert and depth of cut under MQL environment on surface roughness

From Figure 5.7 (c) it is seen that surface roughness increases with an increase in depth of cut. Because, as the depth of cut increases cutting forces also increase due to higher tool vibrations resulting in an increase in the surface roughness. From the Figure 5.7 (c) it was observed that low surface roughness was obtained in Design 2 cutting insert machined surface when compared to normal and Design 1 cutting insert machined surfaces. It has been observed that at depth of cut 0.5 mm, cutting velocity of 150 m/min and feed rate of 0.5 mm/rev surface roughness was 0.96 µm, 0.72 µm and 0.52 µm in the normal insert, Design 1 and Design 2 cutting insert, respectively. At this condition Design, 2 cutting insert reduces the surface roughness by 45% and 27% over the normal insert and Design 1 cutting insert. This variation is mainly due to the effect of micro-holes on the cutting insert with a different orientation which lowers the cutting forces. The results showed that by changing the depth of cut from 0.5 mm to 1.5 mm with a constant feed rate of 0.5 mm/rev and cutting velocity of 150 m/min conditions Design 2 cutting insert reduces the surface roughness by 39% and 18% compared to normal insert and Design 1 cutting insert.

Table 5.4 shows the SEM images of machined surfaces under normal insert, Design 1 and Design 2 cutting insert. Lower voids, material debris, smeared material and low-intensity surface peaks were observed in machined surfaces.

Table 5.4 SEM Images of machined surfaces at different machining conditions

Cutting conditions	Cutting Inserts		
	Normal Insert	Design 1 Insert	Design 2 Insert
Low Cutting velocity (100 m/min)	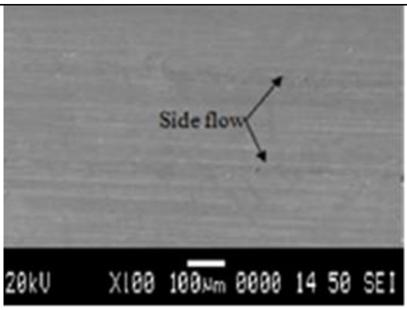 Side flow 20kV X100 100μm 0000 14 50 SEI	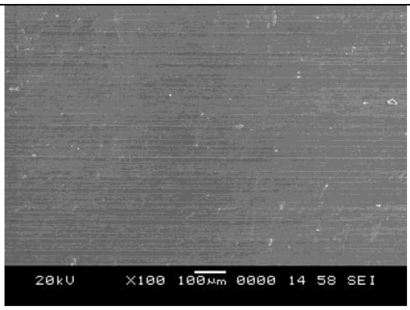 20kV X100 100μm 0000 14 58 SEI	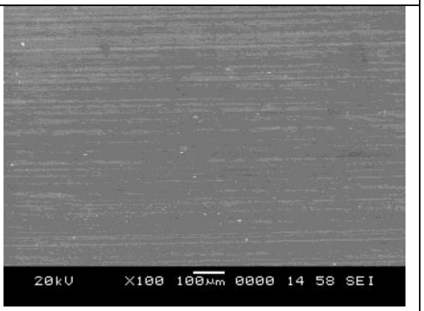 20kV X100 100μm 0000 14 58 SEI
High Cutting velocity (200 m/min)	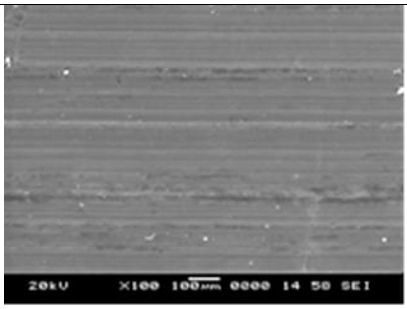 20kV X100 100μm 0000 14 50 SEI	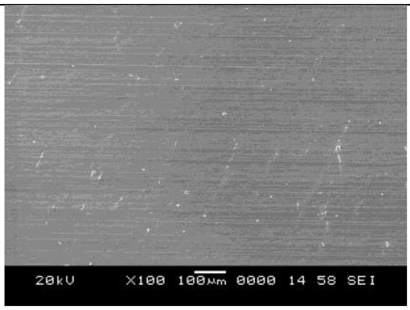 20kV X100 100μm 0000 14 58 SEI	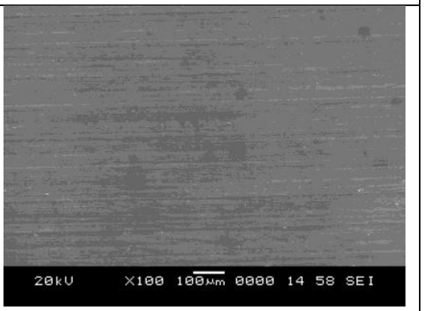 20kV X100 100μm 0000 14 58 SEI
Low Feed rate (0.1 mm/rev)	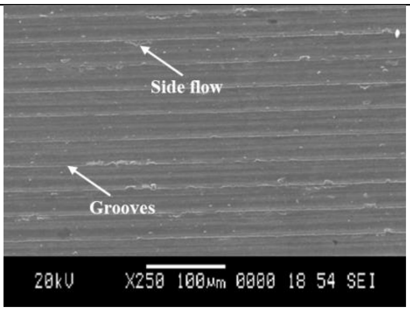 Side flow Grooves 20kV X250 100μm 0000 18 54 SEI	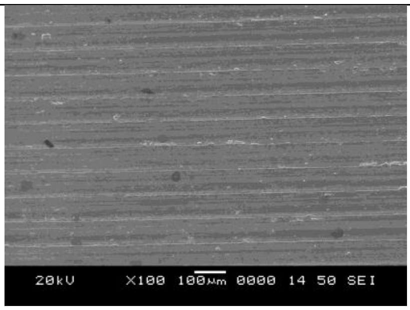 20kV X100 100μm 0000 14 50 SEI	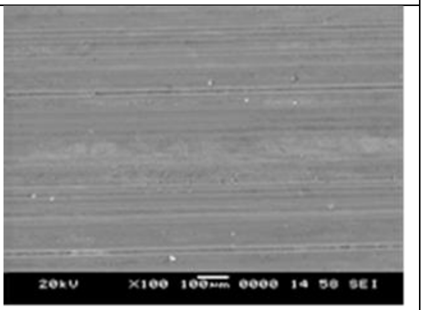 20kV X100 100μm 0000 14 50 SEI

High Feed rate (0.5 mm/rev)	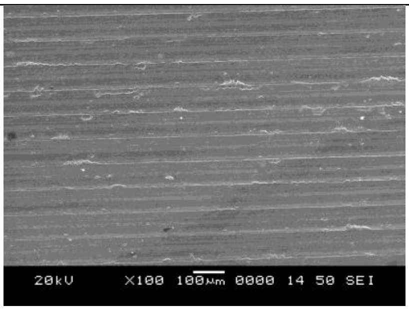 20kV X100 100µm 0000 14 50 SEI	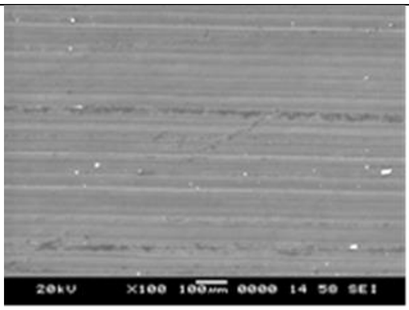 20kV X100 100µm 0000 14 50 SEI	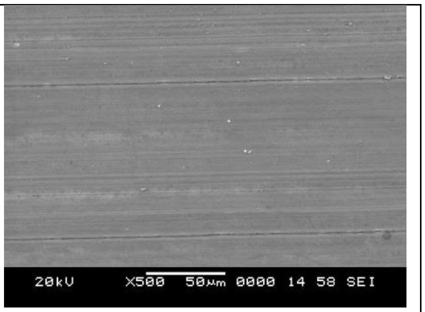 20kV X500 50µm 0000 14 58 SEI
Low depth of cut (0.5 mm)	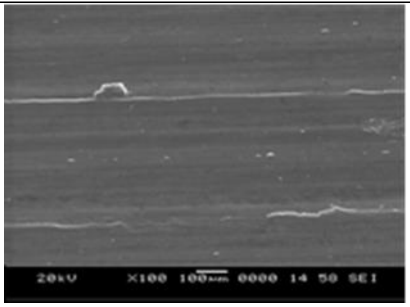 20kV X100 100µm 0000 14 50 SEI	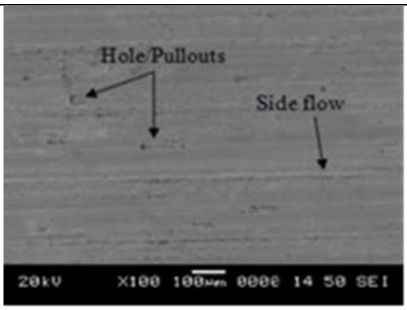 Hole/Pullouts Side flow 20kV X100 100µm 0000 14 50 SEI	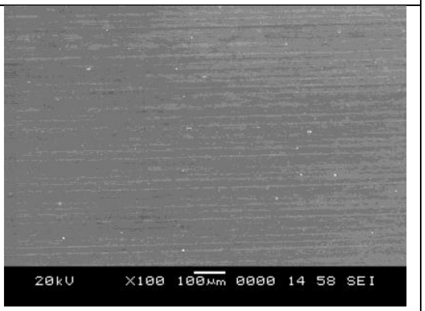 20kV X100 100µm 0000 14 58 SEI
High depth of cut (1.5 mm)	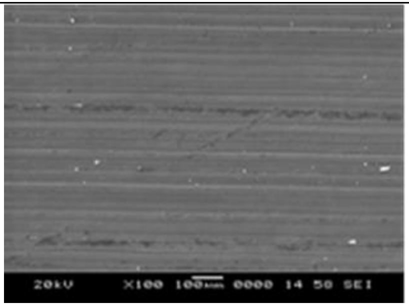 20kV X100 100µm 0000 14 50 SEI	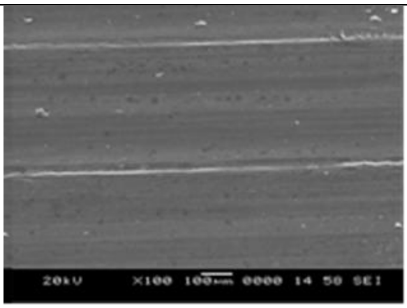 20kV X100 100µm 0000 14 50 SEI	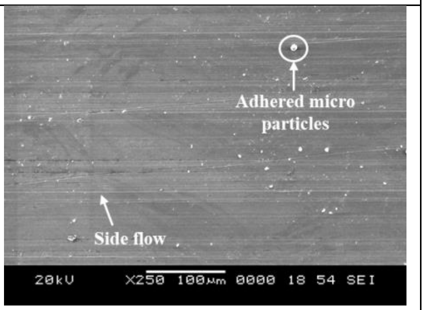 Adhered micro particles Side flow 20kV X250 100µm 0000 18 54 SEI

5.7 CHIP MORPHOLOGY

In metal cutting application, chip type plays a significant role in the machining performance. The long, continuous chip can create hindrance to the operator in conventional machine shop as well production. Also, these can damage the machined surface and cutting tool. Hence, it can increase the maintenance cost. Table 5.5 shows images of chips collected during the experimental work carried out under MQL condition with normal insert and designed insert. It is observed that as cutting velocity increases, chip thickness reduces. Because as cutting velocity increases tool-chip contact length decreases. This leads to a decrease in chip thickness (Bermingham et al. 2012). When the cutting velocity is varied from low to high with a constant feed rate and depth of cut of

0.5 mm/rev and 1 mm, in machining with normal insert, chip morphology changes were observed from long serrated thick tabular chips to very long snarled tabular chips. At the same cutting condition, machining with Design 1 and Design 2 cutting insert, chip morphology changes from medium tabular, medium fine chips to very short ribbon chips. This effect is mainly due to the micro-pool lubrication at the cutting zone effectively reducing the cutting temperatures leads to the chips changes from ductile to the brittle nature resulting improved chip breakability. At higher cutting velocities, minimum thickness chips were observed in machining with Design 2 cutting insert compared to normal insert and Design 1 cutting insert. This effect is because of the retaining the sharp edge of cutting tool by lubrication through micro-holes on the cutting inserts and avoidance of built-up-edges thus reduces the residuals on the chip surface (Venkata Ramana et al. 2014). From SEM images it is evident that less residues were observed in Design 2 cutting insert as shown in Table 5.6. In general when the feed rate increases the chip thickness increases. In the present work, the same results were observed. When the feed rate is varied from low to high with a constant cutting velocity of 150 m/min and depth of cut of 1 mm, there are certain changes observed in chip morphology during machining with normal and modified cutting inserts. The chips are very long with tubular structure and closely curled thin chips to long snarl chips in machining with normal insert and Design 1 cutting insert which are hindrance to the machining operation. Hence, this increases the tool wear and also impairs the surface finish greatly leading to more particle residues on machined surface as shown in Table 5.6 (SEM). Whereas in machining with Design 2 cutting insert, chip morphology changes from short tabular and closely curled thin chips with minimum thickness and less presence of residue particles on the machined surface under same machining condition. It has been found that when the depth of cut increases, chip thickness increases rapidly. This is due to the enhancement in the machinability rate. When the depth of cut changes from low to high, with a constant cutting velocity of 150 m/min and feed rate of 0.5 mm/rev, chip shape changes from thin medium tabular chips to very long thick tabular chips in the normal insert and Design 1 cutting insert. At the same cutting condition, it was observed that chip shape changed from thin short tabular to thick arc type chips as shown in Table 5.6. This effect is mainly due to the reduction of cutting temperatures at the machining zone.

Table 5.5 Chips images at different machining conditions

Cutting conditions	Cutting Inserts		
	Normal Insert	Design 1 Insert	Design 2 Insert
100 m/min (Low cutting velocity)	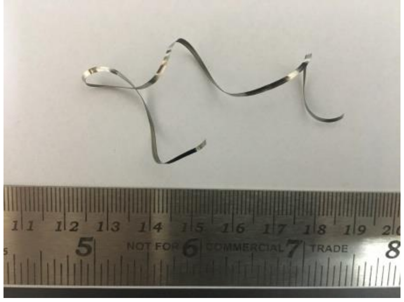	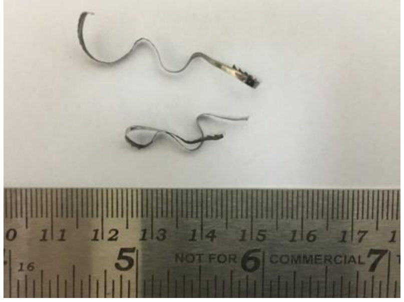	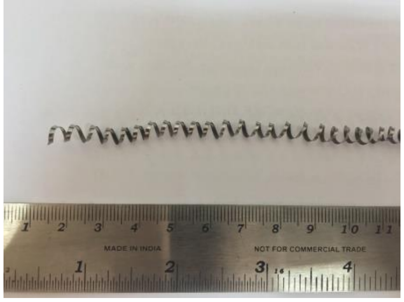
200 m/min (High cutting velocity)	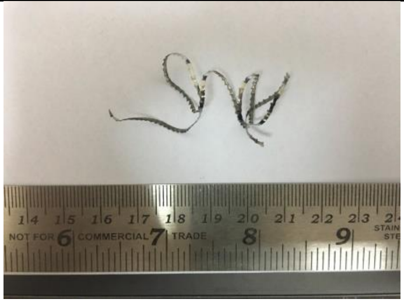	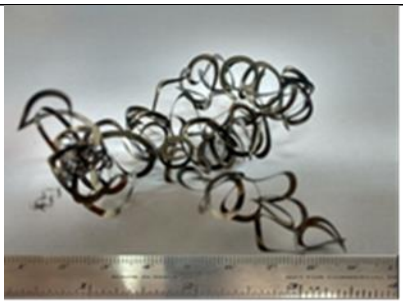	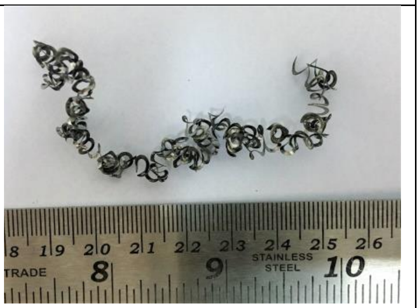
0.1 mm/rev (Low feed rate)	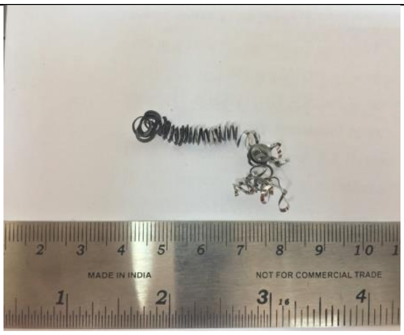	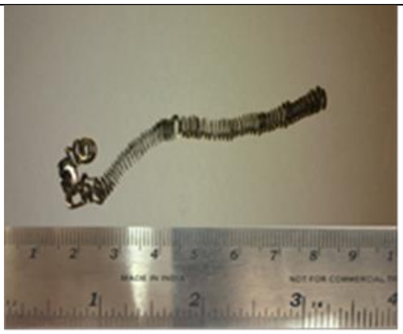	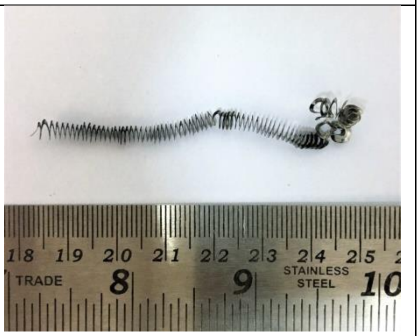
0.5 mm/rev (High feed rate)	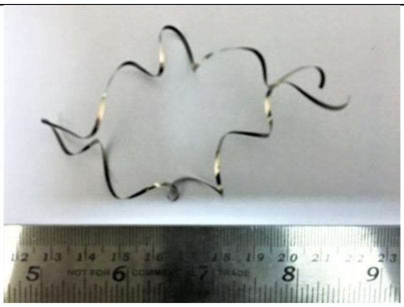	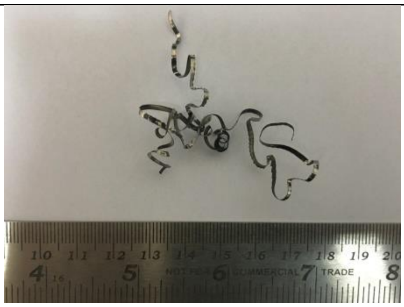	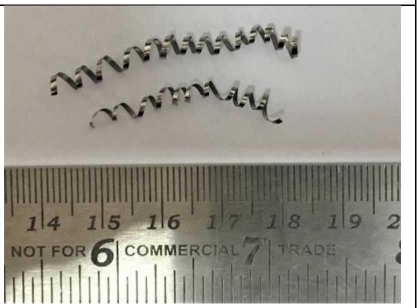

0.5 mm (Low depth of cut)	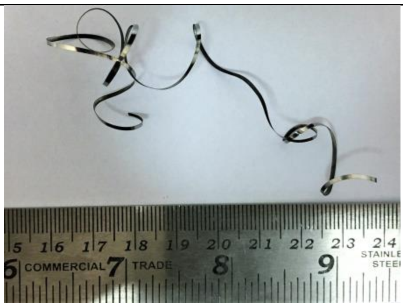	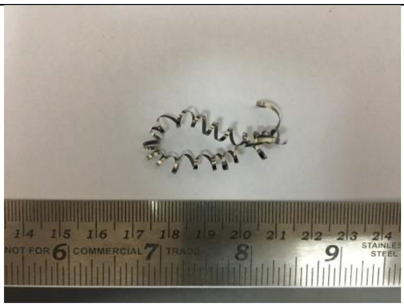	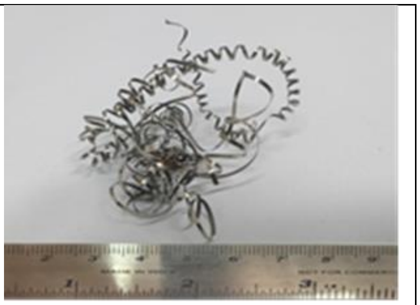
1.25 mm (High depth of cut)	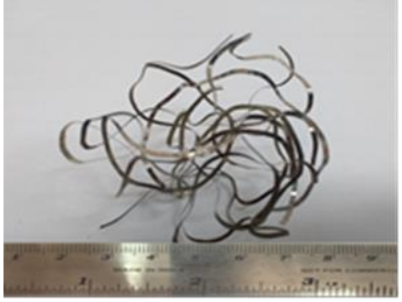	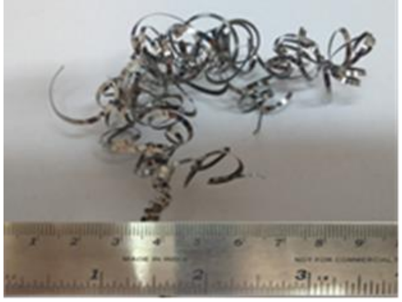	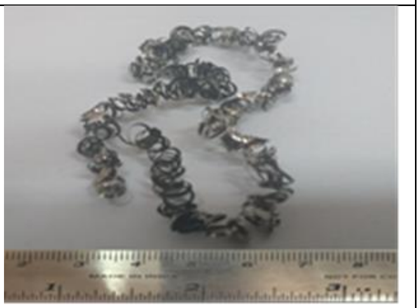

Table 5.6 SEM images of the chip-morphology at different machining conditions

Cutting conditions	Cutting Inserts		
	Normal Insert	Design 1 Insert	Design 2 Insert
100 m/min (Low cutting velocity)	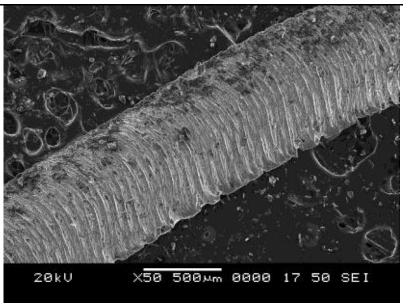 20kV X50 500µm 0000 17 50 SEI	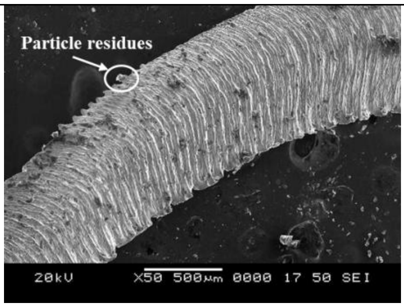 Particle residues 20kV X50 500µm 0000 17 50 SEI	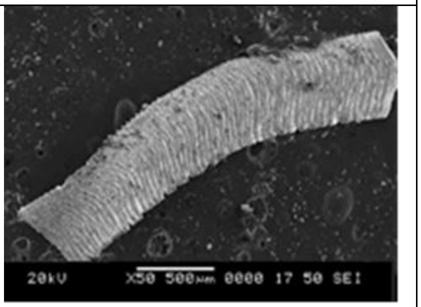 20kV X50 500µm 0000 17 50 SEI
200 m/min (High cutting velocity)	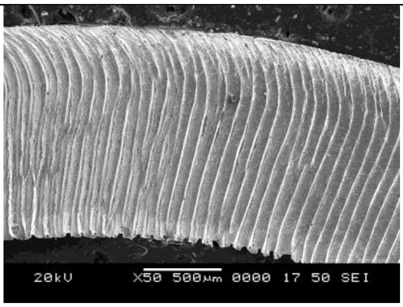 20kV X50 500µm 0000 17 50 SEI	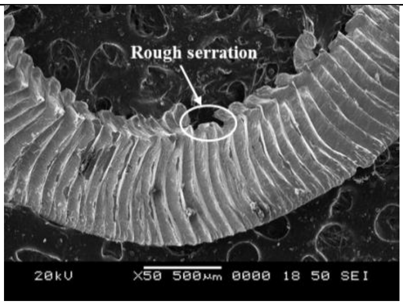 Rough serration 20kV X50 500µm 0000 18 50 SEI	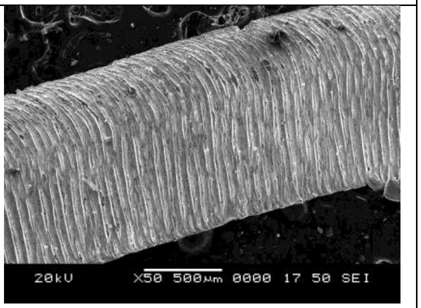 20kV X50 500µm 0000 17 50 SEI

0.1 mm/rev (Low feed rate)	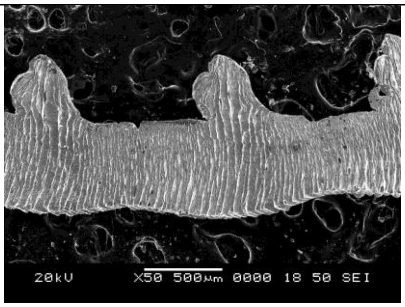 20kV X50 500µm 0000 18 50 SEI	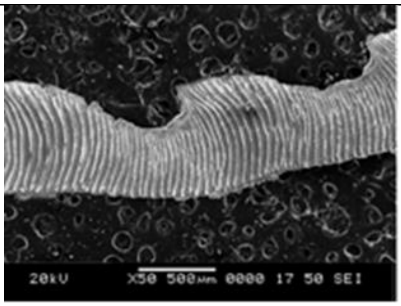 20kV X50 500µm 0000 17 50 SEI	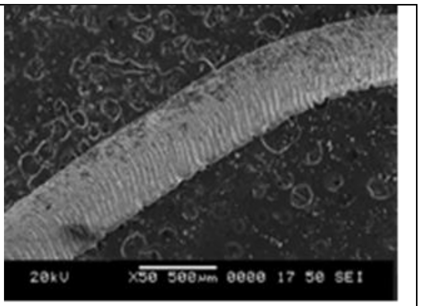 20kV X50 500µm 0000 17 50 SEI
0.5 mm/rev (High feed rate)	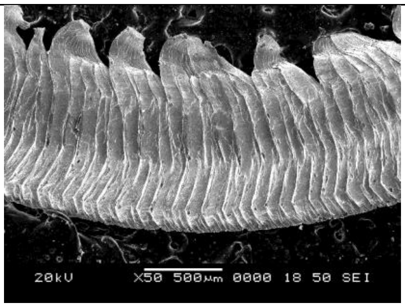 20kV X50 500µm 0000 18 50 SEI	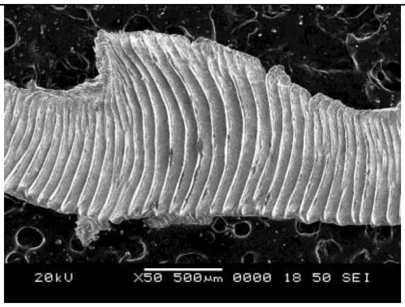 20kV X50 500µm 0000 18 50 SEI	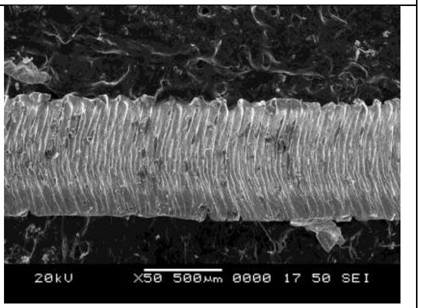 20kV X50 500µm 0000 17 50 SEI
0.5 mm (Low depth of cut)	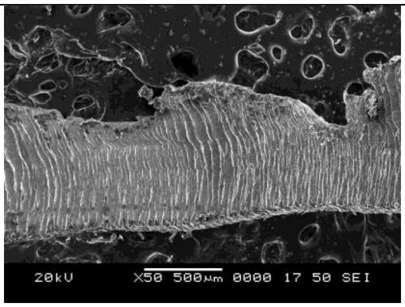 20kV X50 500µm 0000 17 50 SEI	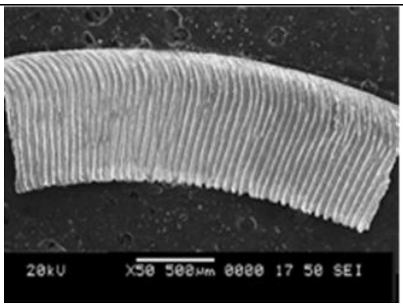 20kV X50 500µm 0000 17 50 SEI	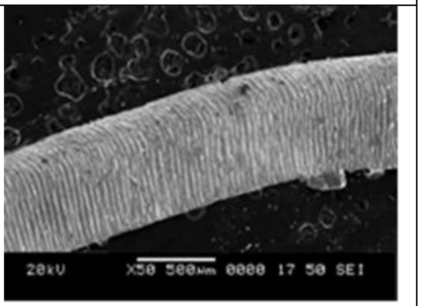 20kV X50 500µm 0000 17 50 SEI
1.25 mm (High depth of cut)	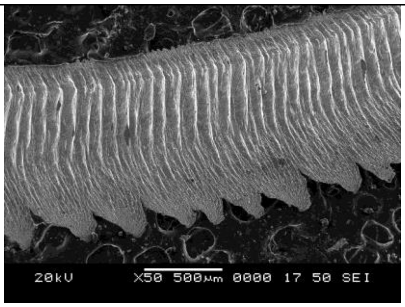 20kV X50 500µm 0000 17 50 SEI	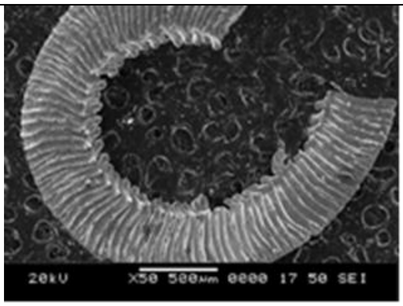 20kV X50 500µm 0000 17 50 SEI	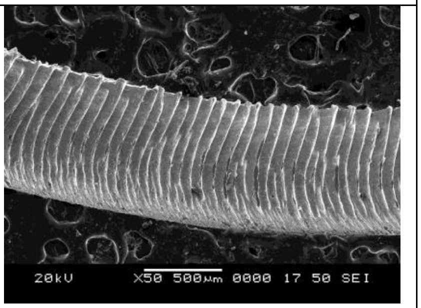 20kV X50 500µm 0000 17 50 SEI

5.8 MICROHARDNESS

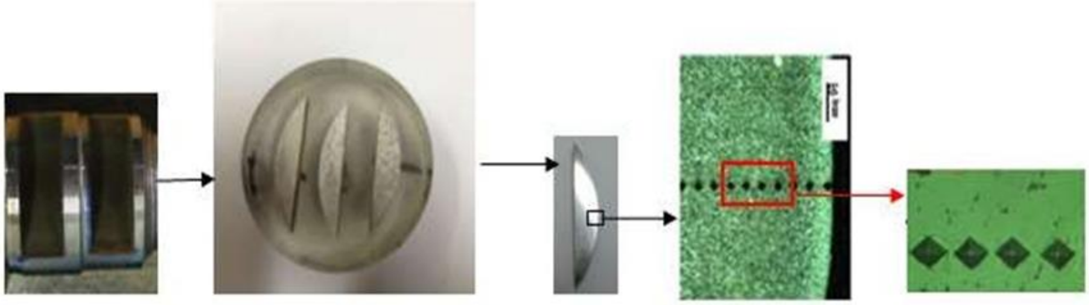

Figure 5.8 Sample preparation methodology for measurement of microhardness

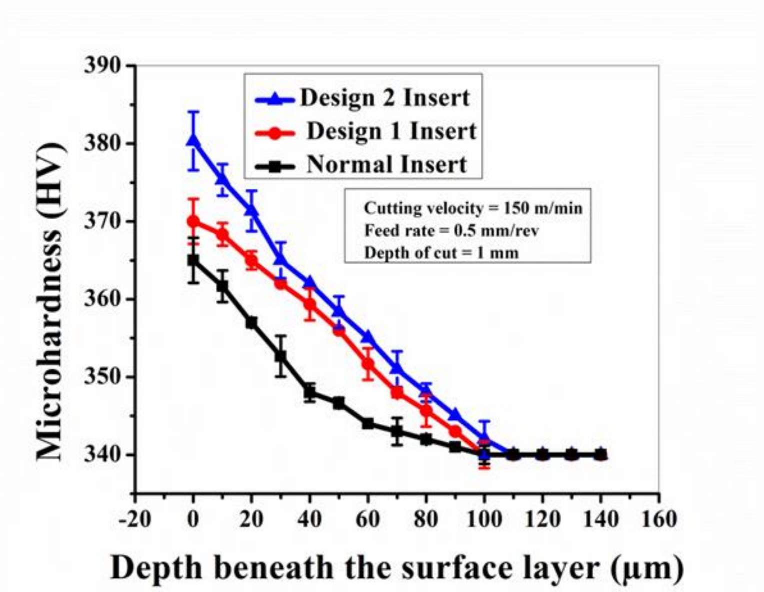

Figure 5.9 Microhardness profiles of the normal insert, Design 1 and Design 2 cutting insert machined surface

In any manufacturing industry, the applications of material processing technology plays a vital role due to its surface and sub-surface hardness which notably affects the fatigue life and wear resistance of the finished product. The improvement of the wear resistance properties could be increased with increase in microhardness of the machined surfaces. During turning, the cutting force required to cause the tearing of the chips as the tool advances induces a severe plastic deformation at surface and subsurface layers. This deformation results in cold working that affects the metal ductility, hardness, and strength (Davim 2010). To measure the microhardness of the machined sample, the procedure is as shown in Figure 5.8. Firstly, the machined sample was cut to a required dimension sample to analyze the sub-surface hardness using wire electric discharge machining into a semicircular shape. Later the semi-circular samples are polished to the mirror-like surface with different grades of emery papers and diamond paste. Figure 5.9 depicts the microhardness profiles of Ti-6Al-4V alloy machined surface with normal and modified cutting inserts. The indentation size is of 20µm with the load of 200gf and a dwell time of 10 seconds was chosen. The initial reading was started at a distance of 50 µm from the sample zero end (machined end) to the beneath surface until it reaches the bulk material microhardness (raw material microhardness). Figure 5.9 shows the effect of modified insert machined surface and normal insert machined surface microhardness, under MQL environment. It was observed that the microhardness trend decreases as there is an increase in depth of the machined surface. At the given condition 380 HV, 370 HV and 365 HV were obtained for Design 2, Design 1 and normal insert machined surface samples under MQL environment and gradually reduced to the bulk material microhardness (Wan et al. 2012). There was 4% - 5% increase in the subsurface microhardness when compared with normal insert and Design 1 cutting insert machined surface, respectively. The increase of microhardness is due to the splashing effect of mist lubricant at cutting zone through the modified cutting insert, there is no much increase in cutting temperature which leads to the work hardening which can be maintained at a certain temperature. More severe plastic deformation at low cutting temperature leads to an increase in work hardening. If the temperature rises, the work-hardening is reduced due to the dynamic recovery or recrystallization of the material. This effect lowers the work-hardening (Chetan et al. 2016). This increase in microhardness of the material helps in the improvement of fracture and fatigue life of the machined surface of the Ti-6Al-4V alloy.

5.9 EFFECT OF MICRO-HOLES IN MQL ENVIRONMENT AND PROCESS PARAMETERS ON SURFACE TOPOGRAPHY

5.9.1 Effect of the modified insert and cutting velocity under MQL environment on surface topography

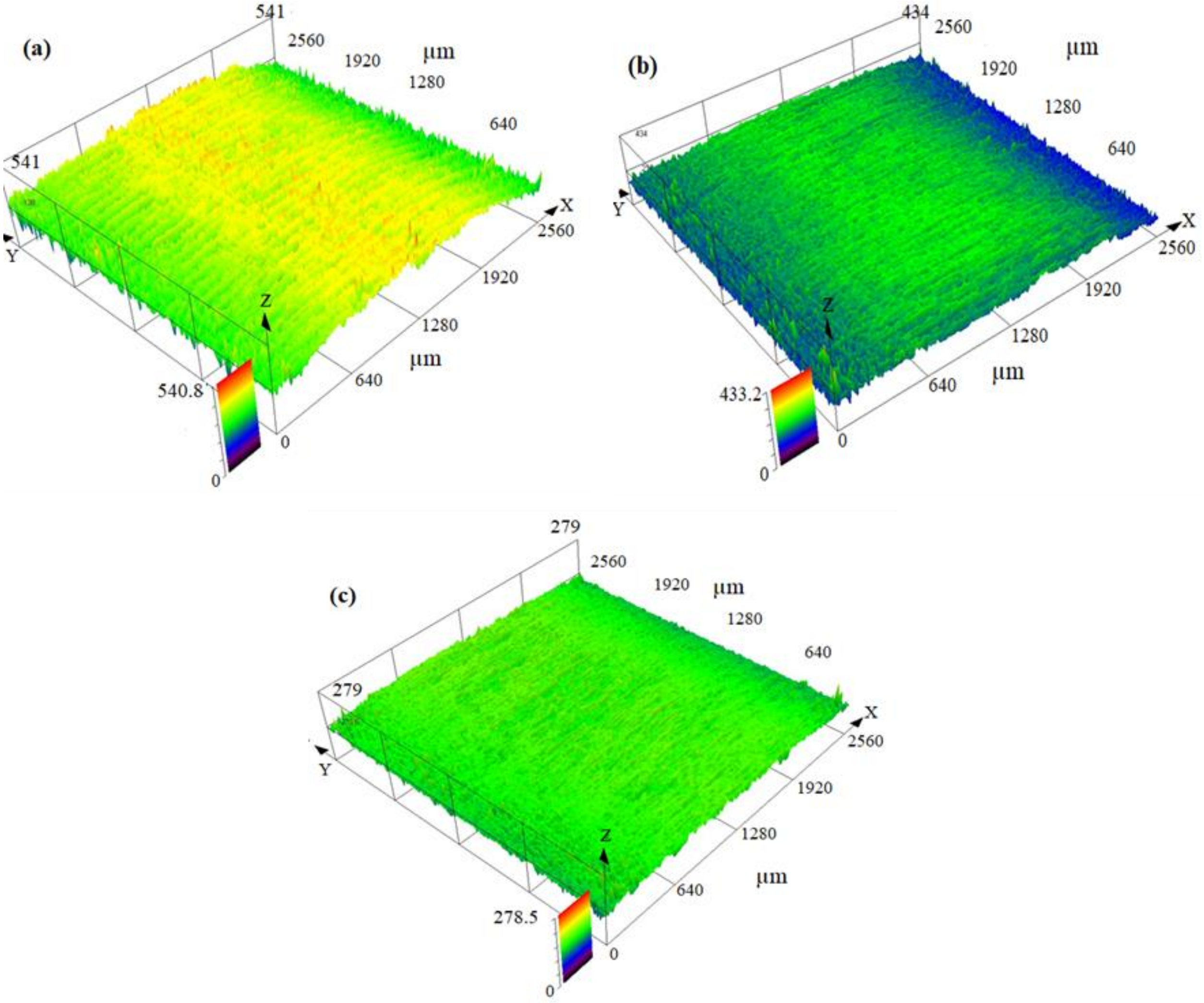

Figure 5.10 Confocal images of surface topography at cutting velocity = 100 m/min, feed rate = 0.5 mm/rev and depth of cut = 1 mm under MQL cooling environments (a) normal cutting insert machined surface (b) Design 1 cutting insert machined surface (c) Design 2 cutting insert machined surface.

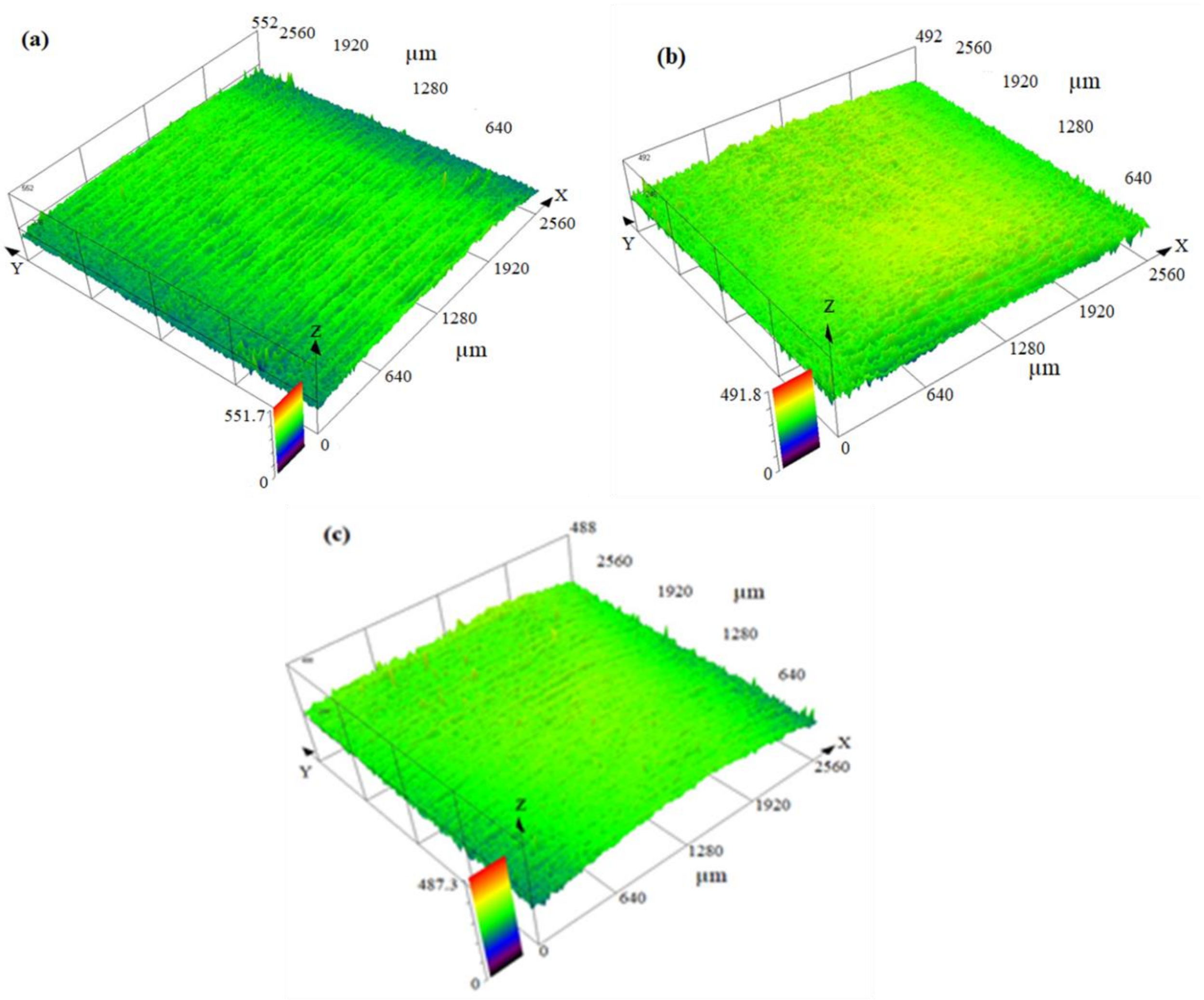

Figure 5.11 Confocal images of surface topography at cutting velocity = 200 m/min, feed rate = 0.5 mm/rev and depth of cut = 1 mm under MQL cooling environments (a) normal cutting insert machined surface (b) Design 1 cutting insert machined surface (c) Design 2 cutting insert machined surface.

Figures 5.10 and 5.11 depict the confocal imagining of surface topography obtained under the normal insert machined surface and modified insert machined surface. At a low cutting velocity of 100 m/min, modified insert Design 2 cutting insert machined surface produced less peak intensity and uniform surface compared to normal insert machined surface and Design 1 insert machined surface, respectively. At the higher cutting velocity at 200 m/min, with better low-intensity peak and the refined uniform surface was obtained in Design 2 cutting insert machined surface when compared to normal and Design 1 cutting insert machined surface under MQL environment. This result was observed due to its less tool wear and built up edge formation compared to other cutting inserts machined surface. Secondly, it may be due to a reduction in cutting temperature with machining under micro-pool lubrication, which causes less thermal distortion on the Design 2 insert machined surface (Ginting and Nouari 2009; Pereira et al. 2016). From Figures 5.10 and 5.11, it can be observed that as the cutting velocity increases, the surface roughness peak intensity of the machined surface also decreases in both the normal and modified cutting inserts machining. This is due to the thermal softening effect of the material at higher cutting conditions which reduces the surface defects through the micro-pool lubrication.

5.9.2 Effect of the modified insert and feed rate under MQL environment on surface topography

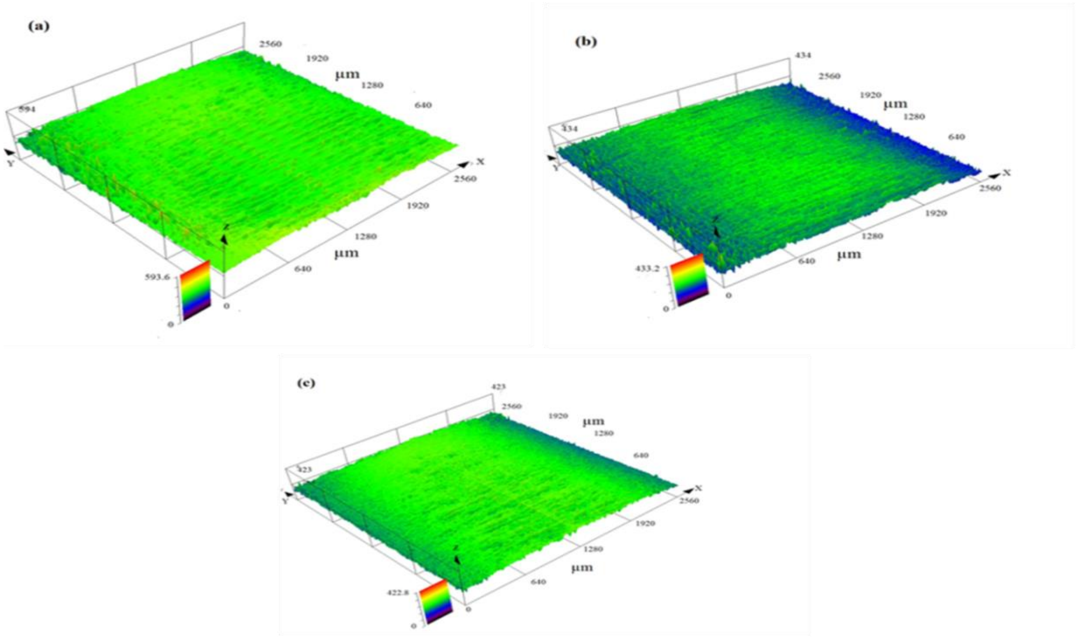

Figure 5.12 Confocal images of surface topography at cutting velocity 150 m/min, feed rate 0.1 mm/rev and depth of cut 1 mm under (a) normal insert machining, (b) Design 1 cutting insert machining and (c) Design 2 cutting insert.

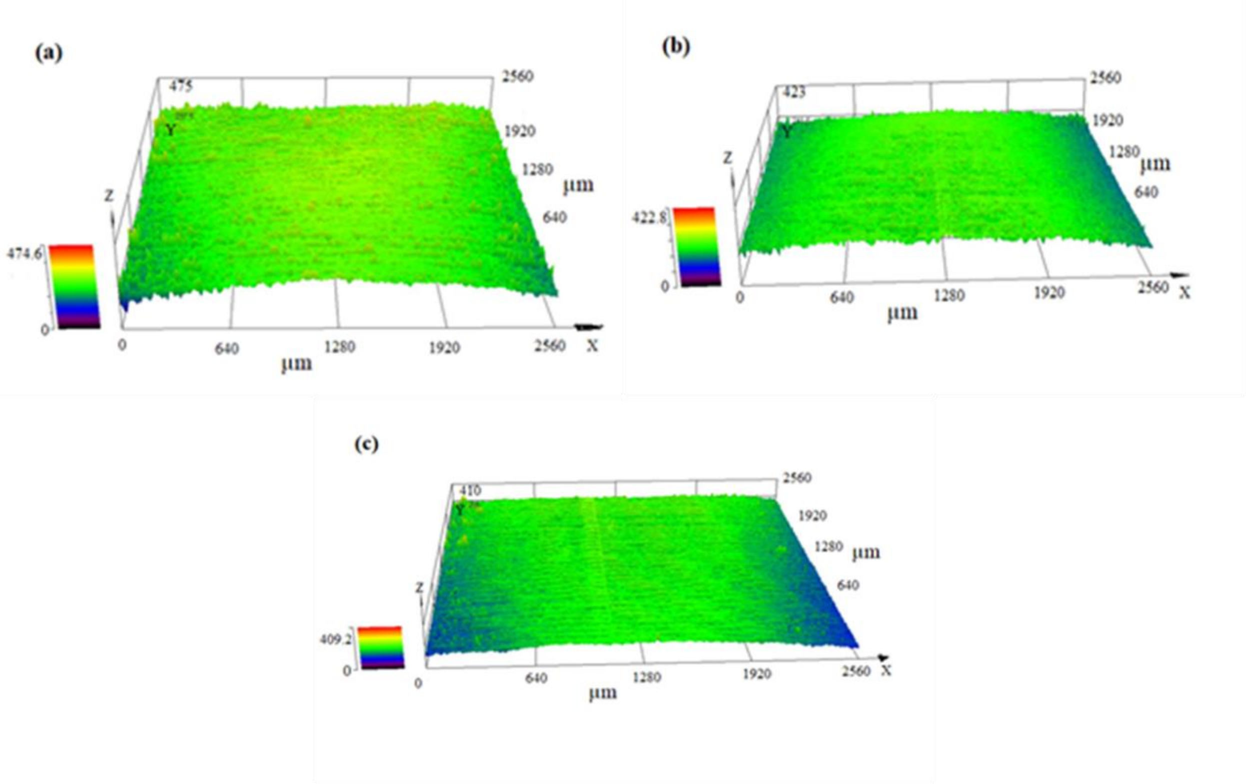

Figure 5.13 Confocal images of surface topography at cutting velocity 150 m/min, feed rate 0.5 mm/rev and depth of cut 1 mm under (a) normal insert machining, (b) Design 1 cutting insert machining and (c) Design 2 cutting insert.

Figures 5.12 and 5.13 shows the 3D confocal images of surface topography under normal insert and modified cutting insert machined surfaces. From the Figure 5.12 and 5.13, it can be observed that as feed rate is increased from 0.1 mm/rev to 0.5 mm/rev, the surface intensity peak of the machined surface is also increased. This rise in intensity of peak is due to the increase in tool wear as feed rate increases. At a lower feed rate of 0.1 mm/rev, Design 2 cutting insert (Figure 5.12(c)) produced lower surface intensity peaks when compared to normal insert and Design 1 cutting insert, respectively. In particular, the normal insert machined surface produced more waviness and higher intensity peaks, due to larger feed marks caused by the higher cutting temperature. These results agree with the literature (Ibrahim et al. 2009; Pereira et al. 2016). At the higher feed rate of 0.5

mm/rev, it is observed that the peak intensity is increasing in both the normal and modified cutting inserts as shown in Figure 5.13. This effect is due to the adherence of chip flow towards the cutting tool which increases the feed marks due to the higher cutting temperatures.

5.9.3 Effect of the modified insert and depth of cut under MQL environment on surface topography

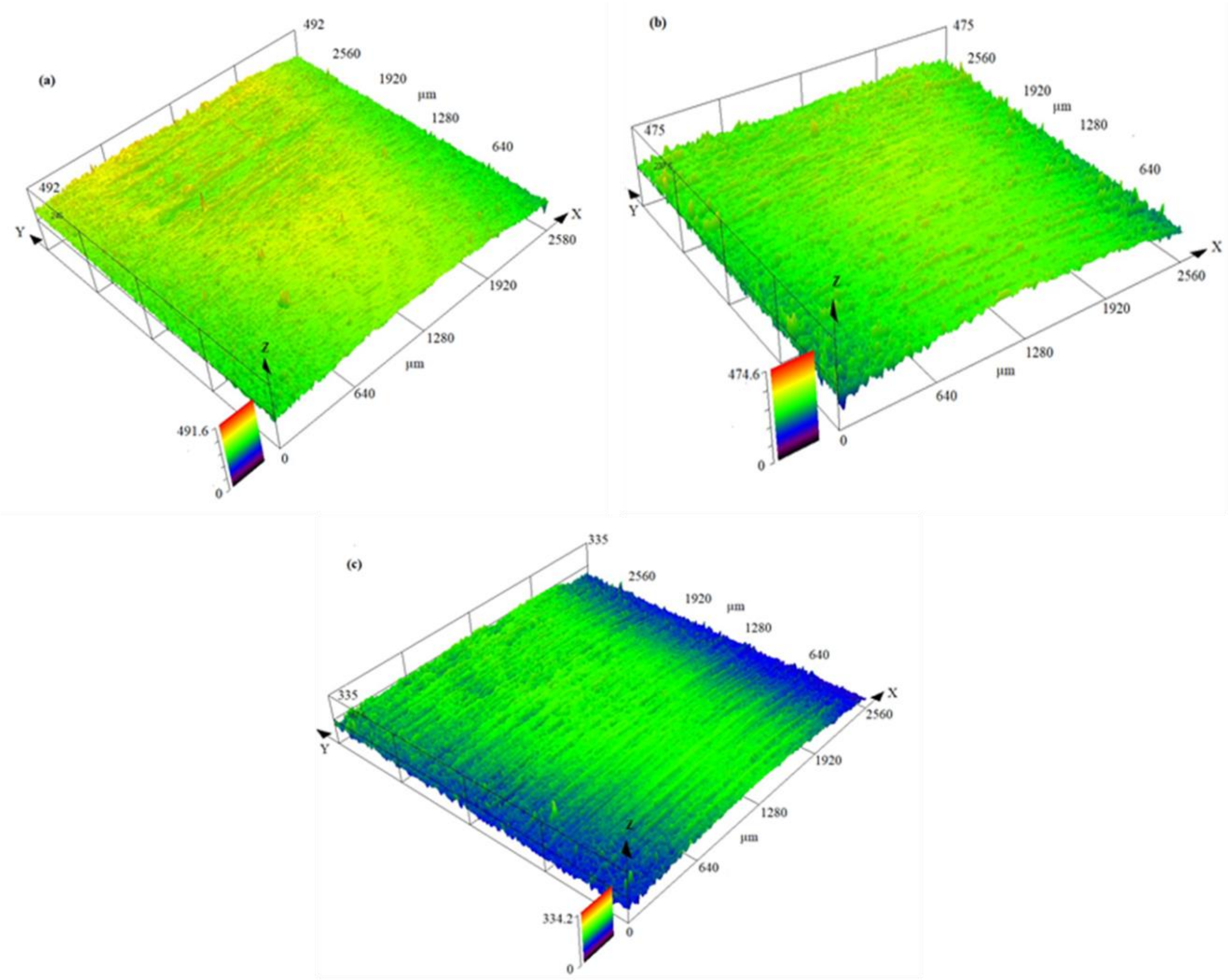

Figure 5.14 Confocal images of surface topography at cutting velocity 150 m/min, feed rate 0.5 mm/rev and depth of cut 0.5 mm under (a) normal insert machining, (b) Design 1 cutting insert machining and (c) Design 2 cutting insert.

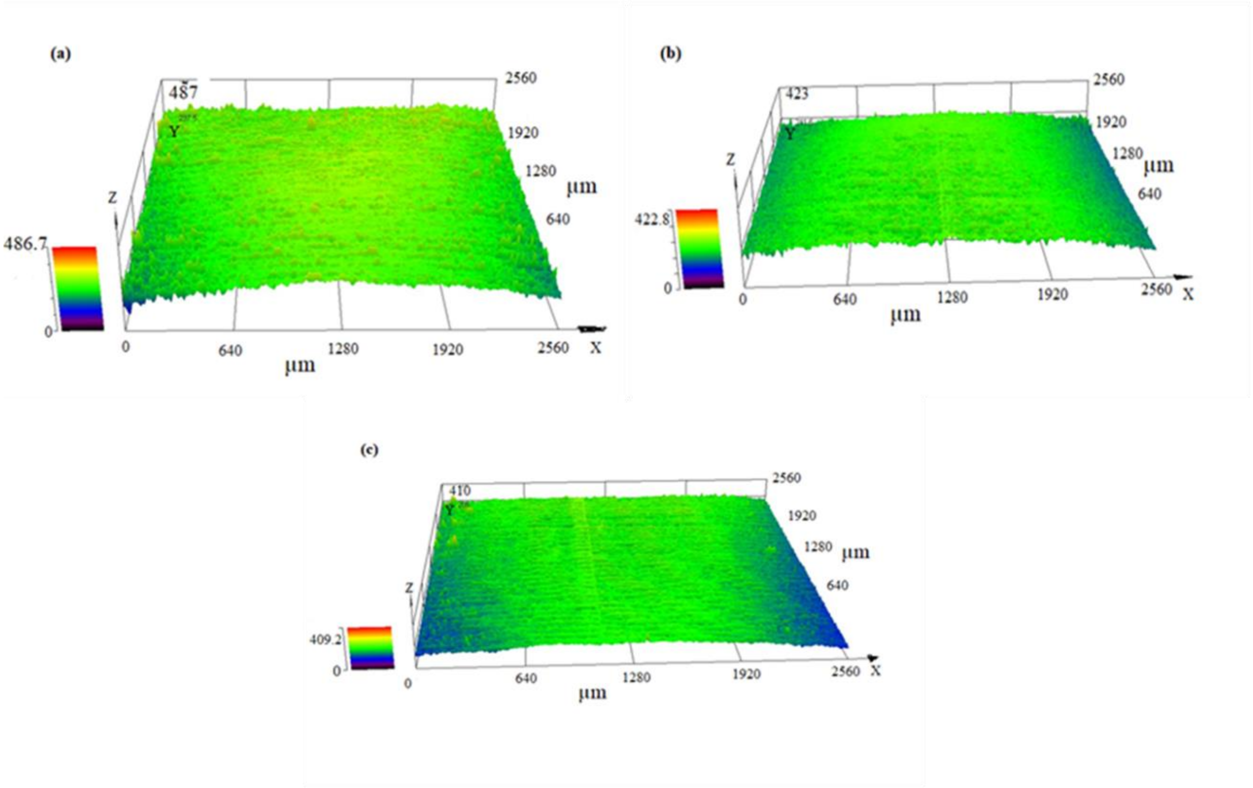

Figure 5.15 Confocal images of surface topography at cutting velocity 150 m/min, feed rate 0.5 mm/rev and depth of cut 1.5 mm under (a) normal insert machining, (b) Design 1 cutting insert machining and (c) Design 2 cutting insert µm.

From Figures 5.14 and 5.15, it is observed that the peak and valley height of the machined surface increases with the increase in the depth of the cut. This is due to larger tool wear with an increase in depth of cut. The Design 2 cutting insert under MQL environment machined sample has reduced peak intensity when compared to normal and Design 1 cutting inserts. The increase in the peak intensity is due to the increase in cutting temperature which is increased due to an increase in depth of cut. As a result, the proper lubrication through micro-holes helped in reduction of cutting temperature which in turn helped in the improvement of the product quality.

5.10 EFFECT OF MICRO-HOLES IN MQL ENVIRONMENT AND PROCESS PARAMETERS ON MATERIAL REMOVAL RATE

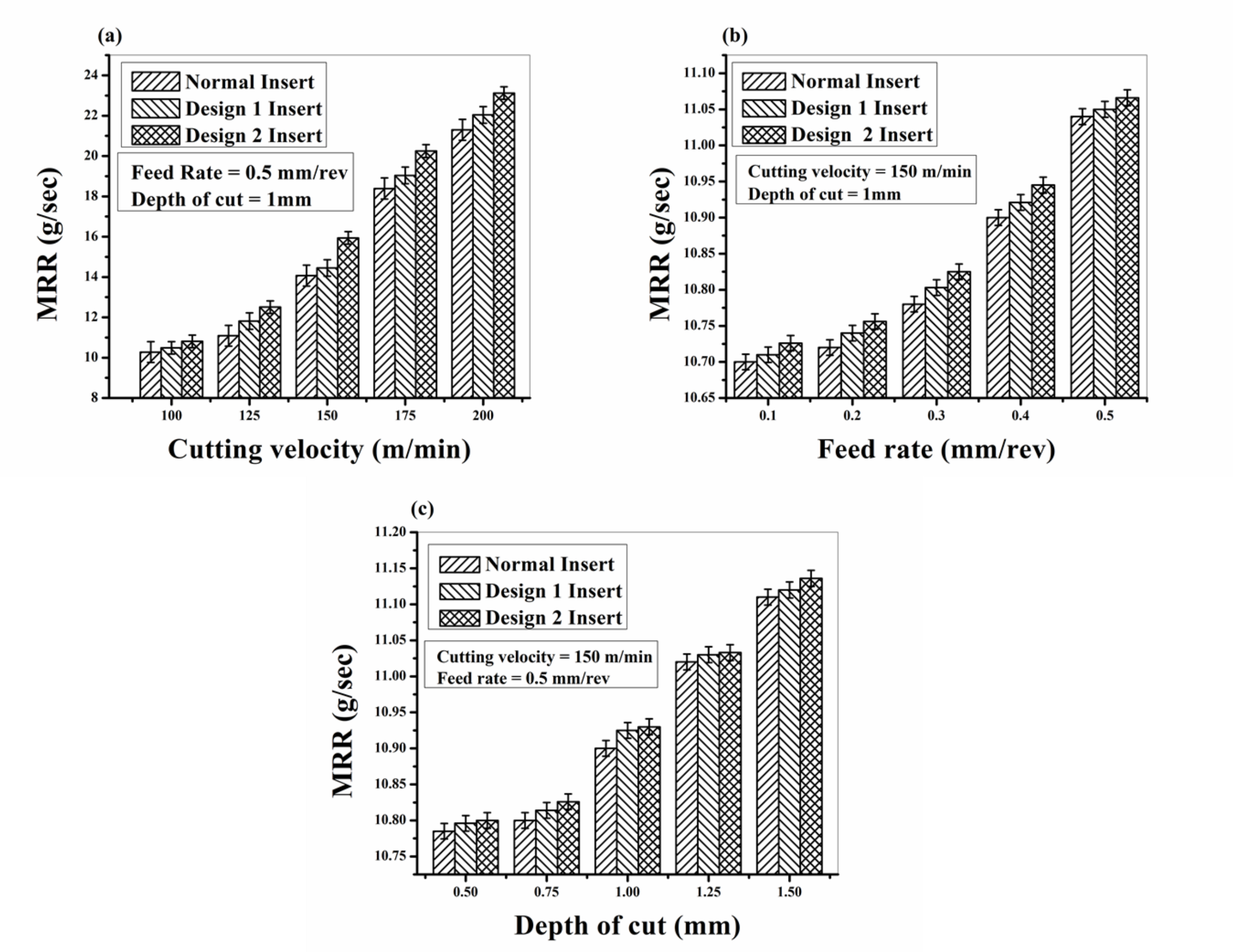

Figure 5.16 Effect of (a) cutting velocity (b) Feed rate and (c) Depth of cut on Material Removal Rate (MRR) with normal and modified insert under MQL environment

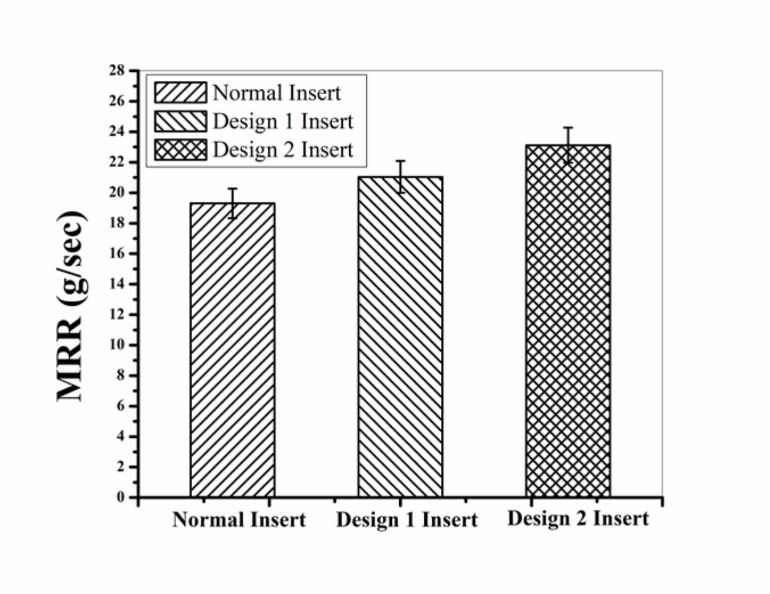

Figure 5.17 MRR measurements by keeping surface roughness as reference

From Figure 5.16 (a)-(c) it is observed that as cutting velocity, feed rate and depth of cut increases then MRR also increases accordingly. Because MRR has a directly proportional relationship with the cutting velocity, feed rate and depth of cut, thus causes an increase in MRR. This effect is observed due to a reduction in chip reduction coefficient resulting in higher MRR (Maity and Swain 2008). When the cutting velocity, feed rate and depth of cut increases from minimum to maximum values, there is no much variations in the MRR for the normal insert and modified insert with the same machining conditions. In this case, the weight of the material is similar in all three machining conditions with different inserts and the only difference is in the machining time. The machining time will be less as the cutting conditions increases. So to avoid the deviancy in this calculation, the MRR is calculated based on the considering the best surface roughness value that is obtained during certain machining condition. In this research, the Design 2 cutting insert machined under cutting conditions of 150 m/min, 0.5 mm/rev and depth of cut of 1mm showed the best surface roughness value of about 0.42μm was the least surface roughness that was obtained. By keeping this surface roughness value as a reference, the machining of the Ti-6Al-4V alloy was performed with normal insert and

Design 1 cutting insert. When the machining was performed for normal insert and Design 1 cutting insert using the same cutting condition, the surface roughness value was increased. To obtain the preferred surface roughness value during normal insert and Design 1 insert machining, the variation in the cutting velocity and feed rate was considered and the experiments were performed on trial and error method. When experiments were performed in such conditions there was an increase in machining time which reduced the MRR value when compared to Design 2 insert machining as depicted in Figure 5.17. From the Figure 5.17, it is observed that the MRR is increased upto 16%-25% in Design 2 cutting insert when compared to normal insert and Design 1 cutting insert, respectively. This improvement in the MRR is due to the reduction in tool wear, resulting in an improved surface finish with minimum machining time.

5.11 SUMMARY

Experiments were conducted on Ti-6Al-4V alloy in MQL condition with machining under normal insert and modified cutting insert, following conclusions were drawn from the experimental results.

- It was observed that as the cutting velocity, feed rate and depth of cut increases, the cutting temperature, flank wear and MRR increased respectively under all the machining environments. Whereas, in the case of cutting vibration and surface roughness, decreasing trend was observed at cutting velocity increasing condition and increasing trend was found for feed rate and depth of cut increasing conditions, respectively. In overall, Design 2 modified cutting insert attained the positive results in terms of cutting temperature, tool wear, cutting vibration and MRR over the normal insert and modified Design 1 cutting insert machining conditions.
- The maximum cutting temperature drop found in Design 2, when compared with normal cutting insert was 24% and when compared with design 1 insert was 15%, respectively.
- The maximum tool flank wear reductions observed in Design 2 modified insert was 62% and 40%, respectively, over normal and Design 1 cutting insert machining.

- The maximum surface reduction in Design 2 cutting insert machining was found to be 40% and 25%, respectively, compared to normal and Design 1 cutting insert.
- The cutting vibration during machining was reduced by 35% and 20% by Design 2 cutting insert when compared to normal and Design 1 cutting insert machining.
- Design 2 modified cutting insert machining increased the MRR to a maximum of 16% and 25% respectively over compared to normal and Design 1 cutting insert machining.
- Design 2 modified cutting insert machining produced favourable chip forms with less residual at all the cutting velocities by improving the chip breakability capability compared to other cutting insert machining.
- In overall, Design 2 cutting insert improved the surface and subsurface properties positively, resulting in improved performance of the product compared to other cutting insert machining conditions.
- From the health, environmentally clean and productivity point of view, MQL machining environment with Design 2 cutting insert satisfies the machining requirements compared to normal insert and Design 1 cutting insert machining conditions.

This chapter explained the comparison between different micro-hole textured PCD Insert with the normal PCD Insert under MQL environment. The results showed that Design 2 pattern of PCD insert was proved as the best design by comparing with different performance indexes. Further to prove that whether the design is suitable for other cutting material, PCBN was selected for machining of Ti-6Al-4V alloy with the Design 2 pattern and the results were compared with Design 2 PCD insert.

CHAPTER-6

COMPARITIVE STUDY OF CUTTING INSERTS FOR Ti-6Al-4V ALLOYS

6.1 INTRODUCTION

This chapter describes the comparison of Polycrystalline diamond (PCD) inserts and Polycrystalline Cubic Boron Nitride (PCBN) insert with respect to machining of Ti-6Al-4V alloy. The effect of an individual parameter such as feed rate under MQL environment is studied on performance characteristics such as cutting temperature, machining vibrations, tool flank wear, chip morphology, chip-reduction coefficient and surface integrity (surface roughness and microhardness). This comparison study is performed to investigate the cutting tool material properties in machining Ti-6Al-4V alloy using the surface modification techniques. The surface defects, tool wear, chip morphology and chip-reduction coefficient are studied based on the SEM images.

6.2 EXPERIMENTAL PLAN

The experimental plan is based on OFATA as explained in the previous chapter. Since feed rate is the most influencing parameter in turning operation. The variation in feed rate is studied by keeping cutting velocity and depth of cut constant. The feed rate is varied from 0.1 mm/rev to 0.5 mm/rev by keeping the cutting velocity of 150 m/min and depth of cut of 1 mm constant, respectively. The turning of the Ti-6Al-4V alloy is performed with a modified insert i.e., Design 2 which shows better effectiveness when compared to normal and Design 1 cutting insert. The Design 2 pattern was drilled on PCD and PCBN insert using the electric discharge super drilling machine. The material properties of PCD and PCBN insert are as shown in Table 6.1. These two are the hardest materials that are suitable for machining of the Ti-6Al-4V alloy. The following performance characteristics namely cutting temperature, machining vibrations in cutting speed direction, chip morphology, chip-reduction coefficient, tool flank wear and surface integrity were investigated under MQL environment for the modified PCD and PCBN inserts.

Table 6.1 Material properties of PCD and PCBN inserts

Material	**Density (g/cm^3)**	**Poisson's ratio**	**Modulus of elasticity (GPa)**	**Thermal conductivity (W/(m.K))**	**Thermal expansion (10^{-6}/°C)**
PCD	3.5	0.07	890	816	2.5
PCBN	3.45	0.176	400	740	1.2

6.3 MODIFIED CUTTING INSERTS WITH MICRO-HOLE AS SURFACE TEXTURE

The surface texturing of cutting tools plays a very important role in the improvement of tribological properties. In this research, micro-holes were selected as textured pattern on PCD and PCBN inserts. The micro-holes were drilled with the help of electric discharge super drilling machine on the rake and flank face of cutting inserts along the main cutting edge. The copper wire was used in drilling the micro-holes with water as a dielectric medium. The micro-holes were drilled with the dimension of 0.6 mm diameter and depth of the hole was 1mm, respectively. Before the drilling of micro-holes, the insert was cleaned with acetone and the inspection of micro-holes was carried out using SEM. Figure 6.1 (a) and (b) show the actual PCD and PCBN inserts with the micro-hole texture pattern. The designs of micro-hole orientation were selected based on trial and error approach and were simulated using DEFORM-3D software and the best design was selected for experimentation.

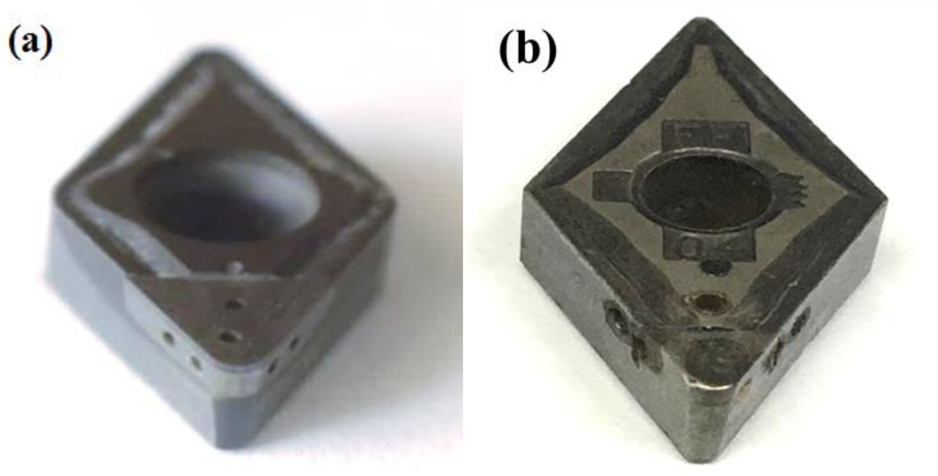

Figure 6.1 The Micro-hole texture (a) PCD Insert (b) PCBN Insert

6.4 EFFECT OF MICRO-HOLES IN PCD AND PCBN INSERTS DURING MACHINING UNDER MQL ENVIRONMENT ON CUTTING TEMPERATURE

Cutting temperature plays an important role in the manufacturing of the component. Cutting temperature was measured with the infrared thermometer gun. The gun was held manually by hand and the infrared light was made to focus on the tool-chip interface. The highest cutting temperature measured during machining was considered as the cutting temperature value. Figure 6.2 depicts the comparison of modified PCD and PCBN insert machining of Ti-6Al-4V alloy under varying feed rate. Low thermal conductivity and specific volume of the heat in Ti-6Al-4V material result in high cutting temperatures (Pramanik 2014). From Figure 6.2, it is observed that as there is an increase in feed rate, the cutting temperature also increases in both the modified PCD and PCBN inserts. But comparatively, the cutting temperatures are higher in PCBN insert than PCD insert. Most of the harder tool materials available in the market are not appropriate for machining of the Ti-6Al-4V alloy. The PCBN inserts experience larger groove wear on the flank and rake face of the insert due to the higher cutting temperature compared to PCD insert. Thus, PCBN tool material is not much suitable for the machining of Ti-6Al-4V alloy machining with modification of insert also (Pramanik et al. 2013). The sintered PCD insert exhibits effective machining with modification. It reduces the cutting temperature and also avoids the galling of material at the tip interface reducing the tool wear. Cutting temperatures of 120°C and 140°C were observed when machining with micro-hole textured PCD and PCBN insert, respectively at a cutting velocity of 150 m/min, feed rate of about 0.5 mm/rev and depth of cut of 1 mm. From Figure 6.2, the cutting temperature observed in modified PCD insert when compared to modified PCBN insert is less by 14.2%, respectively.

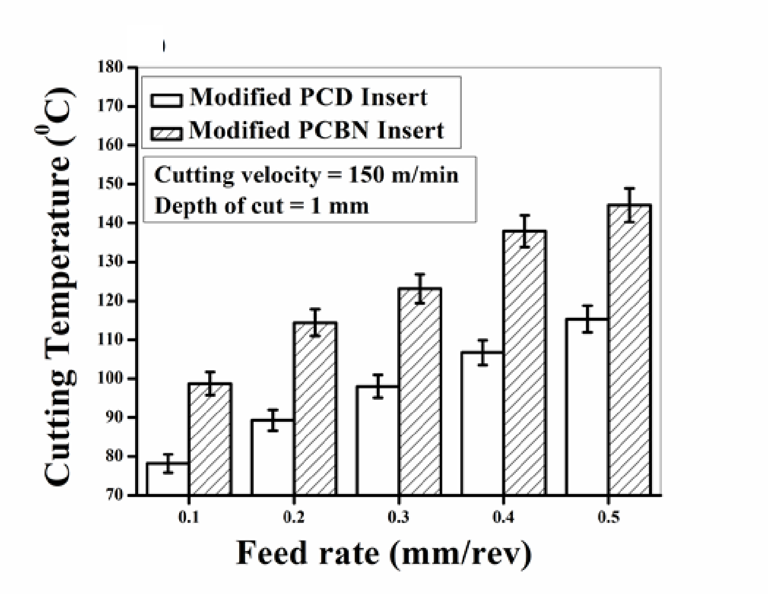

Figure 6.2 Effect of varying feed rate on cutting temperature

6.5 EFFECT OF MICRO-HOLES IN PCD AND PCBN INSERTS DURING MACHINING UNDER MQL ENVIRONMENT ON CUTTING VIBRATION IN CUTTING SPEED DIRECTION

Usually, vibration will be present at the workpiece and tool interface in the machining process. The vibration signals are measured with the help of triaxial accelerometer mounted on the tool holder, which is further connected to DAQ with the help of BNC cable. The vibrations from cutting speed direction (V_y) were selected for further studies. The other two directions showed negligible vibrations when compared with cutting speed direction. Since vibration is common in machining Ti-6Al-4V alloy, due to its significant relative motion at the cutting interface, the cyclic generation of forces and chatter are formed. With respect to the machining with modified PCD and PCBN inserts, the vibration amplitudes show substantial increase at around 3.4-3.8 kHz of the frequency range. The frequency range obtained is close to the natural frequency of the tool holder which is around 3.1 kHz for the tool overhang length of 100mm. Similar observations were observed in the research of Fang et al. (2011) during machining of high-speed Inconel 718. Figure 6.3 shows the variation in the vibration amplitude of modified PCD and PCBN inserts. The comparison of results shows that the modified PCBN insert machining has higher amplitudes when compared to modified PCD insert. The cutting vibration in modified PCD insert is less by 20% when compared to the machining with modified PCBN insert. This observation is due to the micro-pool lubrication at the machining zone, which reduces the friction at the chip-tool interface. Since, there is reduction in friction there is no much built-up edge chip formation. Whereas in PCBN insert, due to the material property there is less reduction in cutting temperature, which lead to an increase in the friction at cutting interface and there is a formation of BUE on the tool, hence, cutting vibration increases. Generally, diffusion and dislocation are the reasons for the damage of the modified PCBN insert. However in PCD insert due to the micro-holes lubrication through the MQL system there is a decrease in the coefficient of friction which reduces the shear angle and decreases the cutting tool vibration. In spite of micro-hole lubrication in the PCBN insert, due to material properties, the chips are welded to the rake face resulting in tool wear.

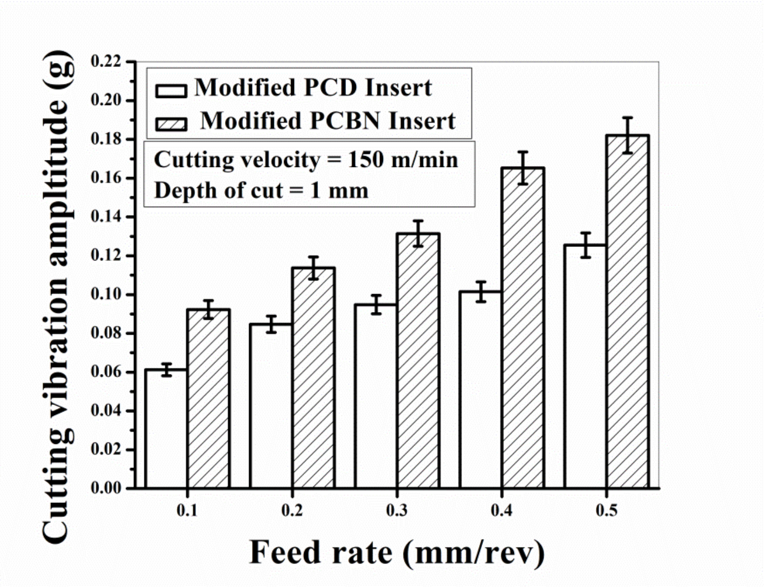

Figure 6.3 Machining vibrations with modified PCD and PCBN insert with a varying feed rate

6.6 EFFECT OF MICRO-HOLES IN PCD AND PCBN INSERTS DURING MACHINING UNDER MQL ENVIRONMENT ON CUTTING TOOL FLANK WEAR

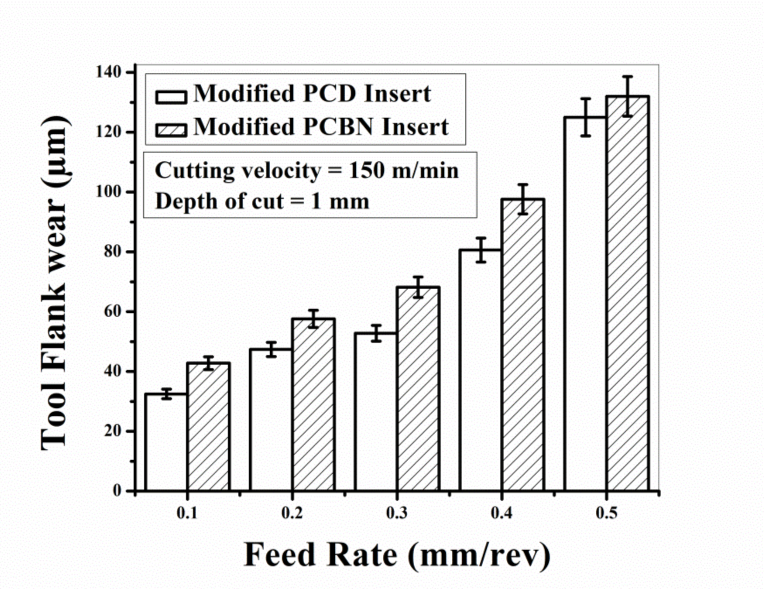

Figure 6.4 Effect of varying feed rate on tool flank wear

Figure 6.4 illustrates the impact of feed rate on the tool flank wear. As the feed rate increases, the tool flank wear also increases in both the modified PCD and PCBN inserts machining under MQL environment. This increasing trend is due to the increase in the cutting temperature which weakens the strength of the cutting tool, causing tool wear. Tool flank wear of 138µm was observed in modified PCBN insert while it was 115µm for modified PCD insert, at the feed rate of 0.5 mm/rev. In the case of modified PCD insert, for machining under MQL environment, it was noted that the reduction in tool flank wear is 16.6% is observed for modified PCBN insert machining.

Table 6.2 SEM images of tool flank wear

Parameters	**Modified PCD Insert**	**Modified PCBN Insert**
Feed rate (0.3 mm/rev)	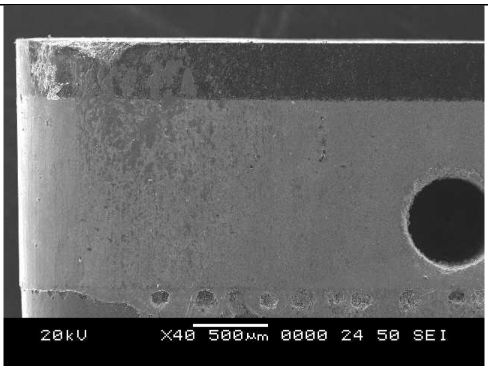 20kV X40 500µm 0000 24 50 SEI	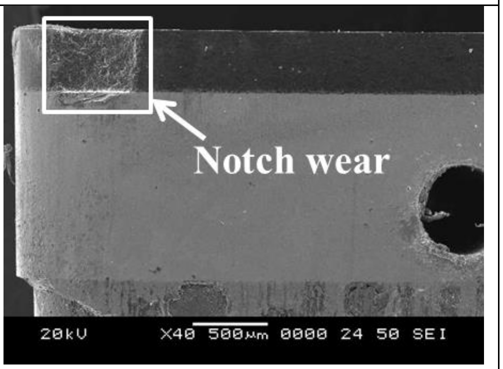 Notch wear 20kV X40 500µm 0000 24 50 SEI
Feed rate (0.5 mm/rev)	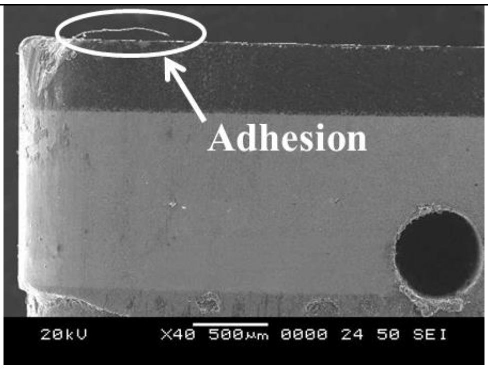 Adhesion 20kV X40 500µm 0000 24 50 SEI	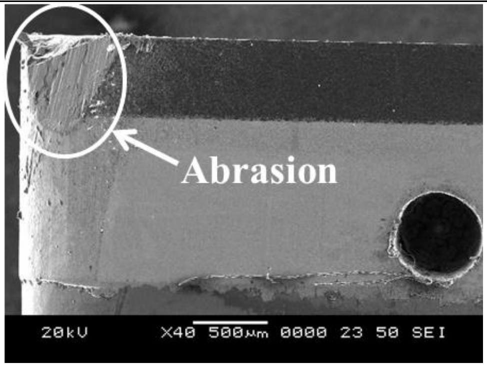 Abrasion 20kV X40 500µm 0000 23 50 SEI

Table 6.2 shows the SEM images for the tool flank regions of the modified PCD and PCBN inserts in machining of Ti-6Al-4V alloy under MQL environment. The SEM images were taken after 5 minutes of machining with each modified inserts. From Table 6.2, it can be observed that tool flank wear is dominant in both the modified inserts.

Modified PCBN inserts show the higher wear distribution compared to the modified PCD insert. This rise in tool flank wear is due to the rise in cutting temperature and high cyclic stress, as well as the adhesion of Ti-6Al-4V alloy to the tooltip during the machining process. The CBN material readily reacts with the Ti-6Al-4V alloy at a higher cutting temperature and welds easily to the tool edge. This welded material is forced to be removed during the machining process which results in the severe tool wear. Since the machining vibrations and cutting heat generated during the machining process are high under the given cutting parameters. It can be assumed that higher temperature is the main reason that causes the adhesion of workpiece material on the tool tip. The same observation has been reported by Honghua et al. (2012).

6.7 EFFECT OF MICRO-HOLES IN PCD AND PCBN INSERTS DURING MACHINING UNDER MQL ENVIRONMENT ON CHIP MORPHOLOGY

The chips produced under modified PCD and PCBN were studied under SEM to study the pattern and segmentation of the chips. Few samples of chip micrographs are shown in Table 6.3. It can be observed from the SEM images that there is chip serration that is running across the whole width of the chips at all feed rates from 0.3 mm/rev to 0.5 mm/rev. From Table 6.3, the chips of PCBN have more primary serrations and also the secondary saw tooth formation at the free end of the chips. The chips obtained from modified PCD insert machining show primary serrations and there is not much of saw tooth formation at the free end of the chips. This serration formation is mainly due to the higher cutting temperatures that are formed at the chip-tool interface zone. Since there is more cutting temperature in case of modified PCBN insert, there is secondary saw tooth formation also as a built-up edge. This sawtooth chip easily welds to the tooltip and also leads to scratch marks on the workpiece resulting in tool wear and poor surface dimensional accuracy. The chip of PCD inserts doesn’t have much sawtooth edges due to MQL splash of coolant through the micro-holes which impinge at the cutting interface. Due to the micro-pool lubrication, the temperature is reduced and the continuous chips are formed which improve the surface dimensional accuracy of the material also improves the tool life.

Table 6.3 SEM images of the chips obtained at machining with modified PCD and PCBN inserts

Parameters	**Modified PCD Insert**	**Modified PCBN Insert**
Feed rate (0.3 mm/rev)	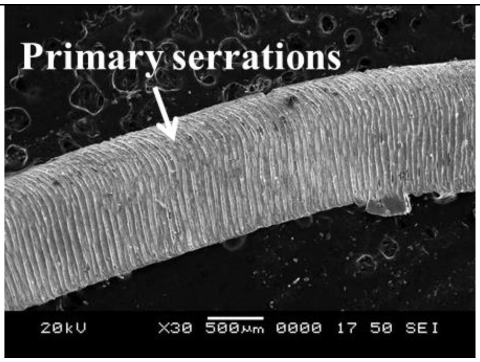 Primary serrations 20kV X30 500µm 0000 17 50 SEI	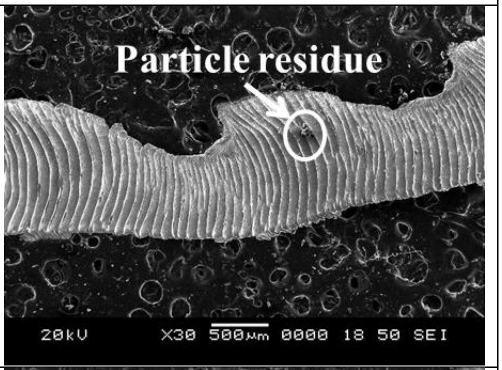 Particle residue 20kV X30 500µm 0000 18 50 SEI
Feed rate (0.5 mm/rev)	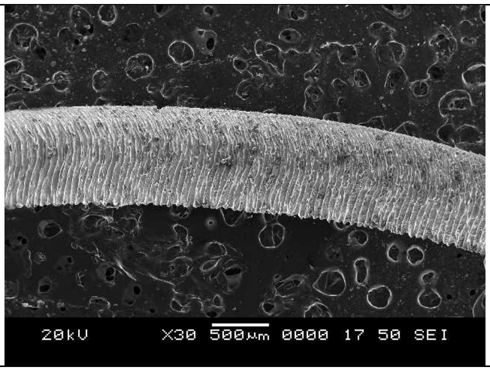 20kV X30 500µm 0000 17 50 SEI	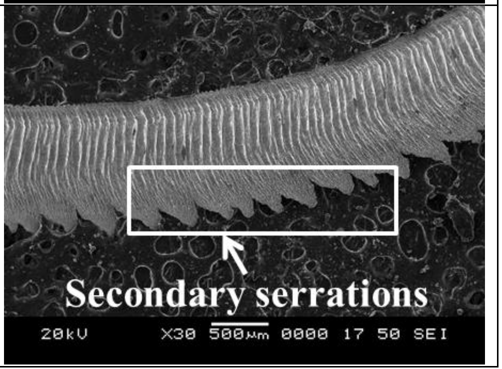 Secondary serrations 20kV X30 500µm 0000 17 50 SEI

6.8 EFFECT OF MICRO-HOLES IN PCD AND PCBN INSERTS MACHINING UNDER MQL ENVIRONMENT ON CHIP REDUCTION COEFFICIENT

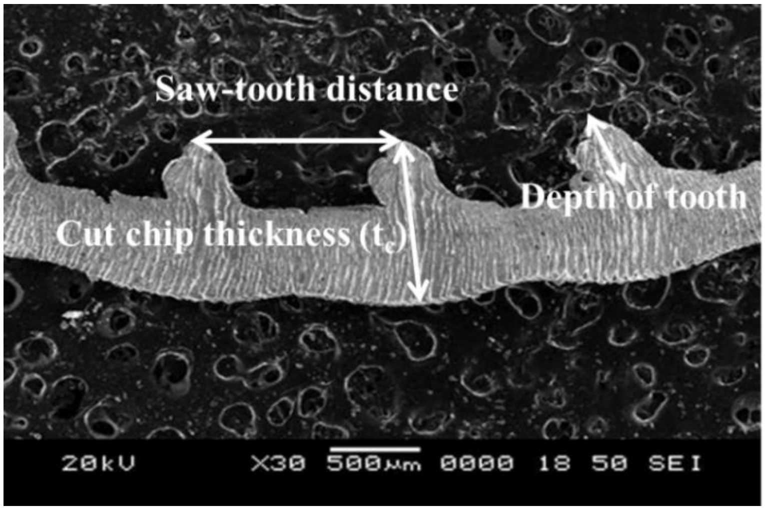

Saw-tooth distance
Depth of tooth
Cut chip thickness (t_c)
20kV X30 500μm 0000 18 50 SEI

Figure 6.5 SEM image of a cross-section of a chip showing some chip features under MQL environment

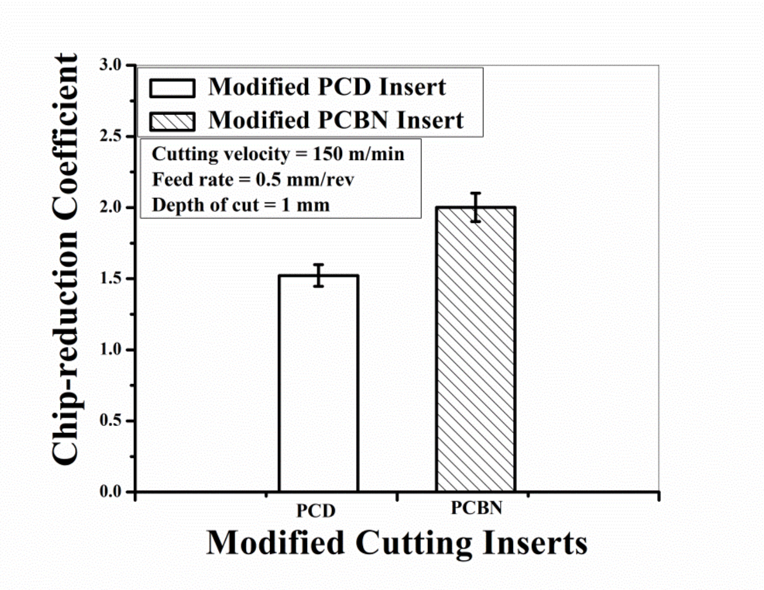

Figure 6.6 The chip-reduction coefficient of modified PCD and PCBN inserts

The chip reduction coefficient is the ratio of the pre-machined and post machined chip thickness. The chip reduction coefficient is mainly influenced by the frictional coefficient, tool wear and the built-up edge formation during the machining process. It is calculated by using Equation 6.1, as described by Thakur and Gangopadhyay (2016).

$$\gamma = \frac{t_c}{t_{uc}} \qquad (6.1)$$

$$t_{uc} = f\ sin\text{ø} \qquad (6.2)$$

Where $'\gamma'$ is the chip reduction coefficient, $'t_c'$ is the cut chip thickness, $'t_{uc}'$ is the uncut chip thickness calculated using Equation 6.2, ‘f ’ is the feed rate and ‘ø’ is the approach angle (93°).

The chip-thickness was measured with the help of SEM images of cross section features of the chip as shown in Figure 6.5. The chip clearly depicts the tooth spacing, chip thickness and depth of the tooth. The effect of machining with modified PCD insert and PCBN insert under the MQL environment on chip reduction coefficient is as shown in Figure 6.6. The chip thickness was measured at 3 different locations and the average of the values was selected for the statistical accuracy. Evidently, the modified PCBN insert resulted in an increase in chip reduction coefficient compared to the modified PCD insert. The higher coefficient of friction in modified PCBN insert is due to the increase in frictional force at the chip-tool interface. The chip reduction coefficient was reduced by 25% in modified PCD insert when compared to modified PCBN insert. The reduction in chip reduction coefficient is due to the decrease in the frictional force at the cutting interface which is due to the proper lubrication through micro-holes and the material properties of the cutting tool. This chip reduction coefficient helps to evaluate the chip thickness which has major influences on the performance indexes such as cutting temperature, tool wear and the cutting forces (Thakur and Gangopadhyay 2016). Thus the lower chip reduction coefficient helps in the improvement of tool life and surface dimensional accuracy.

6.9 EFFECT OF MICRO-HOLES IN PCD AND PCBN INSERTS DURING MACHINING UNDER MQL ENVIRONMENT ON THE SURFACE ROUGHNESS

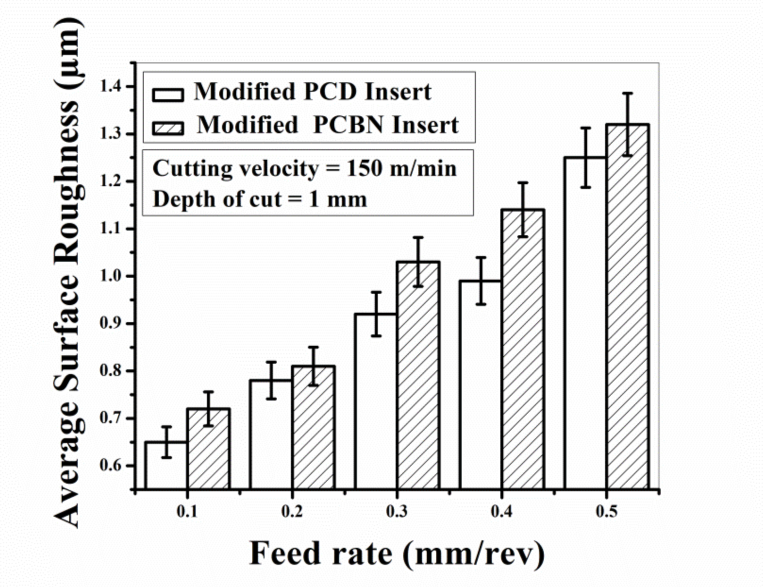

Figure 6.7 Average surface roughness of machined surface with the modified PCD and PCBN insert

Table 6.4 SEM images of surface roughness

Parameters	**Modified PCD Insert**	**Modified PCBN Insert**
Feed rate (0.3 mm/rev)	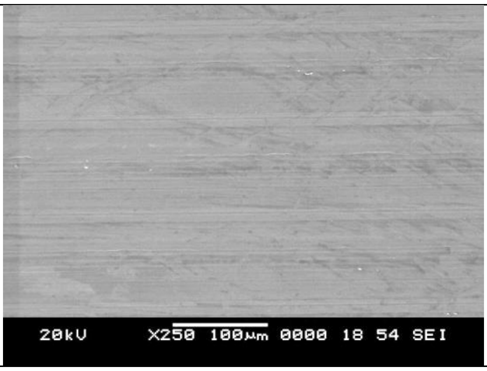 20kV X250 100µm 0000 18 54 SEI	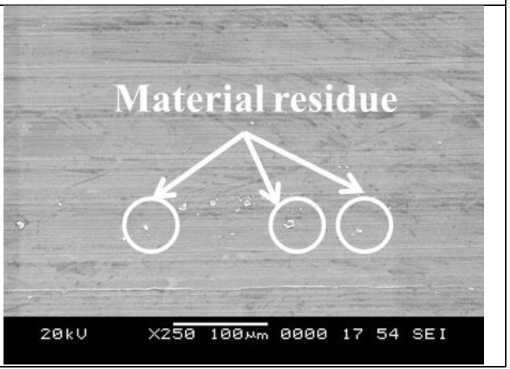 Material residue 20kV X250 100µm 0000 17 54 SEI

Feed rate (0.5 mm/rev)	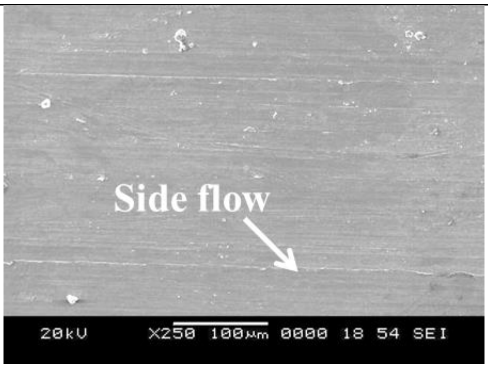	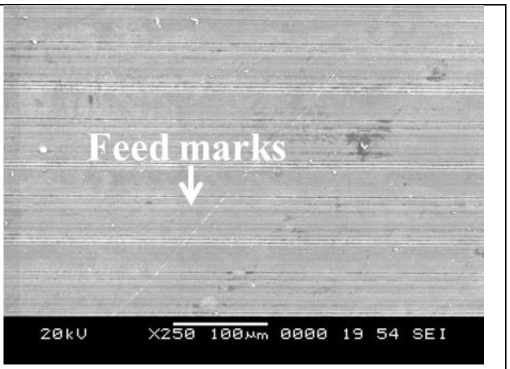

The surface roughness is an important parameter in the manufacturing industry. This parameter also influences the tool life and also the performance of the products. In the present study, the average surface roughness (R_a) was considered as the quality measure. Figure 6.7 depicts the average surface roughness values of the machined surface with modified PCD and PCBN inserts, respectively. The average surface roughness value of the machined surface of Ti-6Al-4V alloy with modified PCD insert was found to be 0.65µm at the initial feed rate of 0.1 mm/rev and increased to 1.05µm at the higher feed rate of 0.5 mm/rev. In the case of modified PCBN insert the average surface roughness at 0.1 mm/rev was 0.75µm and increased to 1.38µm at the feed rate of 0.5 mm/rev, respectively. It is observed from Figure 6.7 that as feed rate increases, the surface roughness also increases in both the modified PCD and PCBN inserts. Comparatively, the surface roughness is reduced in modified PCD insert either at initial feed rate or at higher feed rate. This reduction is due to the proper selection of tool material which reduces the cutting temperature with the micro-pool lubrication and avoids the weldability of the work material to the tooltip. Overall, when the feed rate increased from 0.1 mm/rev to 0.5 mm/rev, machining with modified PCD insert exhibited better surface finish contrast to modified PCBN insert machining. The surface roughness observed in modified PCD insert was reduced by 20% when compared to modified PCBN insert, respectively.

Table 6.4 shows the SEM images of the machined samples with modified PCD and PCBN inserts at varying feed rates, respectively. More feed marks and material residues can be observed on work material during machining with modified PCBN insert compared to modified PCD insert. It is due to the higher cutting temperature which reacts with the tool material leading to the inaccurate surface finish.

6.10 EFFECT OF MICRO-HOLES IN PCD AND PCBN INSERTS MACHINING UNDER MQL ENVIRONMENT ON CUTTING MICROHARDNESS

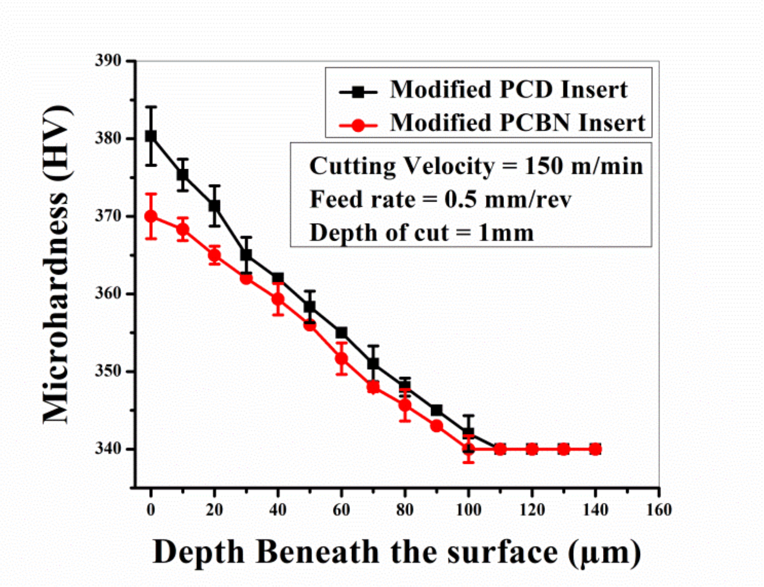

Figure 6.8 Microhardness value beneath the surface roughness machining with modified PCD and PCBN insert

The surface and subsurface hardness have a significant role because these are responsible for the wear resistance and fatigue life of the final product. Higher microhardness increases the wear resistance of the material. Figure 6.8 shows the plots of microhardness beneath the machined surface with the modified PCD and PCBN inserts. The initial reading was started at a distance of 50µm from the machined end to the surface beneath until it reaches the material bulk hardness. Figure 6.8 depicts the effect of modified PCD and PCBN inserts under the MQL environment. The trend of microhardness decreases as there is an increase in depth of the machined surface. At the given condition, 380 Hv and 370 Hv were obtained for modified PCD insert and modified PCBN insert respectively under MQL environment and there is a gradual decrease to bulk material hardness (Che-Haron and Jawaid 2005). There was 6% improvement in the microhardness of modified PCD insert when compared to modified PCBN insert. The increase of microhardness is due to the effect of splashing of mist lubricant at cutting zone through the modified cutting insert. Not much increase in cutting temperature is observed which leads to the work hardening. More severe plastic deformation at low cutting temperature leads to an increase in work hardening (Quan and Ye 2003).

6.11 SUMMARY

The micro-holes on both the PCD and PCBN inserts were drilled successfully with the help of electric discharge super drilling machine. The modified inserts with PCD and PCBN were evaluated with the performance indexes such as cutting temperature, machining vibrations, tool flank wear chip morphology and surface integrity characteristics. From the observed performance of the modified inserts, the following conclusions can be drawn:

- It was observed that as feed rate increases, the cutting temperature, machining vibrations, tool flank wear and surface roughness increases.
- In overall performances modified PCD insert with MQL environment obtained the positive results in terms of all the performance characteristics when compared to modified PCBN insert.
- The cutting temperature drop of 15% was observed in the modified PCD insert when compared to modified PCBN insert. Hence, the modified PCD insert would be functionally better than the PCBN insert, respectively.
- The cutting vibration amplitudes were observed at 3.2 kHz, close to the natural frequency of the tool holder. The cutting speed direction vibration amplitudes were selected in the present study. The highest vibration amplitudes were found in modified PCBN inserts when compared to modified PCD insert. Overall, 20% reduction in machining vibrations was observed in modified PCD insert.

- The tool flank wear and surface roughness of 17% and 20% were reduced in the modified PCD insert under MQL environment with contrast to modified PCBN insert.
- The modified PCD inserts produced the favourable chip flow with minimum serrations and less material residues at varying feed rates compared to modified PCBN insert.
- In overall, the micro-hole texture PCD insert improved the subsurface microhardness with an increase in the wear resistance of the work material.
- Finally, it can be concluded that the modified PCD inserts with MQL system shows the better performance characteristics in all possible standards and is better to be used in machining of the Ti-6Al-4V alloy.

From all the above chapters it was understood that PCD insert with modifications on rake and flank face showed the better performance in machining of Ti-6Al-4V alloy through the turning operation by verifying with different performance indexes and also by using different cutting tool materials. Further to check the accuracy of the experimental results, the prediction of the machining process is carried out using the Adaptive Neuro-Fuzzy Inference System (ANFIS) which is explained in next chapter.

CHAPTER-7

PREDICTION OF PERFORMANCE INDEXES USING ADAPTIVE NEURO-FUZZY INFERENCE SYSTEM (ANFIS)

7.1 INTRODUCTION

Adaptive Neuro-fuzzy Inference System (ANFIS) is a combination of neural network and fuzzy systems. In the ANFIS prediction system, the neural network is used to define the parameters of fuzzy systems. The need for the manual optimization of the fuzzy system is removed by the ANFIS. "A neural network is used to automatically tune the system parameters, for example, the membership function bounds, leading to improved performance without operator intervention. The neuro-fuzzy system with the learning capability of the neural network and with the advantages of the rule-base fuzzy system can improve the performance significantly and can provide a mechanism to incorporate past observations into the classification process" (Rai et al. 2015). The researches on the study of ANFIS strategy made it clear that the hybrid structure with neural network and fuzzy system are beneficial in fields such as the applicability of the existing algorithms for an Artificial Neural Network (ANNs), and the direct adaptation of knowledge articulated with fuzzy rules. An adaptive network, as the name suggests is a network structure which consists of directional links and nodes, with the input and output behaviour that is determined by the values of the parameters through which the nodes are connected (Walia et al. 2015). The advantages of using ANFIS is that it does not require human expertize to solve the complex problems since ANFIS uses the IF-THEN rules. The large choice of membership functions can be used to define a model and also speed up with the convergence time.

The neural network and fuzzy logic are both the universal estimators. The functions are estimated to any prescribed accuracy, with the sufficient fuzzy rules and as well as the hidden neuron layers. The gradient descent algorithms and back-propagation techniques are used to adjust the membership functions of parameters (fuzzy sets) and the weights for the defuzzification (neural network) for the fuzzy neural network. For the prediction process, ANFIS uses these two techniques for the updating of the parameters. The main objective of the ANFIS is to integrate the fuzzy system and the neural network. The adaptive network is one of the examples of a feedforward neural network with multiple layers as shown in Figure 7.1. The supervised learning algorithm is often used in the learning process. In addition, the adaptive network has the architecture characteristics that consist of number of adaptive nodes which is represented by square symbol and the fixed nodes represented as circle symbol (Figure 7.1) are interconnected directly without any weight value between them. Each and every node in the network has different functions and tasks, and the output depends on the incoming signals and parameters that are available in the node. The advantage of using fuzzy is that prior knowledge is denoted into set of constraints to decrease the optimization in the research space. By the implementation of the backpropagation technique, a structured network is used to automate the fuzzy controls that are utilized from the neural network. To define the membership functions, the parameters are fine-tuned with the gradient descent algorithm employed in ANFIS. The adaptive system uses the hybrid learning algorithm to identify the parameters of Sugeno-type fuzzy inference systems. It applies the combination of least-square method and backpropagation gradient descent method for training Fuzzy Inference System (FIS) membership function parameters to emulate a given training dataset.

The neurons in ANFIS have different structures

- The Membership function is described by parameterized soft trapezoids (Generalized Bell Functions).
- Functions are linear regressions and multiplication with *w*, i.e., normalized weights ω, and Output (Algebraic Sum).
- The Normalization is by Sum and arithmetic division.
- The rules are differentiable as T-norm function with AND operator.

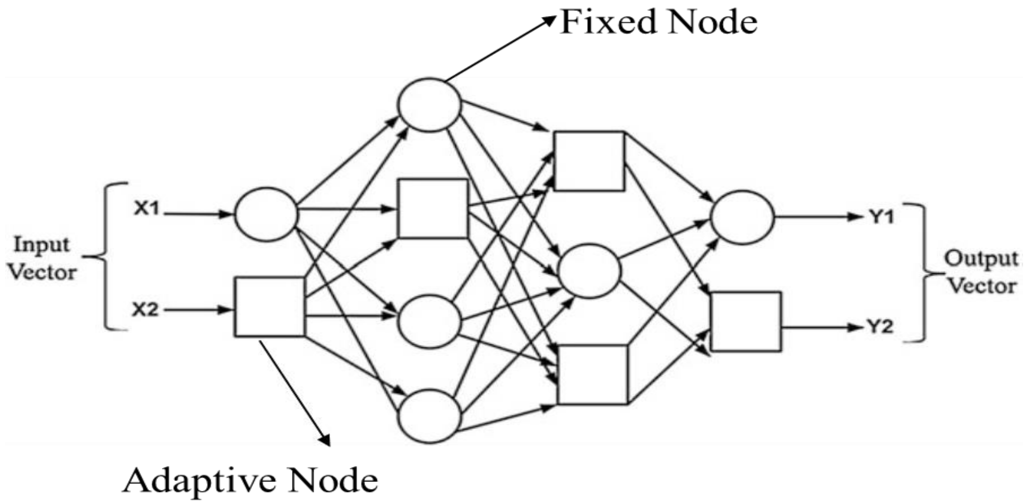

Figure 7.1 Architecture of Adaptive Network

7.1.1 ANFIS Architecture

ANFIS architecture is an adaptive network that uses supervised learning on learning algorithm, which has similar function model of Takagi-Sugeno fuzzy inference system. ANFIS is one implementation that has gained some popularity since it is included in the MATLAB application. The ANFIS structure defined by Jang in 1993 (Jang 1993) is a common architecture that is used commonly. In MATLAB ANFIS, the adaptive network consists of five layers in the feedforward network as shown in Figure 7.2. All the links and network have the unit weights so that the network is changed only through the changes that are interlinked in the inside nodes.

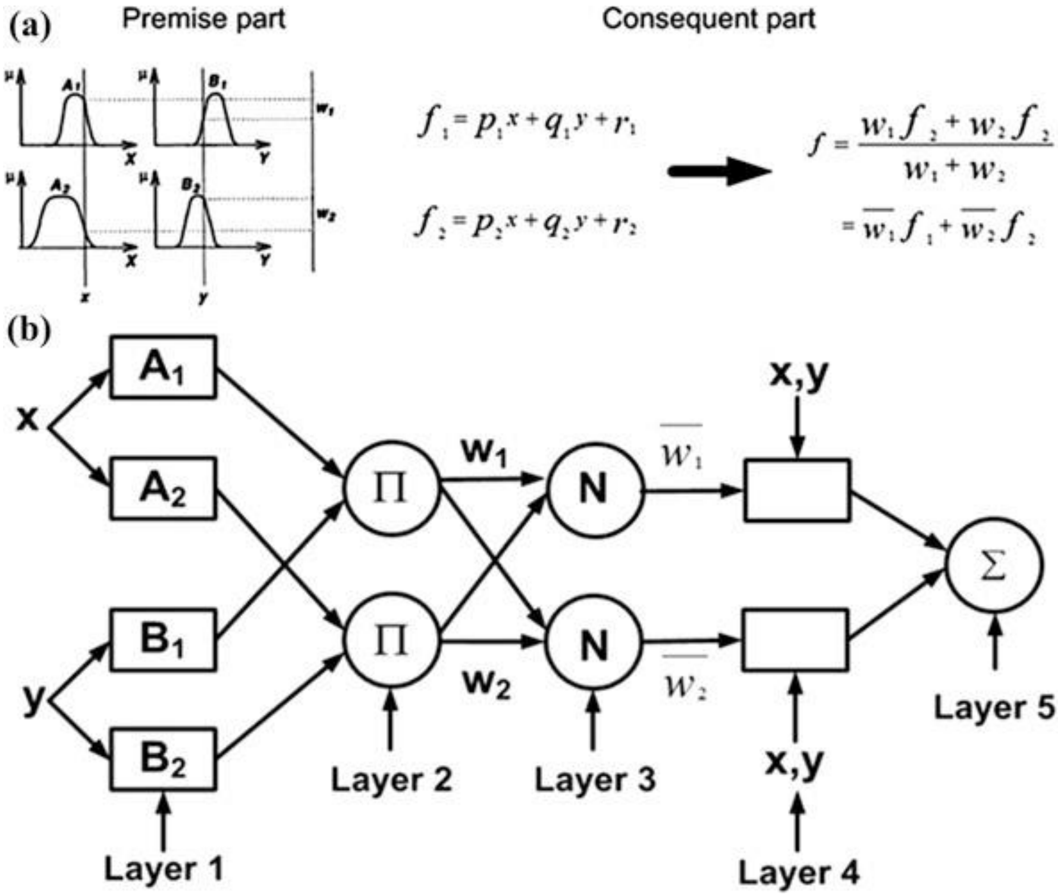
(a)
Premise part
Consequent part
μ
A_1
B_1
A_2
B_2
X
Y
x
y
w_1
w_2
$f_1 = p_1x + q_1y + r_1$
$f_2 = p_2x + q_2y + r_2$
$f = \frac{w_1 f_1 + w_2 f_2}{w_1 + w_2} = \overline{w_1} f_1 + \overline{w_2} f_2$
(b)
x
y
A_1
A_2
B_1
B_2
Π
Π
w_1
w_2
N
N
$\overline{w_1}$
$\overline{w_2}$
x,y
x,y
Σ
Layer 1
Layer 2
Layer 3
Layer 4
Layer 5

Figure 7.2 (a) A two input first-order Sugeno Fuzzy model with two rules (b) equivalent ANFIS architecture (Suparta and Alhasa 2013)

To explain the ANFIS architecture, let’s assume that the system is defined to have two inputs: x and y and one output z. The first-order Sugeno fuzzy model with two if-then rules having fuzzy set A_1, B_1, A_2, and B_2 is expressed as follows.

Rule 1: If x is A_1 and y is B_1, then $f1 = p_1x + q_1y + r_1$,

Rule 2: If x is A_2 and y is B_2, then $f2 = p_2x + q_2y + r_2$,

Where f_i is the output and p_i, q_i and r_i are the design parameters that are determined during the training process, and A_i and B_i are the fuzzy sets.

Implementation of ANIFS architecture using the two rules is shown in Figure 7.2. There are five layers in ANFIS architecture which are explained as follows.

Layer 1: It is also known as a fuzzification layer where each node represents a node function. The function of the node is to generate a membership grade of a linguistic label.

$$\mathbf{O}_{\boldsymbol{i}}^{\mathbf{1}} = \boldsymbol{\mu}\boldsymbol{A}_{\boldsymbol{i}}(\mathbf{x}), \quad \mathbf{for\ i = 1, 2} \tag{7.1}$$

Where x is the input to node i; A_i is the linguistic label that is based on the membership function.

O_i^j is the output of the ith node and jth layer.

Layer 2: This is also known as the product layer. Using the rule of multiplication each node in this layer calculates the firing strength.

$$\mathbf{O}_{\boldsymbol{i}}^{\mathbf{2}} = \mathbf{w}_{\boldsymbol{i}} = \boldsymbol{\mu}\boldsymbol{A}_{\boldsymbol{i}}(\mathbf{x}) * \boldsymbol{\mu}\boldsymbol{B}_{\boldsymbol{i}}(\mathbf{y}), \quad \mathbf{i = 1, 2.} \tag{7.2}$$

Layer 3: This is known as the rule layer in which each node calculates the ratio of individual rule's firing strength to a total of all firing strengths.

$$\mathbf{O}_{\boldsymbol{i}}^{\mathbf{3}} = \overline{\boldsymbol{w}}_{\boldsymbol{i}} = \frac{\boldsymbol{w}_{\boldsymbol{i}}}{\boldsymbol{w}_{\mathbf{1}}+\boldsymbol{w}_{\mathbf{2}}}, \ \boldsymbol{i} = \mathbf{1, 2.} \tag{7.3}$$

$\overline{w}_i$ is the normalized firing strength.

Layer 4: This is known as defuzzification layer where the node calculates the contribution of the ith rule to the overall output i.

$$\mathbf{O}_{\boldsymbol{i}}^{\mathbf{4}} = \overline{\boldsymbol{w}}_{\boldsymbol{i}} * \mathbf{f}_{\boldsymbol{i}} = \overline{\boldsymbol{w}}_{\boldsymbol{i}}(\mathbf{p}_{\boldsymbol{i}} * \mathbf{x} + \mathbf{q}_{\boldsymbol{i}} * \mathbf{y} + \mathbf{r}_{\boldsymbol{i}}) \tag{7.4}$$

Where $\overline{w}_i$ is the output of Layer 3, of the parameter set $\{p_i, q_i, r_i\}$.

Layer 5: This is known as the output layer. It has only one node which calculates the summation of contribution from each rule coming from the nodes of the defuzzification layer to produce ANFIS output, as given in Equation 7.5.

$$\mathbf{O}_{\boldsymbol{i}}^{\mathbf{5}} = \sum_{i} \overline{\boldsymbol{w}}_{\boldsymbol{i}} * \mathbf{fi} = \frac{\sum_{i} \overline{\boldsymbol{w}}_{\boldsymbol{i}} * \mathbf{fi}}{\sum_{i} \overline{\boldsymbol{w}}_{\boldsymbol{i}}} \qquad \textbf{(7.5)}$$

7.1.2 Learning Algorithm of ANFIS

The learning algorithm of ANFIS architecture is nothing but tuning the parameters to the modifiable parameters, namely {a_i, b_i, c_i} and {p_i, q_i, r_i}, to match the training data of ANFIS output. When the premise parameters and membership functions are fixed, the output of the ANFIS model can be written as

$$\boldsymbol{f} = \frac{\boldsymbol{w_1}}{\boldsymbol{w_1}+\boldsymbol{w_2}}\boldsymbol{f_1} + \frac{\boldsymbol{w_2}}{\boldsymbol{w_1}+\boldsymbol{w_2}}\boldsymbol{f_2} \qquad \textbf{(7.6)}$$

Further by substituting Eq. (7.3) into (7.6) yields

$$\boldsymbol{f} = \overline{\boldsymbol{w}}_{\boldsymbol{1}}\boldsymbol{f_1} + \overline{\boldsymbol{w}}_{\boldsymbol{2}}\boldsymbol{f_2} \qquad \textbf{(7.7)}$$

Substituting the fuzzy IF-THEN rules into Eq. (7.6), it becomes

$$\boldsymbol{f} = \overline{\boldsymbol{w}}_{\boldsymbol{1}}(\boldsymbol{p_1 x} + \boldsymbol{q_1 y} + \boldsymbol{r_1}) + \overline{\boldsymbol{w}}_{\boldsymbol{2}}(\boldsymbol{p_2 x} + \boldsymbol{q_2 y} + \boldsymbol{r_2}) \qquad \textbf{(7.8)}$$

After rearrangement, the output can be expressed as

$$\boldsymbol{f} = (\overline{\boldsymbol{w}}_{\boldsymbol{1}}\boldsymbol{x})\boldsymbol{p_1} + (\overline{\boldsymbol{w}}_{\boldsymbol{1}}\boldsymbol{y})\boldsymbol{q_1} + (\overline{\boldsymbol{w}}_{\boldsymbol{1}})\boldsymbol{r_1} + (\overline{\boldsymbol{w}}_{\boldsymbol{2}}\boldsymbol{x})\boldsymbol{p_2} + (\overline{\boldsymbol{w}}_{\boldsymbol{2}}\boldsymbol{y})\boldsymbol{q_2} + (\overline{\boldsymbol{w}}_{\boldsymbol{1}})\boldsymbol{r_2} \qquad \textbf{(7.9)}$$

This is the linear combination of the adjustable parameters p_1, q_1, r_1, p_2, q_2 and r_2. The least square method can be used to identify the optimal values of the parameters easily. If the membership functions are not fixed, the search space becomes larger and the training of the data set becomes slower. The set of gradient descent method algorithm and least squares method is being adapted as a hybrid combination to solve this problem. The least square method (forward pass) optimizes the parameters consequently with the fixed membership function. Once the optimal consequent parameters are found, the backpropagation method starts immediately. The gradient descent method (backward pass) is used to adjust the membership functions that are corresponding to the fuzzy sets in the input domain.

7.2 EXPERIMENTAL PLAN

In this chapter, the experimental plan is selected based on the L27 orthogonal array of Taguchi Design of Experiment. This type of experimental design is selected to study the prediction strategy using Adaptive Neuro-Fuzzy Inference System (ANFIS) on the performance characteristics such as cutting temperature, machining vibrations, tool flank wear and surface roughness. The turning experiments were performed on CNC 'MAXTURN' lathe with Ti-6Al-4V alloy as the workpiece and modified PCD insert (Design 2) as the cutting insert, respectively. The controllable variables that are selected for the experimentation are as shown in Table 7.1. The selection of process parameters is been done based on the previous trial experiments that are conducted. The experimental data of 27 sets were collected, out of which 75% of data sets were selected as training data and the remaining 25% data-sets as the testing data. The neuro-fuzzy inference system was trained with 22 data sets with the 100 epochs. To verify the accuracy of the prediction, other 6 data-sets were used. The training was conducted using Sugeno type fuzzy inference system with 27 rules, three membership function of each of the three input parameters (Cutting velocity, Feed rate and Depth of cut). The hybrid algorithm of gradient descent learning and least square with the linear output is selected for training and testing of the ANFIS model. The membership function is categorized into low, medium and high for each input parameter. The analysis of experimental data was conducted on MATLAB R2015a workstation. The data input to the ANFIS workbench was uploaded with four columns, the first three columns were treated as input parameters and the last column was treated as output for the training of FIS. The experimental data is utilized to train FIS using gauss membership function.

Table 7.1 Controllable Factors and their levels for experimentation

Controllable Factors	Level 1	Level 2	Level 3
Cutting Velocity (m/min)	100	125	150
Feed Rate (mm/rev)	0.3	0.4	0.5
Depth of Cut (mm)	0.5	0.75	1

7.3 ANFIS MODELLING FOR CUTTING TEMPERATURE PREDICTION

The cutting temperature was measured with the help of an infrared thermometer gun, which was hand-held manually during the machining of Ti-6Al-4V alloy using modified PCD insert. The cutting temperature plays an important role in any of the machining operations. This is one of the important performance indices in turning operation. The higher cutting temperature during machining leads to tool wear resulting in lower surface integrity. To reduce the cutting temperature at machining zone, the cutting insert is modified with the micro-hole pattern on rake and flank face which helps the coolant to flow directly to machining zone and helps in reducing the cutting temperature. The lubrication method was made through the MQL system. This chapter deals with the formulation of an ANFIS model for cutting temperature prediction, which is treated as the function of cutting velocity, feed rate and depth of cut during the machining of the Ti-6Al-4V alloy. The chapter also includes the results of the experiments performed to validate the ANFIS model for cutting temperature predicted.

Table 7.2 shows the experimentally obtained cutting temperature values during machining of the Ti-6Al-4V alloy as well as those predicted by ANFIS model by varying cutting velocity, feed rate and depth of cut. From Table 7.2, it can be observed that the percentage of relative error between the experimental and corresponding ANFIS predicted values for validation ranges from +3.44 to -1.40, for the gauss membership function (Gauss MF). Maximum error corresponds to process parameters of cutting velocity of 100 m/min, the feed rate of 0.3 mm/rev and depth of cut of 0.5 mm. Minimum relative error was obtained for cutting velocity of 150 m/min, the feed rate of 0.3 mm/rev and depth of cut of 0.5 mm, respectively. The percentage of error between experimental and ANFIS predicted results at various cutting parameter values for an entire range of data is within 3.44%. This suggests that the model has gained sufficient knowledge regarding the relationship between the input and output parameters. Hence, this model can be used to predict the cutting temperature obtained during the machining of Ti-6Al-4V alloy using the modified PCD insert, respectively.

The testing of model is done to provide the relationship between the predicted values and the corresponding experimental values. Figure 7.3 represents the plot of experimental and predicted values of cutting temperature measured during machining of Ti-6Al-4V alloy using the ANFIS. It can be observed from Figure 7.3 that there is a close agreement between the experimental and predicted values of cutting temperature by varying the cutting parameters. Figure 7.4 depicts the linear fit plot of the cutting temperature for validation of the ANFIS model. The straight line in Figure 7.4 represents the perfect fit between the experimental and predicted values of cutting temperature. The square dots represent the predicted cutting temperature values. The distance between the square dot and the line represents the deviation of predicted values from the corresponding experimental values. Figure 7.5 and 7.6 represent the surface plots of cutting conditions to study the variable nature of cutting temperature.

Table 7.2 Comparison of cutting temperature predicted by trained ANFIS model with the experimentally obtained cutting temperature for machining Ti-6Al-4V alloy

Experimental Trail	Cutting Velocity (m/min)	Feed rate (mm/rev)	Depth of cut (mm)	Experimental Cutting Temperature (°C)	Predicted Cutting Temperature (°C)	Relative Error (%)
1	100	0.3	0.5	23.5	22.6901	3.446393
2	100	0.4	0.75	49.2	48.25811	1.914405
3	150	0.3	0.5	28.1	28.49366	-1.40093
4	150	0.4	1	56.25	55.62537	1.110453

5	200	0.3	0.75	46.8	45.85672	2.015559
6	200	0.5	0.5	30.1	29.59074	1.691893

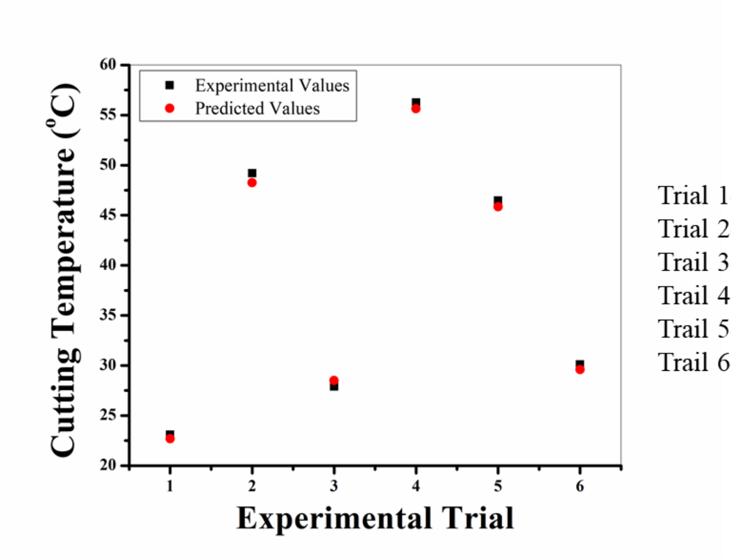

Trial 1- 100m/min, 0.3mm/rev, 0.5mm
Trial 2- 100m/min, 0.4mm/rev, 0.75mm
Trail 3- 150m/min, 0.3mm/rev, 0.5mm
Trail 4- 150m/min, 0.4mm/rev, 1mm
Trail 5- 200m/min, 0.3mm/rev, 0.5mm
Trail 6- 200m/min, 0.5mm/rev, 0.5mm

Figure 7.3 Plots showing the comparison of experimental values and predicted values of cutting temperature by ANFIS

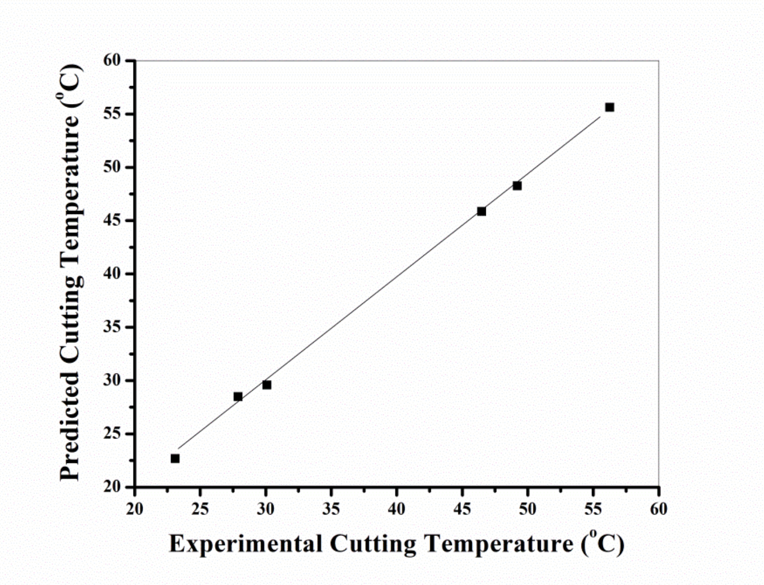

Figure 7.4 Scatter Plot showing the variation of cutting temperature for experimental and predicted values using ANFIS

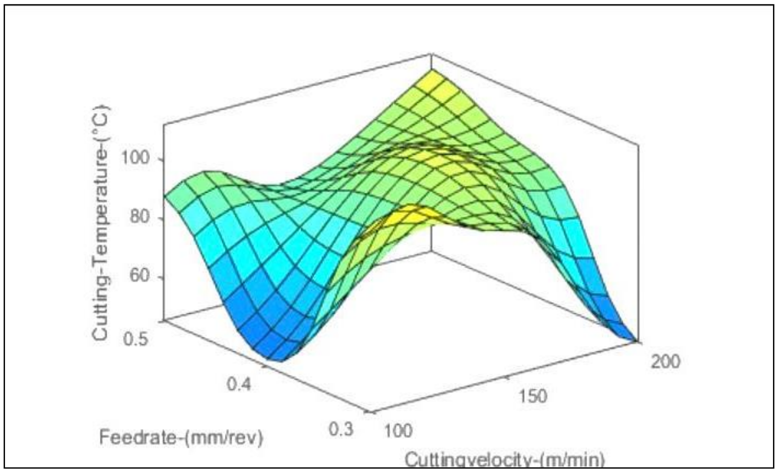

Figure 7.5 3D surface plot for cutting velocity vs feed rate of cutting temperature

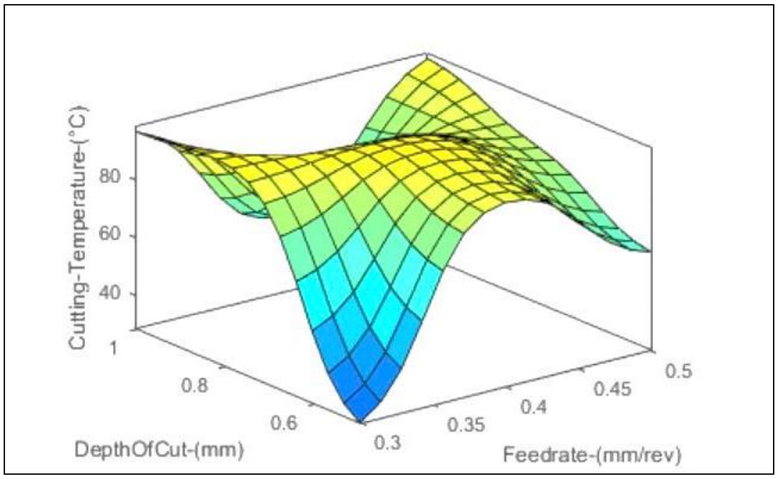

Figure 7.6 3D surface plot for feed rate vs depth of cut of cutting temperature

7.4 ANFIS MODELLING FOR VIBRATION PREDICTION

High-speed machining is the quite old application, but the analysis of vibration signal in high-speed machining is being popular now-a-days in machining of Ti-6Al-4V alloy and other difficult-to-cut materials. No machining system is perfectly rigid. Hence, the vibration is present in any of the machining operations at tool and workpiece interface. In machining of Ti-6Al-4V alloy, the vibration is more susceptible due to the self-excited vibrations that occur at the cutting tool and workpiece (Fang et al. 2011; Pramanik and Littlefair 2015). The vibration signals were fetched with the help of tri-axial accelerometer which was mounted on the tool holder, which was further connected to DAQ with the help of BNC cables and to the workstation. The vibration signals were fetched in all three directions. The cutting vibration amplitude was selected based on the natural frequency of the tool holder. The cutting vibration amplitude from cutting speed direction is studied in this research. The cutting vibration amplitude fetched during machining of Ti-6Al-4V alloy using modified PCD insert predicted using ANFIS model is discussed in this chapter. The machining of the Ti-6Al-4V alloy is performed at varying cutting velocity, feed rate and depth of cut. The model is trained with 75% of the data collected from the Taguchi's orthogonal array and the remaining data set is used to validate the model. Table 7.3 presents the experimental and predicted values of machining vibrations amplitude fetched during machining of Ti-6Al-4V alloy using the ANFIS model. To obtain the convergence of mean square error, the model was trained upto 100 epochs. The maximum relative error that is obtained during validation is +2.04% and the minimum relative error obtained was -2.76%. Since there is minimal in relative error, the ANFIS model is suitable for the prediction of machining vibrations that are produced during the machining of the Ti-6Al-4V alloy. Figure 7.7 shows the experimental and predicted values of vibrations amplitude, which proves the close convergence between the predicted and experimental values. Figure 7.8 depicts the direct comparison between the predicted values generated from the ANFIS model and the experimental values through the linear fit plot. From Figure 7.8, it is confirmed that the predicted values and the experimental values have a good agreement with each other. The closeness of the R-value of the regression line to unity indicates the high accuracy of the predicted data carried out during the training and testing data. Figure 7.9 and 7.10 show the surface plot generated during testing and training of the ANFIS model. This further confirms the potential of ANFIS modelling as an efficient prediction tool for generalizing the input and output complex correlations.

Table 7.3 Comparison of machining vibrations amplitude predicted by trained ANFIS model with the experimentally obtained machining vibrations amplitude for machining Ti-6Al-4V alloy

Experimental Trail	Cutting Velocity (m/min)	Feed rate (mm/rev)	Depth of cut (mm)	Experimental Cutting Vibration amplitude (g)	Predicted Cutting Vibration amplitude (g)	Relative Error (%)
1	100	0.3	0.5	0.1012	0.099128	2.047786
2	100	0.4	0.75	0.1396	0.137018	1.849438
3	150	0.3	0.5	0.0846	0.083936	0.784949
4	150	0.4	1	0.0608	0.062231	-2.35327
5	200	0.3	0.75	0.203	0.201233	0.870338
6	200	0.5	0.5	0.1321	0.135759	-2.76968

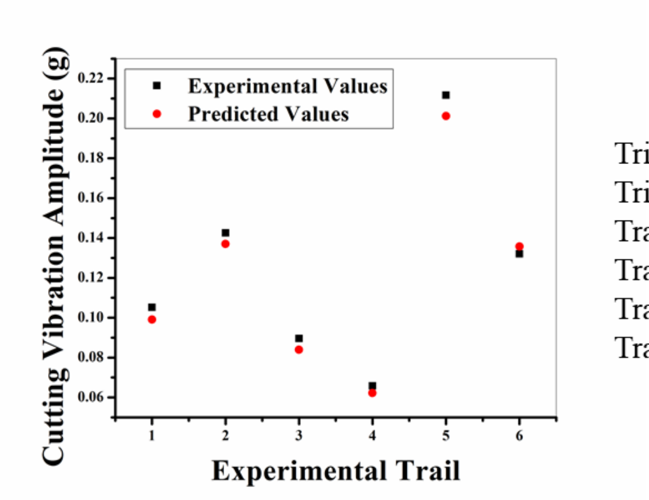

Trial 1- 100m/min, 0.3mm/rev, 0.5mm
Trial 2- 100m/min, 0.4mm/rev, 0.75mm
Trail 3- 150m/min, 0.3mm/rev, 0.5mm
Trail 4- 150m/min, 0.4mm/rev, 1mm
Trail 5- 200m/min, 0.3mm/rev, 0.5mm
Trail 6- 200m/min, 0.5mm/rev, 0.5mm

Figure 7.7 Plots showing the comparison of experimental values and predicted values of machining vibrations amplitude by ANFIS

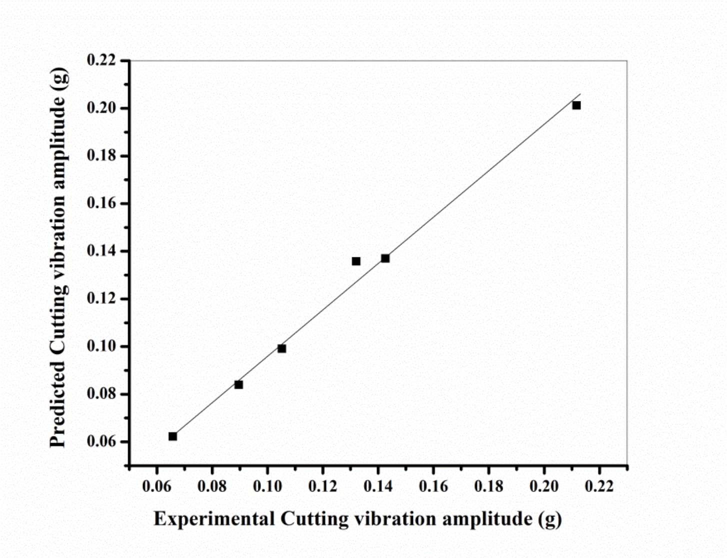

Figure 7.8 Scatter Plot showing the variation of machining vibrations amplitude for experimental and predicted values using ANFIS

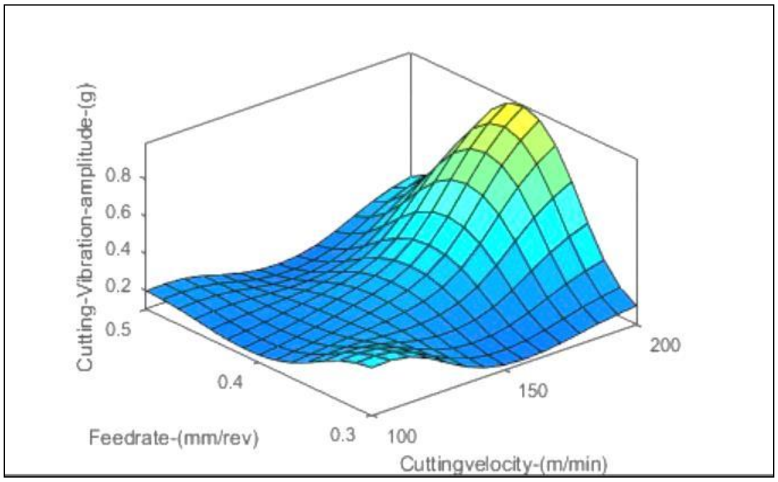

Figure 7.9 3D surface plot for cutting velocity vs feed rate of machining vibrations amplitude

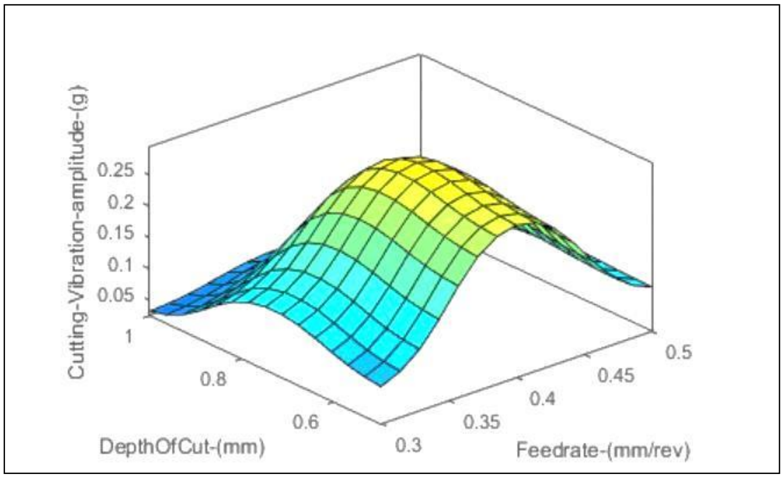

Figure 7.10 3D surface plot for feed rate vs depth of cut of machining vibrations amplitude

7.5 ANFIS MODELLING FOR TOOL FLANK WEAR PREDICTION

The tool flank wear is the main tool wear that is occurring in the turning operation. This is primarily attributed to the rubbing of the tool along the mechanical surfaces. The tool wear is observed due to the high cutting temperatures that are generated in the machining zone. To minimize this cutting temperature and improve the tool wear, the micro-holes have been drilled on the rake and flank face of the PCD insert through which cutting fluids are passed at machining zone to reduce the cutting temperature. The comparison of tool flank wear that was measured after machining of Ti-6Al-4V alloy using the modified PCD insert and prediction is presented in Table 7.4 with a relative error. From the Table 7.4, it is observed that the relative error of tool flank wear between the experimental and predictive values using ANFIS model ranges between -2.37% to 3.09%, respectively. Figure 7.11 shows the close tolerance of the experimental and predicted values obtained during the machining of the Ti-6Al-4V alloy. Figure 7.12 shows the plot depicting the direct comparison between the predicted values from the ANFIS model and experimentally observed values of tool flank wear. The square dots in Figure 7.12 show the closer values of experimental and predicted values with the adjusted square value of

0.98. The R value which is close to one represents the excellent generalization of input and output relationship. Figures 7.13 and 7.14 represent the surface plots generated in ANFIS model due to the interaction of cutting parameters during testing and training of the model.

Table 7.4 Comparison of tool flank wear predicted by trained ANFIS model with the experimentally obtained tool flank wear for machining Ti-6Al-4V alloy

Experimental Trail	Cutting Velocity (m/min)	Feed rate (mm/rev)	Depth of cut (mm)	Experimental Tool Flank Wear (µm)	Predicted Tool Flank Wear (µm)	Relative Error (%)
1	100	0.3	0.5	11.5	11.14403	3.095423
2	100	0.4	0.75	31.8	32.55682	-2.37992
3	150	0.3	0.5	21.2	20.79861	1.893338
4	150	0.4	1	50.25	49.84407	0.807824
5	200	0.3	0.75	35.5	34.98167	1.460074
6	200	0.5	0.5	25.8	25.14218	2.549698

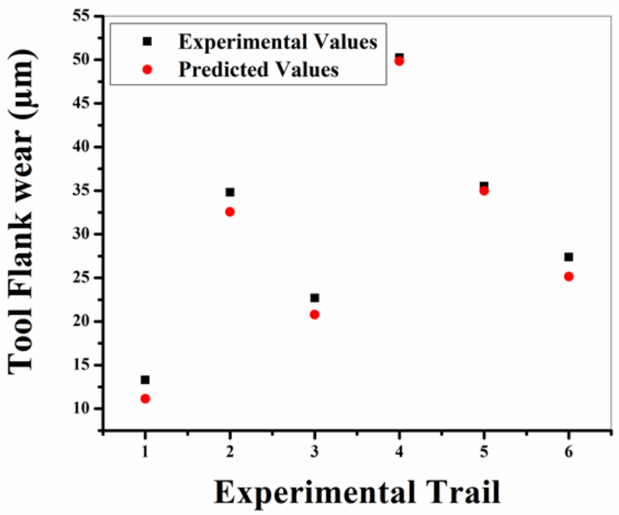

Trial 1- 100m/min, 0.3mm/rev, 0.5mm
Trial 2- 100m/min, 0.4mm/rev, 0.75mm
Trail 3- 150m/min, 0.3mm/rev, 0.5mm
Trail 4- 150m/min, 0.4mm/rev, 1mm
Trail 5- 200m/min, 0.3mm/rev, 0.5mm
Trail 6- 200m/min, 0.5mm/rev, 0.5mm

Figure 7.11 Plots showing the comparison of experimental values and predicted values of tool flank wear by ANFIS

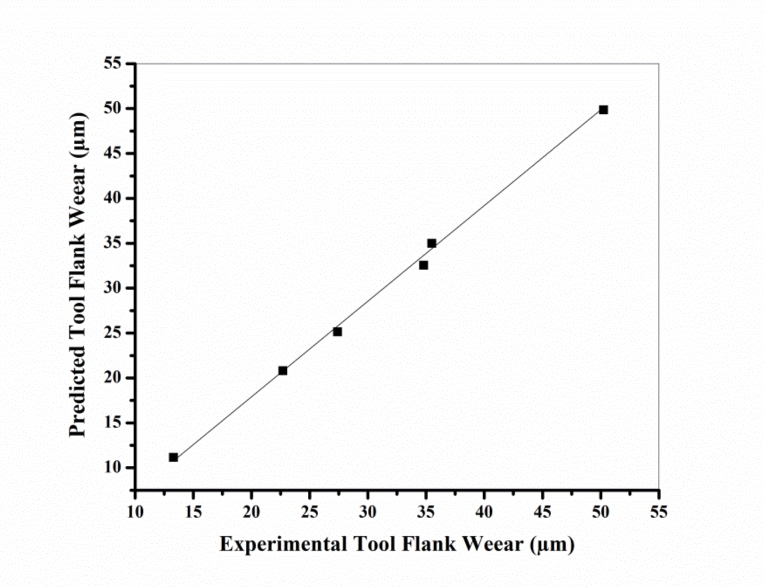

Figure 7.12 Scatter Plot showing the variation of tool flank wear for experimental and predicted values using ANFIS

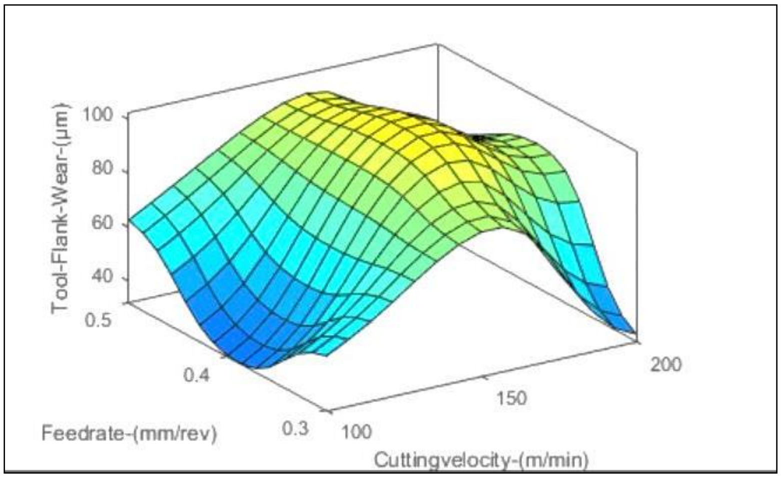

Figure 7.13 3D surface plot for cutting velocity vs feed rate of tool flank wear

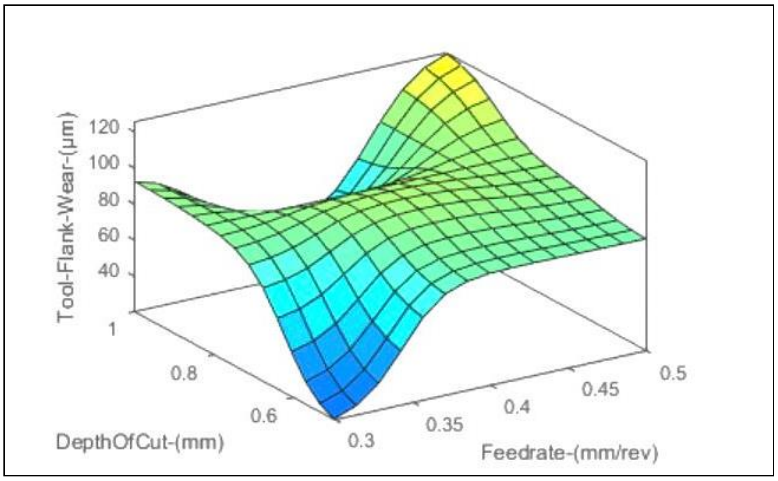

Figure 7.14 3D surface plot for feed rate vs depth of cut of tool flank wear

7.6 ANFIS MODELLING FOR SURFACE ROUGHNESS PREDICTION

The measurement of the surface roughness of machined materials plays a very important role in the finishing of the product. The quality of the product is mainly based on the surface roughness. The surface roughness was measured after 5 minutes of machining Ti-6Al-4V alloy using the modified PCD insert. Table 7.5 shows the validation data of experimentally obtained average surface roughness values of Ti-6Al-4V alloy machined surface as those predicted by ANFIS model by varying the cutting velocity, feed rate and depth of cut. Figure 7.15 provides the comparison of average surface roughness values predicted by the ANFIS model and experimental values. From Table 7.5, it can be observed that the percentage of relative error between the experimental and corresponding ANFIS predicted values range from +3.07 to -4.32. The maximum relative error is corresponding to the cutting velocity of 100 m/min, feed rate of 0.3 mm/rev and depth of cut of 0.5 mm and the minimum relative error corresponds to the process parameters of cutting velocity 150m/min, feed rate of 0.3 mm/rev and depth of cut of 0.5 mm, respectively. The relative error between the experimental and predicted values of entire process parameter variation ranges within the 3.07%. Hence, the model can be used to predict the average surface roughness of the Ti-6Al-4V alloy machined surface. The linear plot in Figure 7.16 represents the perfect fit of the predicted values with the adjusted R square value of 0.97. The value of the regression coefficient close to one represents the close proximity of predicted and target values. Figures 7.17 and 7.18 represent the surface plots obtained during the interaction of cutting parameters. The plot explains the relationship of process parameters during the testing and training of the ANFIS model.

Table 7.5 Comparison of surface roughness predicted by trained ANFIS model with the experimentally obtained surface roughness for machining Ti-6Al-4V alloy

Experimental Trail	Cutting Velocity (m/min)	Feed rate (mm/rev)	Depth of cut (mm)	Experimental Surface Roughness (μm)	Predicted Surface Roughness (μm)	Relative Error (%)
1	100	0.3	0.5	0.148	0.143452	3.073196
2	100	0.4	0.75	0.332	0.330012	0.598898
3	150	0.3	0.5	0.14	0.146049	-4.32072
4	150	0.4	1	0.402	0.38786	3.517307
5	200	0.3	0.75	0.213	0.207341	2.656869
6	200	0.5	0.5	0.132	0.127864	3.133471

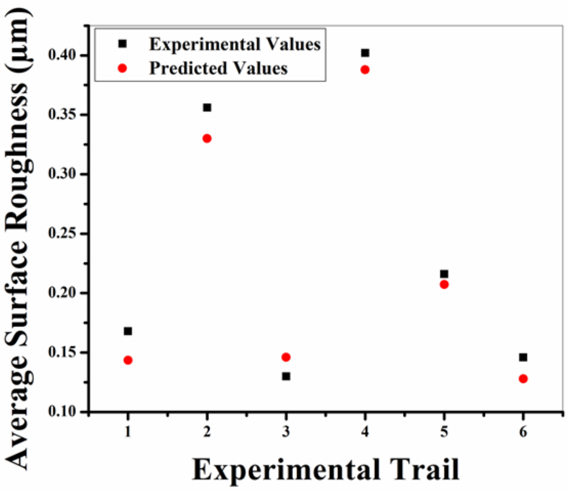

Trial 1- 100m/min, 0.3mm/rev, 0.5mm
Trial 2- 100m/min, 0.4mm/rev, 0.75mm
Trail 3- 150m/min, 0.3mm/rev, 0.5mm
Trail 4- 150m/min, 0.4mm/rev, 1mm
Trail 5- 200m/min, 0.3mm/rev, 0.5mm
Trail 6- 200m/min, 0.5mm/rev, 0.5mm

Figure 7.15 Plots showing the comparison of experimental values and predicted values of surface roughness by ANFIS

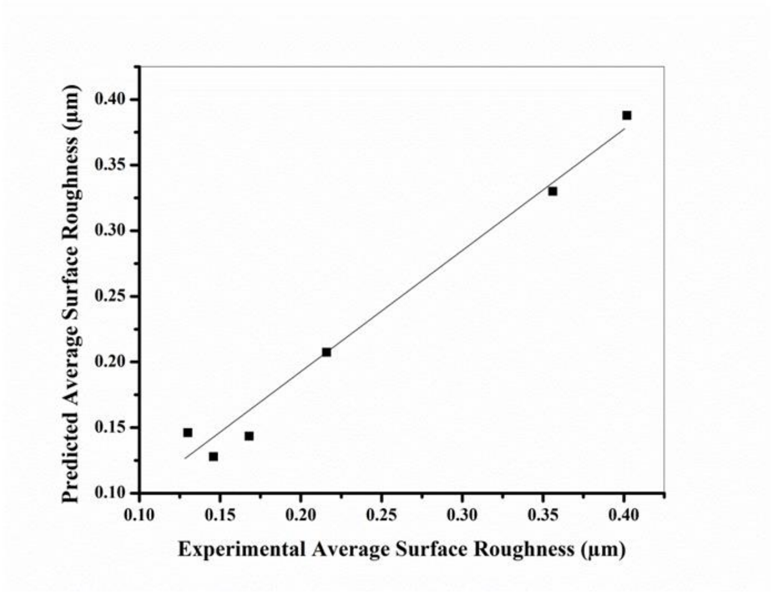

Figure 7.16 Scatter Plot showing the variation of surface roughness for experimental and predicted values using ANFIS

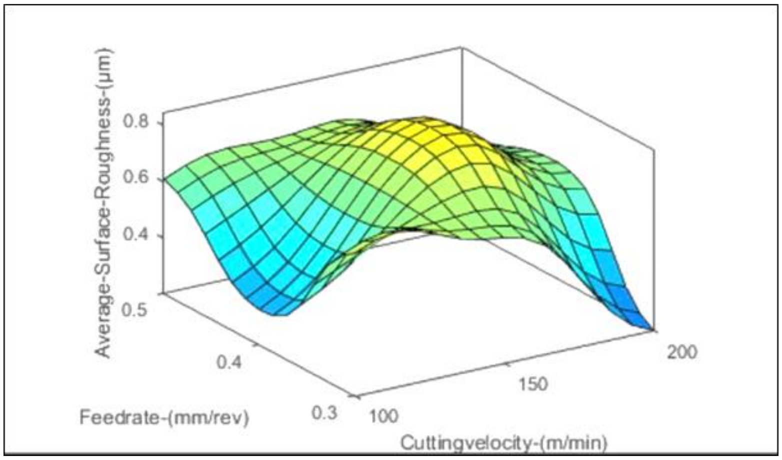

Figure 7.17 3D surface plot for cutting velocity vs feed rate of surface roughness

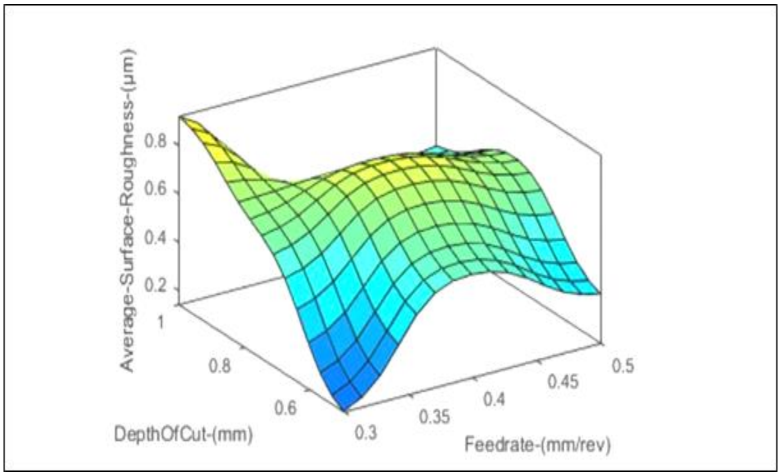

Figure 7.18 3D surface plot for feed rate vs depth of cut of surface roughness

7.7 SUMMARY

An investigation to predict the cutting temperature, machining vibrations, tool flank wear and surface roughness obtained during machining of Ti-6Al-4V alloy using a modified insert are presented in this work. An ANFIS model is used to predict the performance characteristics. The following conclusions can be drawn from the ANFIS prediction model:

- The developed Adaptive Neuro-Fuzzy Inference System model successfully predicted the cutting temperature, machining vibrations, tool flank wear and surface roughness in turning of Ti-6Al-4V alloy with modified PCD insert.
- The percentage of error between validation data ranges from -1.40% to +3.44% for the cutting temperature obtained at the machining zone.
- The majority of the predictions done by the ANFIS model for machining vibrations are within the range of -2.76 to +2.04, respectively.
- The percentage of relative error predicted by the ANFIS model for tool flank wear is within the range of -2.37% to +3.09%.
- The relative percentage error for surface roughness ranges from 3.07% to -1.40% for the validation data.

- The developed ANFIS model with the gauss membership function accurately represents the correlation between the turning process parameters and the performance characteristics.

CHAPTER-8

CONCLUSIONS AND SCOPE FOR FUTURE WORK

8.1 CONCLUSIONS

In the present work, the surface texturing with micro-holes patterns were fabricated on rake and flank face of the cutting insets. The turning experiments were performed under MQL environment with cutting parameters such as cutting velocity, feed rate and depth of cut, to investigate the effect of process parameters on cutting temperature, machining vibrations, tool flank wear, chip morphology and surface integrity (surface roughness, surface topography and microhardness) during the machining of Ti-6Al-4V alloy. Optimization and prediction studies of surface textured inserts have been carried out under the MQL environment. Single object optimization is studied based on the Taguchi technique and ANOVA was used to find the most influencing parameter on each response. Adaptive Neuro-Fuzzy Inference System (ANFIS) has been used as a predictive modelling tool to analyze the responses. The following conclusions were drawn from the experimental and predictive results.

- In the present study, an attempt has been made to make use of micro-holed textured PCD insert for reducing tool wear and increase the tool life. The design of different micro-holed textured inserts was carried out using Pro-E modelling software. In this analytical process, the improvements in the modified inserts over normal inserts have been successfully justified in terms of cutting force, cutting temperature, effective stress, effective strain and total deformations.
- In static analysis investigation using ANSYS 16.0, it was observed that there was not much stress concentration in the micro-hole textured insert which was due to the reduction in cutting force when compared to normal insert. Hence, it was proved that

mechanical strength is not affected by surface textures provided on the inserts. It is also proved that there is no catastrophic failure occurring during machining of the Ti-6Al-4V alloy.

- From the dynamic simulations using DEFORM-3D software, it was observed that micro-hole textured inserts with Design 2, 4, 6 and 7 showed best performance in terms of cutting temperature, stress and strain distributions and also in a decrease of cutting force. Based on the best performance among these modified inserts Design 4 and Design 6 were selected as best insert patterns and investigated for further validation.
- Taguchi technique determined the optimum cutting parameters for the improvement of the turning performance characteristics significantly while machining Ti-6Al-4V alloy. And from ANOVA, it was observed that surface roughness and cutting temperature were significantly affected by Feed rate and Cutting velocity with the contribution of 63.89% and 45.41%, respectively.
- From the health, environmentally clean and productivity improvement point of view, MQL machining satisfies the requirements when compared to dry machining conditions.
- Turning performance characteristics like cutting temperature, tool flank wear and MRR were observed with increasing trend when the turning process parameters like cutting velocity, feed rate and depth of cut increases under MQL condition in normal and modified inserts machining. Whereas, in case of machining vibrations and surface roughness, decreasing trend was observed at the increasing cutting velocity and increasing trend was observed for an increase in feed rate and depth of cut during machining with normal and modified inserts, respectively. In overall, the Design 2 modified insert (with through holes) machining under MQL environment attained the positive results in terms of all turning performance characteristics compared to normal insert and Design 1 insert machining under MQL environment, respectively.
- To identify suitability of insert material for machining of Ti-6Al-4V alloy, the modified PCD insert was compared with the modified PCBN inserts under MQL

environment. From the results of performance characteristics, it was observed that modified PCD inserts showed better performance when compared to PCBN inserts.

- An ANFIS model is developed to aid in decision making. It predicted the workpiece surface roughness, tool flank wear, machining vibrations and cutting zone temperatures, during machining of Ti-6Al-4V alloy using the modified insert with micro-hole texture pattern under MQL environment. The error of the performance characteristics values predicted by ANFIS with gauss membership function is only 4%-5%, reaching accuracy as high as 95-96%, respectively.

8.2 SCOPE FOR FUTURE WORK

Although a lot of work has been carried out on machinability studies of Ti-6Al-4V alloy under MQL environment using the modified insert thoroughly, still, there is a scope on machinability studies of Ti-6Al-4V alloy using modified cutting inserts. Here, some of the suggestions may be useful for future investigations.

- Machinability studies can be carried out by using different cooling strategies like MQL, cryogenic and high-pressure cooling with some more modifications on the cutting inserts.
- Further, for the comparison of the experimental results of modified inserts machining, some other techniques such as abrasion test or non-destructive techniques can be implemented for further investigations.
- Determination of optimum process parameters like white layer formation, microstructure study for investigation of the grain boundaries and cutting force can be studied.

REFERENCES

Ali, M. H., Khidhir, B. A., Mohamed, B., and Oshkour, A.A. (2012). “Prediction of High Cutting Speed Parameters for Ti-6Al-4V by Using Finite Element Modeling.” *Int. J. Model. Optim.*, 2(1), 31–35.

Amin, A. K. M. N., Ismail, A. F., and Nor Khairusshima, M. K. (2007). “Effectiveness of uncoated WC-Co and PCD inserts in end milling of titanium alloy-Ti-6Al-4V.” *J. Mater. Process. Technol.*, 192, 147–158.

Arrazola, P. J., Garay, a., Iriarte, L. M., Armendia, M., Marya, S., and Maître, F. Le. (2009). “Machinability of titanium alloys (Ti6Al4V and Ti555.3).” *J. Mater. Process. Technol.*, 209(5), 2223–2230.

Arrazola, P. J., Kortabarria, A., Madariaga, A., Esnaola, J. A., Fernandez, E., Cappellini, C., Ulutan, D., and Özel, T. (2014). “On the machining induced residual stresses in IN718 nickel-based alloy: Experiments and predictions with finite element simulation.” *Simul. Model. Pract. Theory*, 41, 87–103.

Arulkirubakaran, D., Senthilkumar, V., and Kumawat, V. (2016). “Effect of micro-textured tools on machining of Ti-6Al-4V alloy: An experimental and numerical approach.” *Int. J. Refract. Met. Hard Mater.*, 54, 165–177.

Attanasio, A., Ceretti, E., Fiorentino, A., Cappellini, C., and Giardini, C. (2010). “Investigation and FEM-based simulation of tool wear in turning operations with uncoated carbide tools.” *Wear*, 269(5–6), 344–350.

Ayed, Y., Germain, G., Ammar, A., and Furet, B. (2015). “Tool wear analysis and improvement of cutting conditions using the high-pressure water-jet assistance when machining the Ti17 titanium alloy." *Precis. Eng.*, 42, 294–301.

Balažic, M., and Kopač, J. (2010). "Machining of titanium alloy Ti-6Al-4V for biomedical applications." *Stroj. Vestnik/Journal Mech. Eng.*, 56(3), 1–5.

Baradie, M. A. El. (1996a). "Cutting fluids: Part I. Characterisation." *J. Mater. Process. Technol.*, 56(1–4), 786–797.

Baradie, M. A. El. (1996b). "Cutting fluids: Part II. Recycling and clean machining." *J. Mater. Process. Technol.*, 56(1–4), 798–806.

Bayoumi, A. E., and Xie, J. Q. (1995). "Some metallurgical aspects of chip formation in cutting Ti-6wt.%Al-4wt.%V alloy." *Mater. Sci. Eng. A*, 190(1–2), 173–180.

Bermingham, M. J., Palanisamy, S., Kent, D., and Dargusch, M. S. (2012). "A comparison of cryogenic and high pressure emulsion cooling technologies on tool life and chip morphology in Ti-6Al-4V cutting." *J. Mater. Process. Technol.*, 212(4), 752–765.

Bhatt, A., Attia, H., Vargas, R., and Thomson, V. (2010). "Wear mechanisms of WC coated and uncoated tools in finish turning of Inconel 718." *Tribol. Int.*, 43(5–6), 1113–1121.

Bhuiyan, M. S. H., Choudhury, I. a., and Dahari, M. (2014). "Monitoring the tool wear, surface roughness and chip formation occurrences using multiple sensors in turning." *J. Manuf. Syst.*, 33(4), 476–487.

Bragov, A., Konstantinov, A., Lomunov, A., Sergeichev, I., and Fedulov, B. (2009). "Experimental and numerical analysis of high strain rate response of Ti-6Al-4V titanium alloy." *J. Phys. IV,* 137, 1465.

Çalışkan, H., and Küçükköse, M. (2015). "The effect of aCN/TiAlN coating on tool wear, cutting force, surface finish and chip morphology in face milling of Ti6Al4V superalloy." *Int. J. Refract. Met. Hard Mater.*, 50, 304–312.

Campbell Jr, F. C. (2011). *Manufacturing technology for aerospace structural materials*. Elsevier.

Çaydaş, U., Hasçalik, A., and Ekici, S. (2009). "An adaptive neuro-fuzzy inference system (ANFIS) model for wire-EDM." *Expert Syst. Appl.*, 36(3), 6135–6139.

Ceretti, E., Fallböhmer, P., Wu, W. T., and Altan, T. (1996). "Application of 2D FEM to chip formation in orthogonal cutting." *J. Mater. Process. Technol.*, 59(1–2), 169–180.

Chauhan, S. R., and Dass, K. (2012). "Optimization of machining parameters in turning of titanium (Grade-5) alloy using response surface methodology." *Mater. Manuf. Process.*, 27(5), 531–537.

Che-Haron, C. H., and Jawaid, A. (2005). "The effect of machining on surface integrity of titanium alloy Ti-6% Al-4% V." *J. Mater. Process. Technol.*, 166(2), 188–192.

Chen, B., Chen, X., Li, B., He, Z., Cao, H., and Cai, G. (2011). "Reliability estimation for cutting tools based on logistic regression model using vibration signals." *Mech. Syst. Signal Process.*, 25(7), 2526–2537.

Cherukuri, R., and Molian, P. (2003). "Lathe turning of titanium using pulsed laser deposited, ultra-hard boride coatings of carbide inserts." *Mach. Sci. Technol.*, 7(1), 119–135.

Chetan, Ghosh, S., and Rao, P. V. (2016). “Environment Friendly Machining of Ni-Cr-Co Based Super Alloy using Different Sustainable Techniques.” *Mater. Manuf. Process.*, 31(7), 852–859.

Chiappini, E., Tirelli, S., Albertelli, P., Strano, M., and Monno, M. (2014). “On the mechanics of chip formation in Ti-6Al-4V turning with spindle speed variation.” *Int. J. Mach. Tools Manuf.*, 77, 16–26.

Chinchanikar, S., and Choudhury, S. K. (2014). “Hard turning using HiPIMS-coated carbide tools : Wear behavior under dry and minimum quantity lubrication (MQL).” *Measurement*, 55, 536–548.

Chiou, R. Y., Aynbinder, V., Stepanskiy, L. G., Lu, L., Rauniar, S., Chen, J. S. J., and North, M. T. (2005). “Analytical study of the effect of heat pipe cooling in machining.” *Am. Soc. Mech. Eng. Manuf. Eng. Div. MED*, 16, 13-21.

Coz G. Le, M. Marinescu , A. Devillez , and D. Dudzinski, L. V. (2012). “Measuring temperature of rotating cutting tools: Application to MQL drilling and dry milling of aerospace alloys.” *Appl. Therm. Eng.*, 36(1), 434–441.

D’, G., Mello, N. A., Pai, P. S., Puneet, N. P., and Fang, N. (2016). “Surface roughness evaluation using machining vibrations in high speed turning of Ti-6Al-4V - an experimental approach.” *Int. J. Mach. Mach. Mater.*, 18(3), 288.

Da Silva, W. M., Suarez, M. P., Machado, A. R., and Costa, H. L. (2013). “Effect of laser surface modification on the micro-abrasive wear resistance of coated cemented carbide tools.” *Wear*, 302(1–2), 1230–1240.

Dabnun, M. A., Hashmi, M. S. J., and El-Baradie, M. A. (2005). “Surface roughness prediction model by design of experiments for turning machinable glass-ceramic (Macor).” *J. Mater. Process. Technol.*, 164, 1289–1293.

Daghini, L., Archenti, A., and Nicolescu, C. M. (2009). “Design , Implementation and Analysis of Composite Material Dampers for Turning Operations.” *World Acad. Sci. Eng. Technol.*, 53(4), 613–620.

Dass, K., and Chauhan, S. R. (2011). “Machinability Study of Titanium (Grade-5) Alloy Using Design of Experiment Technique.” *Engineering*, 3(6), 609–621.

Davim, J. P. (Ed.). (2010). “*Surface integrity in machining*”, London: Springer, Vol. 1848828742.

Debnath, S., Reddy, M. M., and Yi, Q. S. (2016). “Influence of cutting fluid conditions and cutting parameters on surface roughness and tool wear in turning process using Taguchi method.” *Measurement*, 78, 111–119.

Deiab, I., Waqar, S., and Pervaiz, S. (2014). “Analysis of Lubrication Strategies for Sustainable Machining during Turning of Titanium Ti - 6Al - 4V alloy.” *Procedia CIRP*, 17, 766–771.

Dhananchezian, M., Kumar, M. P., and Sornakumar, T. (2011). “Cryogenic Turning of AISI 304 Stainless Steel with Modified Tungsten Carbide Tool Inserts.” *Mater. Manuf. Process.*, 26(5), 781–785.

Dhar, N. R., Islam, M. W., Islam, S., and Mithu, M. A. H. (2006). “The influence of minimum quantity of lubrication (MQL) on cutting temperature, chip and dimensional accuracy in turning AISI-1040 steel.” *J. Mater. Process. Technol.*, 171(1), 93–99.

Dorlin, T., Fromentin, G., and Costes, J. (2015). “Analysis and modelling of the contact radius effect on the cutting forces in cylindrical and face turning of Ti6Al4V titanium alloy.” *Procedia CIRP*, 31, 185–190.

Ebersbach, S., and Peng, Z. (2008). “Expert system development for vibration analysis in machine condition monitoring.” *Expert Syst. Appl.*, 34(1), 291–299.

Enomoto, T., Sugihara, T., Yukinaga, S., Hirose, K., and Satake, U. (2012). “Highly wear-resistant cutting tools with textured surfaces in steel cutting.” *CIRP Ann. - Manuf. Technol.*, 61(1), 571–574.

Etsion, I. (2004). “Improving tribological performance of mechanical components by laser surface texturing.” *Tribol. Lett.*, 17(4), 733–737.

Ezilarasan, C., Senthil Kumar, V. S., and Velayudham, A. (2014). “Theoretical predictions and experimental validations on machining the Nimonic C-263 super alloy.” *Simul. Model. Pract. Theory*, 40, 192–207.

Ezugwu, E. O. (2004). “High speed machining of aero-engine alloys.” *J. Brazilian Soc. Mech. Sci. Eng.*, 26(1), 1–11.

Ezugwu, E. O. (2005). “Key improvements in the machining of difficult-to-cut aerospace superalloys.” *Int. J. Mach. Tools Manuf.*, 45(12–13), 1353–1367.

Ezugwu, E. O., and Wang, Z. M. (1997). “Titanium alloys and their machinability.” *J. Mater. Process. Technol.*, 68(3), 262–274.

Ezugwu, E. O., Bonney, J., and Yamane, Y. (2003). “An overview of the machinability of aeroengine alloys.” *J. Mater. Process. Technol.,*134(2), 233-253.

Fahad, M., Mativenga, P. T., and Sheikh, M. A. (2012). “A comparative study of multilayer and functionally graded coated tools in high-speed machining.” *Int. J. Adv. Manuf. Technol.*, 62(1–4), 43–57.

Fang, N., Pai, P. S., and Edwards, N. (2012). “Tool-Edge Wear and Wavelet Packet Transform Analysis in High-Speed Machining of Inconel 718.” *J. Mech. Eng.,* 58(3), 191–202.

Fang, N., Pai, P. S., and Mosquea, S. (2011). “Effect of tool edge wear on the cutting forces and vibrations in high-speed finish machining of Inconel 718: An experimental study and wavelet transform analysis.” *Int. J. Adv. Manuf. Technol.*, 52(1–4), 65–77.

Filice, L., Micari, F., Rizzuti, S., and Umbrello, D. (2007). “A critical analysis on the friction modelling in orthogonal machining.” *Int. J. Mach. Tools Manuf.*, 47(3–4), 709–714.

Ginting, A., and Nouari, M. (2009). “Surface integrity of dry machined titanium alloys.” *Int. J. Mach. Tools Manuf.*, 49(3–4), 325–332.

Guo, Y. B., Li, W., and Jawahir, I. S. (2009). “Surface integrity characterization and prediction in machining of hardened and difficult-to-machine alloys: A state-of-art research review and analysis.” *Mach. Sci. Technol.*, 13(4), 437–470.

Hao, X., Cui, W., Li, L., Li, H., Khan, A. M., and He, N. (2018). “Cutting performance of textured polycrystalline diamond tools with composite lyophilic/lyophobic wettabilities.” *J. Mater. Process. Technol.*, 260, 1–8.

Harms, A., Denkena, B., Lhermet, N., Tools, M., and Technologies, C. (2004). “Tool Adaptor for Active Vibration Control in turning operations.” *In 9th Int. Conf. on New Actu.*, 14–16.

Harsha, N., Kumar, I. A., Raju, K. S. R., and Rajesh, S. (2018). “Prediction of Machinability characteristics of Ti6Al4V alloy using Neural Networks and Neuro-Fuzzy techniques.” *Mater. Today Proc.*, 5(2), 8454–8463.

Hasçalik, A., and Çaydaş, U. (2007). “Electrical discharge machining of titanium alloy (Ti-6Al-4V).” *Appl. Surf. Sci.*, 253(22), 9007–9016.

Hong, S. Y., Ding, Y., and Jeong, J. (2002). “Experimental evaluation of friction coefficient and liquid nitrogen lubrication effect in cryogenic machining.” *Mach. Sci. Technol.*, 6(2), 235–250.

Honghua, S. U., Peng, L. I. U., Yucan, F. U., and Jiuhua, X. U. (2012). “Tool Life and Surface Integrity in High-speed Milling of Titanium Alloy TA15 with PCD/PCBN Tools.” *Chinese J. Aeronaut.*, 25(5), 784–790.

Hua, J., and Shivpuri, R. (2004). “Prediction of chip morphology and segmentation during the machining of titanium alloys.” *J. Mater. Process. Technol.*, 150(1–2), 124–133.

Huang, P. L., Li, J. F., Sun, J., and Zhou, J. (2014). “Study on performance in dry milling aeronautical titanium alloy thin-wall components with two types of tools.” *J. Clean. Prod.*, 67, 258–264.

Ibrahim, G. A., Che Haron, C. H., and Ghani, J. A. (2009). “Surface integrity of Ti-6Al-

4V ELI when machined using coated carbide tools under dry cutting condition." *Int. J. Mech. Mater. Eng.*, 4(2), 191–196.

Jaffery, S. I., and Mativenga, P. T. (2009). "Assessment of the machinability of Ti-6Al-4V alloy using the wear map approach." *Int. J. Adv. Manuf. Technol.*, 40(7–8), 687–696.

Jang J S, S. C. T. and M. E. (1993). *ANFIS (Adaptive Neuro-Fuzzy Inference Systems), Neuro Fuzzy and Soft Computing-A Computational Approach to Learning and Machine Intelligence*. PHI Learning Pvt Ltd.

Jantunen, E. (2002). "A summary of methods applied to tool condition monitoring in drilling." *Int. J. Mach. Tools Manuf.*, 42(9), 997–1010.

Jen, T., Tuchowski, F., and Chen, Y. (2005). "Investigation of Thermosyphon Cooling for Drilling Operation : An Experimental Study." *Am. Soc. Mech. Eng. Manuf. Eng. IMECE*, 59-67.

Jesudass Thomas, S., and Kalaichelvan, K. (2018). "Comparative study of the effect of surface texturing on cutting tool in dry cutting." *Mater. Manuf. Process.*, 33(6), 683–694.

Jianxin, D., Ze, W., Yunsong, L., Ting, Q., and Jie, C. (2012). "Performance of carbide tools with textured rake-face filled with solid lubricants in dry cutting processes." *Int. J. Refract. Met. Hard Mater.*, 30, 164–172.

Kalpakjian, S., Schmid, S. R., & Sekar, K. S. (2014). *Manufacturing Engineering and Technology*. Delhi: Addison Wesley, Longman (Singapore) Pte. Ltd.

Karpat, Y. (2011). "Temperature dependent flow softening of titanium alloy Ti6Al4V: An investigation using finite element simulation of machining." *J. Mater. Process.*

Technol., 211(4), 737–749.

Kawasegi, N., Sugimori, H., Morimoto, H., Morita, N., and Hori, I. (2009). “Development of cutting tools with microscale and nanoscale textures to improve frictional behavior.” *Precis. Eng.*, 33, 248–254.

Klocke, F., and Eisenblätter, G. (1998). “Dry cutting - State of research.” *VDI Berichte*, 46(1399), 159–188.

Kouam, J., Songmene, V., Balazinski, M., and Hendrick, P. (2015). “Effects of minimum quantity lubricating (MQL) conditions on machining of 7075-T6 aluminum alloy.” *Int. J. Adv. Manuf. Technol.*, 79(5–8), 1325–1334.

Kovac P., D. R., Savkovic, V. P. B., and Gostimirovic, M. (2013). “Application of fuzzy logic and regression analysis for modeling surface roughness in face milliing.” *J. Intell. Manuf.*, 24(4), 755–762.

Kumar, J. P., & Thirumurugan, K. (2012). “Optimization of Machining Parameters for Milling Titanium Using Taguchi Method.” *Int. J. Adv. Eng. Technol.*, 3(2), 108–113.

Kümmel, J., Braun, D., Gibmeier, J., Schneider, J., Greiner, C., Schulze, V., and Wanner, A. (2015). “Study on micro texturing of uncoated cemented carbide cutting tools for wear improvement and built-up edge stabilisation.” *J. Mater. Process. Technol.*, 215, 62–70.

Kuppaswamy G. (1996). *Principles of Metal Cutting*. Universities Press.

Kuzu, A. T., Bijanzad, A., and Bakkal, M. (2015). “Experimental Investigations of Machinability in the Turning of Compacted Graphite Iron using Minimum Quantity

Lubrication." *Mach. Sci. Technol.*, 19(4), 559–576.

Lei, S., Devarajan, S., and Chang, Z. (2009). "A study of micropool lubricated cutting tool in machining of mild steel." *J. Mater. Process. Technol.*, 209, 1612–1620.

Lesuer, D. R. (2000). *Experimental Investigations of Material Models for Ti-6Al-4V Titanium and 2024-T3 Aluminum: Final Report*. California.

Li, L., Li, Z. Y., Wei, X. T., and Cheng, X. (2015). "Machining characteristics of inconel 718 by sinking-EDM and wire-EDM." *Mater. Manuf. Process.*, 30(8), 968–973.

Li, Y., Deng, J., Chai, Y., and Fan, W. (2016). "Surface textures on cemented carbide cutting tools by micro EDM assisted with high-frequency vibration." *Int. J. Adv. Manuf. Technol.*, 82(9–12), 2157–2165.

Liang, L., Liu, X., Li, X., and Li, Y.-Y. (2015). "Wear mechanisms of WC–10Ni3Al carbide tool in dry turning of Ti6Al4V." *Int. J. Refract. Met. Hard Mater.*, 48, 272–285.

Lo, S. W., & Wilson, W. R. (1999). "A Theoretical Model of Micro-Pool Lubrication in Metal Forming." *J. Tribol.*, 121(4), 731-738.

Lorentzon, J., and Järvstråt, N. (2008). "Modelling tool wear in cemented-carbide machining alloy 718." *Int. J. Mach. Tools Manuf.*, 48(10), 1072–1080.

Lorentzon, J., Järvstråt, N., and Josefson, B. L. (2009). "Modelling chip formation of alloy 718." *J. Mater. Process. Technol.*, 209(10), 4645–4653.

M'Saoubi;, R., Outeiro, J. C., Chandrasekaran, H., Jr., O. W. D., and Jawahir, I. S.

(2008). “A review of surface integrity in machining and its impact on functional performance and life of machined products.” *Int. J. Sustain. Manuf.,* 1(1-2), 203-236.

Ma, C., and Zhu, H. (2011). “An optimum design model for textured surface with elliptical-shape dimples under hydrodynamic lubrication.” *Tribol. Int.*, 44(9), 987–995.

Ma, J., Duong, N. H., and Lei, S. (2015). “Finite element investigation of friction and wear of microgrooved cutting tool in dry machining of AISI 1045 steel.” *Proc. Inst. Mech. Eng. Part J J. Eng. Tribol.*, 229(4), 449–464.

Ma, J., Duong, N. H., and Lei, S. (2015). “Numerical investigation of the performance of microbump textured cutting tool in dry machining of AISI 1045 steel.” *J. Manuf. Process.*, 19, 194-204.

Machado, Á. R., and Wallbank, J. (1997). “The effect of extremely low lubricant volumes in machining.” *Wear*, 210(1–2), 76–82.

Machai, C., and Biermann, D. (2011). “Machining of β-titanium-alloy Ti-10V-2Fe-3Al under cryogenic conditions: Cooling with carbon dioxide snow.” *J. Mater. Process. Technol.*, 211(6), 1175–1183.

Madhukar, S., Shravan, A., Vidyanand, P., and Reddy, G. S. (2016). “A Critical review on Minimum Quantity Lubrication (MQL) Coolant System for Machining.” *Int. J. Curr. Eng. Technol.,* 6(5), 1745-1751.

Mahdavinejad, R. A., and Saeedy, S. (2011). “Investigation of the influential parameters of machining of AISI 304 stainless steel.” *Sadhana*, 36(6), 963–970.

Maher, I., Eltaib, M. E. H., Sarhan, A. A., and El-Zahry, R. M. (2015). “Cutting force-based adaptive neuro-fuzzy approach for accurate surface roughness prediction in end milling operation for intelligent machining." *Int. J. Adv. Manuf. Technol.,* 76(5–8), 1459–1467.

Maity, K. P., and Swain, P. K. (2008). "An experimental investigation of hot-machining to predict tool life." *J. Mater. Process. Technol.*, 198(1–3), 344–349.

Manivel, D., and Gandhinathan, R. (2016). "Optimization of surface roughness and tool wear in hard turning of austempered ductile iron (grade 3) using Taguchi method." *Measurement,* 93, 108–116.

Manjaiah, M., Narendranath, S., and Basavarajappa, S. (2016). "Wire Electro Discharge Machining Performance of TiNiCu Shape Memory Alloy." *Silicon,* 8(3), 467–475.

Manna, A. (2013). "Multi-response optimisation of machining parameters during drilling LM6Mg15SiC-Al-MMC based on Grey relational analysis." *Int. J. Mach. Mach. Mater.*, 14(3), 275–294.

Montgomery D.C. (1987). *Design and analysis of experiments-Second edition*. Quality and Reliability Engineering International.

Montgomery D.C. (2017). *Design and Analysis of Experiments*. John Wiley & sons, Inc.

Mori, M., and Furuta, M. (1999). "High-Speed Machining of Titanium by New PCD Tools." *SAE Technical Paper,* (No. 1999-01-2296).

Nabhani, F. (2001). "Wear mechanisms of ultra-hard cutting tools materials." *J. Mater. Process. Technol.,* 115(3), 402–412.

Nandy, A. K., Gowrishankar, M. C., and Paul, S. (2009). "Some studies on high-pressure cooling in turning of Ti-6Al-4V.” *Int. J. Mach. Tools Manuf.*, 49(2), 182–198.

Narutaki, N., Murakoshi, A., Motonishi, S., and Takeyama, H. (1983). “Study on machining of titanium alloys.” *CIRP Ann.*, 32(1), 65–69.

Niketh, S., and Samuel, G. L. (2018). “Surface texturing for tribology enhancement and its application on drill tool for the sustainable machining of titanium alloy.” *J. Clean. Prod.*, 167, 253–270.

Nithyanandam, J., LalDas, S., and Palanikumar, K. (2014). “Surface Roughness Analysis in Turning of Titanium Alloy by Nanocoated Carbide Insert.” *Procedia Mater. Sci.*, 5, 2159–2168.

Nouari, M., and Makich, H. (2013). “Experimental investigation on the effect of the material microstructure on tool wear when machining hard titanium alloys : Ti-6Al-4V and Ti-555.” *Int. J. Refract. Met. Hard Mater.*, 41, 259–269.

Oosthuizen G A, Akdogan G, D. D. and T. N. F. (2010). “A Review of the Machinability of Titanium Alloys.” *Res. Dev. South African Inst. Mech. Eng.*, 26, 43–52.

Ota, M., Okida, J., Harada, T., Toda, N., and Sumiya, H. (2009). “High speed cutting of titanium alloy with PCD tools.” *Key Eng. Mater.*, 389, 157–162.

Ozcelik, B., Kuram, E., and Simsek, B. T. (2011). “Comparison of dry and wet end milling of AISI 316 stainless steel.” *Mater. Manuf. Process.*, 26(8), 1041–1049.

Palanisamy, D., and Senthil, P. (2017). “Development of ANFIS model and machinability study on dry turning of cryo-treated PH stainless steel with various inserts." *Mater. Manuf. Process.*, 32(6), 654–669.

Patil, H. B., Chavan, P. B., and Kazi, S. H. (2013). "Effects of Cryogenic on Tool Steels-a Review." *Int. J. Mech. Prod. Eng.*, 1(1), 31–36.

Pawade, R. S., and Joshi, S. S. (2011). "Mechanism of chip formation in high-speed turning of inconel 718." *Mach. Sci. Technol.*, 15(1), 132–152.

Pereira, O., Rodríguez, A., Fernández-Abia, A. I., Barreiro, J., & de Lacalle, L. L. (2016). "Cryogenic and minimum quantity lubrication for an eco-efficiency turning of AISI 304." *J. Clean. Prod.*, 139, 440–449.

Phadke M. S. (1995). *Quality Engineering using Robust Design*. Prentice Hall PTR.
Pramanik, A. (2014). "Problems and solutions in machining of titanium alloys." *Int. J. Adv. Manuf. Technol.*, 70(5–8), 919–928.

Pramanik, A., and Littlefair, G. (2015). "Machining of titanium alloy (Ti-6Al-4V)-theory to application." *Mach. Sci. Technol.*, 19(1), 1–49.

Pramanik, A., Islam, M. N., Basak, A., and Littlefair, G. (2013). "Machining and Tool Wear Mechanisms during Machining Titanium Alloys." *Adv. Mater. Res.*, Trans Tech Publications, 651, 338–343.

Prashanth, B., and Krishnaraj, J. (2017). "Optimization of Surface Roughness of Titanium Alloy Ti-6Al-4V Using Taguchi Technique." *Int. J. Civ. Eng. Technol.*, 8(7), 115–121.

Quan, Y., and Ye, B. (2003). "The effect of machining on the surface properties of

SiC/Al composites." *J. Mater. Process. Technol.*, 138(1–3), 464–467.

Rahim, E. A., and Sasahara, H. (2011). "A study of the effect of palm oil as MQL lubricant on high speed drilling of titanium alloys." *Tribol. Int.*, 44(3), 309–317.

Rahman, M., Kumar, A. S., and Salam, M. U. (2002). "Experimental evaluation on the effect of minimal quantities of lubricant in milling." *Int. J Mach. Tool Manu.*, 42(5), 539–547.

Rahman, M., San WONG, Y., & Zareena, A. R. (2003). "Machinability of Titanium Alloys." *JSME Int. J. Ser. C*, 46(1), 107–115.

Rahman, M., Wang, Z. G., & Wong, Y. S. (2006). "A Review on High-Speed Machining of Titanium Alloys." *JSME Int. J. Ser. C*, 49(1), 11–20.

Rai, A. A., Pai, P. S., & Rao, B. S. (2015). "Prediction models for performance and emissions of a dual fuel CI engine using ANFIS." *Sadhana - Acad. Proc. Eng. Sci.*, 40(2), 515–535.

Ramana, M. V., Rao, G. K. M., and Rao, D. H. (2014). "CHIP morphology in turning of Ti-6Al-4V ALLOY under different machining conditions." *J. Prod. Eng.*, 17(1), 27-32.

Ramana, M. V., Srinivasulu, K., and Rao, G. K. M. (2011). "Performance Evaluation and Selection of Optimal Parameters in Turning of Ti-6Al-4V Alloy Under Different Cooling Conditions." *Int. J Inn. Tech. & Crea. Eng.*, 1(5), 10–21.

Ramesh, S., Karunamoorthy, L., and Palanikumar, K. (2012). "Measurement and analysis of surface roughness in turning of aerospace titanium alloy (gr5)." *Measurement*, 45(5), 1266–1276.

Ravi Kumar, S. M., and Kulkarni, S. K. (2017). "Analysis of Hard Machining of Titanium Alloy by Taguchi Method." *Mater. Today Proc.*, 4(10), 10729–10738.

Rehorn, A. G., Jiang, J., and Orban, P. E. (2005). "State-of-the-art methods and results in tool condition monitoring: A review." *Int. J. Adv. Manuf. Technol.*, 26(7–8), 693–710.

Ren, J., Zhou, J., and Wei, J. (2015). "Optimization of cutter geometric parameters in end milling of titanium alloy using the grey-taguchi method." *Adv. Mech. Eng.*, 7(2), 721093.

Ren, Q., Balazinski, M., Baron, L., Jemielniak, K., Botez, R., and Achiche, S. (2014). "Type-2 fuzzy tool condition monitoring system based on acoustic emission in micromilling." *Inf. Sci. (Ny).*, 255, 121–134.

Revankar, G. D., Shetty, R., Rao, S. S., and Gaitonde, V. N. (2014). "Analysis of surface roughness and hardness in titanium alloy machining with polycrystalline diamond tool under different lubricating modes." *Mater. Res.*, 17(4), 1010–1022.

Revuru, R. S., Zhang, J. Z., Posinasetti, N. R., and Kidd, T. (2018). "Optimization of titanium alloys turning operation in varied cutting fluid conditions with multiple machining performance characteristics." *Int. J. Adv. Manuf. Technol.*, 95(1–4), 1451–1463.

Ross P J. (1996). *Taguchi techniques for quality engineering: loss function, orthogonal experiments, parameter and tolerance design*. McGraw-Hill, New York.

Rowe, W. B., Li, Y., Mills, B., and Allanson, D. R. (1996). "Application of intelligent

CNC in grinding.” *Comput. Ind.*, 31(1), 45–60.

Sahin, Y., and Motorcu, A. R. (2004). “Surface Roughness Prediction Model in Machining of Carbon Steel by PVD Coated Cutting Tools.” *Am. J. Appl. Sci.*, 1(1), 12–17.

Sarıkaya, M., Yılmaz, V., and Güllü, A. (2016). “Analysis of cutting parameters and cooling/lubrication methods for sustainable machining in turning of Haynes 25 superalloy.” *J. Clean. Prod.*, 133, 172–181.

Sarkheyli, A., Zain, A. M., and Sharif, S. (2015). “A multi-performance prediction model based on ANFIS and new modified-GA for machining processes.” *J. Intell. Manuf.*, 26(4), 703–716.

Selvakumar, S., Ravikumar, R., and Raja, K. (2012). “Designing and Conducting Experiments for Optimization of satisfactory Cutting conditions in Micro Turning by using Titanium Alloy.” *Int. J. Sci. Eng. Res.*, 3(8), 1–9.

Senthilkumar, N., Ganapathy, T., and Tamizharasan, T. (2014). “Optimisation of machining and geometrical parameters in turning process using Taguchi method.” *Aust. J. Mech. Eng.*, 12(2), 233-246.

Sharma, J., and Sidhu, B. S. (2014). “Investigation of effects of dry and near dry machining on AISI D2 steel using vegetable oil.” *J. Clean. Prod.*, 66, 619–623.

Sharma, P., Chakradhar, D., and Narendranath, S. (2015). “Evaluation of WEDM performance characteristics of Inconel 706 for turbine disk application.” *Mater. Des.*, 88, 558–566.

Sharma, V. S., Dogra, M., and Suri, N. M. (2009). “Cooling techniques for improved productivity in turning.” *Int. J. Mach. Tools Manuf.*, 49(6), 435–453.

Sharma, V., and Pandey, P. M. (2016). “Recent advances in turning with textured cutting tools: A review.” *J. Clean. Prod.*, 137, 701–715.

Shaw, M. C. (1984). *Metal Cutting Principles*. Clarendon Press. U.S.

Shaw, M. C. (2005). *Metal cutting principles–Oxford series on advanced manufacturing*. Oxford University Press, New York (USA).

Shokrani, A., Dhokia, V., and Newman, S. T. (2012). “Environmentally conscious machining of difficult-to-machine materials with regard to cutting fluids.” *Int. J. Mach. Tools Manuf.*, 57, 83–101.

Song, D. Y., Otani, N., Aoki, T., Kamakoshi, Y., Ohara, Y., and Tamaki, H. (2005). “A new approach to cutting state monitoring in end-mill machining.” *Int. J. Mach. Tools Manuf.*, 45(7–8), 909–921.

Sreejith, P. S., and Ngoi, B. K. A. (2000). “Dry machining: Machining of the future.” *J. Mater. Process. Technol.*, 101(1), 287–291.

Srivastava, A. K., Zhang, X., Tim, B., and Cadigan, S. (2011). “Investigations on turning Ti-6Al-4V titanium alloy using super-finished tool edge geometry generated by micro-machining process (MMP).” *CIRP Ann. Manuf. Technol.*, 1(3), 4–9.

Su, Y., He, N., Li, L., and Li, X. L. (2006). “An experimental investigation of effects of cooling/lubrication conditions on tool wear in high-speed end milling of Ti-6Al-4V.” *Wear*, 261(7–8), 760–766.

Su, Y., Li, L., He, N., and Zhao, W. (2014). "Experimental study of fiber laser surface texturing of polycrystalline diamond tools." *Int. J. Refract. Met. Hard Mater.,* 45, 117–124.

Sugihara, T., and Enomoto, T. (2009). "Development of a cutting tool with a nano/micro-textured surface-Improvement of anti-adhesive effect by considering the texture patterns." *Precis. Eng.,* 33, 425–429.

Sugihara, T., and Enomoto, T. (2012). "Improving anti-adhesion in aluminum alloy cutting by micro stripe texture." *Precis. Eng.,* 36(2), 229–237.

Sugihara, T., and Enomoto, T. (2013). "Crater and flank wear resistance of cutting tools having micro textured surfaces." *Precis. Eng.,* 37(4), 888–896.

Suparta, W., and Alhasa, K. M. (2013). "A comparison of ANFIS and MLP models for the prediction of precipitable water vapor." *Int. Conf. Sp. Sci. Commun. Iconsp.,* IEEE, 243–248.

Sutherland, J. W., Kulur, V. N., King, N. C., and Turkovich, B. F. von. (2000). "An Experimental Investigation of Air Quality in Wet and Dry Turning." *CIRP Ann. - Manuf. Technol.,* 49(1), 61–64.

Taguchi. (1986). *Introduction to quality engineering: designing quality into product and processes*. Asian Productivity Organization, Tokyo.

Thakur, A., and Gangopadhyay, S. (2016). "Dry machining of nickel-based super alloy as a sustainable alternative using TiN/TiAlN coated tool." *J. Clean. Prod.,* 129, 256–268.

Thakur, D. G., Ramamoorthy, B., and Vijayaraghavan, L. (2009). “Machinability investigation of Inconel 718 in high-speed turning.” *Int. J. Adv. Manuf. Technol.*, 45(5–6), 421–429.

Thomas Childs, Katsuhiro Maekawa, Toshiyuki Obikawa, Y. Y. (2000). *Metal machining: theory and applications*. Arnold, Paris.

Trent E. M and Wright P.K. (2000). *Metal Cutting*. Butterworth-Heinemann, Boston, USA.

Umbrello, D., M’Saoubi, R., and Outeiro, J. C. (2007). “The influence of Johnson-Cook material constants on finite element simulation of machining of AISI 316L steel.” *Int. J. Mach. Tools Manuf.*, 47(3–4), 462–470.

Umbrello, D., Rizzuti, S., Outeiro, J. C., Shivpuri, R., and M’Saoubi, R. (2008). “Hardness-based flow stress for numerical simulation of hard machining AISI H13 tool steel.” *J. Mater. Process. Technol.*, 199(1), 64–73.

Usui, E. and Shirakashi, T. (1982). “Mechanics of machining-from ‘descriptive’ to ‘predictive’ theory.” *ASME Pub.*, 7, 13–35.

Vardhaman, B. S. A., Amarnath, M., Jhodkar, D., Ramkumar, J., Chelladurai, H., & Roy, M. K. (2018). “Influence of coconut oil on tribological behavior of carbide cutting tool insert during turning operation.” *J. Brazilian Soc. Mech. Sci. Eng.*, 40(9), 450.

Veiga, C., and Davim, J. P. (2013). “Review on Machinability of Titanium Alloys : the Process Perspective.” *Rev. Adv. Mater. Sci.*, 34(2), 148–164.

Vijay Sekar, K. S., and Pradeep Kumar, M. (2011). “Finite element simulations of Ti6Al4V titanium alloy machining to assess material model parameters of the Johnson-

Cook constitutive equation.” *J. Brazilian Soc. Mech. Sci. Eng.*, 33(2), 203–211.

Walia, N., Singh, H., and Sharma, A. (2015). “ANFIS: Adaptive neuro-fuzzy inference system-a survey.” *Int. J. Comput. Appl.*, 123(13), 32–38.

Wan, Z. P., Zhu, Y. E., Liu, H. W., and Tang, Y. (2012). “Microstructure evolution of adiabatic shear bands and mechanisms of saw-tooth chip formation in machining Ti6Al4V.” *Mater. Sci. Eng. A*, 531, 155–163.

Wang, T., Huang, W., Liu, X., Li, Y., and Wang, Y. (2014a). “Experimental study of two-phase mechanical face Seals with laser surface texturing.” *Tribol. Int.*, 72, 90–97.

Wang, Z., Nakashima, S., and Larson, M. (2014b). “Energy efficient machining of titanium alloys by controlling cutting temperature and vibration.” *Procedia CIRP*, 17, 523–528.

Webzell S. (2007). *Exotic Substrates*.

Wilks, J., & Wilks, E. (1991). *Properties and applications of diamond*. Oxford: Butterworth-Heinemann.

Wu, X., Tao, N., Hong, Y., Liu, G., Xu, B., Lu, J., and Lu, K. (2005). “Strain-induced grain refinement of cobalt during surface mechanical attrition treatment.” *Acta Mater.*, 53(3), 681–691.

Wu, Z., Yang, Y., and Luo, C. (2016). “Design, fabrication and dry cutting performance of pulsating heat pipe self-cooling tools.” *J. Clean. Prod.*, 124, 276–282.

Xing, Y., Deng, J., Li, S., Yue, H., Meng, R., and Gao, P. (2014a). “Cutting performance and wear characteristics of Al_2O_3/TiC ceramic cutting tools with WS2/Zr soft-coatings and nano-textures in dry cutting.” *Wear*, 318(1–2), 12–26.
Xing, Y., Deng, J., Zhang, K., Zhang, G., and Gao, H. (2014b). “Effect of femtosecond laser pretreatment on wear resistance of Al_2O_3/TiC ceramic tools in dry cutting.” *Int. J. Refract. Met. Hard Mater.*, 43, 291–301.

Xing, Y., Deng, J., Zhao, J., Zhang, G., and Zhang, K. (2014c). “Cutting performance and wear mechanism of nanoscale and microscale textured Al_2O_3/TiC ceramic tools in dry cutting of hardened steel.” *Int. J. Refract. Met. Hard Mater.*, 43, 46–58.

Yan, P., Rong, Y., and Wang, G. (2016). “The effect of cutting fluids applied in metal cutting process.” *Proc. Inst. Mech. Eng. Part B J. Eng. Manuf.*, 230(1), 19–37.

Zębala, W., and Słodki, B. (2013). “Cutting data correction in Inconel 718 turning.” *Int. J. Adv. Manuf. Technol.*, *65*(5-8), 881-893.

Zębala, W., Kowalczyk, R., and Matras, A. (2015). “Analysis and Optimization of Sintered Carbides Turning with PCD Tools.” *Procedia Eng.*, 100, 283–290.

Zhang, Y., Outeiro, J. C., and Mabrouki, T. (2015). “On the selection of Johnson-Cook constitutive model parameters for Ti-6Al-4V using three types of numerical models of orthogonal cutting.” *Procedia CIRP*, 31, 112–117.

Zhao, H., Barber, G. C., and Zou, Q. (2002). “A study of flank wear in orthogonal cutting with internal cooling.” *Wear*, 253(9–10), 957–962.

APPENDIX-I

The specification of the Micro-hole fabricated on the PCD and PCBN Inserts

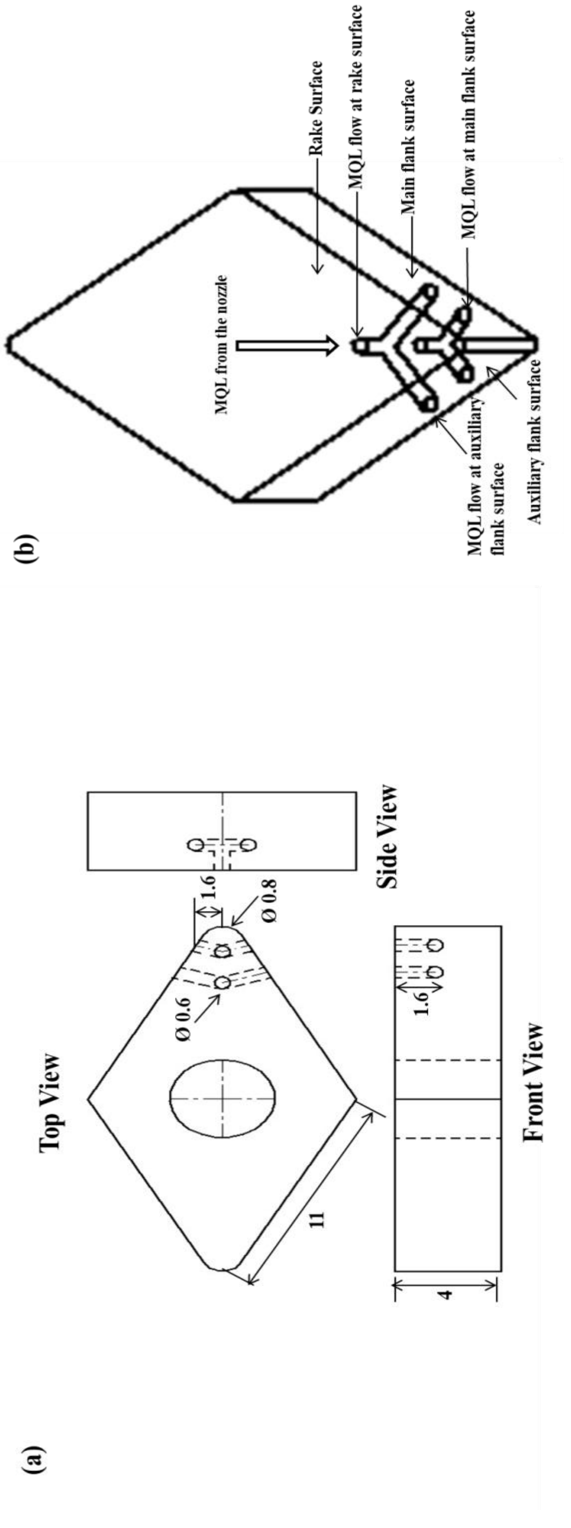
(a)
Top View
Side View
Front View
1.6
Ø 0.8
Ø 0.6
1.6
11
4
(b)
Rake Surface
MQL flow at rake surface
Main flank surface
MQL flow at main flank surface
MQL from the nozzle
MQL flow at auxiliary flank surface
Auxiliary flank surface

(a) Detail drawing of modified cutting inserts (b) Schematic representation of modified cutting insert

APPENDIX-II

BLOCK DIAGRAM OF LABVIEW PROGRAM

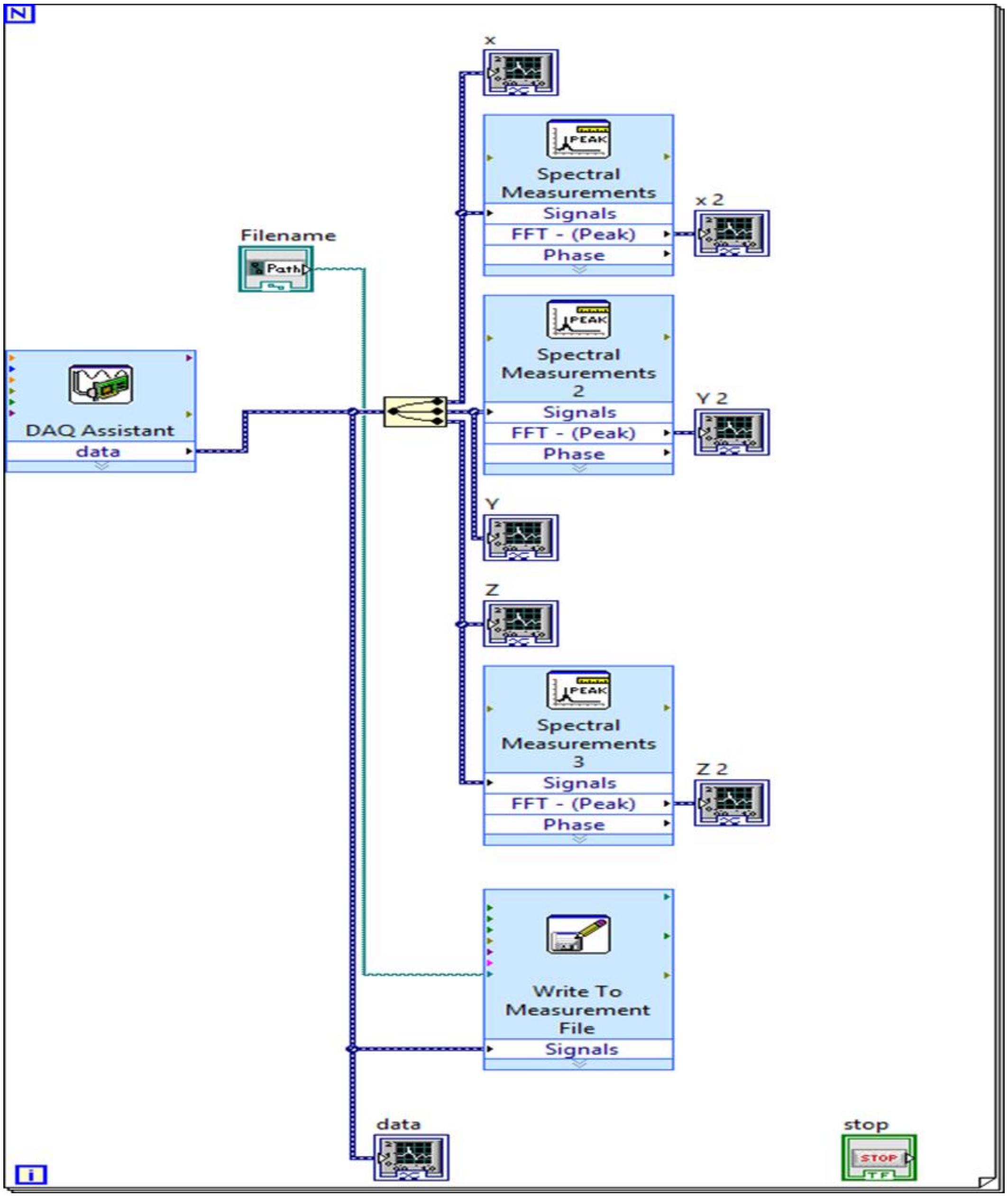
N
x
Spectral Measurements
Signals
FFT - (Peak)
Phase
x 2
Filename
Path
Spectral Measurements 2
Signals
FFT - (Peak)
Phase
Y 2
DAQ Assistant
data
Y
Z
Spectral Measurements 3
Signals
FFT - (Peak)
Phase
Z 2
Write To Measurement File
Signals
data
stop
STOP
TF
i

Block diagram for collecting vibration signals during turning operation

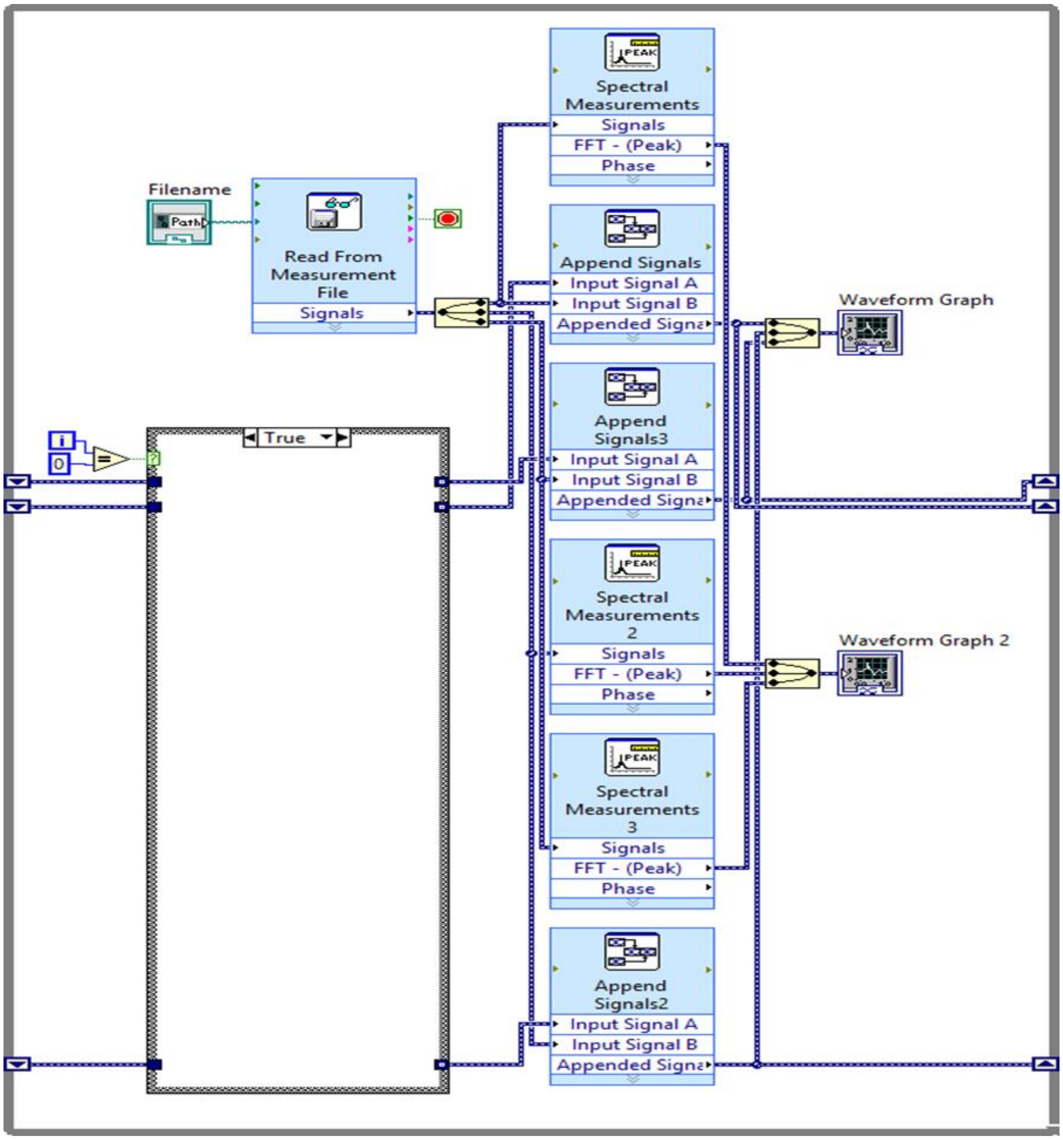
Spectral Measurements
Signals
FFT - (Peak)
Phase
Filename
Path
Read From Measurement File
Signals
Append Signals
Input Signal A
Input Signal B
Appended Signa
Waveform Graph
True
i
0
Append Signals3
Input Signal A
Input Signal B
Appended Signa
Spectral Measurements 2
Signals
FFT - (Peak)
Phase
Waveform Graph 2
Spectral Measurements 3
Signals
FFT - (Peak)
Phase
Append Signals2
Input Signal A
Input Signal B
Appended Signa

Simple block diagram for data fetching from stored vibration signals

List of Publications based on Ph.D. Research Work

Sl. No.	Title of the paper	Authors (in the same order as in the paper. Underline the Research Scholar's name)	Name of the Journal/ Conference/ Symposium, Vol., No., Pages	Month, Year of Publication	Category*
1.	Development of novel cutting tool with a micro-hole pattern on PCD insert in machining of titanium alloy	Charitha M Rao, Shrikantha S Rao, Mervin A Herbert	Journal of Manufacturing Processes, 36, 93–103 doi.org/10.1016/j.jmapro.2018.09.028	October 2018	1
2.	Performance improvement studies for cutting tools with perforated surface in turning of titanium alloy	Charitha M Rao, Shrikantha S Rao, Mervin A Herbert	MATEC Web of Conferences, 144, 03003 doi.org/10.1051/matecconf/201814403003	January 2018	1
3.	Influence of Modified Cutting Inserts in Machining of Ti-6Al-4V Alloy Using PCD Insert	Charitha M Rao, Shrikantha S Rao, Mervin A Herbert	Materials Today: Proceedings, 5, 18426–18432 doi.org/10.1016/j.matpr.2018.06.183	October 2018	1
4.	Studies on the effect of Process Parameters in Turning of Ti-6Al-4V alloy using TOPSIS	Charitha M Rao, Shrikantha S Rao, Mervin A Herbert	International Conference on Advanced Materials and Manufacturing Applications (Paper will be published in IOP Series: Materials and Science Engineering)	August 2018	3
5.	Minimum Quantity Lubrication through the Micro-hole textured PCD and PCBN inserts in machining of the Ti-6Al-4V alloy as a sustainable alternative	Charitha M Rao, Shrikantha S Rao, Mervin A Herbert	Journal of Manufacturing Processes	(Under Review)	1
6.	An experimental and numerical approach to study the performance of micro-holed tools on machining of Ti-6Al-4V alloy	Charitha M Rao, Shrikantha S Rao, Mervin A Herbert	Arabian Journal for Science and Engineering	(Revisions Submitted)	1

*Category:
1: Journal paper, full paper reviewed 2: Journal paper, Abstract reviews 3: Conference/Symposium paper, full paper reviewed 4: Conference/Symposium paper, abstract reviewed 5: Others (including papers in Workshops, NITK Research Bulletins, Short notes etc.)

Miss. Charitha M Rao	Prof. Shrikantha S Rao	Dr. Mervin A Herbert
Research Scholar	Research Guide	Research Guide
Name & Signature, with Date	Name & Signature, with Date	Name & Signature, with Date

BIO-DATA

1. **Name** Charitha M. Rao
2. **Father's Name** M R Manjunatha Rao
3. **Date of Birth** 1/10/1989
4. **Nationality** Indian
5. **Permanent Address** D/o M R Manjunatha Rao, #3324/7, Chirapreetha,
11th Cross, Shankarpura Road, Nanjangudu-571301
Mysuru Dist. Karnataka, India.
6. **E-mail** charithamrao@gmail.com
7. **Mobile Number** +91-9632243324

8. Academic Credentials:

Qualification	University	Institution	Performance	Year of Passing	Class
Ph.D.	NITK	National Institute of Technology Karnataka (NITK), Surathkal	9.25 CGPA	2019	
M.Tech in Computer Integrated Manufacturing	VTU, Belgaum	Dayananda Sagar College of Engineering, Bangalore	79%	2013	FCD
B.E in Industrial & Production Engineering	Autonomous, affiliated to VTU, Belgaum	Malnad College of Engineering, Hassan	8.08 CGPA	2011	FCD

9. Working Experience

Name of the Organization	Duration	Position
K S School of Engineering and Management, Bengaluru	2013-2014	Assistant Professor